

Polymer or Macrocycle?

Cobalt Complexes of Ditopic 2,2':6',2''- Terpyridine Ligands with Flexible Spacers

Inauguraldissertation

zur

Erlangung der Würde eines Doktors der Philosophie

vorgelegt der

Philosophisch-Naturwissenschaftlichen Fakultät

der Universität Basel

von

Emily Kate Harris

aus Grossbritannien

Basel, 2010

Original document stored on the publication server of the University of Basel

edoc.unibas.ch



This work is licenced under the agreement „Attribution Non-Commercial No Derivatives – 2.5 Switzerland“. The complete text may be viewed here:
creativecommons.org/licenses/by-nc-nd/2.5/ch/deed.en

Genehmigt von der Philosophisch-Naturwissenschaftlichen Fakultät
auf Antrag von

Prof. Dr. Edwin Constable

PD Dr. Daniel Häussinger

Basel, den 02.03.2010

Prof. Dr. Eberhard Parlow
Dekan



Attribution-Noncommercial-No Derivative Works 2.5 Switzerland

You are free:



to Share — to copy, distribute and transmit the work

Under the following conditions:



Attribution. You must attribute the work in the manner specified by the author or licensor (but not in any way that suggests that they endorse you or your use of the work).



Noncommercial. You may not use this work for commercial purposes.



No Derivative Works. You may not alter, transform, or build upon this work.

- For any reuse or distribution, you must make clear to others the license terms of this work. The best way to do this is with a link to this web page.
- Any of the above conditions can be waived if you get permission from the copyright holder.
- Nothing in this license impairs or restricts the author's moral rights.

Your fair dealing and other rights are in no way affected by the above.

This is a human-readable summary of the Legal Code (the full license) available in German:
<http://creativecommons.org/licenses/by-nc-nd/2.5/ch/legalcode.de>

Disclaimer:

The Commons Deed is not a license. It is simply a handy reference for understanding the Legal Code (the full license) — it is a human-readable expression of some of its key terms. Think of it as the user-friendly interface to the Legal Code beneath. This Deed itself has no legal value, and its contents do not appear in the actual license. Creative Commons is not a law firm and does not provide legal services. Distributing of, displaying of, or linking to this Commons Deed does not create an attorney-client relationship.

Acknowledgements

First and foremost, I'd like to thank Ed and Catherine for giving me the chance to do my PhD in Switzerland. I very much appreciate having been able to do almost anything I could think of in the lab as long as it involved terpy, glycols and cobalt! Thank you for all your support, advice and encouragement over the last four years.

Next I'd like to thank everyone in Basel who has helped me in some way or another with this project. Thanks to all of you who have taken the time to do any measurements for me; to patiently explain to me how to use various instruments; or to come up with suggestions as to what my results might possibly mean. And also to those of you who have stopped me from doing anything too stupid or who helped me to clear up the mess if it was too late. Thank you especially to Markus, Silvia and Jennifer for solving all my crystal structures. It's really great to be able to see that the molecules I think I've made really do exist! I'd also like to say a big thank you to Jon, for, among many things, teaching me (almost) everything I know about NMR; being willing to answer the same questions over and over again and for lots of thoughtful advice as to what I should try next when the last idea didn't work. Thank you to everyone for making the group such an enjoyable and interesting place to work – it is very much appreciated.

Finally, I'd like to thank my family and friends for all your support and encouragement over the last four years, whether you are here in Basel, on the other side of the world or somewhere in between. In particular, thanks to those of you who have listened to my many concerns over the last year. I couldn't have done it without you!

So, especially for David, "my book" is finally finished!

Abstract

The reaction of transition metal ions with ditopic ligands containing two 2,2':6',2''-terpyridine units linked by flexible spacers can give metallosupramolecular polymers, discrete metallomacrocycles or mixtures of the two. The outcome of the coordination depends on the precise reaction conditions as well as the nature of the spacer and the transition metal salt.

This thesis is concerned with the reaction between cobalt(II) salts and bis(2,2':6',2''-terpyridine) ligands in which the metal-binding domains are linked by flexible oligo(ethylene glycol) spacers. An initial study of the ligands and several model mononuclear bis(2,2':6',2''-terpyridine)cobalt(II) and (III) complexes gave some insight into the solid state and solution properties of these systems, and PGSE NMR spectroscopy was found to be a useful tool for determination of the size of both the ligands and the cobalt(III) complexes in solution. The reaction of the ditopic ligands with cobalt(II) acetate tetrahydrate in pure alcohol was found to cause the decomposition of the ligand and the formation of a mononuclear bis(4'-alkoxy-2,2':6',2''-terpyridine)cobalt(II) complex. This reaction was extended to monotopic 4'-substituted-2,2':6',2''-terpyridines and can be considered as a reaction giving rise to polymer end-capping units, thus influencing the final outcome of the coordination. The effect of the anion on the coordination was considered further, and the speciation of mono- and bis(2,2':6',2''-terpyridine)cobalt(II) complexes in solution was investigated using the 4'-methoxy-2,2':6',2''-terpyridine ligand. The product mixtures were found to depend heavily on the anion, solvent and initial ratio of ligand to metal salt. Similar behaviour was observed for a model ditopic ligand. The presence of the mono(2,2':6',2''-terpyridine)cobalt(II) complexes within a system containing the ditopic ligands would also provide polymer end-capping units, influencing the speciation of these mixtures. Finally, a detailed study of the product mixtures obtained from the reactions of the ditopic ligands with cobalt(II) salts revealed a complex dependence of the speciation of many bis(2,2':6',2''-terpyridine)cobalt(II) complexes on the ligand, anion, solvent, concentration and other seemingly minor reaction parameters. Using the PGSE NMR spectroscopic technique, the sizes of some of the metallomacrocyclic species present in the equilibrium mixtures could be determined. These measurements were in excellent agreement with X-ray crystallographic data. Analysis of initial product mixtures using the same technique suggested that the initial kinetic products of the complexation are significantly larger species.

Contents

Abstract	v
Nomenclature	xi
1 Introduction	1
1.1 <i>Supramolecular chemistry and self-assembly</i>	1
1.2 <i>Metallosupramolecular polymerisation</i>	2
1.3 <i>Formation of discrete molecular species</i>	3
1.4 <i>Examples of metallosupramolecular polymerisation and macrocycle formation with ditopic bis(2,2':6',2"-terpyridine) ligands</i>	3
1.4.1 <i>Metallosupramolecular polymerisation with rigid ditopic bis(2,2':6',2"-terpyridine) ligands</i>	4
1.4.2 <i>Metallosupramolecular polymerisation with flexible ditopic bis(2,2':6',2"-terpyridine) ligands</i>	6
1.4.3 <i>Formation of metallomacrocycles from rigid ditopic bis(2,2':6',2"-terpyridine) ligands</i>	14
1.4.4 <i>Formation of metallomacrocycles from flexible ditopic bis(2,2':6',2"-terpyridine) ligands</i>	18
1.5 <i>Aims of this thesis</i>	24
2 Methods	25
2.1 <i>¹H NMR spectroscopy of cobalt(II) complexes</i>	25
2.1.1 <i>General considerations</i>	25
2.1.2 <i>¹H NMR spectroscopy of bis(2,2':6',2"-terpyridine)cobalt(II) complexes</i>	26
2.2 <i>Diffusion and PGSE NMR Spectroscopy</i>	29
2.2.1 <i>What is diffusion?</i>	29
2.2.2 <i>Limitations of and corrections to the Stokes-Einstein equation</i>	31
2.2.3 <i>What is PGSE NMR spectroscopy and how does it work?</i>	36
2.2.4 <i>Applications of PGSE NMR spectroscopy</i>	39

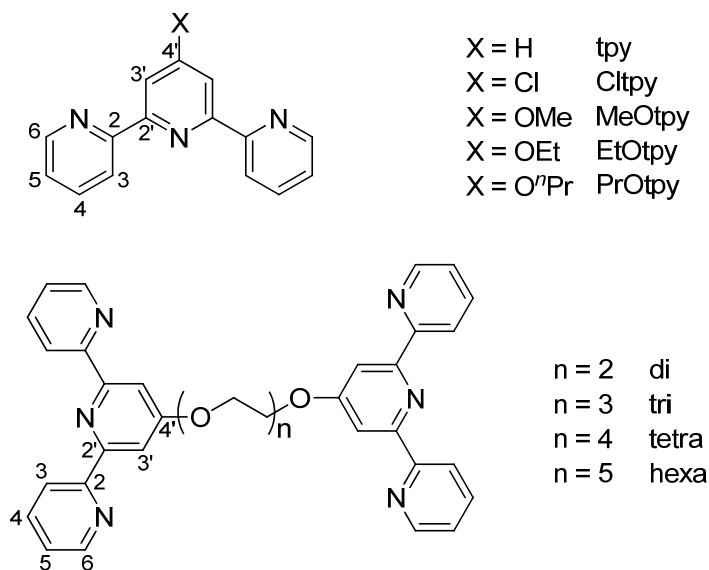
2.2.4.1 Determination of molecular size in metallocsupramolecular systems.....	39
3 Simple Models.....	43
3.1 Introduction.....	43
3.2 Synthesis of the ligands and simple complexes	43
3.2.1 Ligand synthesis.....	43
3.2.1.1 Synthesis of 4'-alkoxy-2,2':6',2"-terpyridine ligands	43
3.2.1.2 Synthesis of bis(terpyridyl)oligo(ethylene glycol) ligands	45
3.2.2 Synthesis of mononuclear cobalt(II) hexafluorophosphate complexes.....	47
3.2.3 Synthesis of mononuclear cobalt(III) hexafluorophosphate complexes	49
3.3 Comparison of X-ray crystal structures of bis(2,2':6',2"-terpyridine) cobalt(II) and cobalt(III) complexes.....	51
3.4 Mononuclear cobalt(II) complexes as models for more complex systems: How fast is the ligand exchange in bis(2,2':6',2"-terpyridine) cobalt(II) hexafluorophosphate complexes?	70
3.5 Ligands and mononuclear cobalt(III) complexes as models for more complex systems: What size are the species in solution?.....	73
3.5.1 Measurement of diffusion coefficients using PGSE NMR spectroscopy	73
3.5.1.1 Mononuclear cobalt(III) complexes	73
3.5.1.2 Ligands	75
3.5.2 Models of the model compounds	76
3.5.2.1 Mononuclear cobalt(III) complexes	76
3.5.2.2 Ligands	79
3.6 Conclusions.....	85
3.7 Experimental	86
4 Solvent Effects	97
4.1 Introduction.....	97
4.2 Alkoxy group exchange in cobalt(II) complexes of bis(terpyridyl)-oligo(ethylene glycol) ligands.....	97

4.3 Alkoxy group exchange in cobalt(II) complexes of 4'-alkoxy-2,2':6',2''-terpyridine ligands	100
4.4 Substituent exchange in cobalt(II) complexes of 4'-chloro-2,2':6',2''-terpyridine	102
4.5 Proposed mechanism for the substituent exchange in cobalt(II) complexes of 4'-substituted-2,2':6',2''-terpyridine ligands	104
4.6 Conclusions	109
4.7 Experimental	110
5 Anion Effects.....	121
5.1 Introduction.....	121
5.2 Initial observations.....	121
5.3 Monotopic 2,2':6',2''-terpyridine ligands as model systems	124
5.3.1 Coordinated acetate anions.....	125
5.3.2 NMR spectroscopic studies with other anions	132
5.3.3 Crystal structures of mono(4'-substituted-2,2':6',2''-terpyridine)cobalt complexes	138
5.4 NMR spectroscopic studies with bis(terpyridyl)tetra(ethylene glycol)	150
5.5 Conclusions	155
5.6 Experimental	157
6 Polymer or Macrocycle?	165
6.1 Introduction.....	165
6.2 Cobalt(II) equilibria.....	165
6.2.1 Reactions with cobalt(II) acetate tetrahydrate.....	165
6.2.1.1 Reactions with bis(terpyridyl)di(ethylene glycol).....	166
6.2.1.2 Reactions with bis(terpyridyl)tri(ethylene glycol)	169
6.2.1.3 Reactions with bis(terpyridyl)tetra(ethylene glycol).....	172
6.2.1.4 Reactions with bis(terpyridyl)hexa(ethylene glycol)	175
6.2.1.5 Comparison of cobalt(II) complexes of bis(terpyridyl)oligo(ethylene glycol) ligands	177

6.2.2 NMR spectroscopic studies with other anions	178
6.2.3 Bulk synthesis	185
6.3 Oxidation.....	187
6.4 X-ray structure determination of macrocycles.....	189
6.5 Measurement of diffusion coefficients with PGSE NMR spectroscopy.....	204
6.5.1 Equilibrium mixtures.....	204
6.5.1.1 Models of the macrocyclic complexes	207
6.5.2 Initial mixtures	212
6.6 Conclusions	215
6.7 Experimental	217
7 General Conclusions	223
8 Appendix	225
8.1 General experimental.....	225
8.1.1 Analytical instrumentation	225
8.1.2 PGSE NMR spectroscopy	225
8.2 X-Ray crystallography.....	226
References	237
CV	247
List of Publications.....	249

Nomenclature

The ligands described in this thesis and the numbering scheme used for NMR spectroscopic assignments are shown in Scheme 0.1. IUPAC nomenclature for ligands and starting materials based on oligo(ethylene glycol)s are given in Table 0.1. For ease of understanding, the trivial names are used in this thesis.



Scheme 0.1 Ligands and numbering scheme for NMR assignments.

Abbreviation	Trivial	IUPAC
-	di(ethylene glycol)	3-oxapentane-1,5-diol
-	tri(ethylene glycol)	3,6-dioxaoctane-1,8-diol
-	tetra(ethylene glycol)	3,6,9-trioxaundecane-1,11-diol
-	hexa(ethylene glycol)	3,6,9,12,15-pentaoxaheptadecane-1,17-diol
di	bis(terpyridyl)di(ethylene glycol)	1,5-bis(2,2':6',2''-terpyridin-4'-yloxy)-3-oxapentane
tri	bis(terpyridyl)tri(ethylene glycol)	1,8-bis(2,2':6',2''-terpyridin-4'-yloxy)-3,6-dioxaoctane
tetra	bis(terpyridyl)tetra(ethylene glycol)	1,11-bis(2,2':6',2''-terpyridin-4'-yloxy)-3,6,9-trioxaundecane
hexa	bis(terpyridyl)hexa(ethylene glycol)	1,17-bis(2,2':6',2''-terpyridin-4'-yloxy)-3,6,9,12,15-pentaoxaheptadecane

Table 0.1 Abbreviations and IUPAC Nomenclature for compounds based on oligo(ethylene glycol)s

1 Introduction

1.1 Supramolecular chemistry and self-assembly

The term "supramolecular chemistry" incorporates the Latin prefix *supra-* meaning "above" or "beyond" and is therefore commonly defined as "chemistry beyond the molecule".¹ However, over the short history of this discipline, the term has come to have several other definitions including "the chemistry of intermolecular interactions or the non-covalent bond", "the formation of elaborate structures using coordination chemistry", or "the controlled organisation of multiple chemical components".²

While chemists have traditionally focused on the synthesis of molecules based on the irreversible formation of strong covalent bonds, supramolecular chemists are interested in the (usually) weak, reversible interactions between molecules. These intermolecular interactions include ion–ion, ion–dipole (including metal–ligand coordination bonds) and dipole–dipole interactions, hydrogen bonding, cation– π , anion– π and π – π interactions.¹ A summary some of these interactions is given in Table 1.1.^{1,3}

Interaction	Energy / kJ mol^{-1}	Stability	Lability	Example
Covalent Carbon	150 – 500	high	low	C–X
Ion–Ion	100 – 350	high	high	NaCl
Metal–Ligand	100 – 350	high	high	1 st row M–L
		high	medium	2 nd row M–L
		high	low	3 rd row M–L
Ion–Dipole (other)	50 – 200	high	high	crown ethers
Dipole–Dipole	5 – 50	low	high	carbonyls
Hydrogen Bond	4 – 60	medium	high	X–H \cdots Y
π – π	5 – 20	low	high	benzene

Table 1.1 Comparison of covalent and intermolecular interactions.^{1,3}

One of the core concepts in supramolecular chemistry is that of "self-assembly", or the spontaneous and reversible association of several molecular components into more complex supramolecular entities.¹ Reversibility of the assembly process is necessary to allow the system to "self-repair", or correct any defects in the initial assembly of the structure, ideally leading to the formation of a single thermodynamically stable product. By careful choice of the components and conditions used, the nature of the final product can often be predicted in advance, enabling the synthesis of supramolecular entities designed to have specific properties.

Much of the inspiration for supramolecular chemistry and self-assembly is drawn from biology, as nature has been self-assembling large, complex and functional structures based on weak interactions for billions of years. Examples of these include proteins, DNA and even viruses. An understanding of the processes that nature uses to build these structures could potentially provide an understanding of life at a level which is currently inconceivable. In the more immediate future, the application of even the most basic of these concepts could result in the development of new materials with remarkable properties.

Supramolecular assemblies based on directional interactions can be divided into two very broad categories; those forming polymeric species, and those forming discrete aggregates.¹ Considering specifically metallosupramolecular chemistry, or the assembly of supramolecular architectures based on metal–ligand interactions,⁴ ligands can be designed accordingly with metal-binding domains arranged in such a way that the formation of either polymers or discrete species is favoured. Alternatively, the metal ion can be protected such that it has only a limited number of coordination sites in a specific geometry available for coordination to the ligands.⁵ If the components are not designed in such a way as to promote the formation of a particular species, the outcome of the coordination is less certain, with the potential formation of polymers, discrete supramolecular species or mixtures of the two.^{6,7}

1.2 Metallosupramolecular polymerisation

The incorporation of metallosupramolecular building-blocks into polymeric systems has become an attractive area of research in polymer chemistry, leading to new materials which combine the properties of polymers with those of metal complexes (catalysis, light-emission, conduction etc.).^{8,9} The properties of the resulting polymers can be tuned to suit individual circumstances by selection of the ligand, an appropriate metal cation and corresponding

counteranion. Differences in the thermodynamic and kinetic stability of the metal complexes within the polymeric system result in different degrees and reversibility of the polymerisation. Modification of the metal centre therefore affects the size of the resulting polymer, the response of the system towards changes in temperature, pH and addition of competing ligands or redox agents, and the physical properties of the material. Adjustment of the counterion alters the intermolecular interactions in the structure and, as a result, the solubility of the final polymer. Based on a single ligand, the synthesis of many different polymers with many distinct properties can therefore be envisaged. Considering in addition the wide variety of potential ligands, many thousands of new polymeric systems can be imagined. Even ligands with identical binding motifs can behave very differently on coordination to metal ions depending on the nature of the spacer linking the binding units.

1.3 Formation of discrete molecular species

Many examples of increasingly complex architectures have already been described in the literature, including molecular squares, cubes, boxes, racks, grids and ladders, cages or capsules, rosettes, catenanes, rotaxanes, helices, knots, and even a nanoscale version of the Borromean rings.¹ The number of possible structures for future self-assembled supramolecular architectures is probably only limited by the imagination of supramolecular chemists.

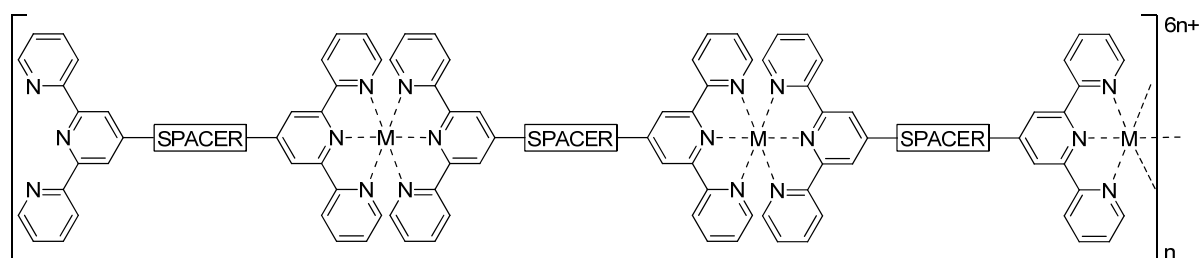
1.4 Examples of metallosupramolecular polymerisation and macrocycle formation with ditopic bis(2,2':6',2''-terpyridine) ligands

2,2':6',2''-Terpyridine-based (tpy) ligands have become attractive building-blocks for the formation of self-assembled species in metallosupramolecular chemistry.¹⁰ These ligands have several advantages over the related bidentate 2,2'-bipyridine (bpy) ligands. One of the most important of these is that, provided that symmetrically substituted ligands are used, the $\{M(tpy)_2\}$ motif is achiral, while the equivalent $\{M(bpy)_3\}$ species gives rise to Δ and Λ enantiomers. This, along with the increased complexity introduced by incorporating three ligands around each metal centre, becomes an important consideration for multinuclear species containing these metal-binding units.^{10, 11} Functionalisation of the 2,2':6',2''-terpyridine unit at the 4'-position preserves the symmetry of the ligand and there are many examples of ditopic bis(2,2':6',2''-terpyridine) ligands linked by a spacer through the 4'-

position. Some of these are described below. Careful design of a rigid spacer can lead to the preferential formation of metallocupramolecular polymers or discrete macrocyclic species. Alternatively, a flexible spacer can be incorporated into the ligand, making the outcome of the coordination to metal ions significantly more uncertain.

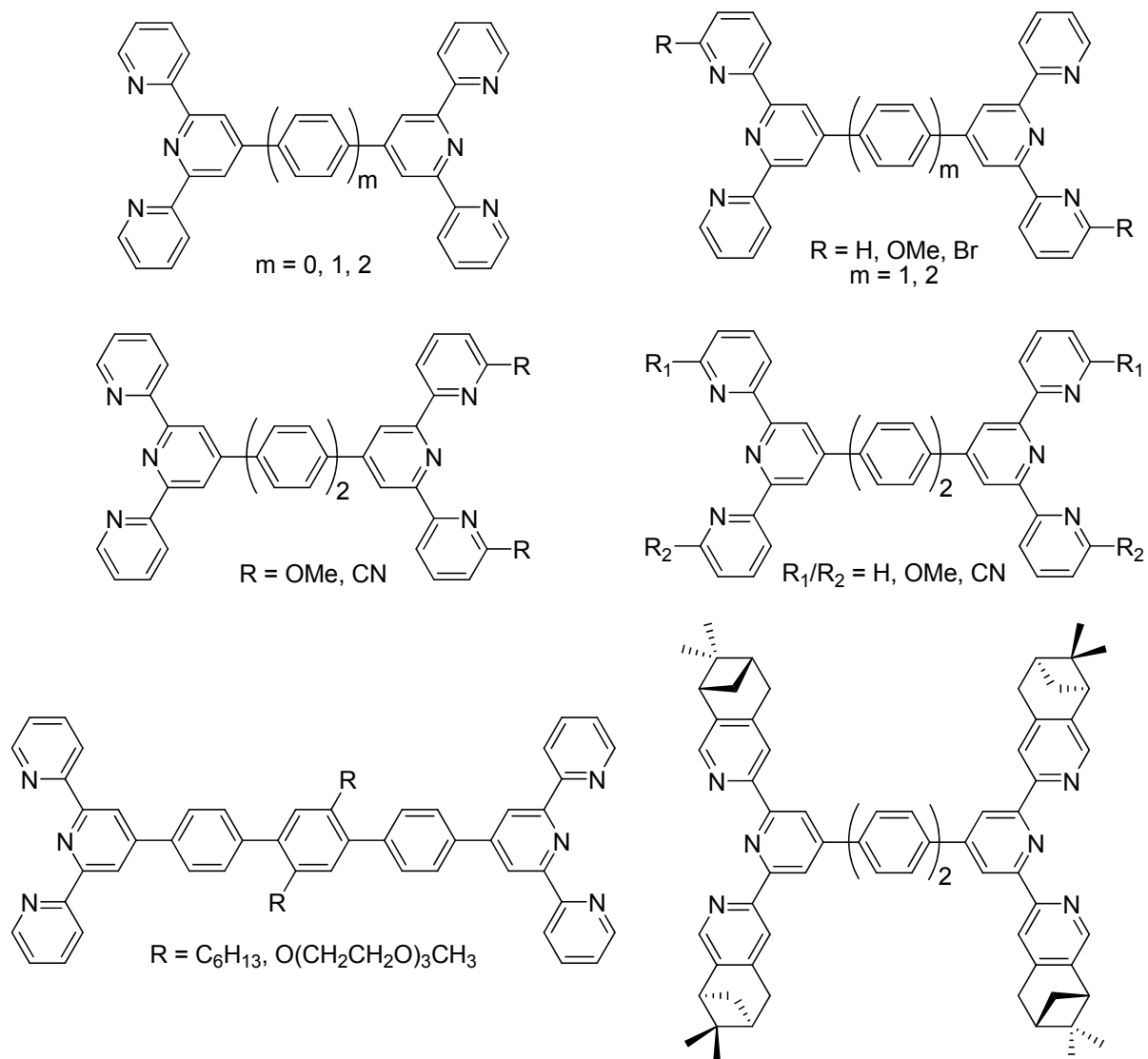
1.4.1 Metallosupramolecular polymerisation with rigid ditopic bis(2,2':6',2''-terpyridine) ligands

Coordination of ditopic bis(2,2':6',2''-terpyridine) ligands containing rigid linear spacers to octahedral transition metal ions can be expected to give linear coordination polymers as shown in Scheme 1.1. Conjugated systems are particularly attractive due to their interesting electrochemical and photophysical properties. Several studies of the synthesis and properties of di- and trinuclear complexes containing this type of ligand have been carried out.¹¹⁻²¹



Scheme 1.1 Schematic representation of a metallosupramolecular polymer incorporating a ditopic bis(4'-substituted-2,2':6',2''-terpyridine) ligand.

One class of ligands used for the construction of rod-like metallosupramolecular polymers is the set of ditopic bis(4'-substituted-2,2':6',2''-terpyridine) ligands linked by phenylene spacer units. Some of these ligands are shown in Scheme 1.2,²²⁻³³ and have been used to synthesise metallosupramolecular polymers incorporating ruthenium(II),^{25, 26, 28, 29, 33} iron(II)^{22, 24, 27, 30, 31, 33} and cobalt(II)^{32, 33} metal ions. In addition, a ruthenium(II)-containing oligomer formed from seven monomer units has been assembled in a stepwise approach.²³

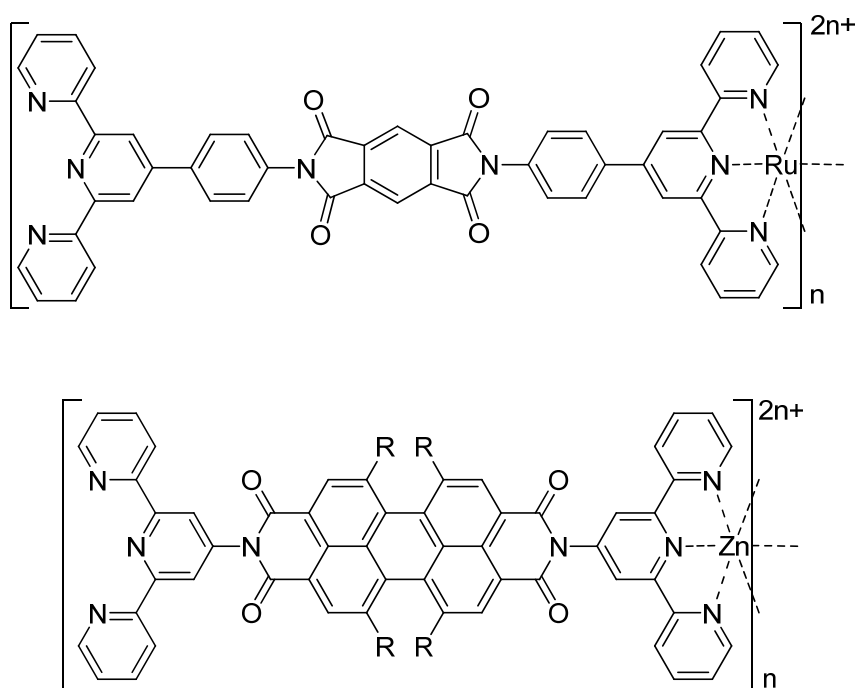


Scheme 1.2 Ditopic bis(2,2':6',2''-terpyridine) ligands with rigid phenylene-based spacers.²²⁻³³

Formation of metallocsupramolecular polymers was suggested by the broadening of the ^1H NMR spectrum,^{22, 25, 26} and confirmed with viscosity measurements^{25, 26} or analytical ultracentrifugation,²² and the synthesis of polymers consisting of at least 25 repeat units has been proposed.^{22, 25, 26, 29} As well as confirming the high molecular weights, viscosity measurements also demonstrated the rod-like structures of the polymers.^{25, 26} The properties and colours of the polymers were found to be easily adjusted by variation of the metal ion or by the introduction of substituents on the terminal pyridine rings of the ligand.³¹⁻³³

Other polymeric systems containing bis(2,2':6',2''-terpyridine) ligands with rigid spacers include ruthenium(II)-containing polyimides (for an example see Scheme 1.3 (top)),

synthesised using a polymerisation reaction between a bis(4'-(4-amino)phenyl-2,2':6',2''-terpyridine)ruthenium(II) complex and several dianhydride monomers,³⁴ and zinc(II)-containing polymers of ditopic bis(2,2':6',2''-terpyridine) ligands with perylene bisimide spacers with up to 35 repeat units (Scheme 1.3 (bottom)).³⁵ A library of other conjugated ditopic bis(2,2':6',2''-terpyridine) ligands with rigid ethene- or ethyne-based spacers and their zinc(II)-containing metallosupramolecular polymers was also recently synthesised,³⁶ illustrating the versatility of this polymerisation approach.



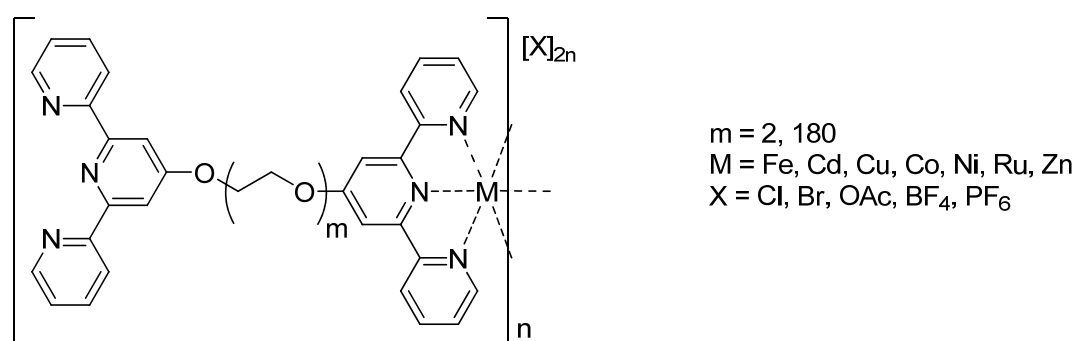
Scheme 1.3 Ruthenium(II)-containing polyimide with a ditopic bis(2,2':6',2''-terpyridine) ligand (top) and zinc(II)-containing polymer with a ditopic bis(2,2':6',2''-terpyridine) ligand with a perylene bisimide spacer (bottom).

1.4.2 Metallosupramolecular polymerisation with flexible ditopic bis(2,2':6',2''-terpyridine) ligands

If, instead of well-defined rigid spacers, a long flexible spacer is used to link the two 2,2':6',2''-terpyridine units, the outcome of the coordination is much less predictable. As well as synthesis of the desired polymer, formation of discrete metallomacrocycles is also possible. The use of ditopic ligands composed of covalent polymers end-functionalised with 2,2':6',2''-

terpyridine units as ligands was in response to the limitations of the existing coordination polymers based on ligands with short rigid spacers described above. These systems are usually sparingly soluble in water and common organic solvents, or require multi-step syntheses in order to incorporate solubilising side-chains. Additionally, the molecular weights of the resulting polymers are limited by the low molecular weights of the ligands.

The coordination chemistry of many divalent transition metal ions with ditopic ligands containing two 2,2':6',2''-terpyridine units linked by a poly(ethylene glycol) spacer has been studied in detail by Schubert.³⁷⁻⁴⁶ In addition, several different counteranions and a model system incorporating a ligand with a shorter chain di(ethylene glycol) spacer have been considered. A summary of the systems studied is shown in Scheme 1.4. The combination of the water-soluble poly(ethylene glycol) with a well-studied bis(2,2':6',2''-terpyridine) complex was anticipated to give water-soluble coordination polymers with interesting properties.



Scheme 1.4 Metallosupramolecular polymers synthesised from bis(terpyridyl)di(ethylene glycol) and bis(terpyridyl)poly(ethylene glycol) ligands.³⁷⁻⁴⁶

The conditions required to synthesise the metallosupramolecular polymers vary depending on the metal ion chosen, but the process is identical to complexation reactions of other 2,2':6',2''-terpyridine ligands with metal ions. An automated parallel synthesis approach has also been developed, although this was found to give species with lower molecular weights.⁴² Formation of the bis(2,2':6',2''-terpyridine)metal complex was confirmed by ¹H NMR measurements and UV/vis titrations, with a maximum extinction coefficient found at a 1L:1M ratio,^{38, 39} and using a chloride counterion gave water-soluble complexes. Evidence for the

formation of extended metallopolymers was obtained using several techniques described below; however the formation of cyclic structures cannot be excluded.

The macroscopic properties of the materials resulting from the complexation of the ligand with all the metal ions used suggested the formation of extended coordination polymers. While the ligand itself was a powdery solid, the complexes had film-forming properties typical of polymers.³⁷⁻⁴¹ Films formed from the short chain di(ethylene glycol)-based ligand were brittle; this was attributed to the high charge density of the resulting polymers,³⁸ while complexes of the poly(ethylene glycol)-based ligand formed flexible films.⁴⁰ The signals in the ¹H NMR spectra of the complexes tended to be broadened, also suggesting the formation of extended coordination polymers.^{39, 41} MALDI-TOF mass spectrometry was expected to provide a useful insight into the molecular weights of the resulting polymers. However, for complexes of the di(ethylene glycol)-based ligand, only peaks corresponding to the free ligand and a [MLX]⁺ species were observed.^{38, 39} As the ¹H NMR spectra showed that no free 2,2':6',2''-terpyridine units remained in solution after the complexation step,³⁹⁻⁴² the metal–ligand bonds were assumed to rupture under the conditions used. Analysis of the polymers formed from the longer chain ligands was more successful using MALDI-TOF mass spectrometry, with signals corresponding to oligomers with up to seven repeating units.^{39, 41} As the length of the polymers predicted by this characterisation technique did not agree with the (longer) lengths determined from other methods (see below), the absence of fragments with higher molecular weight was explained by insufficient desorption or decomplexation under the conditions used.

Viscosity measurements were carried out on all of the synthesised polymers in solution in order to estimate the proportion of high molecular weight species in the product mixtures.^{39-41, 43} The relative viscosity is related to the molecular weight of the polymers and the presence of small cyclic species will thus lead to a solution with a lower viscosity.⁴¹ In all cases, the maximum relative viscosity was obtained at 1L:1M ratios and addition of an excess of metal ions resulted in a decrease in the relative viscosity.^{39, 41} The maximum relative viscosity and the behaviour of the viscosity of the polymer solutions on addition of an excess of metal ions was found to be dependent on the nature of the metal salt used for the complexation. The maximum relative viscosity of polymer solutions of different metal ions increases in the order cadmium(II) < copper(II) < cobalt(II) < nickel(II) < iron(II).^{39, 41} This order corresponds qualitatively to the thermodynamic stability of the bis(2,2':6',2''-terpyridine) complexes.⁴⁷

The behaviour of the polymer solutions on addition of an excess of metal ions was related to the kinetic stability of complexes of the metal ions.^{39, 41} For kinetically very labile complexes such as the bis(2,2':6',2''-terpyridine)cobalt(II) and -copper(II) complexes,⁴⁸ the relative viscosity dropped sharply on addition of an excess of metal ions, whereas for complexes more stable towards ligand exchange such as those of iron(II) and nickel(II),⁴⁸ a more gradual decrease in the relative viscosity was observed.^{39, 41} Changing the anion also had an effect on the value of the maximum relative viscosity of bis(terpyridyl)poly(ethylene glycol)iron(II) polymer solutions.⁴²

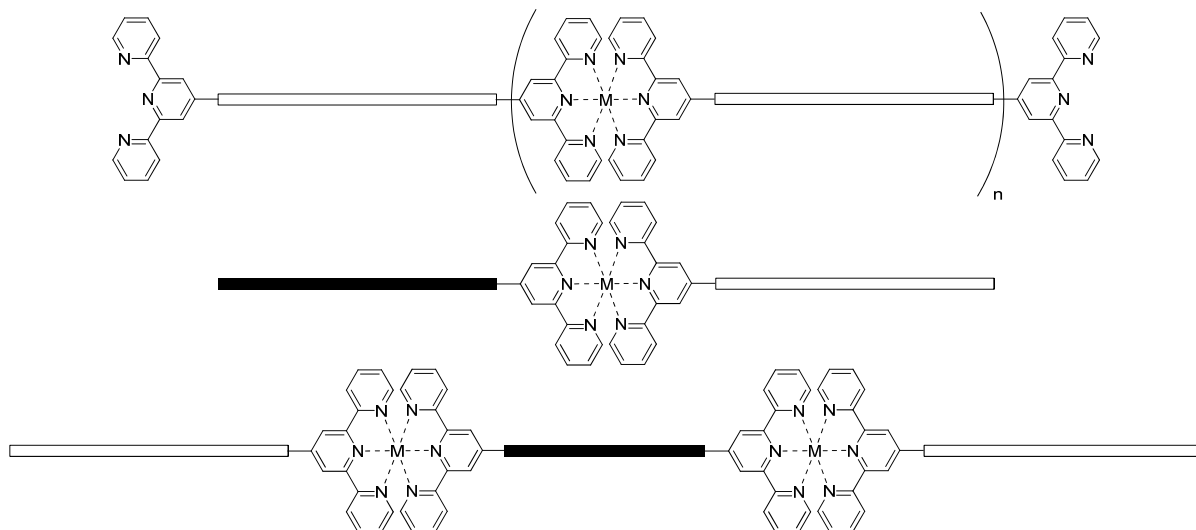
The effect of the reaction conditions on the relative viscosity of the resultant polymer solution has also been studied.^{40, 41, 43} The synthetic procedure can be modified in three ways to give solutions with higher relative viscosities. Firstly, carrying out the reaction at higher concentrations results in higher relative viscosities as intermolecular complexation is favoured under these conditions (when considering a system under kinetic control).^{40, 41, 43} Secondly, an improved mode of metal salt addition, in which two equivalents of the metal salt are initially added to one equivalent of the ligand followed by addition of a second equivalent of the ligand, has also been found to increase the relative viscosity of the resulting polymer solutions.^{41, 43} Using an initial excess of metal salt is expected to result in the formation of mono(2,2':6',2''-terpyridine)metal complexes at both ends of the ligand, thus preventing the formation of [1+1] metallomacrocycles.^{41, 43} Finally, the use of chloroform-ethanol (19:1) in place of ethanol as the solvent for the complexation reaction also leads to solutions with higher relative viscosities.⁴⁰ The 2,2':6',2''-terpyridine moieties are more soluble in chloroform and it is believed that they are therefore more accessible for complexation in this solvent mixture, resulting in a higher degree of polymerisation.³⁹⁻⁴¹ By size exclusion chromatographic studies (see below), it has also been established that the reaction time is important in determining the degree of polymerisation in ruthenium(II)-containing systems.⁴⁵ The highest molecular weights were observed after a reaction time of 12 hours and it was suggested that low molecular weight species are formed first, and then couple to give higher molecular weight polymers. At longer reaction times, the molecular weight decreases slightly. A possible explanation for this is that the complexation is an equilibrium process and the proportion of thermodynamically favoured rings increases with time.⁴⁵

Size exclusion chromatography (SEC) (or gel permeation chromatography (GPC)) is frequently used for the determination of the molecular weights of polymers, but presents

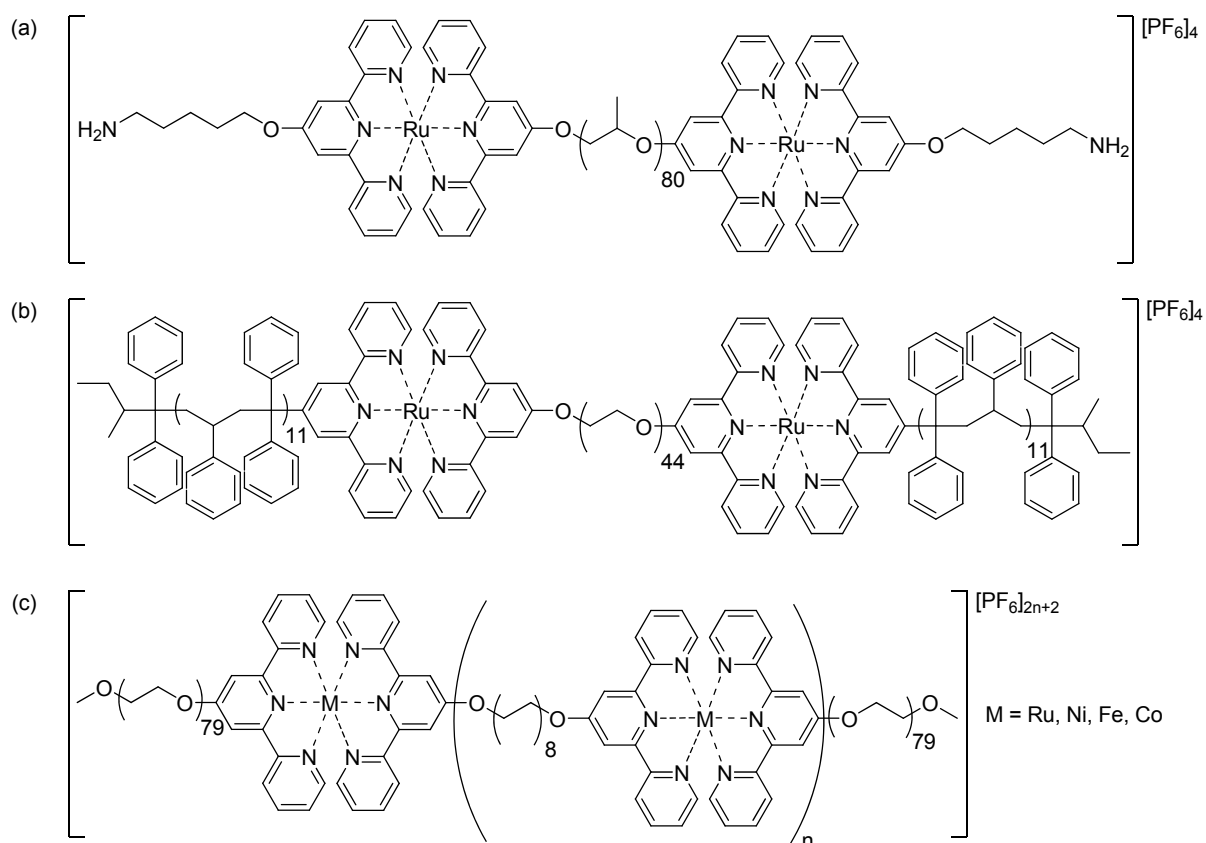
several problems for reversible systems, due to breaking of the metal–ligand bonds and re-equilibration of the product mixture.⁴⁴ In addition, standards for calibration are not usually available for metallosupramolecular polymers. A GPC method was developed for the analysis of a bis(terpyridyl)poly(ethylene glycol)ruthenium(II) tetrafluoroborate metallosupramolecular polymer and the number averaged molecular weight was found to be 138000 g mol⁻¹ with a polydispersity index of 1.55.⁴⁴ This value is in good agreement with the average molecular masses determined by analytical ultracentrifugation (143000 g mol⁻¹)⁴⁴ and from viscosity measurements (123000 g mol⁻¹),⁴⁰ and these molecular weights correspond to polymers with 14 to 16 repeat units. The presence of other macromolecular species, potentially metallomacrocycles, is also suggested by the GPC data. While analytical ultracentrifugation⁴⁹ gives absolute molecular weights, removing the need for calibration standards, both the experimental procedure and the interpretation of the results are time-consuming, making this method unsuitable as a standard characterisation technique.

Studies of the effects of oxidation³⁹ and addition of a competing ligand (HEDTA)^{38, 39} have confirmed the reversibility of the polymerisation. The bis(2,2':6',2''-terpyridine)iron(II) units in the iron(II) polymer of the bis(terpyridyl)di(ethylene glycol) ligand have been found to be stable up to 210 °C,^{38, 39} but cooling to room temperature after heating above this temperature results in a reversible formation of the complexes after 12 hours. The thermal properties and morphology of the linear coordination polymers have also been studied.^{40, 41, 46}

The concept behind these homopolymeric systems was extended and a similar simple synthetic strategy was developed for the formation of metallosupramolecular block copolymers, the covalent analogues of which can be difficult to synthesise using conventional polymerisation techniques.⁵⁰⁻⁵³ The synthesis of metallosupramolecular AB diblock copolymers (see Scheme 1.5) using ruthenium(II) as the metal centre,⁵³⁻⁵⁷ and those proposed more recently with cobalt(III) and nickel(II),⁵⁸ was extended to form metallosupramolecular ABA triblock copolymers based on similar ligands to the homopolymeric systems described above.⁵⁰⁻⁵³ Some of these metallosupramolecular ABA triblock copolymers are shown in Scheme 1.6, showing the versatility of the method.



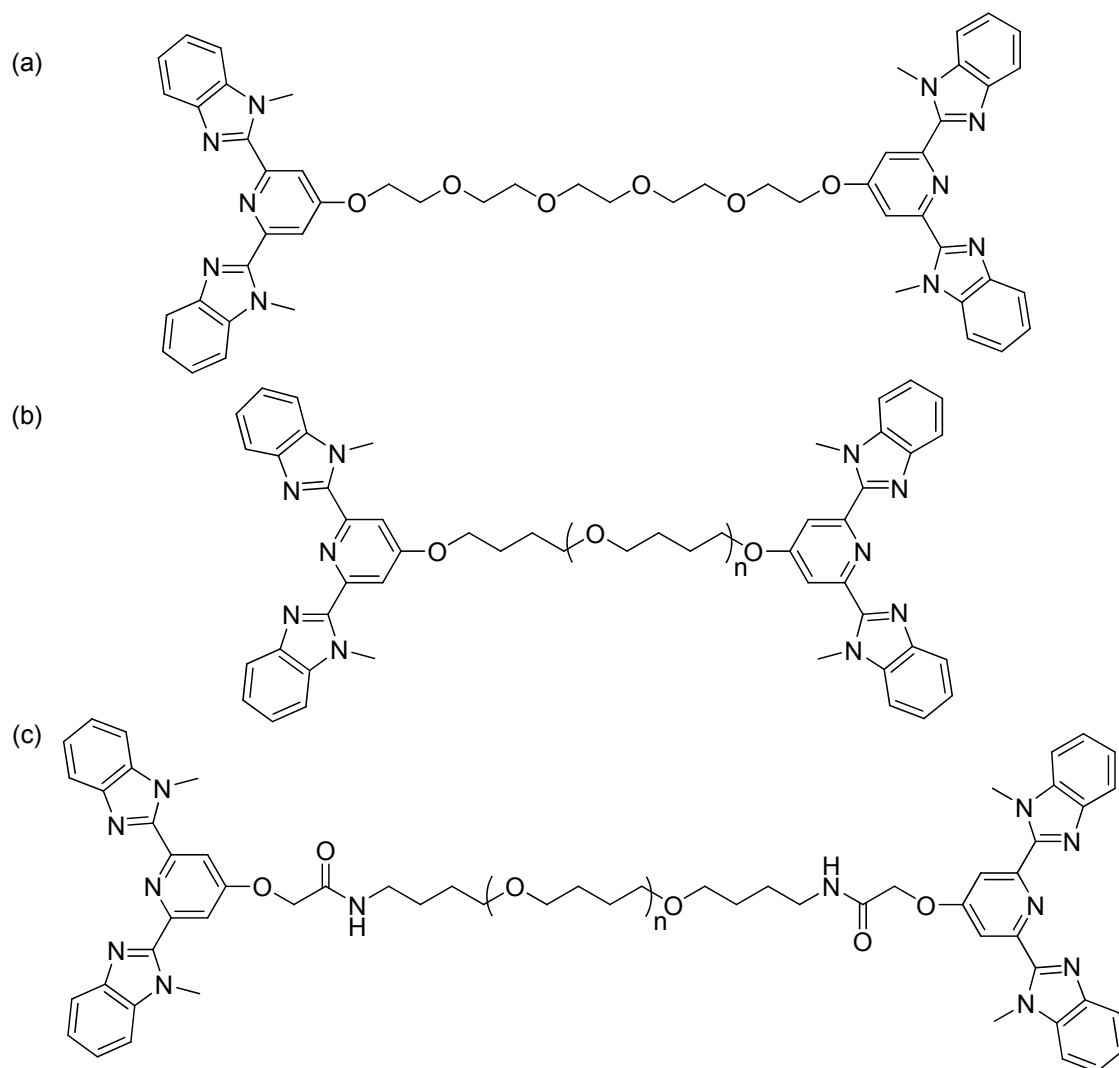
Scheme 1.5 Schematic representation of homopolymers (top), AB diblock (middle) and ABA triblock (bottom) copolymers.



Scheme 1.6 Metallosupramolecular ABA triblock copolymers.⁵⁰⁻⁵³

The copolymer with the amino end groups⁵⁰ (Scheme 1.6(a)) and that with the diphenylethylene ("superpolystyrene" (SPS)) chains⁵³ (Scheme 1.6(b)) were synthesised via a stepwise approach, taking advantage of the ease of formation of heteroleptic bis(2,2':6',2''-terpyridine)ruthenium(II) complexes.⁵⁹ The amino end groups could potentially be used for further copolymerisation or attachment of other supramolecular entities.⁵⁰ The PEG-SPS system is interesting as the combination of the two distinct polymer units in the same molecule can lead to the formation of nanostructures in the bulk material and micelles in solution.⁵³ The micelle-forming polymers shown in Scheme 1.6(c) were synthesised using a one-pot approach.^{51, 52} The molecular weight of the resulting polymers could be adjusted by variation of the relative proportion of the monofunctionalised poly(ethylene glycol) ligand.⁵¹

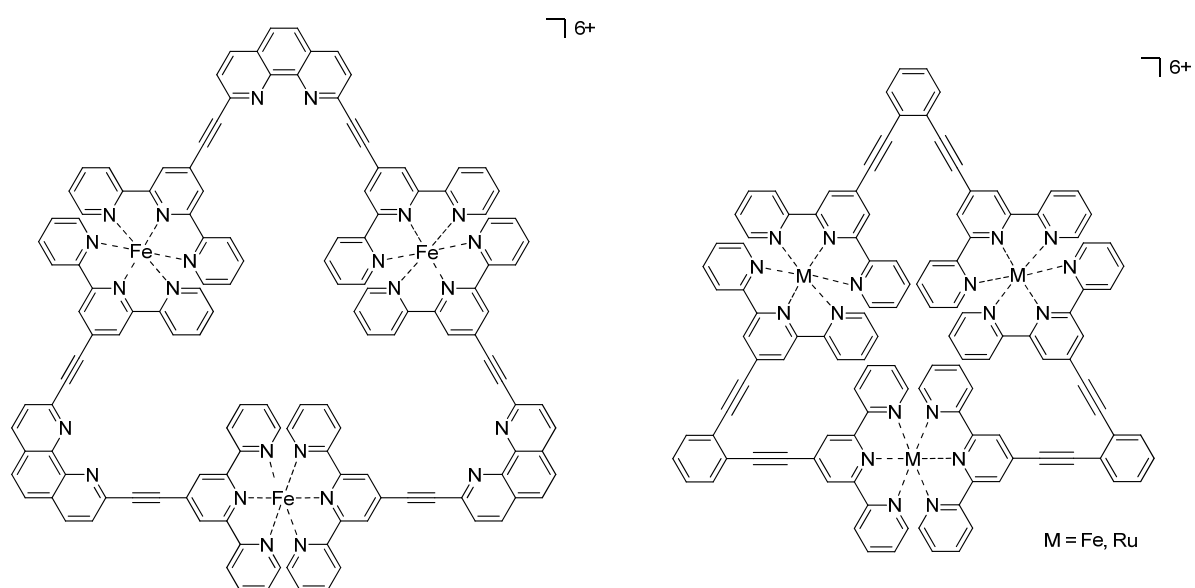
A similar approach with related ligands (Scheme 1.7) was used to build up a library of stimuli-responsive metallosupramolecular systems,⁶⁰⁻⁶⁶ proposed to respond to thermal, chemical, mechanical and light stimuli. The nature of the response can be controlled by the ligand spacer and the transition metal ion. The formation of metallosupramolecular polymers on addition of various transition metal ions was confirmed by viscosity measurements and their thermal properties in the solid state were studied.⁶³ It was proposed that the zinc(II) perchlorate complexes of the short penta(ethylene glycol)-based ligand (Scheme 1.7(a)) contained a higher proportion of metallomacrocycles with respect to the other ligands and metal complexes tested as this complex did not form gels.⁶³ It was later discovered, however, that by changing the sample preparation (solvent, temperature, concentration) of this complex the formation of gels with various morphologies could be achieved.^{64, 66}



Scheme 1.7 Ditopic ligands used for the formation of metallosupramolecular gels.⁶⁰⁻⁶⁶

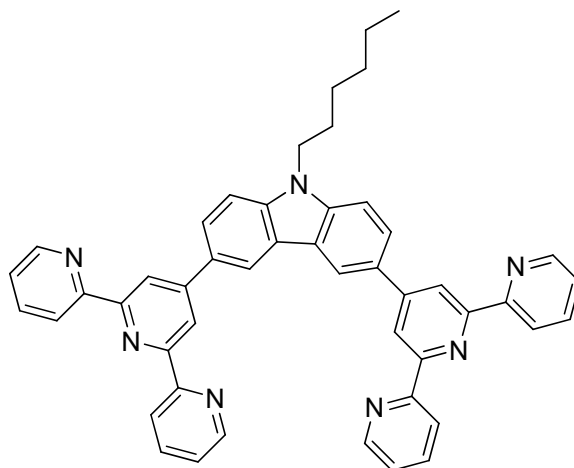
As well as binding transition metal ions in a 2L:1M ratio, these ligands are capable of binding lanthanide ions in a 3L:1M ratio. Mixtures of the penta(ethylene glycol)-based ligand (Scheme 1.7(a)) with transition metal ions (for the linear components) and a small percentage of lanthanide ions to act as cross-linking components were used to synthesise gel-like materials (Scheme 1.8).^{60-62, 65} The order of metal salt addition to the ligand was found to be important, with gel-like materials only formed when the lanthanide salt was introduced before the transition metal salt.⁶² Addition of the lanthanide(III) ions to a large excess of the ditopic ligand is expected to give a trifunctional unit which can act as a cross-linker. If transition metal ions (Zn(II)) are then added, a cross-linked polymer should form. On the other hand, addition of the transition metal ions (97%) before the small amount of lanthanide ions (3%) is

metallomacrocyclic could be synthesised via a stepwise approach, allowing the incorporation of a different metal centre (demonstrated using iron(II)) into the triangular framework.⁶⁸ The complexation of the heterotripic phenanthroline-based ligand with iron(II) salts was studied by electrospray mass spectrometry. Although the angle between the 2,2':6',2''-terpyridine units in the ligand is 60°, significant amounts (26%) of a tetrameric species are also present at equilibrium in acetonitrile solution.⁶⁷



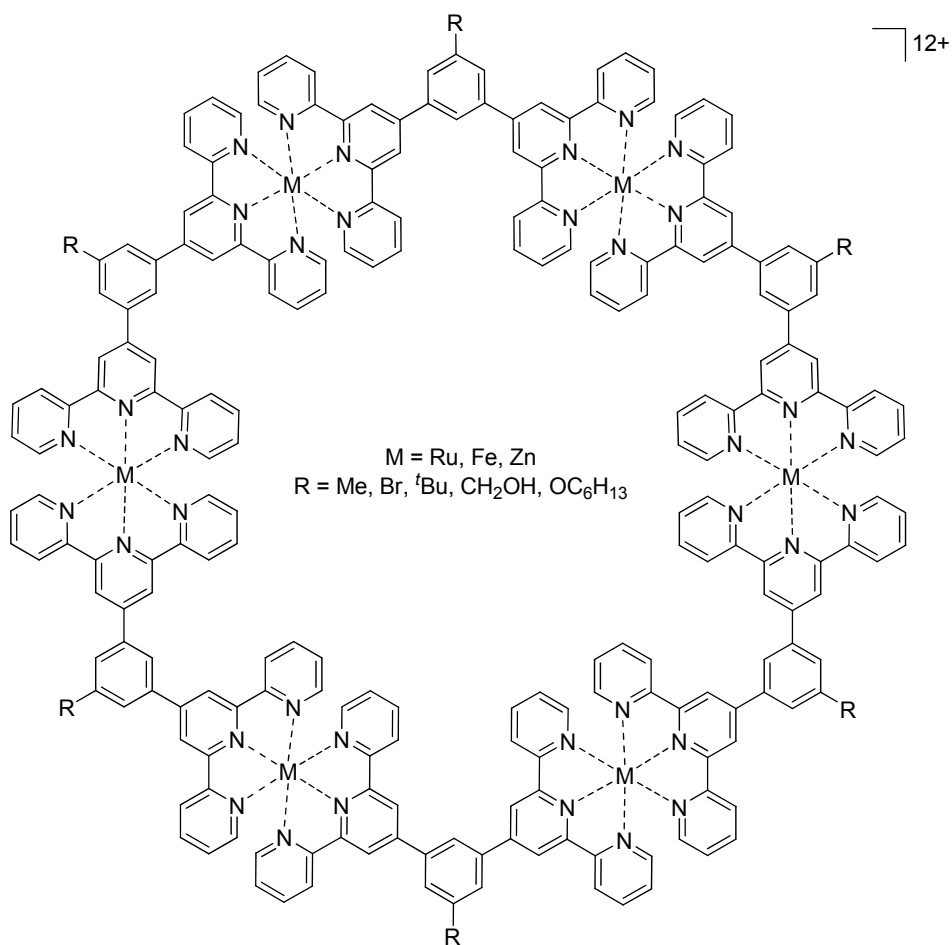
Scheme 1.9 Triangular metallomacrocycles formed from ditopic bis(2,2':6',2''-terpyridine) ligands with rigid spacers.^{67, 68}

The reaction of the ligand shown in Scheme 1.10 with an angle of approximately 105° between the 2,2':6',2''-terpyridine units with iron(II), ruthenium(II) or zinc(II) salts gave pentameric metallomacrocycles.⁶⁹ The study of the photophysical properties of these complexes revealed their potential for use in solar cell devices.



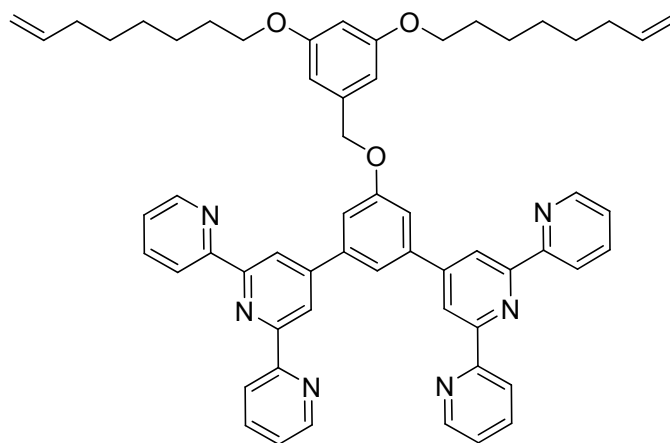
Scheme 1.10 Ditopic bis(2,2':6',2'')-terpyridine) ligand used for the formation of pentameric metallomacrocycles.⁶⁹

Hexagonal metallomacrocycles were synthesised in high yield from rigid ditopic bis(2,2':6',2'')-terpyridine ligands with a 120° angle between the two 2,2':6',2'')-terpyridine units as shown in Scheme 1.11.⁷⁰⁻⁷⁷ The substituent on the phenyl spacer can easily be varied by simple modifications of the ligand synthesis.⁷³ Ruthenium(II) hexagonal metallomacrocycles can be synthesised in either one step from a 1:1 mixture of the ligand (L) and Cl₃RuLRuCl₃ under reducing conditions,^{70, 71} or built up in a stepwise approach⁷⁰⁻⁷² taking advantage of the ease of formation of heteroleptic bis(2,2':6',2'')-terpyridine)ruthenium(II) complexes.⁵⁹ This stepwise approach also opened up the possibility for the formation of heteroleptic macrocycles (with different ligands)^{70, 71} and heterometallic macrocycles, with one, two or three labile iron(II) ions in specific positions in the molecule.⁷² Potential uses for these hexametallomacrocycles are in organic light-emitting diodes⁷⁴ or solar cells.⁷⁸



Scheme 1.11 Hexagonal metallomacrocycles formed from ditopic bis(2,2':6',2''-terpyridine) ligands with rigid spacers.⁷⁰⁻⁷⁷

Similar ligands based on triphenylamine⁷⁸ and an alkyne-bridged structure^{76, 79, 80} were also used to form hexameric metallomacrocycles, demonstrating the potential to modify the size and chemical properties of the resulting structures. Using this hexagonal motif and the ligand shown in Scheme 1.12, it was also possible to form a six-membered metallomacrocycle enclosed within a 114-membered macrocyclic structure.⁸¹ The hexagonal metallomacrocycle was formed by reaction of the ligand with iron(II) salts, then cross-linking of the alkyl chains was performed using ring-closing metathesis with Grubbs' catalyst to give the metallomacrocycle within an organic macrocycle. Demetallation of the complex led to an organic macrocycle which could be purified by chromatography. Treatment of this macrocycle with iron(II) salts led to the reformation of the hexagonal metallomacrocyclic species.



Scheme 1.12 Ditopic bis(2,2':6',2'')-terpyridine) ligand used for the formation of a hexameric metallomacrocyclic within a macrocyclic superstructure.⁸¹

1.4.4 Formation of metallomacrocycles from flexible ditopic bis(2,2':6',2'')-terpyridine) ligands

As mentioned above, the outcome of the coordination of ditopic bis(2,2':6',2'')-terpyridine) ligands with flexible spacers is much less predictable, with the potential formation of polymers or metallomacrocycles of various nuclearities. Some examples of the formation of discrete metallomacrocycles with these ligands are discussed below.

The reaction of ditopic bis(2,2':6',2'')-terpyridine) ligands with oligo(ethylene glycol) spacers with iron(II) or ruthenium(II) salts gave metallomacrocycles (Figure 1.1) in reasonable yields, although all reactions also resulted in variable amounts of an intractable material (immobile on silica) which was assumed to be polymeric.^{82, 83} The nuclearity of the metallomacrocyclic was found to depend on the length of the spacer. The major products from the reaction of longer tetra(ethylene glycol) and hexa(ethylene glycol)-based ligands with ruthenium(II) salts were the [2+2] cyclic species,⁸³ while the reaction of the ligand with the shorter tri(ethylene glycol) spacer with iron(II) salts gave a separable mixture of [3+3] and [4+4] metallomacrocycles.⁸² The labile iron(II) metallomacrocycles were stable in CD₃CN solution for many days and no re-equilibration of products was observed. The reaction of iron(II) salts with the shortest chain ligand gave only polymeric material.⁸³ However, this ligand was used in the formation of heteroleptic ruthenium(II) dimetallomacrocycles using mixtures of the ligands shown in Figure 1.1.⁸³

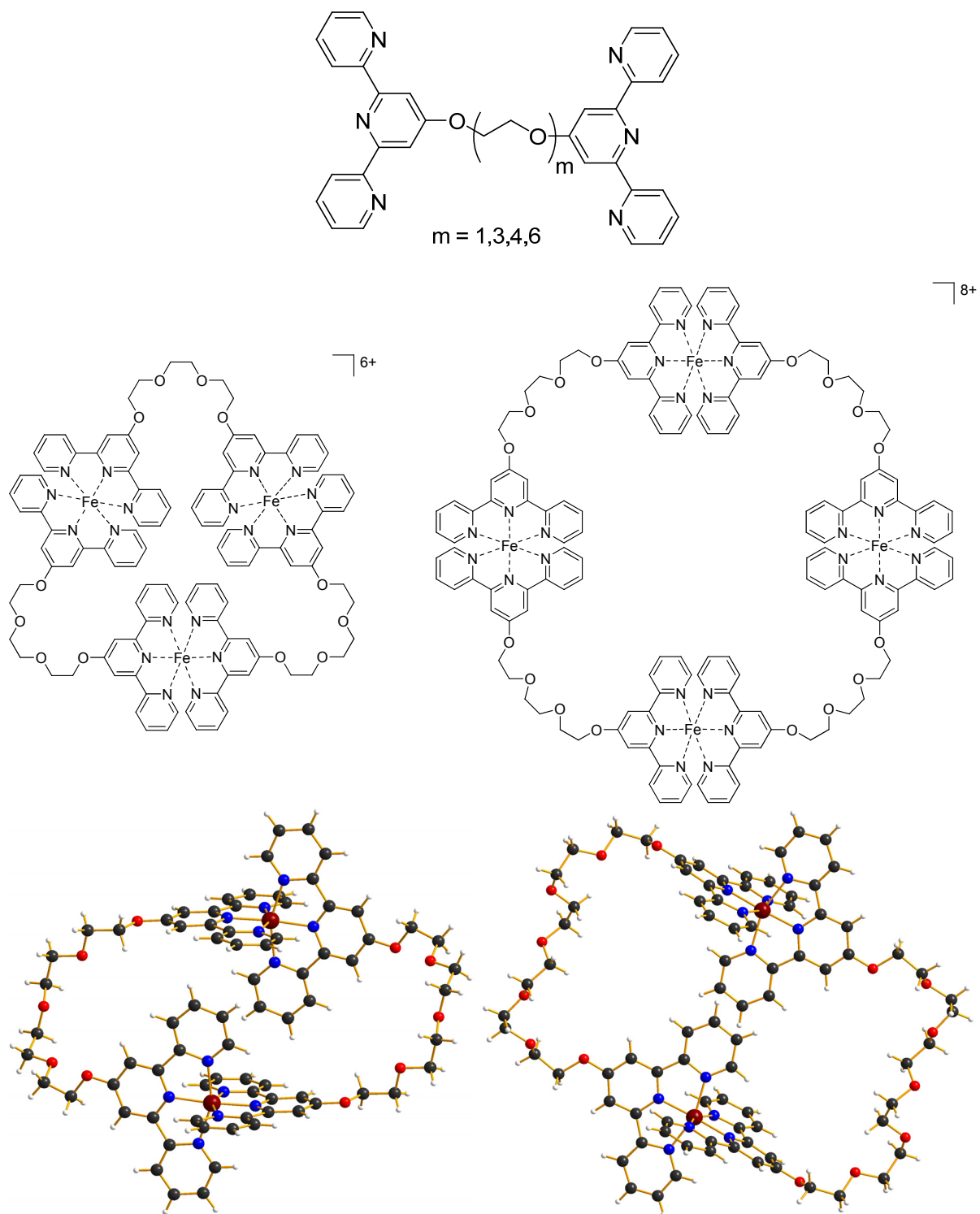
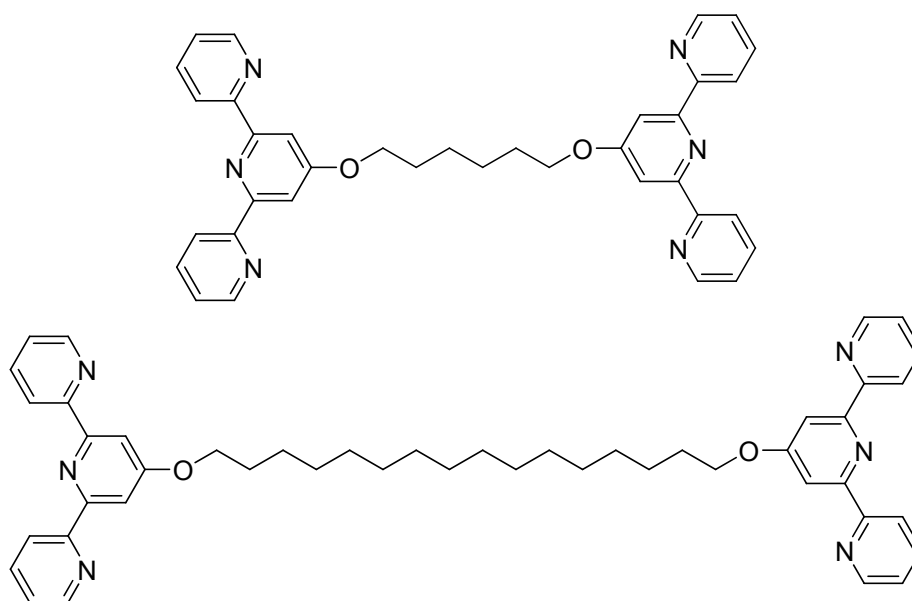


Figure 1.1 Ditopic bis(2,2':6,2''-terpyridine) ligands with oligo(ethylene glycol) spacers and iron(II) and ruthenium(II) metallomacrocyclic cations.^{82, 83}

Iron(II) complexes of the bis(2,2':6',2''-terpyridine) ligands with flexible alkyl spacers shown in Scheme 1.13 were likewise found to be predominantly metallomacrocyclic species.^{84, 85} The reaction of the shorter chain ligand with anhydrous iron(II) chloride at room temperature gave a mixture of species, the speciation of which changed on refluxing the sample, giving signals with more significant upfield shifts in the ¹H NMR spectrum. Two of the six species present in the mixture could be isolated in 46 and 25% yield, and were identified as [3+3] and [4+4] metallomacrocyclic species by MALDI-TOF mass spectrometry.⁸⁴ Refluxing the clean [3+3] macrocycle in acetonitrile solution led to rearrangement of the ligands and formation of the [4+4] species as shown by MALDI-TOF mass spectrometry. MALDI-TOF investigations of the iron(II) complexes of the ligand with the longer spacer formed after reaction at room temperature for one hour suggested the presence of metallomacrocycles with nuclearities of up to [10+10], although the most dominant peak was assigned to a [2+2] species.⁸⁵ These were assumed to be macrocyclic species due to the absence of uncomplexed 2,2':6',2''-terpyridine units in the ¹H NMR spectrum of the product.



Scheme 1.13 Ditopic bis(2,2':6',2''-terpyridine) ligands with alkyl spacers used in the formation of metallomacrocycles.^{84, 85}

A heterotritopic ligand with two terminal 2,2':6',2''-terpyridine binding domains linked to a 2,2'-bipyridine unit through tri(ethylene glycol) spacers formed a single thermodynamic

product after reaction with iron(II) salts at room temperature for 24 hours. This was identified by X-ray structure determination as a [1+1] metallomacrocyclic species, in which the 2,2'-bipyridine unit is uncoordinated (Figure 1.2).⁸⁶

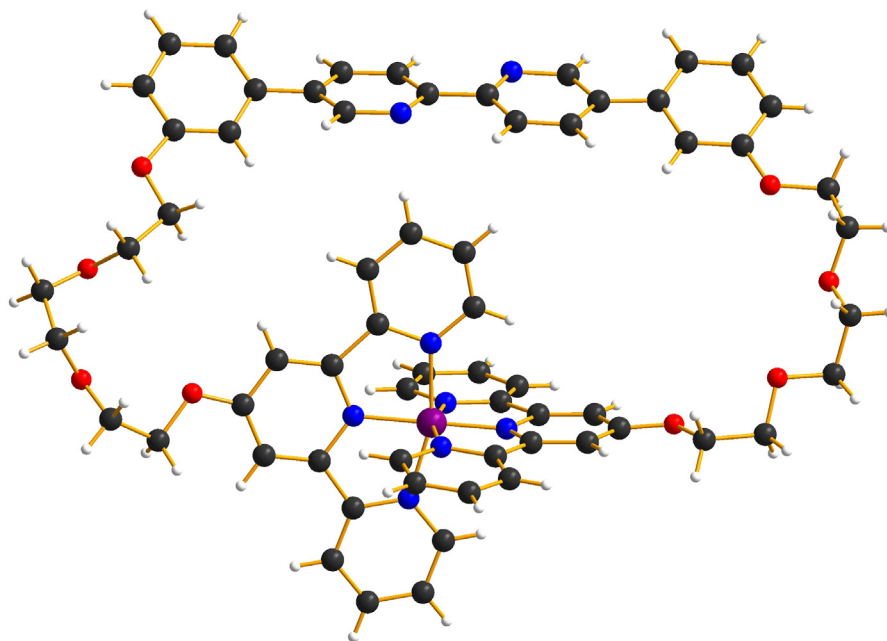


Figure 1.2 X-ray structure of a [1+1] iron(II) metallomacrocyclic species of a heterotripotopic ligand containing two 2,2':6',2''-terpyridine binding domains.⁸⁶

A series of ditopic bis(2,2':6',2''-terpyridine) ligands with flexible naphthalene-centred spacers (Figure 1.3) was used to form metallomacrocyclic species with iron(II) and ruthenium(II) salts.⁸⁷⁻⁹⁰ Complexation of the ligands with the 2,7-disubstituted naphthalene-centred spacer (Figure 1.4(b), $n = 2$ or 3) with iron(II) gave [1+1] metallomacrocyclic species.^{87, 88, 90} The ligand with the shorter spacer ($n = 2$) formed a chiral species in which the naphthalene unit was locked into the cleft between the two 2,2':6',2''-terpyridine units in the iron(II) complex (shown at the bottom left of Figure 1.3).^{87, 88, 90} The ligand with the longer spacer ($n = 3$) also forms a [1+1] metallomacrocyclic species on complexation to iron(II), but the longer length of the spacer allows the rotation of the chain around the bis(2,2':6',2''-terpyridine)iron(II) unit.^{88, 90} Ruthenium(II) complexes of these ligands could also be isolated and were found to be [2+2] and [3+3] ($n = 1$) or [2+2] ($n = 2$ or 3) metallomacrocyclic species. However, the majority of the product mixture was immobile on silica and assumed to be polymeric.^{89, 90}

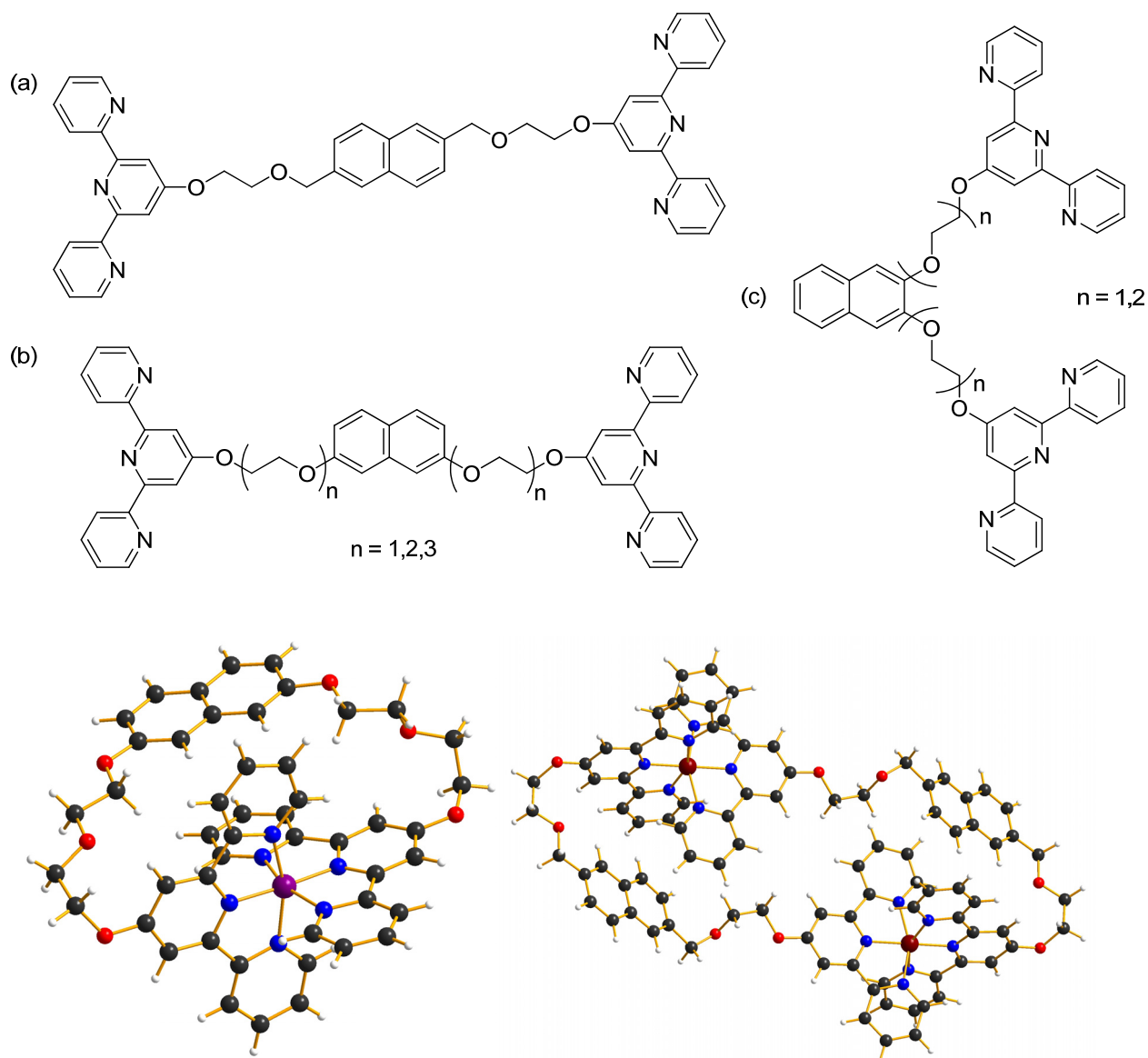


Figure 1.3 Ditopic bis(2,2':6',2''-terpyridine) ligands with naphthalene-centred spacers and examples of [1+1] iron(II) and [2+2] ruthenium(II) metallomacrocycles.⁸⁷⁻⁹⁰

Metallomacrocyclic complexes of iron(II) and ruthenium(II) with the ligand with the 2,6-disubstituted naphthalene-centred spacer (Figure 1.3(a)) were also isolated and found to be [2+2] cyclic species by electrospray mass spectrometry.^{88, 89} In addition, the X-ray crystal structure of the ruthenium(II) complex confirmed this identification (shown at the bottom right of Figure 1.3). Finally, [2+2] metallomacrocyclic species were also formed by the reaction of ruthenium(II) with the ligands with the 2,3-disubstituted naphthalene-centred spacer (Figure 1.3(c)), although again most of the product was an intractable material.⁸⁹ With

iron(II), the nuclearity of the macrocycle was found to depend on the length of the spacer, with the shorter spacer leading to a [3+3] species and the longer spacer forming [2+2] cycles. In each case, the major component of the product mixture could be chromatographically separated and all other products remained on the baseline and were assumed to be polymeric.⁸⁸

Two 5-substituted ditopic bis(2,2':6',2''-terpyridine) ligands linked with flexible alkyl spacers (Figure 1.4) were used to form [1+1] metallomacrocycles with iron(II) and nickel(II) salts.⁹¹ While the ¹H NMR spectrum of the iron(II) complex containing the ligand with the shorter spacer showed a single symmetric species was formed, increasing the length of the spacer led to the additional formation of an unidentified oligomeric species (5 – 10%). The formation of [1+1] metallomacrocycles was confirmed by FAB mass spectrometry of the iron(II) species and X-ray structure determination of the nickel(II) species, shown in Figure 1.4.

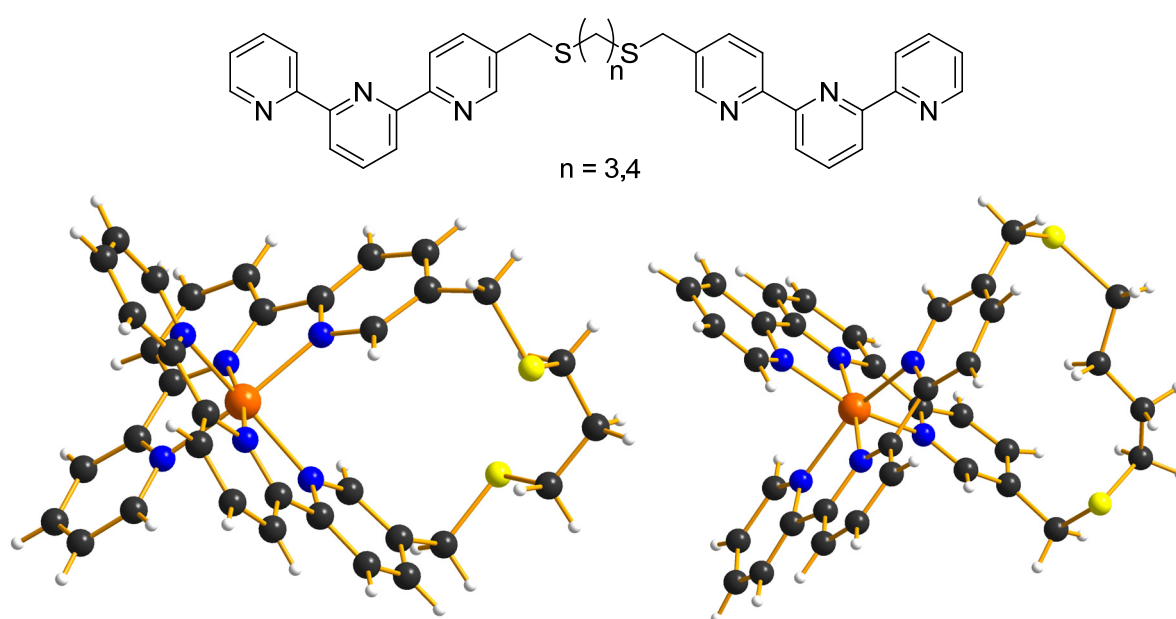


Figure 1.4 Ditopic 5,5''-substituted bis(2,2':6',2''-terpyridine) ligands with alkyl spacers and X-ray structure determinations of [1+1] nickel(II) metallomacrocycles.⁹¹

1.5 Aims of this thesis

The overall aim of this thesis is to assess the extent of polymer or macrocycle formation from the reaction of cobalt(II) salts with ditopic 2,2':6',2''-terpyridine ligands linked by flexible oligo(ethylene glycol) spacers. These ligands have been shown to give both metallosupramolecular polymers and metallomacrocycles on reaction with transition metal salts and many applications have been proposed for the metallosupramolecular polymers based on these ligands. Extensive metallomacrocycle formation in these systems may place significant limitations on the applications of these polymers. Cobalt(II) was chosen as the transition metal ion as it forms labile complexes with 2,2':6',2''-terpyridine, allowing the investigation of dynamic processes. It also offers the advantage of a paramagnetically shifted ^1H NMR spectrum, facilitating the detection and identification of several similar components of a complex mixture.

2 Methods

2.1 ^1H NMR spectroscopy of cobalt(II) complexes

2.1.1 General considerations^{92, 93}

The cobalt(II) ion has a $3d^7$ electronic configuration and in an approximately octahedral environment can adopt either a low-spin ($t_{2g}^6 e_g^1$) or a high-spin ($t_{2g}^5 e_g^2$) ground state. In both cases the complex contains at least one unpaired electron, and is therefore paramagnetic. This does not, however, preclude the use of ^1H NMR spectroscopy as a method for characterisation of cobalt(II)-containing complexes.

The presence of the paramagnetic metal ion in the complex has two important effects on the appearance of the resulting NMR spectrum. Firstly, the spectrum is paramagnetically shifted, with signals observed over a chemical shift range of several hundred ppm. Due to the presence of the unpaired electron, the local magnetic field at the proton is significantly different from the applied magnetic field. In diamagnetic samples, the very small variations in the local magnetic field due to the electron distribution around the observed nucleus (paired electrons in filled orbitals) result in the characteristic chemical shifts of protons in distinct chemical environments. The unpaired electron in a paramagnetic complex has a very large magnetic moment compared with that of a proton. Therefore, the variations in the local magnetic field are much larger than in diamagnetic compounds, and consequently the variation in chemical shift is also much larger, giving rise to a paramagnetically shifted spectrum. Secondly, the signals are significantly broadened in comparison with ^1H NMR spectra of diamagnetic compounds. The coupling of the nuclear spin of the proton and the electronic spin of the unpaired electron results in a very efficient enhancement of the longitudinal (T_1) relaxation mechanism, which dramatically shortens the lifetime of the excited state. According to the Heisenberg uncertainty principle, the shorter (more precisely defined) lifetime of the excited state leads to a poorly defined energy and hence broadened signals in the NMR spectrum. In contrast, the slower relaxation mechanism in diamagnetic samples leads to a more precisely defined energy and sharp NMR signals are observed. With many paramagnetic metal ions, the extent of the broadening of the signals is such that no useful information can be obtained from the NMR spectrum. However, in the case of

bis(2,2':6',2''-terpyridine)cobalt(II) complexes, the broadening is limited such that no ^1H - ^1H coupling is observed, but the signals remain reasonably sharp.

2.1.2 ^1H NMR spectroscopy of bis(2,2':6',2''-terpyridine)cobalt(II) complexes

The unsubstituted bis(2,2':6',2''-terpyridine)cobalt(II) hexafluorophosphate complex has been well investigated by ^1H NMR spectroscopy and the full ^1H NMR spectrum is shown in Figure 2.1. All signals are broad singlets and no ^1H - ^1H coupling can be observed directly. Assignment of the signals is not trivial and is discussed below.

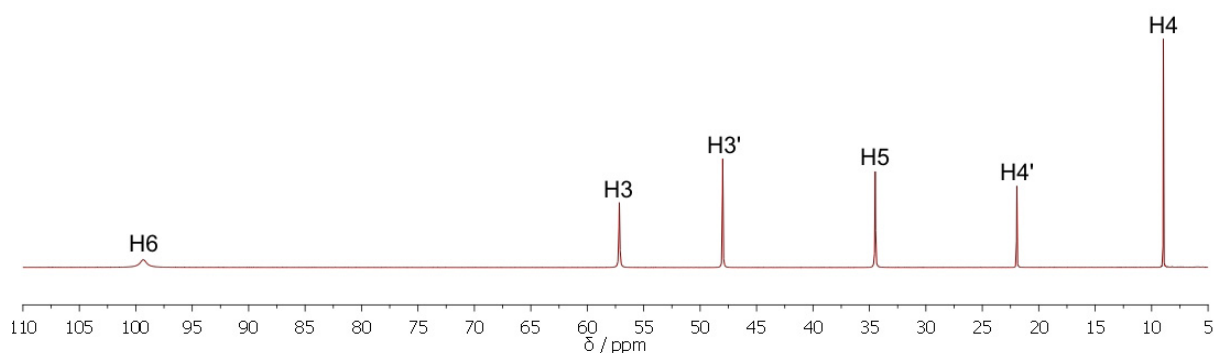


Figure 2.1 Full ^1H NMR spectrum of $[\text{Co}(\text{tpy})_2][\text{PF}_6]_2$ (CD_3CN , 500 MHz, 298 K).

Although the ^1H NMR spectrum of $[\text{Co}(\text{tpy})_2][\text{PF}_6]_2$ was first reported in 1997,⁹⁴ it was initially not possible to assign the spectrum. Using the inversion recovery technique, the longitudinal relaxation times (T_1) of a CD_3CN solution of this complex were determined (see Table 2.1). The efficiency of the relaxation mechanism described above was confirmed by the very short T_1 values as compared to those for the analogous ruthenium(II) complex (1-2 s).⁹⁴ The degree of paramagnetic shifting correlates very well with the value of T_1 with the more shifted signals having a shorter relaxation time.

δ / ppm	assignment	line width at half height / Hz	T_1 / ms
99.8	H ⁶	> 50	1.54
57.2	H ³	46	21.9
48.2	H ^{3'}	30.5	20.9
34.5	H ⁵	34	30.7
21.8	H ^{4'}	25	61.8
8.9	H ⁴	20	78.0

Table 2.1 Chemical shifts⁹⁵ (500 MHz, 298 K), assignments,⁹⁵ line widths at half height⁹⁵ (500 MHz, 298 K) and longitudinal relaxation times⁹⁴ (T_1) (250 MHz) for CD₃CN solutions of [Co(tpy)₂][PF₆]₂.

It was originally thought that it would be impossible to carry out 2D NMR techniques on these cobalt(II) complexes due to the short relaxation times.⁹⁴ However, it was found that the use of a gradient probe allows the observation of weak cross peaks in the ¹H–¹H COSY spectrum of bis(2,2':6',2''-terpyridine)cobalt(II) complexes.^{95, 96} Some preliminary assignments of the signals can be made from the ¹H NMR spectrum and the ¹H–¹H COSY spectrum (shown in Figure 2.2). Based on the integral (2 H), the peak at δ 21.8 ppm can be unambiguously assigned to H^{4'}. This proton couples to H^{3'}, so the signal at δ 48.2 ppm can be assigned based on the cross peak observed in the ¹H–¹H COSY spectrum. The broad highest frequency signal (δ 99.8 ppm) shows no cross peaks in the ¹H–¹H COSY spectrum, but could be subjectively assigned to H⁶, the proton closest to the paramagnetic metal ion, as this proton will be most affected by the paramagnetic relaxation enhancement of the unpaired electron.⁹⁵ The signal at δ 8.9 ppm shows cross peaks to two other signals, so can be assigned to H⁴, as this proton couples to H³ and H⁵. Differentiation between these two protons, however, is not possible using the ¹H–¹H COSY technique, as both only show cross peaks to the signal at δ 8.9 ppm.

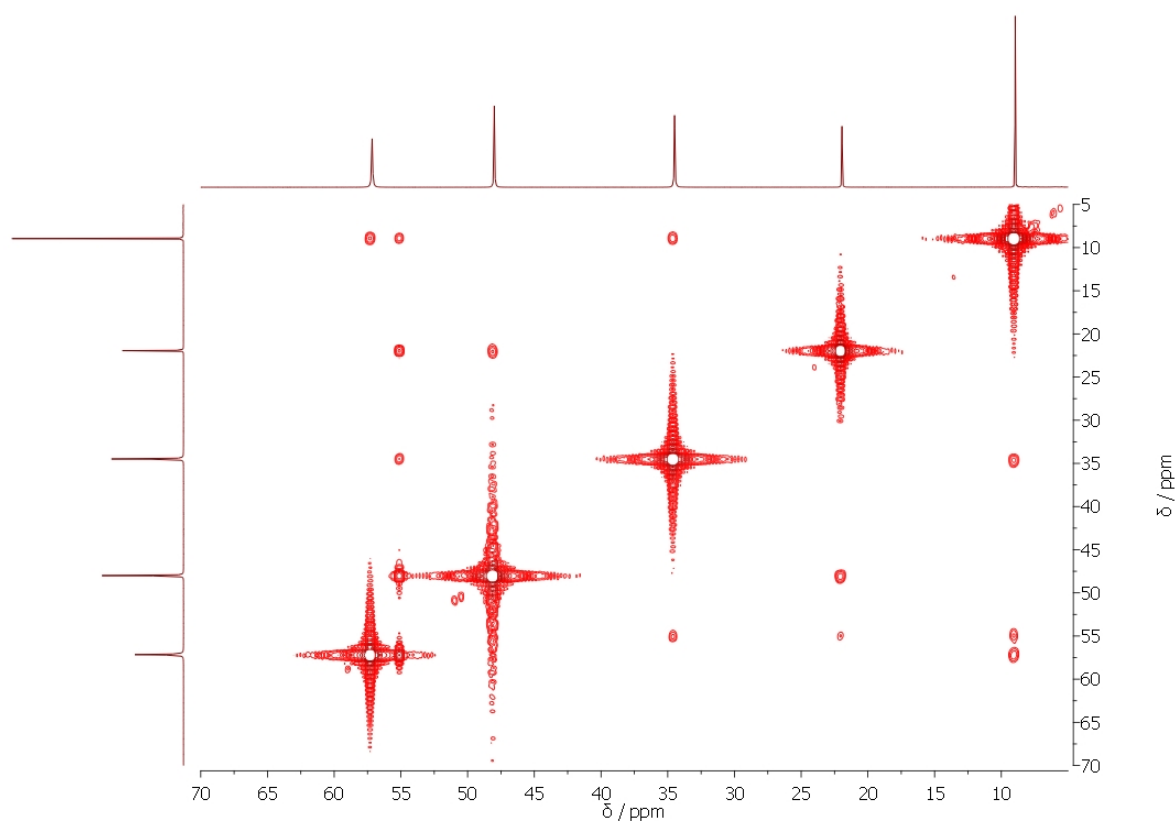
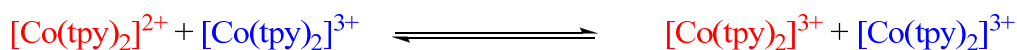


Figure 2.2 A portion of the ^1H - ^1H COSY spectrum of $[\text{Co}(\text{tpy})_2][\text{PF}_6]_2$ (CD_3CN , 500 MHz, 295 K).

The cobalt(III) ion has a d^6 electronic configuration and bis(2,2':6',2''-terpyridine)cobalt(III) complexes are low-spin and diamagnetic, so the ^1H NMR spectrum of $[\text{Co}(\text{tpy})_2][\text{PF}_6]_3$ shows sharp, well-resolved signals in the "normal" range, which can be assigned by standard techniques. A mixture of $[\text{Co}(\text{tpy})_2]^{2+}$ and $[\text{Co}(\text{tpy})_2]^{3+}$ is a classical self-exchange system in which an electron is transferred from the cobalt(II) species to the cobalt(III) species:



The rate constant for the electron transfer reaction is dependent on the anion and the concentration of the cobalt(II) species. At 0 °C with a chloride anion, the rate constant is approximately $40 \text{ M}^{-1}\text{s}^{-1}$. Replacement of the chloride for a nitrate anion results in an increase in the rate of electron transfer.⁹⁷

In the case of fast electron transfer, the interconversion of cobalt(II) and cobalt(III) complexes is identical to a chemical exchange of the cobalt(II) and cobalt(III) centres. Assuming that electron transfer is still fast on the NMR timescale with a hexafluorophosphate anion, this

process can be investigated using chemical exchange spectroscopy (EXSY), which uses the same pulse sequence as nuclear Overhauser effect spectroscopy (NOESY). Using 1D NOE difference spectroscopy, the ^1H NMR spectrum of $[\text{Co}(\text{tpy})_2][\text{PF}_6]_2$ could be unambiguously assigned (see Table 2.1) by correlation of the cobalt(II) signals with the known cobalt(III) signals.^{95,96}

Substituted bis(2,2':6',2''-terpyridine)cobalt(II) complexes have also been studied by ^1H NMR spectroscopy.^{90,94,96,98-100} In most cases, the substituent is in the 4'-position of the terpyridine ligand, and the ^1H NMR spectra of these complexes are very similar. The $\text{H}^{3'}$ proton is most affected by the substitution at the 4'-position and the position of this signal is highly dependent on the nature of the substituent as shown in Table 2.2.

Substituent	H^{95}	S^{90}	Cl^{96}	$\text{O}^{90,96}$	N^{96}
$\delta \text{H}^{3'} / \text{ppm}$	48.2	55.9	59.1	73.8-78.7	82.1-82.3

Table 2.2 Effect of the nature of the substituent on the chemical shift of the peak corresponding to the $\text{H}^{3'}$ proton in ^1H NMR spectra of CD_3CN solutions of cobalt(II) complexes of 4'-substituted-2,2':6',2''-terpyridine ligands.

The cobalt(II) complexes with 4'-substituted ligands are low-spin in solution¹⁰⁰ and the highest frequency resonance (corresponding to H^6) is observed at approximately δ 100 ppm. The cobalt(II) complex of the asymmetric 6-bromo-2,2':6',2''-terpyridine ligand has also been synthesised. This complex is high spin in solution as a result of steric interactions between the ligands which weaken the ligand field and in this case the ^1H NMR spectrum shows resonances at frequencies up to around δ 260 ppm.¹⁰⁰

2.2 Diffusion and PGSE NMR spectroscopy

2.2.1 What is diffusion?

Diffusion is defined as the "migration of matter down a concentration gradient."¹⁰¹ Thus, matter will move via the random Brownian motion of the particles from an area of high concentration to an area of lower concentration, increasing the entropy of the system and resulting eventually in a uniform concentration throughout the entire sample. This process is described by Fick's first law of diffusion (equation 2.1):

$$J = -D \frac{dc}{dx}$$

2.1

where J is the flux (or amount passing through a unit area per unit time) of the particles down the concentration gradient (dc/dx), and the proportionality constant, D , is known as the diffusion coefficient and has units $m^2 s^{-1}$. It follows that the rate of diffusion will be fast when the concentration gradient is steep, and once a uniform concentration of the sample has been reached, no further net flow of matter can occur. However, the particles are still randomly moving in the sample as a result of their thermal energy (self-diffusion). The root-mean-square displacement, $(\langle x^2 \rangle)^{1/2}$, of any particle in the sample at uniform concentration is given by equation 2.2:¹⁰²

$$\sqrt{\langle x^2 \rangle} = \sqrt{nDt}$$

2.2

where n is 2, 4 or 6 for one-, two- or three-dimensional diffusion, respectively, and t is the diffusion time.

Einstein¹⁰³ and von Smoluchowski¹⁰⁴ showed that the diffusion coefficient, D , is related to the nature of the diffusing particle and the medium in which it is diffusing (equation 2.3).

$$D = \frac{kT}{f}$$

2.3

where k is the Boltzmann constant and T is the absolute temperature. The frictional coefficient, f , is related to the size and shape of the diffusing particle and to the viscosity of the solvent. For a spherical particle with radius r diffusing in a continuous medium (i.e. the solvent molecules are small in comparison with the size of the solute molecules) with viscosity η , the frictional coefficient is given by Stokes' relation (equation 2.4):¹⁰¹

$$f_0 = 6\pi\eta r$$

2.4

Combining equations 2.3 and 2.4 gives equation 2.5, the Stokes-Einstein equation, which allows us to obtain information about the size of the diffusing particle through experimental determination of the diffusion coefficient.

$$D = \frac{kT}{6\pi\eta r}$$

2.5

2.2.2 Limitations of and corrections to the Stokes-Einstein equation

As mentioned in section 2.2.1, the Stokes-Einstein equation was derived by assuming that the diffusing particle is (a) spherical and (b) very large in comparison to the solvent molecules. On a molecular scale, these assumptions are often not the case. As a result, several improvements to the Stokes-Einstein equation have been proposed for dealing with non-spherical particles on the molecular scale.^{105, 106}

Considering first the shape of the particle, equations have been derived to determine exact frictional coefficients, f , for prolate (rugby ball) and oblate (disc-shaped) ellipsoid particles (see Figure 2.3) as well as approximate values for other non-spherical shapes, and these equations are given in Table 2.3.¹⁰⁷ The equations are given as ratios of f/f_0 where f_0 is the frictional coefficient for a sphere of the same volume as the ellipsoid or rod (described by equation 2.4) and r_e is the radius of this sphere. Figure 2.4 and Figure 2.5 show graphically how the frictional coefficients depend on the axial ratio (α/β) of an ellipsoid or rod. The frictional coefficient of a non-spherical particle is always greater than that of a sphere of equal volume so the ratio f/f_0 is greater than one.¹⁰⁷

shape	ff_0	r_e
prolate ellipsoid	$\frac{P^{-1/3}(P^2 - 1)^{1/2}}{\ln\left[P + (P^2 - 1)^{1/2}\right]}$	$(\alpha\beta^2)^{1/3}$
oblate ellipsoid	$\frac{(P^2 - 1)^{1/2}}{P^{2/3} \tan^{-1}\left[(P^2 - 1)^{1/2}\right]}$	$(\alpha^2\beta)^{1/3}$
long rod	$\frac{(2/3)^{1/3} P^{2/3}}{\ln 2P - 0.30}$	$\left(\frac{3\alpha\beta^2}{2}\right)^{1/3}$

Table 2.3¹⁰⁷ Equations for the ratios ff_0 , where f is the frictional coefficient of the non-spherical object, f_0 is the frictional coefficient for a sphere of the same volume as the ellipsoid or rod and r_e is the radius of the sphere such that $f_0 = 6\pi\eta r_e$. $P = \alpha/\beta$, where α is the semi-major axis (half-length of a rod) and β is the semi-minor axis (radius of a rod).

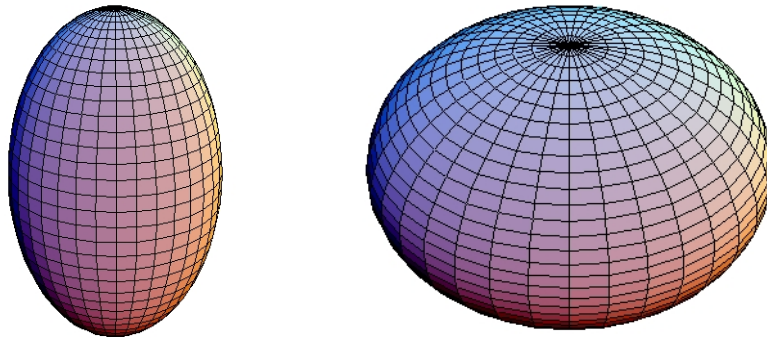


Figure 2.3 Prolate (left) and oblate (right) ellipsoids.

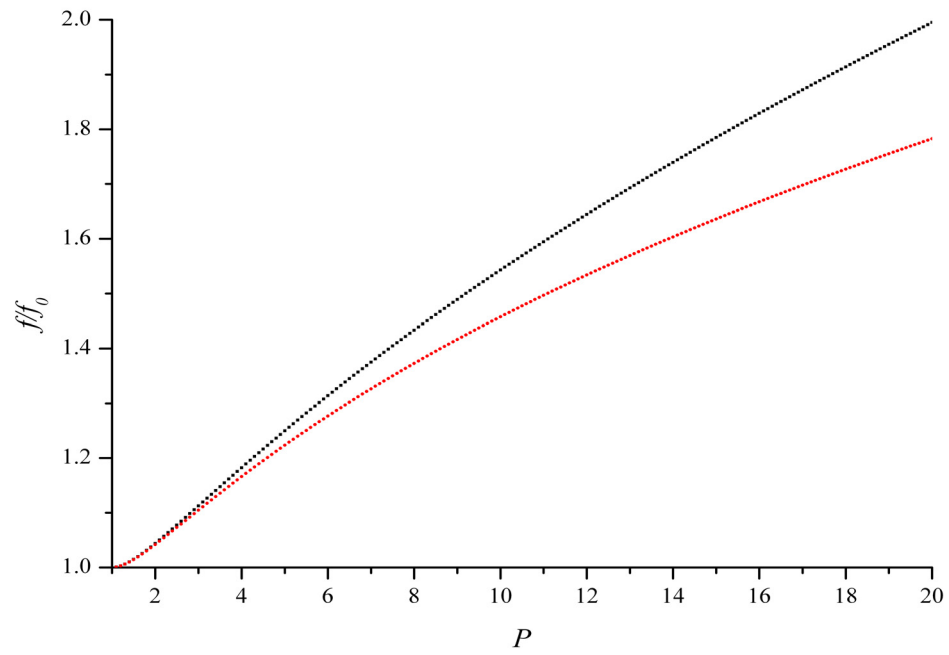


Figure 2.4 Dependence of the frictional coefficient on shape of prolate (black line) and oblate (red line) ellipsoids.

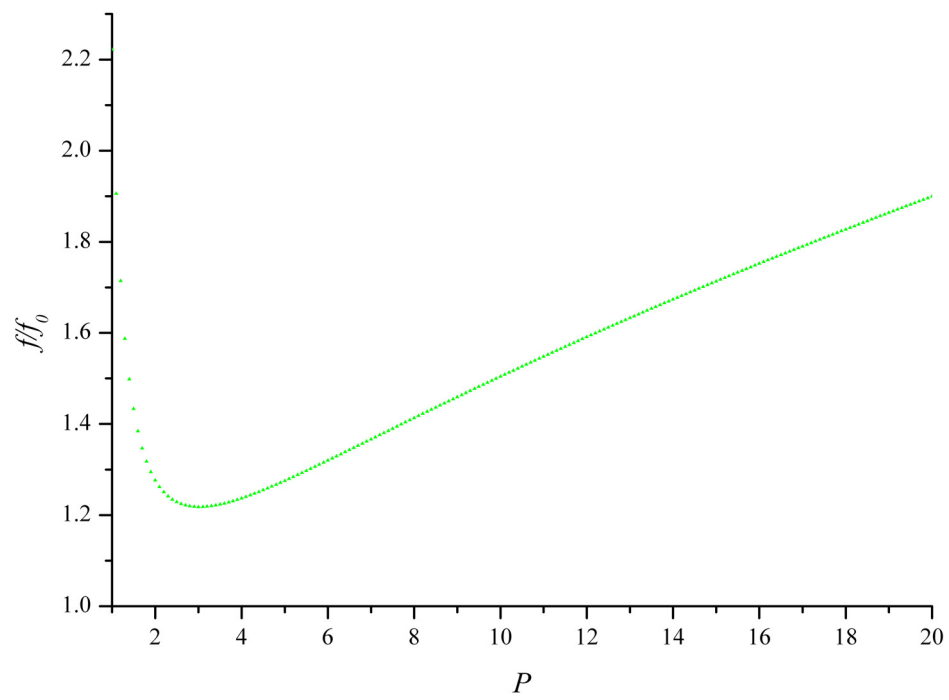


Figure 2.5 Dependence of the frictional coefficient on shape for rod-like shapes.

A modified Stokes-Einstein equation, taking into account the shape of the molecule can therefore be written as:

$$D = \frac{kT}{6\pi\eta r(f/f_0)}$$

2.6

The second assumption of the Stokes-Einstein equation, that the size of the diffusing particle is much larger than that of the solvent molecules and that the solvent therefore behaves as a continuous medium, must also be taken into account when considering the diffusion of particles of molecular size. It has been found that experimentally determined diffusion coefficients for small molecules are consistently higher than predicted by the Stokes-Einstein equation (equation 2.5).^{105, 106}

In the case of a large diffusing particle, it is assumed that a layer of solvent molecules is firmly attached to the exterior surface of the particle. This is known as "stick-boundary" conditions¹⁰⁶ and through the use of classical hydrodynamics results in the factor of 6 in the Stokes' relation.¹⁰⁸ In the other extreme, when the diffusing particle is much smaller than the solvent, it is able to move freely in the void space between the solvent molecules.¹⁰⁹ This situation is known as "slip-boundary" conditions¹⁰⁶ and results in the modification of Stokes' relation to equation 2.7.^{105, 108}

$$f = 4\pi\eta r$$

2.7

There have been many attempts to model the deviations from the Stokes-Einstein equation due to the size of the diffusing particles.^{110, 111} Many of these empirical models are based on very specific series of compounds and are not readily transferable to other systems. For example, models have been based on hydrated¹¹² and non-hydrated¹¹³ ions, as well as approximately spherical neutral molecules¹¹⁴⁻¹¹⁶ and a selection of spherical and ellipsoidal molecules varying from molecular hydrogen to anthracene and *n*-octacosane¹⁰⁵ in a variety of solvents. Through an extensive comparison of empirically or semi-empirically determined diffusion coefficients¹¹¹ it was found that the empirical correction suggested by Spornol and Wirtz¹¹⁴ (equation 2.8) was the most appropriate for non-associating solutes in solutions of low viscosity. This approach takes into account both the radius of the diffusing molecule and

the radius of the solvent, and was based on the study of the diffusion of over one hundred approximately spherical neutral molecules in mostly non-polar solvents.

$$D = \frac{kT}{6\pi\eta r a} \text{ where } a = 0.16 + 0.4 \frac{r}{r_{\text{solvent}}}$$

2.8

where r is the radius of the diffusing molecule and r_{solvent} is the radius of the solvent molecule. Gierer and Wirtz¹¹⁷ developed a theoretical modification (microfrictional theory) to the Stokes-Einstein equation, taking into account the finite thickness of the solvent layers flowing around the diffusing particle (equation 2.9).

$$D = \frac{kT}{6\pi\eta r b} \text{ where } b = \left[1.5 \frac{r_{\text{solvent}}}{r} + \frac{1}{1 + \frac{r_{\text{solvent}}}{r}} \right]^{-1}$$

2.9

Both the empirical¹¹⁴ and the theoretical¹¹⁷ corrections to the Stokes-Einstein equation make the assumption that the interactions between the solute and the solvent are similar to the solvent-solvent interactions. This corresponds to the assumption made by Stokes that the diffusing particle was coated with a layer of solvent molecules, so that only solvent-solvent interactions were present.

Unfortunately, the theoretical model was only able to predict the correct order of magnitude of the diffusion coefficients used by Spagnol and Wirtz¹¹⁴ to develop their empirical modification of the Stokes-Einstein equation. For this reason, the microfrictional theory developed by Wirtz has been improved semi-empirically to give equation 2.10.^{109, 118}

$$D = \frac{kT}{6\pi\eta r c} \text{ where } c = \left[1 + 0.695 \left(\frac{r_{\text{solvent}}}{r} \right)^{2.234} \right]^{-1}$$

2.10

The diffusion coefficients of several small, spherical molecules and a selection of crown ethers in a variety of solvents have been predicted accurately using this modification of the Stokes-Einstein equation. The failure of the Stokes-Einstein equation to accurately predict the diffusion coefficients of non-spherical particles appears to be insignificant in the case of

the crown ethers. This is believed to be due to the rapid molecular rotation of the molecule, which on average gives a spherical shape.¹⁰⁹

So, considering both modifications of the Stokes-Einstein equation in order to take into account the non-spherical nature of the diffusing particle and the non-continuous nature of the solvent, we arrive at the following equation¹⁰⁶ (equation 2.11):

$$D = \frac{kT}{6\pi\eta rc(f/f_0)}$$

2.11

where c is the correction factor for the size (see equation 2.10) and (f/f_0) is the correction factor for the shape (see Table 2.3) of the diffusing particle.

Finally, it must be noted that failing to take into account the increased viscosity of the solution (which increases with concentration of solute) compared to that of the solvent leads to errors in interpreting the diffusion coefficient in terms of the radius of the particle.¹¹⁹

2.2.3 What is PGSE NMR spectroscopy and how does it work?¹²⁰⁻¹²⁴

Pulsed-field gradient spin-echo (PGSE) NMR spectroscopy, first developed in 1965 by Stejskal and Tanner,¹²⁵ is a technique used to measure diffusion coefficients of molecules in solution and, thus, a means of acquiring information on particle size. In recent years, the technique has found widespread application in co-ordination and organometallic chemistry, including supramolecular chemistry (see section 2.2.4).¹²³

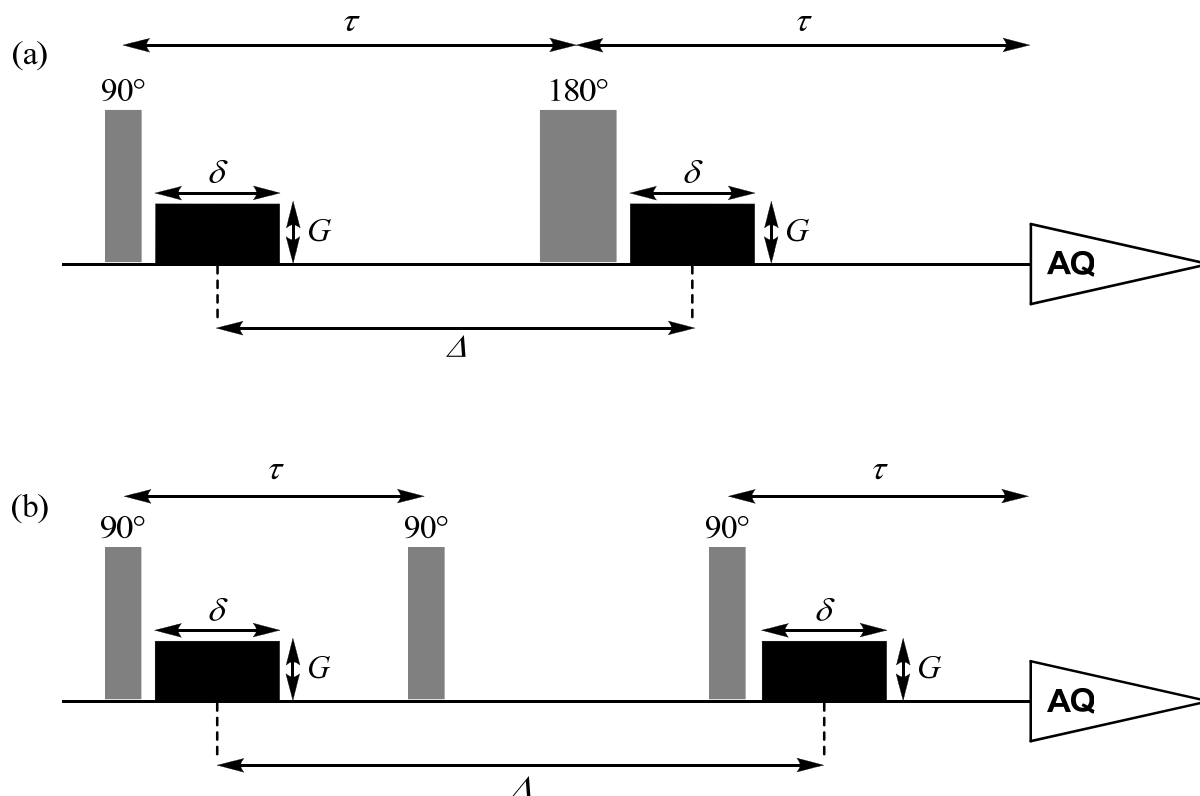


Figure 2.6 Typical pulse sequences for PGSE NMR experiments: (a) the Stejskal-Tanner spin-echo pulse sequence and (b) the stimulated echo pulse sequence.

The basic pulse sequence is based on a spin-echo pulse sequence incorporating two identical gradient pulses and is shown in Figure 2.6(a) with the effect on the magnetisation shown schematically in Figure 2.7. The initial 90° pulse flips the spins from thermal equilibrium along the z -axis into the xy plane. The first gradient pulse of magnitude G and duration δ is then applied, which strongly dephases the magnetisation. The strength of the gradient varies linearly along the z -axis so only spins contained in the same narrow slice of the sample have the same phase angle. Without a gradient field, the magnetisation dephases due to processes such as chemical shift and hetero- and homonuclear coupling evolution and spin-spin (T_2) relaxation. In the PGSE experiment these effects are kept constant by using a fixed value for τ . The application of a 180° pulse reverses the sign of the phase angle. The second gradient pulse, identical (G, δ) to the first and applied after time Δ , refocuses the magnetisation. If no diffusion had occurred during this time, the effects of both gradient pulses would cancel each other out and all spins would be refocused. However, any spins which move out of their narrow slice along the z -axis via Brownian motion experience gradient fields of different

strengths during the two gradient pulses and are therefore not completely refocused. This leads to a decrease in the intensity of the echo signal. The further the spins move along the z -axis from their original positions, the poorer the refocusing and the smaller the echo intensity. Increasing the diffusion time allows the molecules to diffuse further (equation 2.2) and results in a decrease in the intensity of the spin-echo signal. Smaller molecules diffuse faster (equation 2.5), so they move further away from their original slice of the sample in a given diffusion time. As a result, the spins of smaller molecules are more poorly refocused and the intensity of the spin-echo signal is lower for a given gradient pulse length and magnitude.

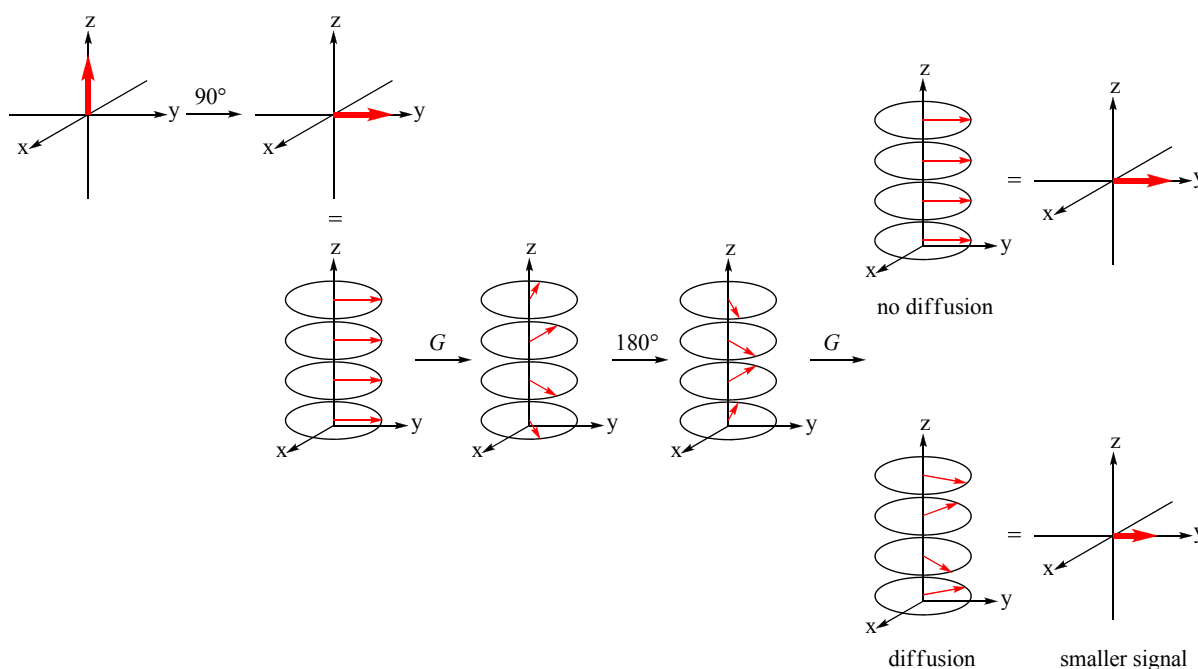


Figure 2.7 Schematic representation of nuclear spins in the Stejskal-Tanner spin-echo pulse sequence.

Several more sophisticated pulse sequences have since superseded the original Stejskal-Tanner spin-echo pulse sequence.¹²⁶⁻¹²⁸ The simplest improvement, the stimulated-echo (STE) method shown in Figure 2.6(b), uses three 90° pulses which allows the phase angles to be stored in the z -direction. This has the advantage that spin-lattice relaxation (T_1), rather than spin-spin relaxation (T_2) is the effective relaxation pathway during the diffusion time. Since T_1 is equal to or longer than T_2 , the signal to noise ratio is improved using the STE pulse sequence.

The intensity of the spin-echo is dependent on the length (δ) and magnitude (G) of the gradient pulse and the diffusion time ($\Delta - \delta/3$) according to Equation 2.12. Thus, a plot of $\ln(I/I_0)$ vs. $\gamma^2 \delta^2 G^2 (\Delta - \delta/3)$ will give a straight line with a slope of $-D$.

$$\ln\left(\frac{I}{I_0}\right) = -\gamma^2 \delta^2 G^2 \left(\Delta - \frac{\delta}{3}\right) D$$

2.12

where I is the observed spin-echo intensity, I_0 is the intensity observed without gradients, γ is the gyromagnetic ratio of the nucleus, δ is the length of the gradient pulse, G is the gradient strength, Δ is the time between the midpoints of the gradients and D is the diffusion coefficient.

2.2.4 Applications of PGSE NMR spectroscopy

Diffusion coefficients have been determined via PGSE NMR techniques for a wide variety of systems. Important applications include the determination of relative or absolute sizes of molecules as well as assessment of the extent of intermolecular interactions.¹²⁹ In the last ten years, the technique has become more commonplace in areas of coordination chemistry, including organometallic^{120-122, 130, 131} and supramolecular^{123, 132} chemistry. The most common application of PGSE NMR spectroscopy is the determination of molecular size through the use of the Stokes-Einstein equation and selected examples of this as applied to metallosupramolecular chemistry are discussed below.

2.2.4.1 Determination of molecular size in metallosupramolecular systems

As described in section 1.5, the aim of this project is to assess the extent of polymer or macrocycle formation from the reaction of flexible ditopic 2,2':6',2''-terpyridine ligands with cobalt(II) salts. PGSE NMR spectroscopy was considered to be a valuable technique for the characterisation of the resulting metallosupramolecular species for several reasons. Firstly, crystallisation of the complexes was expected to be difficult due to their size and the flexibility of the ligands making information on the size and nuclearity of the polymer or macrocycle difficult to obtain. In addition, characterisation by elemental analysis only confirms the ligand:metal ratio, which is the same for [1+1], [2+2] and higher nuclearity species. Finally, the structure, shape and behaviour of these (and other) supramolecular species in solution is an important area of investigation.

There are several examples of the use of PGSE NMR spectroscopy as a technique to determine the relative or absolute sizes of metallomacrocyclic species in solution. Following the structural characterisation of a metallocyclic rectangle, triangle and three-dimensional cage in the solid state by X-ray crystallography, the existence of these supramolecular species in nitromethane solution was confirmed by determination of the molecular radii using PGSE NMR spectroscopy.¹³³ A series of ligands (L), corners ($[\text{Re}(\text{CO})_3\text{Cl}(\text{L})_2]$) and molecular squares of the type $[\text{Re}(\text{CO})_3\text{Cl}(\text{L})_4]$, where L is a rigid ditopic nitrogen donor ligand of varying size, were also investigated by PGSE NMR spectroscopy.¹³⁴ A calibration curve based on the well-characterised members of the series was developed by plotting the measured diffusion coefficients against the inverse of the molecular radii. These were approximated from either crystallographic data or geometry optimisations by treating the molecules as spherical and taking the radius to be half the longest axis of the molecule. The calibration curve was then used to estimate the size of the new molecular square based on the largest ligand and to show that it was neither catenated nor polymeric. Palladium(II) and platinum(II) complexes of a similar, but slightly more flexible, ligand were investigated by ^{31}P PGSE NMR spectroscopy.¹³⁵ Both systems show a concentration and temperature dependent equilibrium between at least two species in dichloromethane or nitrobenzene solution. Mass spectrometric studies confirmed the formation of a dinuclear species but identification of the second species as trinuclear could only be established conclusively from the relative sizes of the species determined from their measured diffusion coefficients. The analysis of mixtures of iron(II) complexes prepared from platinum(II)-centred ditopic 2,2':6',2"-terpyridine ligands by PGSE NMR spectroscopy showed that the reaction of these ligands with iron(II) yields a mixture of di-, tri- and tetranuclear metallomacrocycles as the kinetic products, which over time rearrange to the entropically favoured [2+2] species.¹³⁶ The formation of a double-stranded metallosupramolecular helical polymer which is stable in solution (see Figure 2.8) was also confirmed using PGSE NMR spectroscopy.¹³⁷ The hydrodynamic volumes of the monomer and the polymer were calculated using the Stokes-Einstein equation based on experimentally determined diffusion coefficients and the volume of the polymer found to be 20 times that of the monomer, thus confirming the polymeric structure.

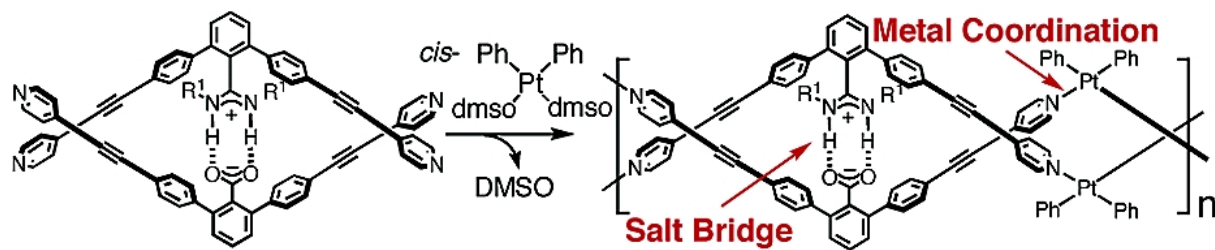


Figure 2.8 Synthesis of double-stranded metallosupramolecular helical polymers. Reproduced from Ref.¹³⁷

3 Simple Models

Ligands and Simple Complexes

3.1 Introduction

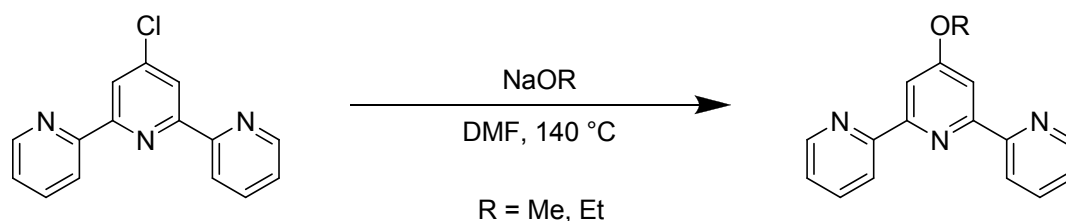
As described in section 1.5, the overall aim of this project is to assess the extent of polymer or macrocycle formation from the reaction of flexible ditopic 2,2':6',2''-terpyridine ligands with cobalt(II) salts. The systems under consideration proved to be extremely complex, so initial investigations into simple model systems were carried out to understand the behaviour of the basic components of the systems. This included the behaviour of the ligands in solution and the solid state, as well as the structural characteristics and dynamic behaviour of some simple mononuclear bis(2,2':6',2''-terpyridine)cobalt complexes, before their incorporation into complex multinuclear assemblies. In addition, these model compounds were studied to establish whether the PGSE NMR spectroscopic technique would be of assistance in the characterisation of these systems and to develop models for the interpretation of the data.

3.2 Synthesis of the ligands and simple complexes

3.2.1 Ligand synthesis

3.2.1.1 Synthesis of 4'-alkoxy-2,2':6',2''-terpyridine ligands

The synthetic route to the monotopic 4'-alkoxy-2,2':6',2''-terpyridine ligands from 4'-chloro-2,2':6',2''-terpyridine and the appropriate sodium alkoxide followed a slightly modified literature procedure^{59, 138} and is shown in Scheme 3.1.



Scheme 3.1 Synthesis of 4'-alkoxy-2,2':6',2''-terpyridine ligands.

The ligands 4'-methoxy-2,2':6',2''-terpyridine and 4'-ethoxy-2,2':6',2''-terpyridine were obtained as white solids in good to excellent yields and characterisation is consistent with literature data,^{59, 138, 139} although previously reported melting points are not consistent with each other or those measured here.

X-ray quality single crystals of 4'-methoxy-2,2':6',2''-terpyridine were obtained by slow evaporation of a chloroform-hexane solution of the ligand. The ligand is essentially planar (angles between the least-squares planes of the pyridine rings containing N1 and N2, and N2 and N3 are 3.33(2)° and 2.07(2)°, respectively) and the terpyridine domain has the expected¹⁴⁰ *trans-trans* conformation which minimises the interactions between the nitrogen lone pairs and between the protons in the 3- and 3'-positions of the terpyridine unit.

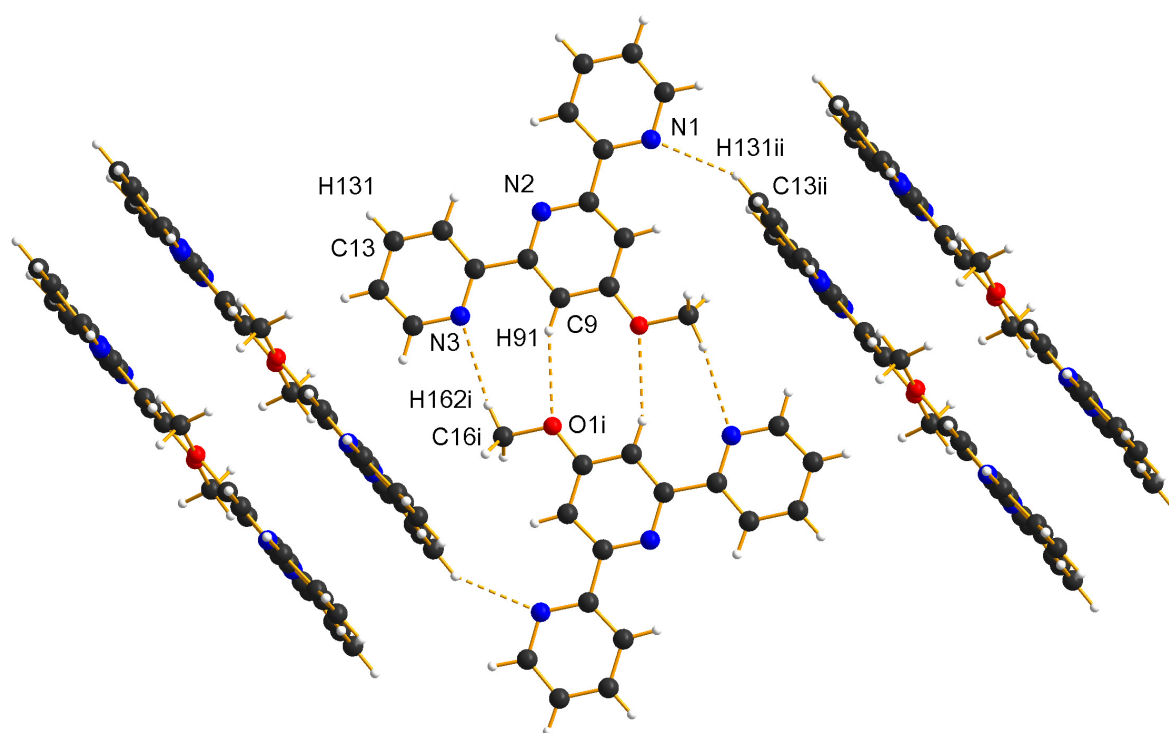


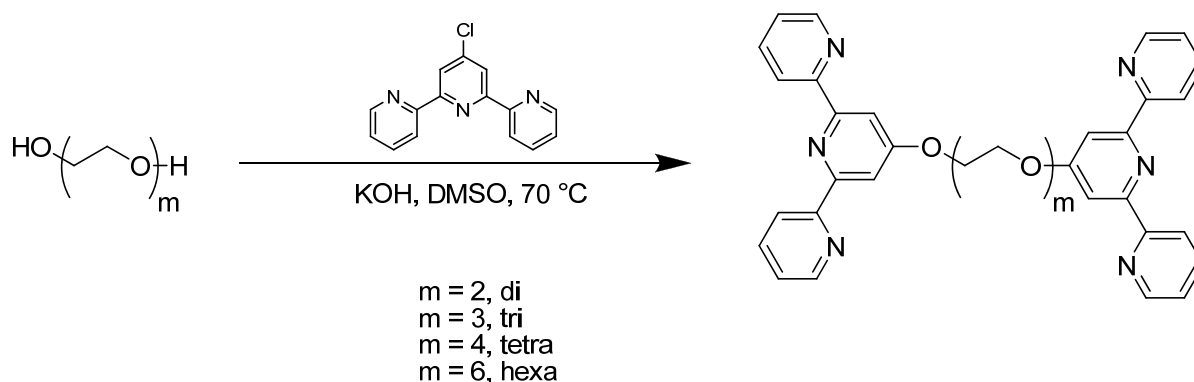
Figure 3.1 Packing of 4'-methoxy-2,2':6',2''-terpyridine ligands (symmetry codes: $i = 1 - x, -y, 1 - z$; $ii = x, 0.5 - y, 0.5 + z$).

The molecules form weakly hydrogen-bonded dimers (shown in Figure 3.1) through the interaction between one of the terminal terpyridine nitrogen atoms and the methyl protons of the methoxy group ($C16^i-H162^i \cdots N3 = 2.55 \text{ \AA}$), and the oxygen atom and the aromatic proton

on the central pyridine ring (C9–H91 \cdots O1ⁱ = 2.60 Å; symmetry code: i = 1 – x, – y, 1 – z). These dimers form π -stacked layers (distance between the layers is 3.3 Å) which interact with approximately perpendicular (angle between the least-squares planes is 82.80(2)°) layers of dimers through weak hydrogen bonding (C13ⁱⁱ–H131ⁱⁱ \cdots N1 = 2.63 Å; symmetry code: ii = x, 0.5 – y, 0.5 + z) which is also shown in Figure 3.1.

3.2.1.2 Synthesis of bis(terpyridyl)oligo(ethylene glycol) ligands

The bis(terpyridyl)oligo(ethylene glycol) ligands were synthesised in good yields by the reaction of the appropriate oligo(ethylene glycol) with 4'-chloro-2,2':6',2''-terpyridine in DMSO in the presence of KOH as shown in Scheme 3.2.



Scheme 3.2 Synthesis of bis(terpyridyl)oligo(ethylene glycol) ligands.

This methodology has been described for the di-,^{38, 39} tetra- and hexa(ethylene glycol)-based ligands⁸³ as well as for poly(ethylene glycol)-based ligands of various lengths.^{37, 39, 41, 141} The ligands could also potentially be synthesised by reaction of 4'-hydroxy-2,2':6',2''-terpyridine with oligoethyleneoxy chlorides, mesylates or tosylates. However, preliminary experiments suggested that this strategy is significantly less reliable and less successful than the published procedure. A two-step synthesis has previously been described for the synthesis of bis(terpyridyl)tri(ethylene glycol),⁸² first forming the monofunctionalised glycol from 2-(2-(2-chloroethoxy)ethoxy)ethanol and 4'-hydroxy-2,2':6',2''-terpyridine, followed by reaction of this intermediate with 4'-chloro-2,2':6',2''-terpyridine. Characterisation is consistent with the previously published data.^{38, 39, 82, 83}

Single crystals of bis(terpyridyl)tri(ethylene glycol) suitable for X-ray diffraction were obtained by slow diffusion of diethyl ether into a THF solution of the ligand. The molecular structure of bis(terpyridyl)tri(ethylene glycol) is shown in Figure 3.2.

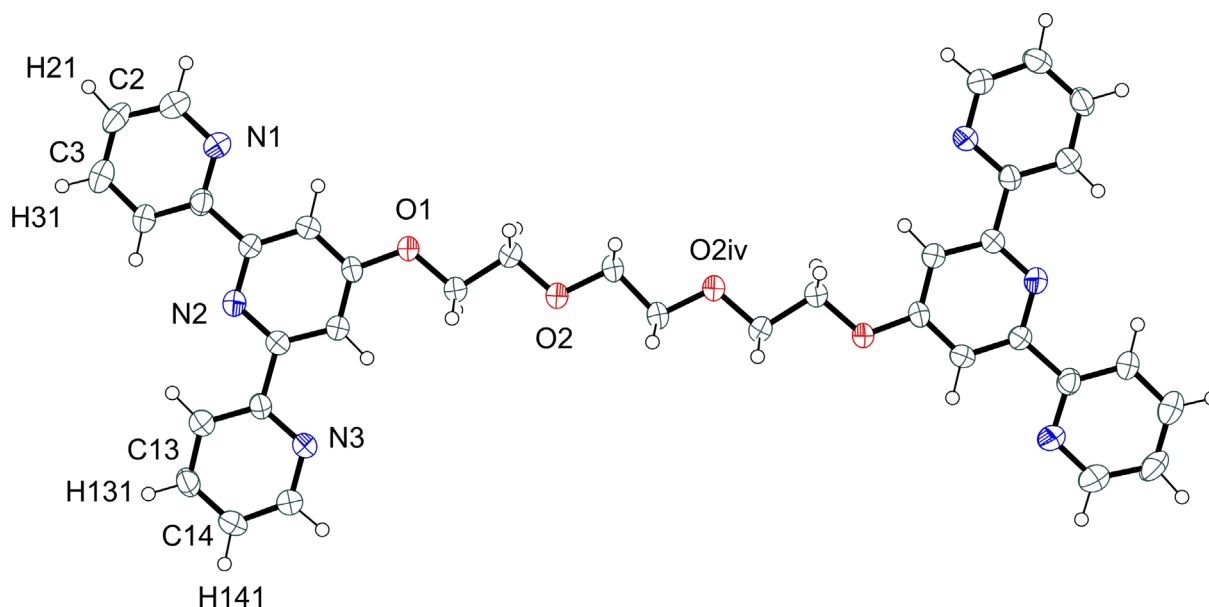


Figure 3.2 Molecular structure of bis(terpyridyl)tri(ethylene glycol) with anisotropic displacement ellipsoids drawn at the 50% probability level (symmetry code: $iv = 2 - x, 1 - y, 2 - z$). Hydrogen atoms are shown as spheres of arbitrary radius.

The ligand is essentially planar (angles between the least-squares planes of the pyridine rings containing N1 and N2, and N2 and N3 are $9.0(1)^\circ$ and $3.8(1)^\circ$, respectively), and the ethyleneoxy chain adopts an extended conformation. The terpyridine domain has the expected¹⁴⁰ *trans-trans* conformation which minimises the interactions between the nitrogen lone pairs and the protons in the 3- and 3'-positions.

The packing in this structure (shown in Figure 3.3) is dominated by weak hydrogen bonding between the terpyridine domain of one ligand and the ethyleneoxy chain ($C13^{iii}-H131^{iii}\cdots O1 = 2.38 \text{ \AA}$; $C3^{iii}-H31^{iii}\cdots O2^{iv} = 2.64 \text{ \AA}$) or the terpyridine nitrogen atoms ($C2^{iii}-H21^{iii}\cdots N3^{iv} = 2.97 \text{ \AA}$, $C14^{iii}-H141^{iii}\cdots N1 = 3.23 \text{ \AA}$) on another (symmetry codes: $iii = 1.5 + x, 0.5 - y, 0.5 + z$, $iv = 2 - x, 1 - y, 2 - z$). The ethyleneoxy chain in this tri(ethylene glycol)-based ligand appears to have the ideal length ($O1-O1^{iv} = 10.545(3) \text{ \AA}$) to accommodate a terpyridine unit ($C2-C14 = 9.586(5) \text{ \AA}$) in the crystal packing. Within each layer, the molecules are

interdigitated, with the terpyridine domain of one ligand fitting along the length of the ethyleneoxy chain of the next. This packing effect could also explain the difficulty in obtaining suitable crystals of any other oligo(ethylene glycol)-based ligand. The stacking of the layers is offset to maximise the π -stacking interaction between the aromatic rings (distance between the layers is 3.4 Å) while minimising the steric repulsion between the ethyleneoxy chains.

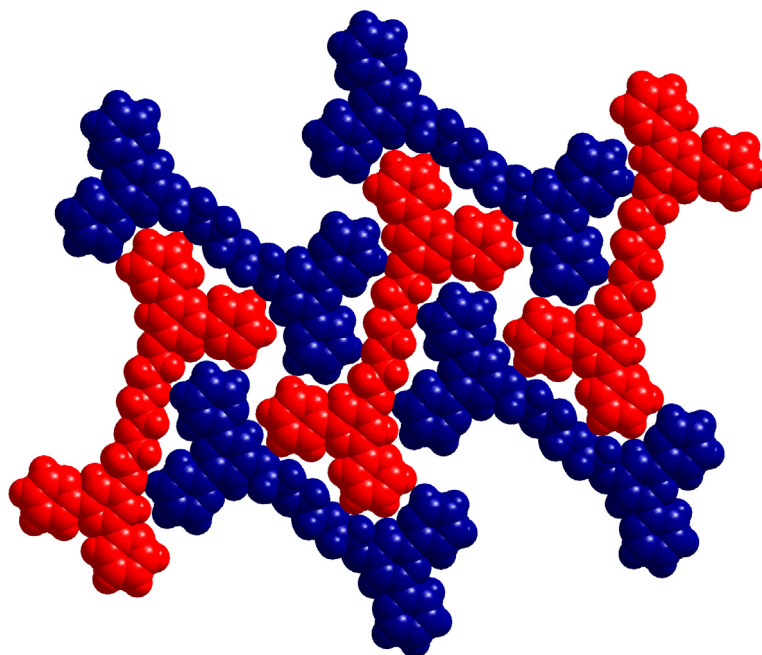
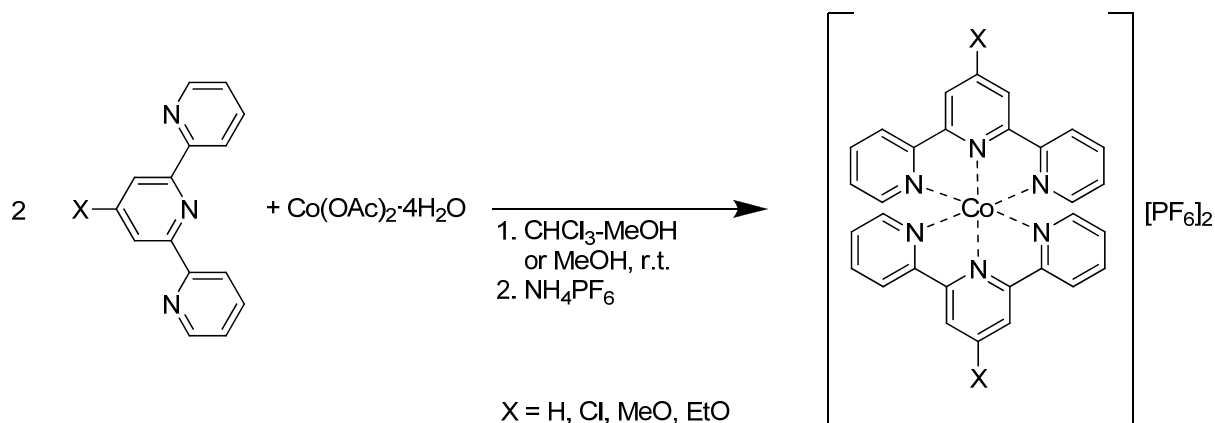


Figure 3.3 Packing arrangement in bis(terpyridyl)tri(ethylene glycol).

3.2.2 Synthesis of mononuclear cobalt(II) hexafluorophosphate complexes

Homoleptic cobalt(II) hexafluorophosphate complexes of the monotopic terpyridine ligands 2,2':6',2''-terpyridine, 4'-chloro-2,2':6',2''-terpyridine, 4'-methoxy-2,2':6',2''-terpyridine and 4'-ethoxy-2,2':6',2''-terpyridine were prepared by the reaction of two equivalents of the ligand with one equivalent of cobalt(II) acetate tetrahydrate at room temperature followed by precipitation of the hexafluorophosphate salt by addition of excess ammonium hexafluorophosphate (see Scheme 3.3). All complexes were obtained in excellent yields.



Scheme 3.3 Synthesis of mononuclear bis(2,2':6',2''-terpyridine)cobalt(II) hexafluorophosphate complexes.

Although the preparation of $[\text{Co}(\text{Cltpy})_2][\text{PF}_6]_2$ and $[\text{Co}(\text{MeOtpy})_2][\text{PF}_6]_2$ have been described previously,¹³⁸ characterisation of these complexes has been limited to elemental analysis and mass spectrometry. Cobalt(II) has a d^7 electronic configuration and the ^1H NMR spectra of the complexes are consequently paramagnetically shifted and broadened such that no multiplet structure is observed. However, as described in Section 2.1, these spectra can be fully assigned and contain much useful chemical information. The complex $[\text{Co}(\text{tpy})_2][\text{PF}_6]_2$ has been studied in detail by ^1H NMR spectroscopy^{94, 95} and will not be discussed here.

It has been shown that the ^1H NMR spectra of bis(2,2':6',2''-terpyridine)cobalt(II) complexes with an oxygen substituent in the 4'-position are very similar.⁹⁰ Altering the substituent in the 4'-position affects primarily the chemical shift of the adjacent H^3 proton as is the case for ligands and diamagnetic complexes of 4'-substituted-2,2':6',2''-terpyridines. The ^1H NMR spectra of $[\text{Co}(\text{Cltpy})_2][\text{PF}_6]_2$, $[\text{Co}(\text{MeOtpy})_2][\text{PF}_6]_2$ and $[\text{Co}(\text{EtOtpy})_2][\text{PF}_6]_2$ were assigned by comparison with literature data and with the aid of ^1H - ^1H COSY spectra. From comparison with spectra of similar complexes,⁹⁰ the most shifted and broadened peak is assigned to H^6 , the proton closest to the paramagnetic centre, the peak at approximately δ 34 ppm is assigned to H^5 , and the least shifted peak (between δ 6 and 9 ppm) is assigned to H^4 . This assignment of H^4 can also be confirmed with a ^1H - ^1H COSY experiment as the signal shows a cross peak to two other signals (H^3 and H^5). On this basis, the peak corresponding to the H^3 proton can also be assigned. Finally, the H^3 signal can be assigned based on the lack of cross peaks in the ^1H - ^1H COSY spectrum. The alkyl protons in $[\text{Co}(\text{MeOtpy})_2][\text{PF}_6]_2$ and $[\text{Co}(\text{EtOtpy})_2][\text{PF}_6]_2$ were assigned by inspection of their integrals. A representative ^1H NMR

spectrum and a ^1H - ^1H COSY spectrum of a CD_3CN solution of $[\text{Co}(\text{Cltpy})_2][\text{PF}_6]_2$ are shown in Figure 3.4.

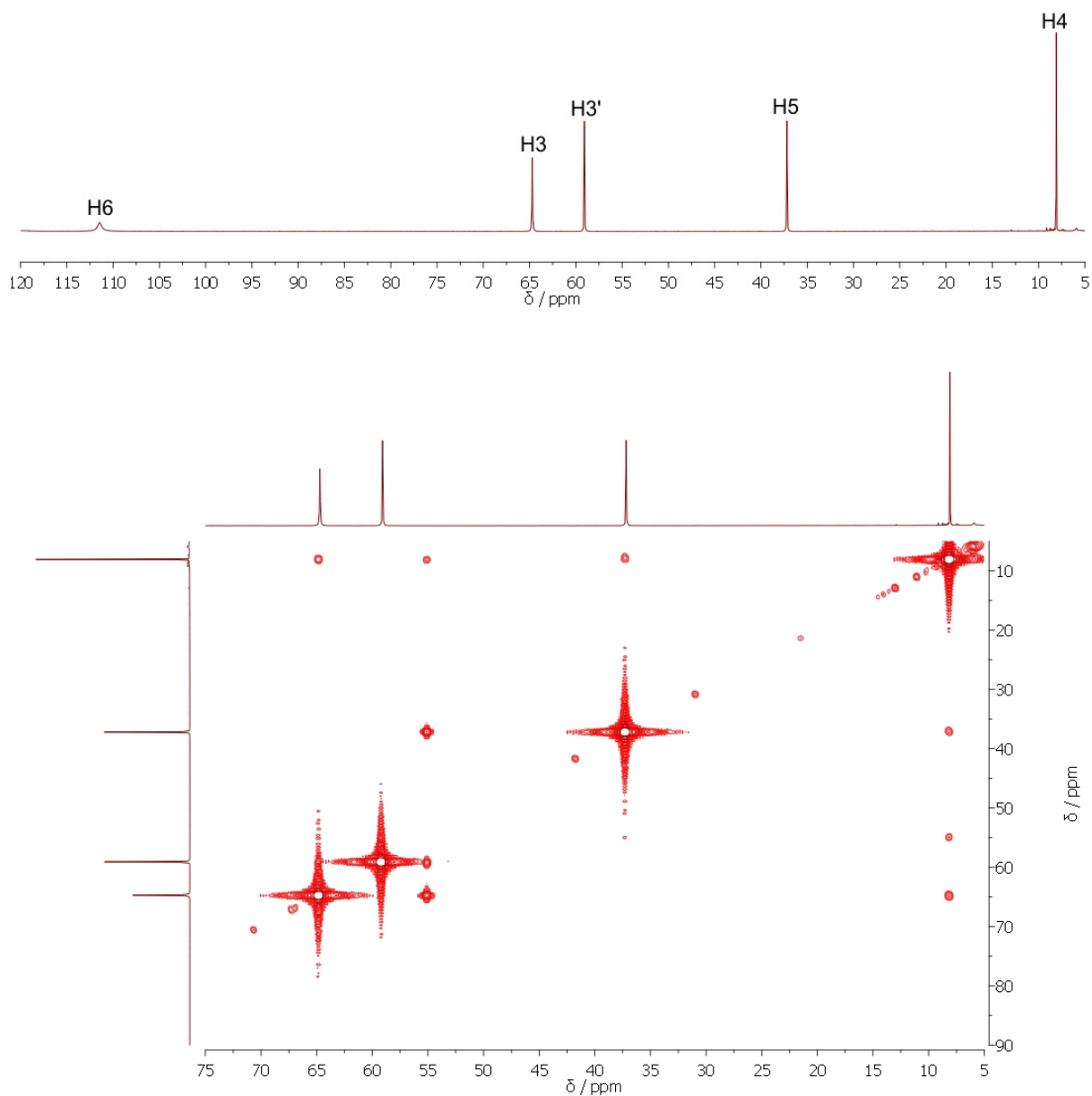
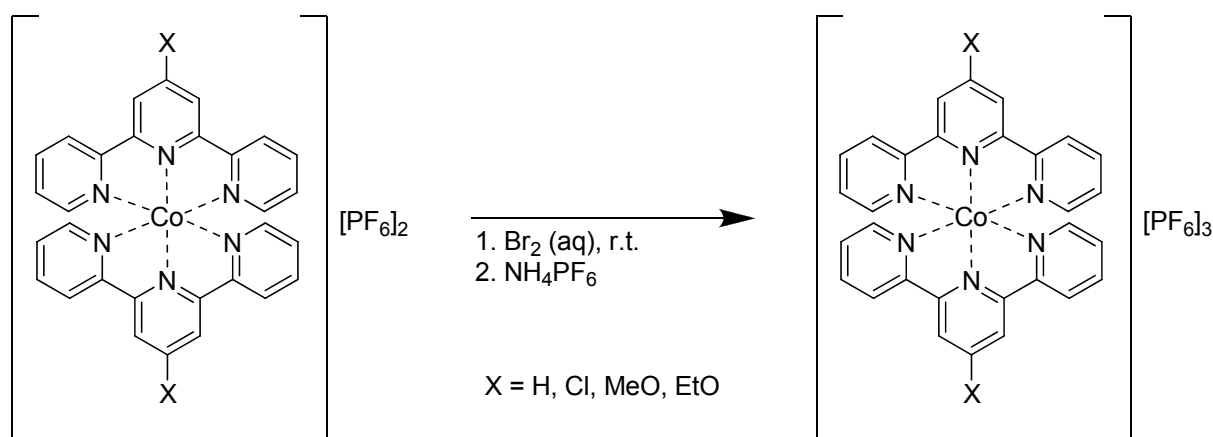


Figure 3.4 Full ^1H NMR spectrum (top) and a portion of the ^1H - ^1H COSY spectrum (bottom) of $[\text{Co}(\text{Cltpy})_2][\text{PF}_6]_2$ (CD_3CN , 500 MHz, 295 K).

3.2.3 Synthesis of mononuclear cobalt(III) hexafluorophosphate complexes

Homoleptic cobalt(III) hexafluorophosphate complexes of the monotopic 2,2':6',2''-terpyridine ligands 2,2':6',2''-terpyridine, 4'-chloro-2,2':6',2''-terpyridine, 4'-methoxy-

2,2':6',2''-terpyridine and 4'-ethoxy-2,2':6',2''-terpyridine were prepared by oxidation of the corresponding cobalt(II) hexafluorophosphate complexes. Initially, aqueous bromine was used as the oxidant, and the hexafluorophosphate salt was precipitated in good to moderate yields by addition of excess ammonium hexafluorophosphate as shown in Scheme 3.4. However, the presence of the bromide ions formed during the oxidation could affect the speciation of complexes involving the ditopic ligands and oxidation of the cobalt(II) complexes using silver(I) hexafluorophosphate was also tested. This approach was unsuccessful for the synthesis of $[\text{Co}(\text{Cltpy})_2][\text{PF}_6]_3$, but in preliminary trials gave good yields of the remaining three cobalt(III) complexes with a much simpler work-up than for the oxidation with bromine.



Scheme 3.4 Synthesis of mononuclear bis(2,2':6',2''-terpyridine)cobalt(III) hexafluorophosphate complexes.

Cobalt(III) has a d^6 configuration and bis(terpyridine)cobalt(III) salts are low-spin and diamagnetic. The ^1H and ^{13}C NMR spectra of the oxidised complexes therefore show signals within the normal ranges and were fully assigned by inspection of the coupling constants¹⁴² (^1H) and using standard 2D methods (see Section 3.7.5). The completion of the oxidation reaction was confirmed by the absence of paramagnetically shifted peaks in the ^1H NMR spectrum. However, the electrospray mass spectra of the cobalt(III) complexes show, in addition to the expected signals ($[\text{M}-\text{PF}_6]^+$, $[\text{M}-2\text{PF}_6]^{2+}$ and $[\text{M}-3\text{PF}_6]^{3+}$), intense peaks which correspond to the analogous cobalt(II) species ($[\text{M}-2\text{PF}_6]^+$, $[\text{M}-3\text{PF}_6]^{2+}$). These cobalt(II) species are believed to form by reduction of the cobalt(III) complex in the mass spectrometer source¹⁴³ as elemental analysis also confirmed the purity of the analytical sample.

3.3 Comparison of X-ray crystal structures of bis(2,2':6',2''-terpyridine)-cobalt(II) and cobalt(III) complexes

Although cobalt(II) complexes of 2,2':6',2''-terpyridine and its derivatives have been well investigated due to their spin-crossover behaviour,¹⁴⁴ there have been very few structural investigations of bis(2,2':6',2''-terpyridine)cobalt(III) complexes,¹⁴⁵⁻¹⁴⁷ and only one comparative study of analogous cobalt(II) and cobalt(III) complexes.¹⁴⁷

Single crystals of the cobalt(II) complexes described in section 3.2.2, $[\text{Co}(\text{tpy})_2][\text{PF}_6]_2 \cdot 2\text{MeCN}$, $[\text{Co}(\text{Cltpy})_2][\text{PF}_6]_2$, $[\text{Co}(\text{MeOtpy})_2][\text{PF}_6]_2$, $[\text{Co}(\text{MeOtpy})_2][\text{PF}_6]_2 \cdot \text{MeCN}$ and $[\text{Co}(\text{EtOtpy})_2][\text{PF}_6]_2 \cdot 2\text{MeCN}$, and the cobalt(III) complexes described in section 3.2.3, $2\{[\text{Co}(\text{tpy})_2][\text{PF}_6]_3\} \cdot 5\text{MeCN}$, $[\text{Co}(\text{Cltpy})_2][\text{PF}_6]_3 \cdot \text{MeCN}$, $[\text{Co}(\text{MeOtpy})_2][\text{PF}_6]_3 \cdot \text{MeCN}$ and $[\text{Co}(\text{EtOtpy})_2][\text{PF}_6]_3 \cdot \text{MeCN}$, were obtained by slow diffusion of diethyl ether into acetonitrile solutions of the complexes. In addition, single crystals of the bromide salt $[\text{Co}(\text{EtOtpy})_2][\text{Br}]_3 \cdot \text{MeCN} \cdot \text{H}_2\text{O}$ and cobalt(II) and cobalt(III) complexes with the ligand 4'-(1-propoxy)-2,2':6',2''-terpyridine (see Chapter 4 for the synthesis), $[\text{Co}(\text{PrOtpy})_2][\text{PF}_6]_2 \cdot \text{MeCN}$, $[\text{Co}(\text{PrOtpy})_2][\text{PF}_6]_2 \cdot \text{MeCN} \cdot \text{Et}_2\text{O}$ and $2\{[\text{Co}(\text{PrOtpy})_2][\text{PF}_6]_3\} \cdot 5\text{MeCN}$, were obtained using the same procedure. The molecular structures of the cations in the cobalt(III) hexafluorophosphate complexes are shown in Figure 3.5 to Figure 3.9. Cobalt–nitrogen bond lengths are given in Table 3.1 and $\text{N}_{\text{terminal}}\text{--Co--N}_{\text{terminal}}$ bond angles and angles between the least-squared planes of the pyridine rings are given in Table 3.2.

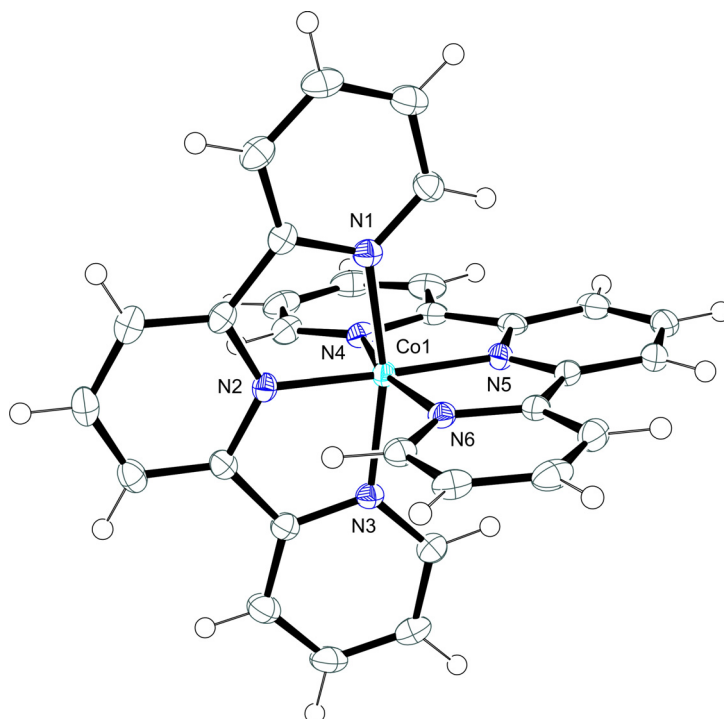


Figure 3.5 Molecular structure of one of the two similar cations in the asymmetric unit of $[\text{Co}(\text{tpy})_2][\text{PF}_6]_3 \cdot 2.5\text{MeCN}$ with anisotropic displacement ellipsoids drawn at the 50% probability level. Hydrogen atoms are shown as spheres of arbitrary radius.

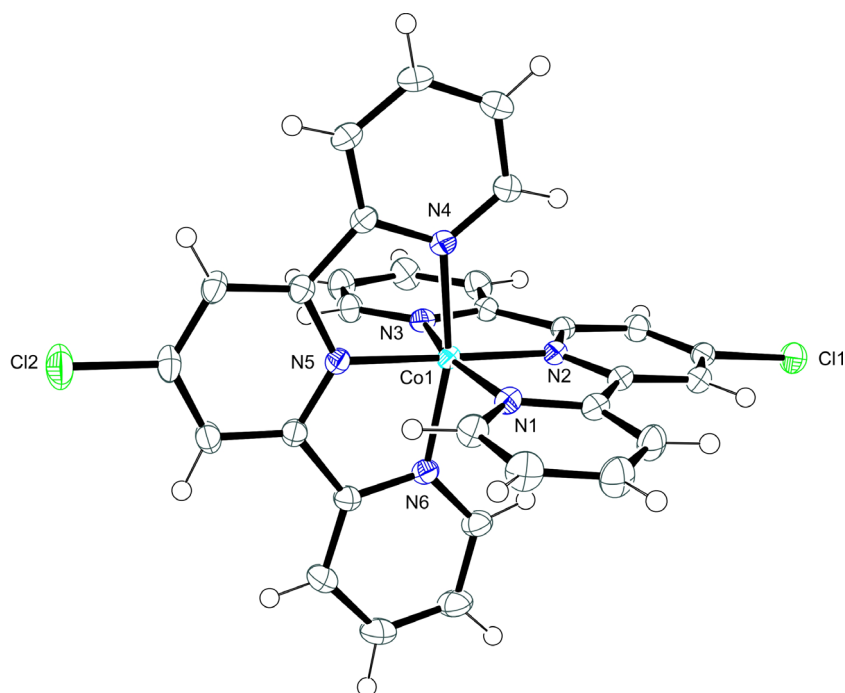


Figure 3.6 Molecular structure of the cation in $[\text{Co}(\text{Cltpy})_2][\text{PF}_6]_3 \cdot \text{MeCN}$ with anisotropic displacement ellipsoids drawn at the 50% probability level. Hydrogen atoms are shown as spheres of arbitrary radius.

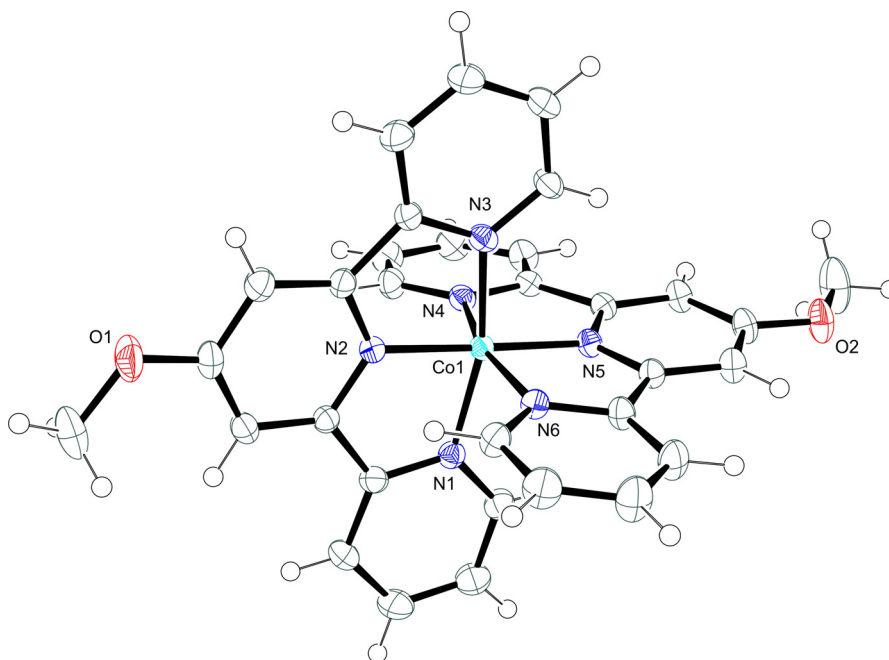


Figure 3.7 Molecular structure of the cation in $[\text{Co}(\text{MeOtpy})_2][\text{PF}_6]_3 \cdot \text{MeCN}$ with anisotropic displacement ellipsoids drawn at the 50% probability level. Hydrogen atoms are shown as spheres of arbitrary radius.

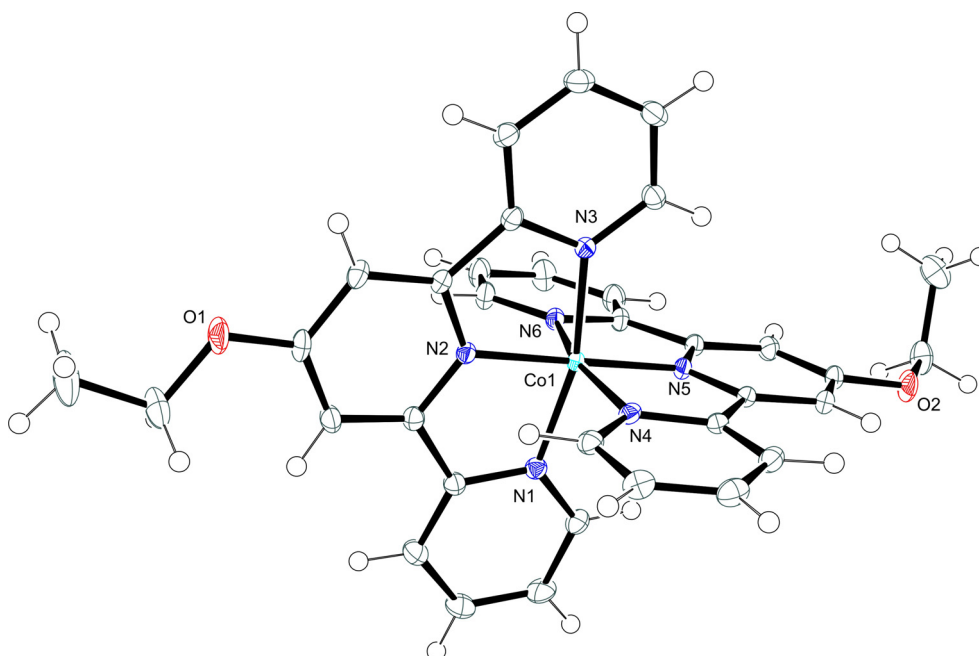


Figure 3.8 Molecular structure of the cation in $[\text{Co}(\text{EtOtpy})_2][\text{PF}_6]_3 \cdot \text{MeCN}$ with anisotropic displacement ellipsoids drawn at the 50% probability level. Hydrogen atoms are shown as spheres of arbitrary radius.

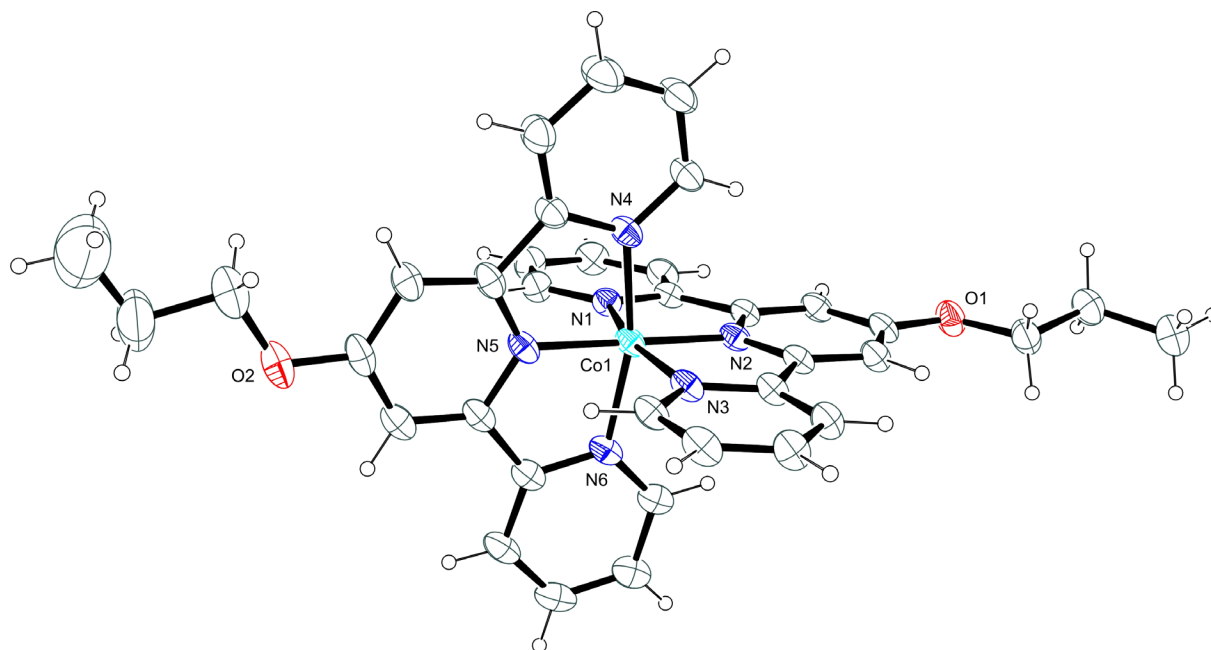


Figure 3.9 Molecular structure of the cation in $2\{[\text{Co}(\text{PrOtpy})_2][\text{PF}_6]_3\} \cdot 5\text{MeCN}$ with anisotropic displacement ellipsoids drawn at the 30% probability level. Hydrogen atoms are shown as spheres of arbitrary radius.

Complex	Co–N1	Co–N2	Co–N3	Co–N4	Co–N5	Co–N6	av. Co–N _t	av. Co–N _c
[Co(tpy) ₂][PF ₆] ₂ ·2MeCN ^a	2.033(3)	1.882(3)	2.045(3)	2.110(3)	1.915(3)	2.116(3)	2.076	1.899
	2.029(3)	1.881(3)	2.038(3)	2.101(3)	1.912(3)	2.102(3)	2.068	1.897
2{[Co(tpy) ₂][PF ₆] ₃ }·5MeCN ^a	1.9545(16)	1.8590(16)	1.9408(16)	1.9595(16)	1.8596(16)	1.9369(16)	1.948	1.859
	1.9348(15)	1.8550(16)	1.9440(15)	1.9457(15)	1.8555(15)	1.9474(16)	1.943	1.855
[Co(Cltpy) ₂][PF ₆] ₂ ^b	2.0973(17)	1.907(2)	2.0973(17)	2.0973(17)	1.907(2)	2.0973(17)	2.097	1.907
[Co(Cltpy) ₂][PF ₆] ₃ ·MeCN	1.9397(13)	1.8591(13)	1.9495(13)	1.9477(13)	1.8637(13)	1.9481(13)	1.946	1.861
[Co(MeOtpy) ₂][PF ₆] ₂	2.073(5)	1.924(5)	2.068(5)	2.135(5)	1.948(5)	2.138(5)	2.104	1.936
[Co(MeOtpy) ₂][PF ₆] ₂ ·MeCN	2.108(2)	1.913(2)	2.118(2)	2.068(2)	1.903(2)	2.056(2)	2.088	1.908
[Co(MeOtpy) ₂][PF ₆] ₃ ·MeCN	1.945(2)	1.857(2)	1.941(2)	1.943(2)	1.856(2)	1.947(2)	1.944	1.857
[Co(EtOtpy) ₂][PF ₆] ₂ ·2MeCN	2.156(3)	1.919(3)	2.161(3)	2.007(3)	1.874(3)	2.009(3)	2.083	1.897
[Co(EtOtpy) ₂][PF ₆] ₃ ·MeCN	1.9458(14)	1.8603(12)	1.9502(13)	1.9561(14)	1.8585(12)	1.9461(14)	1.950	1.859
[Co(EtOtpy) ₂][Br] ₃ ·MeCN·H ₂ O	1.949(4)	1.853(4)	1.943(4)	1.947(5)	1.853(4)	1.933(5)	1.943	1.853
[Co(PrOtpy) ₂][PF ₆] ₂ ·MeCN ^a	2.1331(14)	2.0147(13)	2.1214(13)	2.1751(15)	2.0282(15)	2.1751(16)	2.151	2.021
	2.1332(14)	1.9762(13)	2.1190(14)	2.0982(14)	1.9693(15)	2.1161(16)	2.117	1.973
[Co(PrOtpy) ₂][PF ₆] ₂ ·MeCN·Et ₂ O	2.1617(13)	2.0375(11)	2.1433(12)	2.1526(12)	2.0404(11)	2.1726(13)	2.158	2.039
2{[Co(PrOtpy) ₂][PF ₆] ₃ }·5MeCN	1.951(3)	1.859(3)	1.940(3)	1.944(3)	1.849(3)	1.944(3)	1.945	1.854

Table 3.1 Cobalt–nitrogen bond lengths (Å) in mononuclear bis(2,2':6',2''-terpyridine)cobalt(II) (white) and cobalt(III) (yellow) complexes. N1, N2 and N3 belong to one terpyridine ligand and N4, N5 and N6 belong to the other terpyridine ligand. N2 and N5 are the nitrogen atoms in the central pyridine rings. N_c = N_{central}, N_t = N_{terminal}. The numbering of the atoms in the table does not always correspond to the numbering of the atoms in the cif file. (a = The numbering of the second cation in the asymmetric unit uses the labels N7–12 in the cif file, b = Due to symmetry, N2 and N5 are equivalent and are labelled N2 in the cif file. N1, N3, N4 and N6 are also equivalent and are labelled N9 in the cif file.)

Complex	N1–Co–N3	N4–Co–N6	angle between least-squared planes containing:			
			N1 and N2	N2 and N3	N4 and N5	N5 and N6
[Co(tpy) ₂][PF ₆] ₂ ·2MeCN ^a	161.63(12)	159.23(12)	0.27(11)	3.89(11)	3.57(12)	2.36(13)
	161.84(12)	159.30(11)	2.24(12)	2.07(11)	3.26(11)	6.85(11)
2{[Co(tpy) ₂][PF ₆] ₃ }·5MeCN ^a	164.92(7)	165.08(7)	2.52(6)	7.33(6)	2.98(7)	0.85(6)
	165.54(7)	165.55(7)	1.71(5)	8.13(6)	4.34(6)	6.15(6)
[Co(Cltpy) ₂][PF ₆] ₂ ^b	159.18(10)	159.18(10)	0	0	0	0
[Co(Cltpy) ₂][PF ₆] ₃ ·MeCN	164.56(6)	164.4(6)	5.87(6)	5.87(6)	6.69(6)	2.30(4)
[Co(MeOtpy) ₂][PF ₆] ₂	159.36(18)	157.50(18)	1.78(17)	8.4(2)	0.29(19)	3.51(19)
[Co(MeOtpy) ₂][PF ₆] ₂ ·MeCN	158.72(8)	159.87(8)	0.31(8)	1.49(8)	4.12(7)	10.30(8)
[Co(MeOtpy) ₂][PF ₆] ₃ ·MeCN	164.48(10)	164.31(9)	5.20(9)	6.36(10)	7.51(9)	5.89(9)
[Co(EtOtpy) ₂][PF ₆] ₂ ·2MeCN	157.65(11)	162.14(12)	3.43(14)	7.46(11)	5.59(11)	1.53(9)
[Co(EtOtpy) ₂][PF ₆] ₃ ·MeCN	164.21(6)	164.17(6)	5.58(5)	3.78(4)	6.19(6)	3.20(6)
[Co(EtOtpy) ₂][Br] ₃ ·MeCN·H ₂ O	165.22(19)	164.8(2)	2.0(2)	2.49(18)	4.0(2)	5.8(2)
[Co(PrOtpy) ₂][PF ₆] ₂ ·MeCN ^a	153.82(5)	152.25(6)	5.45(5)	2.03(5)	9.86(6)	14.71(6)
	155.51(5)	155.89(6)	10.36(5)	6.03(5)	4.81(6)	8.07(7)
[Co(PrOtpy) ₂][PF ₆] ₂ ·MeCN·Et ₂ O	152.38(4)	152.47(4)	9.19(5)	6.16(4)	11.36(4)	10.16(5)
2{[Co(PrOtpy) ₂][PF ₆] ₃ }·5MeCN	164.45(12)	164.73(13)	3.48(12)	1.72(12)	1.55(12)	3.31(13)

Table 3.2 Selected bond angles and angles between least-squared planes (°) in mononuclear bis(2,2':6',2''-terpyridine)cobalt(II) (white) and cobalt(III) (yellow) complexes. N1, N2 and N3 belong to one terpyridine ligand and N4, N5 and N6 belong to the other terpyridine ligand. N2 and N5 are the nitrogen atoms in the central pyridine rings. The numbering of the atoms in the table does not always correspond to the numbering of the atoms in the cif file. (a = The numbering of the second cation in the asymmetric unit uses the labels N7–12 in the cif file, b = Due to symmetry, N2 and N5 are equivalent and are labelled N2 in the cif file. N1, N3, N4 and N6 are also equivalent and are labelled N9 in the cif file.)

In all the complexes, the cobalt ion is found in a distorted octahedral environment with two 2,2':6',2''-terpyridine ligands bound in a bis-meridional conformation. Cobalt–nitrogen bond lengths in the cobalt(II) complexes range from 1.874(3) to 2.1751(16) Å, with the Co–N_{central} bond lengths consistently shorter (1.874(3) – 2.0404(11) Å) than the Co–N_{terminal} bond lengths in the same cation (2.007(3) – 2.1751(16) Å). In the cobalt(III) complexes, the variation in cobalt–nitrogen bond lengths is much smaller, with the Co–N_{central} bond lengths between 1.849(3) and 1.8603(12) Å and the Co–N_{terminal} bond lengths between 1.933(5) and 1.9595(17) Å. The N_{terminal}–Co–N_{terminal} bite angles for the cobalt(II) complexes range from 152.25(6) to 162.14(12)° while in the cobalt(III) complexes, this angle is 5 to 12° larger and much less variable (164.21(6) to 165.55(7)°). This suggests that the substituent in the 4'-position of the terpyridine has little effect on the environment around the cobalt(III) ion. Comparison of the two complexes with the 4'-ethoxy-2,2':6',2''-terpyridine ligand, [Co(EtOtpy)₂][PF₆]₃·MeCN (Co–N_{terminal} = 1.9458(14) – 1.9561(14) Å, Co–N_{central} = 1.8585(12) and 1.8603(12) Å) and [Co(EtOtpy)₂][Br]₃·MeCN·H₂O (Co–N_{terminal} = 1.933(5) and 1.949(4) Å, Co–N_{central} = 1.853(4) Å), shows that the anion and solvate molecules also have little effect on the geometry of the cobalt(III) ion.

On the other hand, the geometry around the cobalt(II) ion in bis(2,2':6',2''-terpyridine) complexes is heavily dependent on the substituent, anion and presence of solvate molecules in the crystal structure (see Table 3.1). The cobalt(II) ion has a 3d⁷ electronic configuration and can adopt either a low-spin (t_{2g}⁶e_g¹) or a high-spin (t_{2g}⁵e_g²) ground state. When the difference between the ligand field strength and the spin pairing energy is of a similar magnitude to the thermal energy, a crossover between the two states is observed. The dependence of the magnetic properties of bis(2,2':6',2''-terpyridine)cobalt(II) salts on the anion and degree of solvation was first observed in 1962⁴⁸ and has since then been widely studied. Measured magnetic moments are temperature dependent and span a continuous range from the calculated low-spin value (1.8 – 2.2 μ_B) to the expected high-spin value (4.7 – 5.2 μ_B),¹⁴⁴ and can be considered to give an indication of the position of the spin state equilibrium. X-ray crystal structures and magnetic moments of the bis(2,2':6',2''-terpyridine)cobalt(II) cation with a variety of anions (bromide,¹⁴⁸ thiocyanate,¹⁴⁹ perchlorate,^{150, 151} iodide,¹⁵² nitrate¹⁵³) have been determined and the effect of the spin state on the cobalt–nitrogen bond length considered.¹⁵¹ It was found that the Co–N_{central} distance changes by up to 0.21 Å and the Co–N_{terminal} distance by approximately 0.07 Å between the two spin states. At 120 K, the iodide

dihydrate has a magnetic moment corresponding to a fully low-spin species ($2.2 \mu_B$) and the cobalt–nitrogen bond lengths of the structure ($\text{Co–N}_{\text{terminal}} = 2.083(4) \text{ \AA}$, $\text{Co–N}_{\text{central}} = 1.912(5) \text{ \AA}$) can therefore be considered typical for a low-spin bis(2,2':6',2''-terpyridine)cobalt(II) species.¹⁵² In contrast, the highest magnetic moment for an unsubstituted bis(2,2':6',2''-terpyridine)cobalt(II) salt ($4.2 \mu_B$) was measured for the perchlorate salt with 1.3 water molecules at 295 K.¹⁵¹ The cobalt–nitrogen bond lengths in this structure ($\text{Co–N}_{\text{terminal}} = 2.133(5) \text{ and } 2.140(5) \text{ \AA}$, $\text{Co–N}_{\text{central}} = 2.030(6) \text{ and } 2.026(6) \text{ \AA}$) are significantly longer than in structures with smaller magnetic moments. The only bis(2,2':6',2''-terpyridine)cobalt(II) structure with longer cobalt–nitrogen bond lengths ($\text{Co–N}_{\text{terminal}} = 2.189(3) \text{ and } 2.180(3) \text{ \AA}$, $\text{Co–N}_{\text{central}} = 2.101(4) \text{ and } 2.075(3) \text{ \AA}$) is the nitrate dihydrate,¹⁵³ but unfortunately the magnetic properties of this complex were not studied. The variation in both magnetic moments and cobalt–nitrogen bond lengths is continuous and complexes with intermediate magnetic moments also show intermediate cobalt–nitrogen bond lengths.

More recently, the magnetic and structural properties of a series of cobalt(II) complexes of the 4'-hydroxy-2,2':6',2''-terpyridine ligand with a variety of anions¹⁵⁴⁻¹⁵⁶ and of 4'-alkoxy-2,2':6',2''-terpyridine ligands with varying alkyl chain lengths and several anions¹⁵⁷⁻¹⁶⁰ have also been investigated.

It is difficult to make any general comments about the trends in the cobalt–nitrogen bond lengths as the substituent in the 4'-position of the 2,2':6',2''-terpyridine is varied and it is clear that the spin-state and geometry of the cobalt(II) ion are extremely sensitive to lattice forces in the crystal. The cobalt–nitrogen bond lengths in the bis(2,2':6',2''-terpyridine)cobalt(II) complexes described in this chapter range from approximate low-spin values ($[\text{Co}(\text{tpy})_2][\text{PF}_6]_2 \cdot 2\text{MeCN}$, $\text{Co–N}_{\text{central}} = 1.881(3) - 1.915(3) \text{ \AA}$, $[\text{Co}(\text{Cltpy})_2][\text{PF}_6]_2$, $\text{Co–N}_{\text{central}} = 1.907(2) \text{ \AA}$, $[\text{Co}(\text{MeOtpy})_2][\text{PF}_6]_2 \cdot \text{MeCN}$, $\text{Co–N}_{\text{central}} = 1.903(2) \text{ and } 1.913(2) \text{ \AA}$, $[\text{Co}(\text{EtOtpy})_2][\text{PF}_6]_2 \cdot 2\text{MeCN}$, $\text{Co–N}_{\text{central}} = 1.874(3) \text{ and } 1.919(3) \text{ \AA}$) to approximate high-spin values ($[\text{Co}(\text{PrOtpy})_2][\text{PF}_6]_2 \cdot \text{MeCN} \cdot \text{Et}_2\text{O}$, $\text{Co–N}_{\text{central}} = 2.0375(11) \text{ and } 2.0404(11) \text{ \AA}$). It is clear that the degree of solvation significantly affects the cobalt–nitrogen bond lengths through comparison of $[\text{Co}(\text{MeOtpy})_2][\text{PF}_6]_2$ and $[\text{Co}(\text{MeOtpy})_2][\text{PF}_6]_2 \cdot \text{MeCN}$, in which the $\text{Co–N}_{\text{central}}$ bond lengths are $1.924(5) \text{ and } 1.948(5) \text{ \AA}$, and $1.903(2) \text{ and } 1.913(2) \text{ \AA}$, respectively. Comparison of the structures of the two independent cations in the complex $[\text{Co}(\text{PrOtpy})_2][\text{PF}_6]_2 \cdot \text{MeCN}$ and closer inspection of the structure of

[Co(EtOtpy)₂][PF₆]₂·2MeCN suggests that even more subtle lattice effects must also influence the geometry of the cobalt(II) ion in these systems. The Co–N_{central} bond lengths in the two cations in [Co(PrOtpy)₂][PF₆]₂·MeCN are 2.0147(13) and 2.0282(15) Å, and 1.9762(13) and 1.9693(15) Å, with an average difference of 0.048 Å, which is approximately a quarter of the change in this bond length between high and low spin states. In the case of [Co(EtOtpy)₂][PF₆]₂·2MeCN, one of the terpyridine units is bound 0.045 Å more closely to the cobalt ion than the other (Co–N_{central} = 1.919(3) and 1.874(3) Å). This has been observed previously in the complexes [Co(HOtpy)₂][BF₄][SiF₆]_{0.5} (Co–N_{central}(293 K) = 1.894(2) and 1.946(2) Å, Co–N_{central}(105 K) = 1.871(3) and 1.943(3) Å),¹⁵⁵ and [Co(H₁₇C₈Otpy)₂][ClO₄]₂ (Co–N_{central} = 1.918(3) and 1.865(3) Å),¹⁶⁰ although no explanation was given.

The intermolecular interactions between the bis(2,2':6',2''-terpyridine)cobalt(II) cation and the anions and solvent molecules present in the lattice undoubtedly have a significant effect on the spin-state and hence the geometry around the cobalt(II) ion. An attempt to relate the differences in the position of the spin equilibrium of the cobalt(II) ion to packing effects in the crystal in unsubstituted bis(2,2':6',2''-terpyridine)cobalt(II) complexes, considering interactions between the ligands, anions and solvent molecules and their positions relative to the cobalt ion, disorder in the anion positions and distortions in the bis(2,2':6',2''-terpyridine)cobalt(II) cation, concluded that "any conclusions made would be a gross oversimplification of a very complex situation."¹⁵¹

The crystal packing of the complexes described in this chapter show a wide variety of different structural features and, although evidently significant, correlation of the packing effects and the geometry around the cobalt(II) ion is not possible.

The complex [Co(tpy)₂][PF₆]₂·2MeCN crystallises in the chiral space group *P*4₃ with two independent molecules in the asymmetric unit. The cations pack in two-dimensional layers (Figure 3.10) through the well-known tpy embrace motif,¹⁶¹ in which each cation participates in four offset face-to-face π–π interactions (distance between the planes = 3.5 Å) and eight edge-to-face C–H⋯π interactions with the shortest C–H⋯π distances being 2.48 and 2.54 Å.

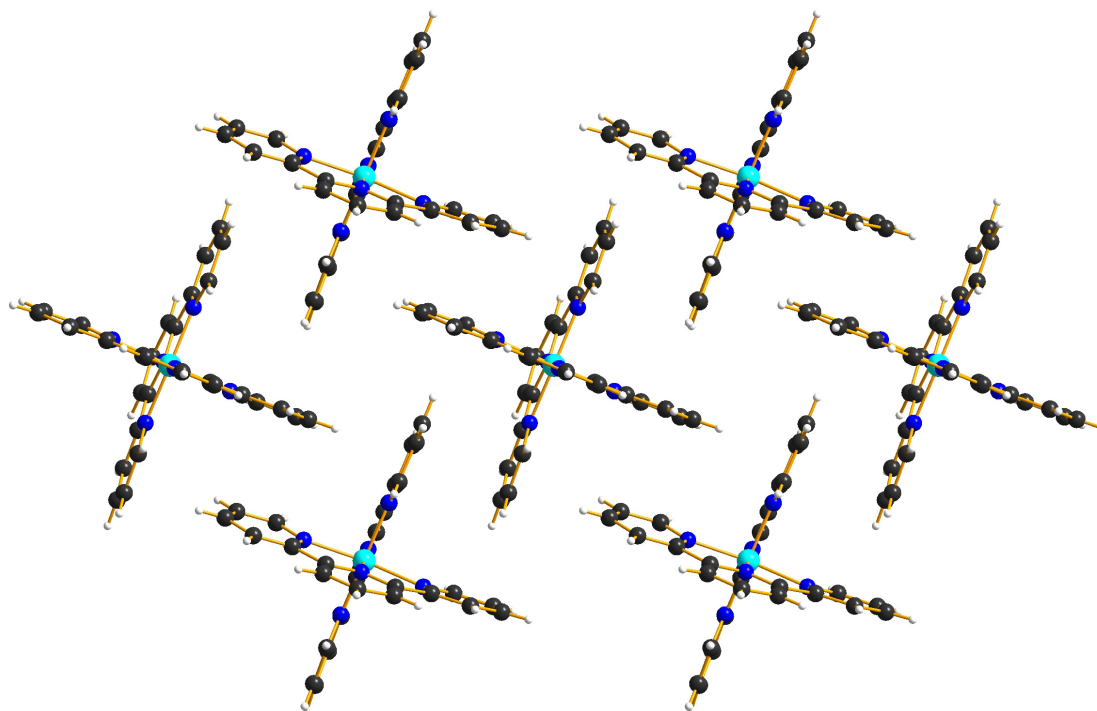


Figure 3.10 View of the cations in the two-dimensional layer structure in $[\text{Co}(\text{tpy})_2][\text{PF}_6]_2 \cdot 2\text{MeCN}$.

The two-dimensional layers of cations are connected via weak non-classical C–H···F or C–H···N hydrogen bonds between the pyridyl rings and the anions and the acetonitrile molecules, which form a layer between the sheets of cations. The cations arrange in a helical structure along the crystallographic c -axis (Figure 3.11), leading to the adoption of a chiral space group.

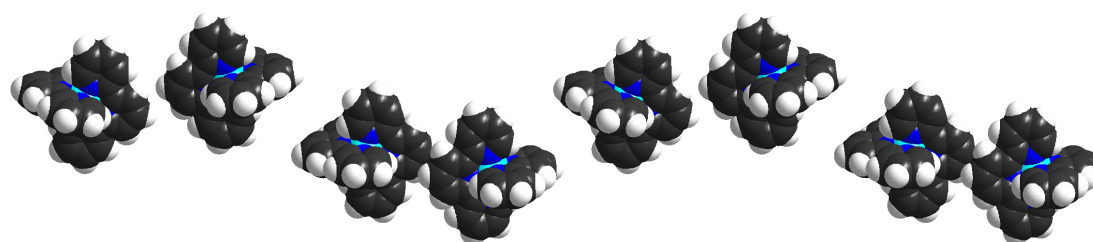


Figure 3.11 Helical chains of cations in $[\text{Co}(\text{tpy})_2][\text{PF}_6]_2 \cdot 2\text{MeCN}$.

The packing in the structure of $[\text{Co}(\text{Cltpy})_2][\text{PF}_6]_2$ is also dominated by two-dimensional layers of the well-known tpy embrace motif,¹⁶¹ in which each cation participates in four offset face-to-face π – π interactions (distance between the planes = 3.6 Å) and eight edge-to-face C–

H $\cdots\pi$ interactions (C11–H16 $\cdots\pi^v = 3.10$ Å, symmetry code: $v = -x, y, -z$). Alternating layers of cations are rotated by 45° relative to one another and the chloro substituent in the 4'-position is directed into the space between four terpyridine units in the adjacent layer (see Figure 3.12). The layers of cations are connected via C–H \cdots F hydrogen bonds between the pyridyl rings and the anions.

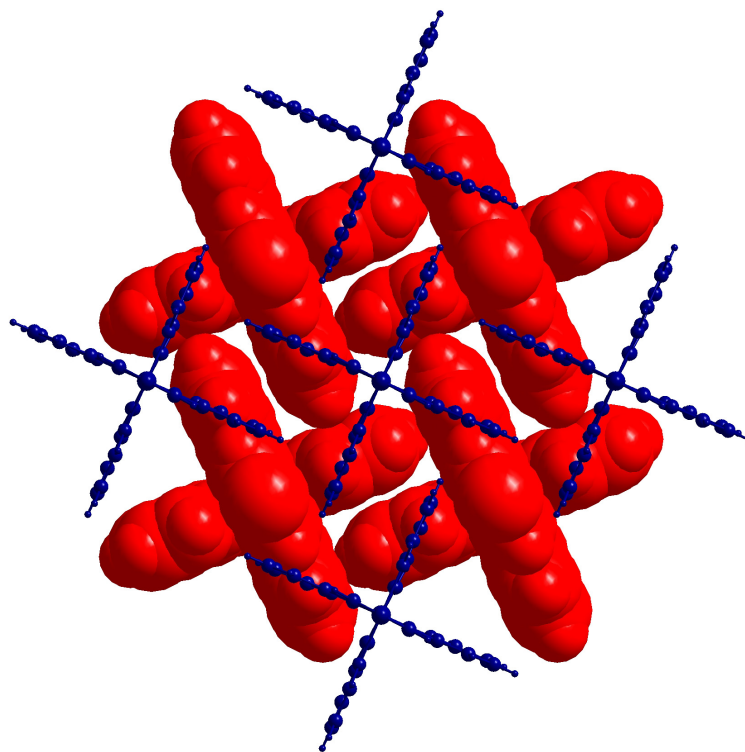


Figure 3.12 View of the two-dimensional layer structure in $[\text{Co}(\text{Cltpy})_2][\text{PF}_6]_2$. The $[\text{PF}_6]^-$ anions fit into grooves formed between the central pyridine rings and form layers between layers of cations.

Two-dimensional layers of cations offset by 45° to adjacent layers are also observed in $[\text{Co}(\text{MeOtpy})_2][\text{PF}_6]_2 \cdot \text{MeCN}$ as shown in Figure 3.13. In this case, each cation participates in three offset face-to-face π – π interactions (distance between the planes = 3.5 Å) and six edge-to-face C–H $\cdots\pi$ interactions (C13–H131 $\cdots\pi^{\text{vi}} = 2.68$ Å, C2–H21 $\cdots\pi^{\text{vii}} = 2.89$ Å, C29–H291 $\cdots\pi^{\text{viii}} = 3.06$ Å; symmetry codes: $\text{vi} = 1 - x, 1 - y, 1 - z$, $\text{vii} = 0.5 - x, 1.5 - y, z$, $\text{viii} = 0.5 - x, 0.5 - y, z$). The remaining terminal pyridine ring forms a hydrogen bond to the acetonitrile molecule (C16–H181 $\cdots\text{N}7^{\text{ix}} = 2.66$ Å; symmetry code: $\text{ix} = x, 1 + y, z$), which fills the spaces between the chains of π -stacked cations.

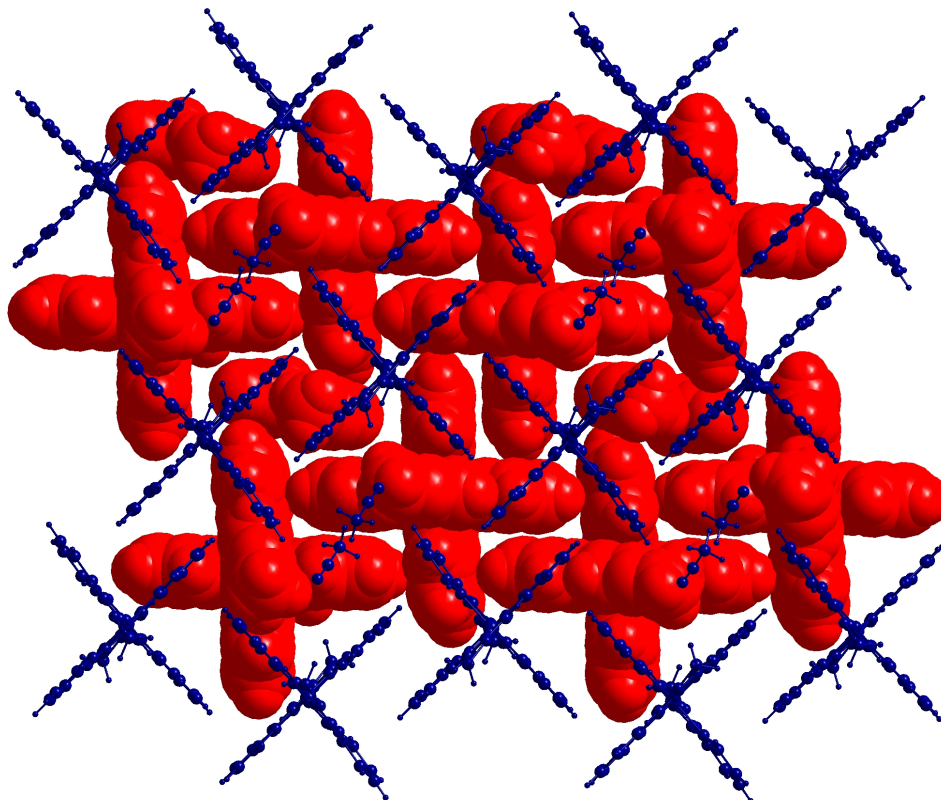


Figure 3.13 View of the two-dimensional layer structure in $[\text{Co}(\text{MeOtpy})_2][\text{PF}_6]_2 \cdot \text{MeCN}$ showing only the cations and acetonitrile molecules within the layer structure.

In this structure, the layers are also connected via $\text{C}-\text{H}\cdots\text{F}$ hydrogen bonds between the pyridyl rings and the anions. A second interaction between the layers of cations involves the oxygen atoms of the methoxy groups, which form weak hydrogen bonds to the aromatic protons with $\text{C}-\text{H}\cdots\text{O}$ distances of approximately 2.9 Å.

This hydrogen bonding interaction is more important in the packing of $[\text{Co}(\text{MeOtpy})_2][\text{PF}_6]_2$ and even disrupts the two-dimensional layer structure of terpy embraces. Instead, the cations form one-dimensional chains as shown in Figure 3.14 with each cation participating in four $\text{C}-\text{H}\cdots\text{O}$ hydrogen bonds ($\text{C}30^x-\text{H}301^x\cdots\text{O}1 = 2.68$ Å, $\text{C}15^{\text{vi}}-\text{H}151^{\text{vi}}\cdots\text{O}2 = 2.91$ Å; symmetry codes: $x = 2 - x, 1 - y, 1 - z$, $\text{vi} = 1 - x, 1 - y, 1 - z$).

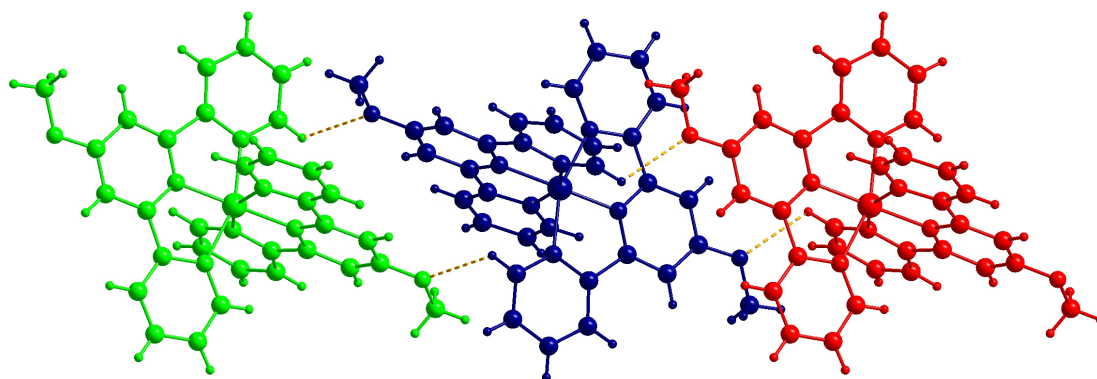


Figure 3.14 Chain of hydrogen bonded cations in the structure of $[\text{Co}(\text{MeOtpy})_2][\text{PF}_6]_2$.

Interaction between the chains is via $\text{C}-\text{H}\cdots\text{F}$ hydrogen bonds between the pyridyl rings and the anions with $\text{C}-\text{H}\cdots\text{F}$ distances as short as 2.3 Å. The arrangement of the chains is shown in Figure 3.15.

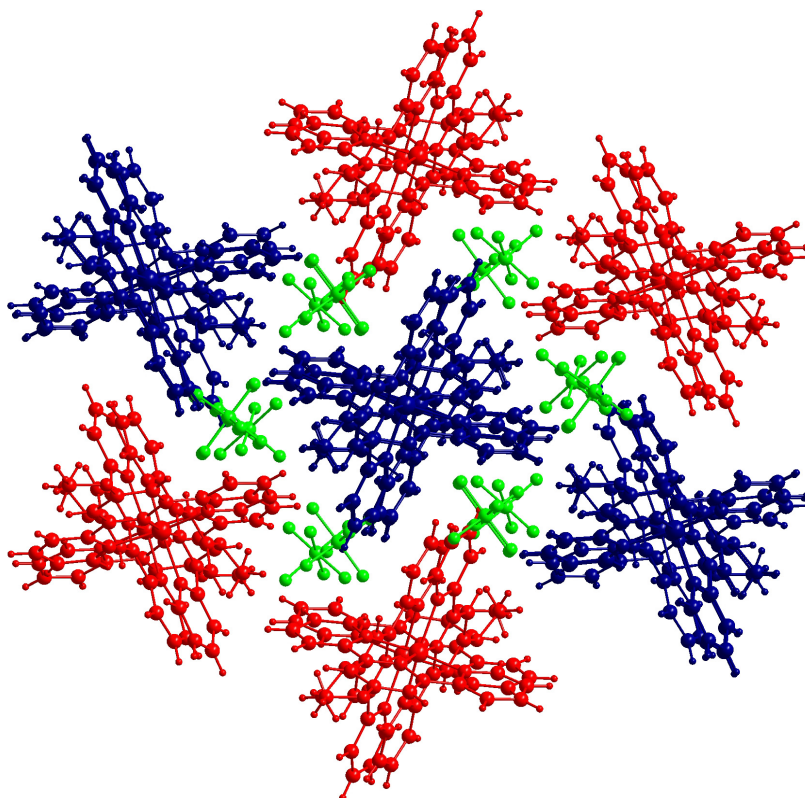


Figure 3.15 Packing of the chains in the structure of $[\text{Co}(\text{MeOtpy})_2][\text{PF}_6]_2$ showing the $[\text{PF}_6]^-$ anions (green) between the chains.

The same hydrogen bonding motif ($C15^{xi}-H151^{xi}\cdots O1 = 2.94 \text{ \AA}$, $C16^{ii}-H161^{ii}\cdots O2 = 2.82 \text{ \AA}$; symmetry codes: $xi = x, 0.5 - y, -0.5 - z$, $ii = x, 0.5 - y, 0.5 + z$) is observed in the structure of $[Co(EtOtpy)_2][PF_6]_2 \cdot 2MeCN$ and the one-dimensional chains are shown in Figure 3.16.

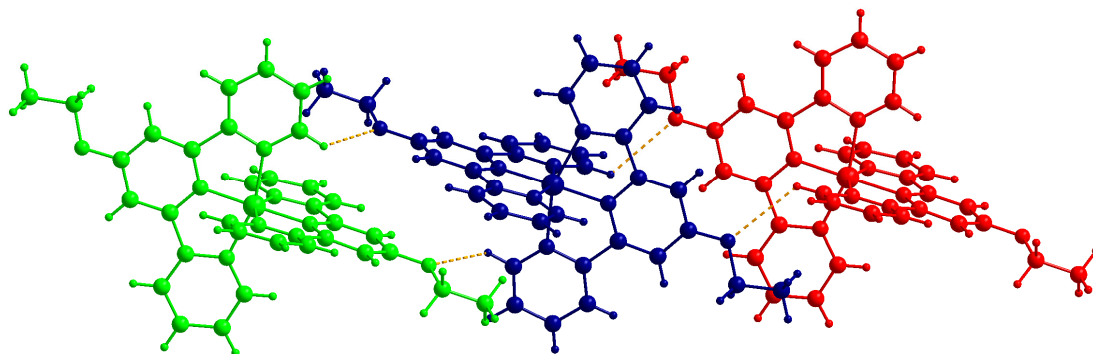


Figure 3.16 Chain of hydrogen bonded cations in the structure of $[Co(EtOtpy)_2][PF_6]_2 \cdot 2MeCN$.

Again, interaction between the chains is through $C-H\cdots F$ hydrogen bonds between the pyridyl rings and the anions. However, packing of the chains in $[Co(EtOtpy)_2][PF_6]_2 \cdot 2MeCN$ is not the same as that in $[Co(MeOtpy)_2][PF_6]_2$, as shown in Figure 3.17, and the acetonitrile molecules occupy channels between chains of cations. Interactions between the acetonitrile molecules and the cations are in the form of $C-H\cdots N$ hydrogen bonds ($C4-H41\cdots N7^{xi} = 2.77 \text{ \AA}$, $C16-H161\cdots N8 = 2.81 \text{ \AA}$; symmetry code: $xi = x, 0.5 - y, -0.5 - z$).

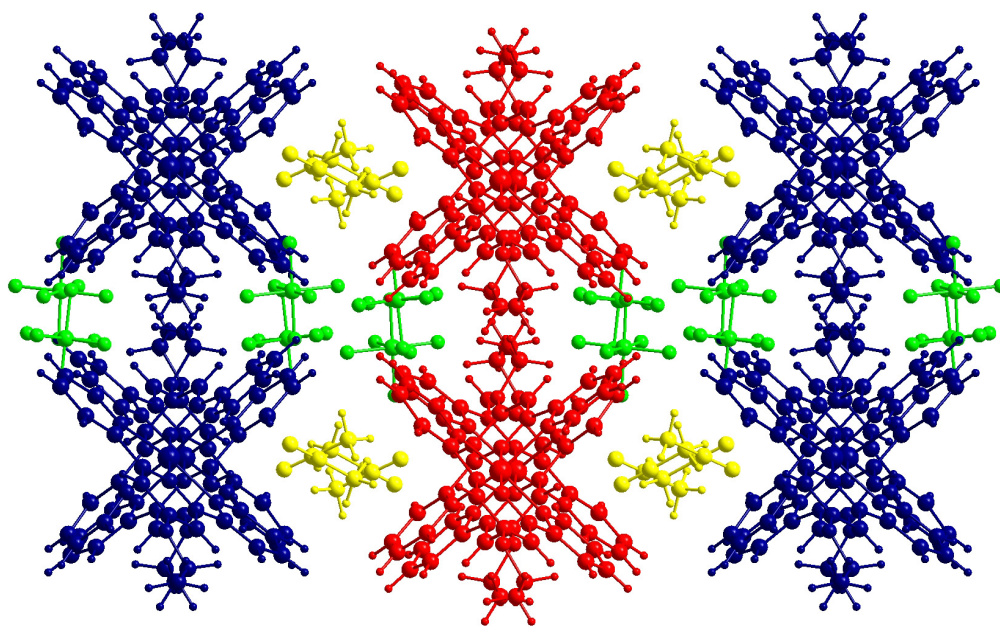


Figure 3.17 Packing of the chains in the structure of $[\text{Co}(\text{EtOtpy})_2][\text{PF}_6]_2 \cdot 2\text{MeCN}$ showing the $[\text{PF}_6]^-$ anions (green) between the chains and the acetonitrile molecules (yellow) in channels.

The structure of $[\text{Co}(\text{PrOtpy})_2][\text{PF}_6]_2 \cdot \text{MeCN}$ contains two independent cations in the asymmetric unit and the ligands in this structure show the greatest deviation from planarity (angle between the least-squared planes containing N5 and N6 = $14.71(6)^\circ$). In the packing of $[\text{Co}(\text{PrOtpy})_2][\text{PF}_6]_2 \cdot \text{MeCN}$, the tpy embrace motif is again observed. In this case, the cations are arranged in one-dimensional chains in which each cation participates in two offset face-to-face π - π (distance between the planes = 3.6 \AA) and four edge-to-face C-H \cdots π interactions (C-H \cdots π distances between 2.74 and 3.20 \AA). These chains interact with neighbouring chains via one further offset face-to-face π - π interaction and two edge-to-face interactions (C-H \cdots π distances 3.18 and 3.20 \AA), forming two-dimensional layers as shown in Figure 3.18. The arrangement of the cations in these layers is analogous to the arrangement in the structure of $[\text{Co}(\text{MeOtpy})_2][\text{PF}_6]_2 \cdot \text{MeCN}$, but the acetonitrile molecules are not incorporated into the layer. Two of the $[\text{PF}_6]^-$ anions in the structure are ordered, and take part in C-H \cdots F hydrogen bonds with the aromatic protons within the layer.

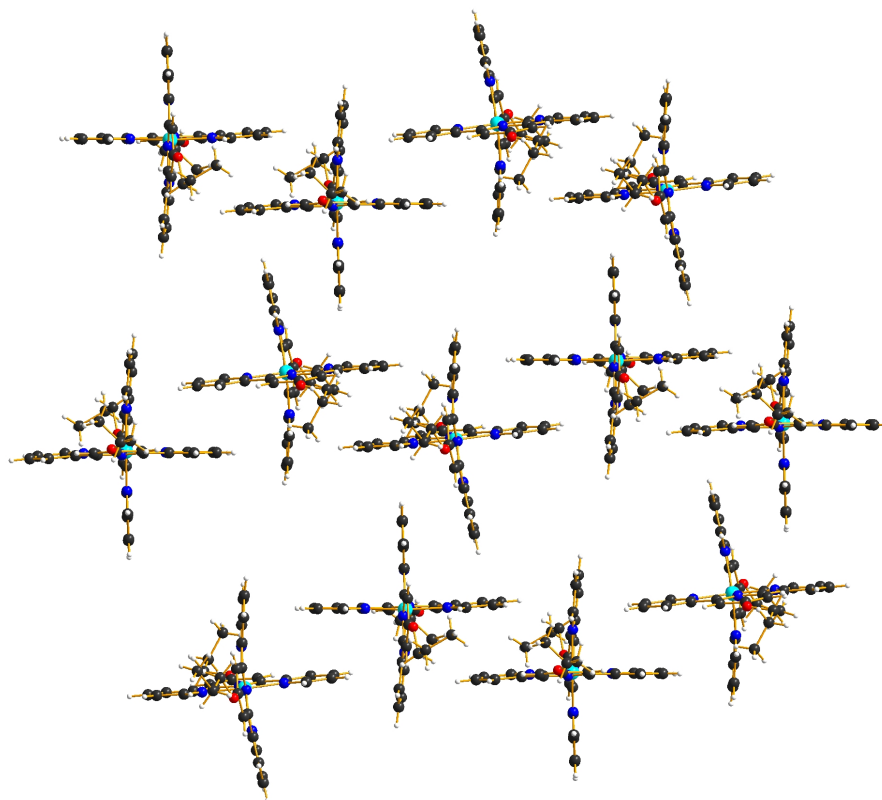


Figure 3.18 View of the cations in the two-dimensional layer structure in $[\text{Co}(\text{PrOtpy})_2][\text{PF}_6]_2 \cdot \text{MeCN}$, showing the offset face-to-face π - π and edge-to-face $\text{C}-\text{H} \cdots \pi$ interactions as well as the distortions in the ligands.

Unlike the packing in $[\text{Co}(\text{MeOtpy})_2][\text{PF}_6]_2 \cdot \text{MeCN}$, adjacent layers are not rotated by 45° relative to each other, but instead stack in a parallel fashion as shown in Figure 3.19. The propoxy groups of the ligands fit into the spaces in the layers (which are filled with acetonitrile molecules in $[\text{Co}(\text{MeOtpy})_2][\text{PF}_6]_2 \cdot \text{MeCN}$). The two remaining anions, which are highly disordered, and the acetonitrile molecules fill the remaining spaces between the layers. The acetonitrile molecules form $\text{C}-\text{H} \cdots \text{N}$ hydrogen bonds with aromatic protons from the terminal pyridine rings of the ligand ($\text{C}77-\text{H}771 \cdots \text{N}37^{\text{xii}} = 2.63 \text{ \AA}$, $\text{C}29-\text{H}291 \cdots \text{N}39^{\text{xiii}} = 2.61 \text{ \AA}$; symmetry codes: $\text{xii} = 1 - x, 1 - y, -1 - z$, $\text{xiii} = -1 + x, y, z$).

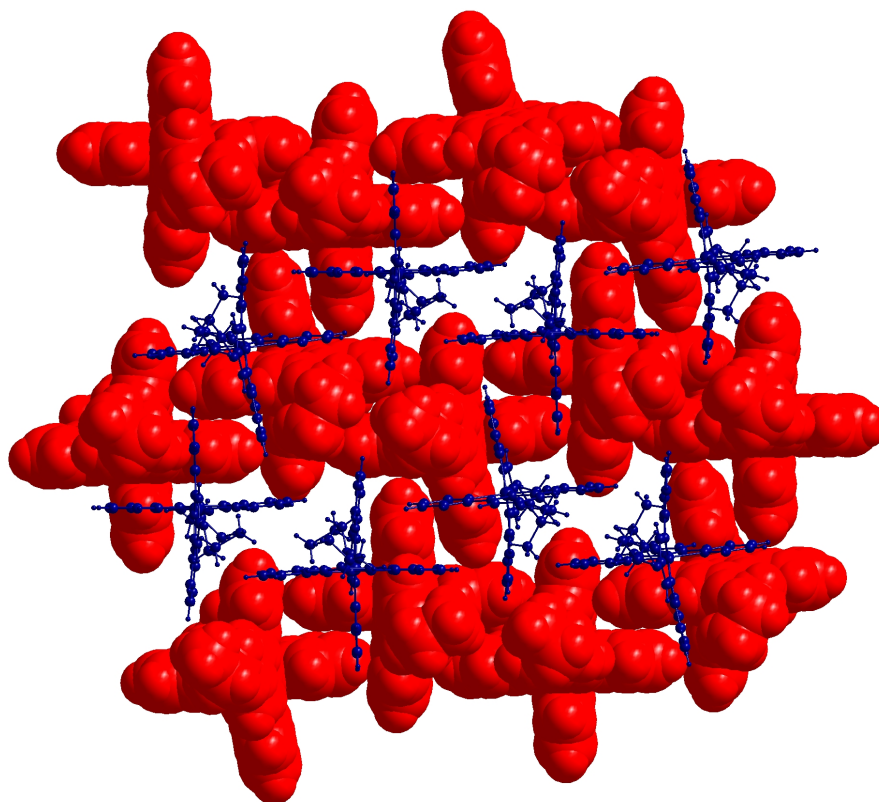


Figure 3.19 Packing of the layers in $[\text{Co}(\text{PrOtpy})_2][\text{PF}_6]_2 \cdot \text{MeCN}$ showing only the cations.

In the structure of $[\text{Co}(\text{PrOtpy})_2][\text{PF}_6]_2 \cdot \text{MeCN} \cdot \text{Et}_2\text{O}$, the cations again form one dimensional chains through two offset face-to-face π - π (distance between the planes = 3.4 Å) and four edge-to-face C-H \cdots π interactions (C14-H141 \cdots π^{xiv} = 2.92 Å, C17-H171 \cdots π^{xv} = 3.00 Å; symmetry codes: $\text{xiv} = 0.5 - x, -0.5 + y, 0.5 - z$, $\text{xv} = 0.5 - x, 0.5 + y, 0.5 - z$), but the arrangement of the cations is not the same as in $[\text{Co}(\text{PrOtpy})_2][\text{PF}_6]_2 \cdot \text{MeCN}$. These chains are arranged into a two-dimensional layer structure as shown in Figure 3.20, however, in this case interaction between the chains does not involve any further π - π or C-H \cdots π interactions. Instead, weak C-H \cdots F hydrogen bonds are the principal forces holding the layer structure together. These C-H \cdots F interactions also occur between cations in the same chain. The acetonitrile molecules occupy channels in the larger spaces between the chains of cations and interact via C-H \cdots N hydrogen bonds with alternating cations (C3-H31 \cdots N $^{\text{xvi}}$ = 2.53 Å; symmetry code: $\text{xvi} = 0.5 + x, 1.5 - y, -0.5 - z$). Highly disordered diethyl ether molecules occupy the smaller channels between the chains of cations.

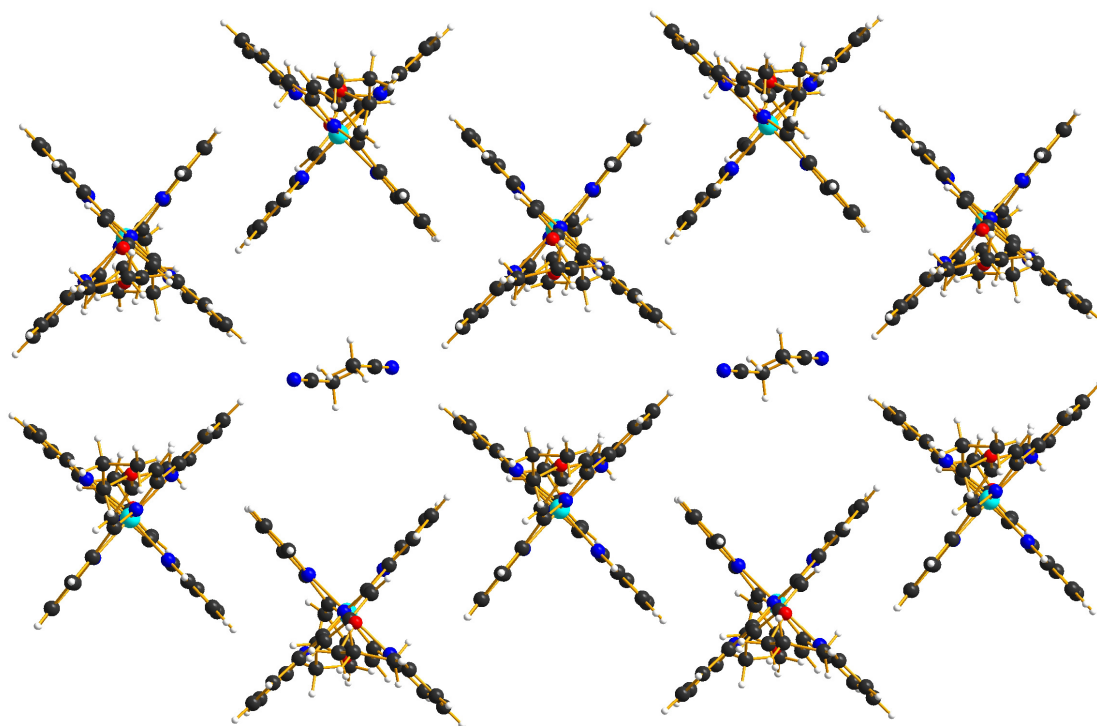


Figure 3.20 Two-dimensional layer structure in $[\text{Co}(\text{PrOtpy})_2][\text{PF}_6]_2 \cdot \text{MeCN} \cdot \text{Et}_2\text{O}$, showing only the cations and acetonitrile molecules.

Similar to the packing of the layers in $[\text{Co}(\text{PrOtpy})_2][\text{PF}_6]_2 \cdot \text{MeCN}$, the layers of cations in $[\text{Co}(\text{PrOtpy})_2][\text{PF}_6]_2 \cdot \text{MeCN} \cdot \text{Et}_2\text{O}$ also stack in a parallel fashion relative to one another, and the propoxy groups of the ligands fit into the spaces between the cations and acetonitrile molecules in the layers above and below as shown in Figure 3.21. The interactions between the layers are primarily $\text{C}-\text{H} \cdots \text{F}$ hydrogen bonds.

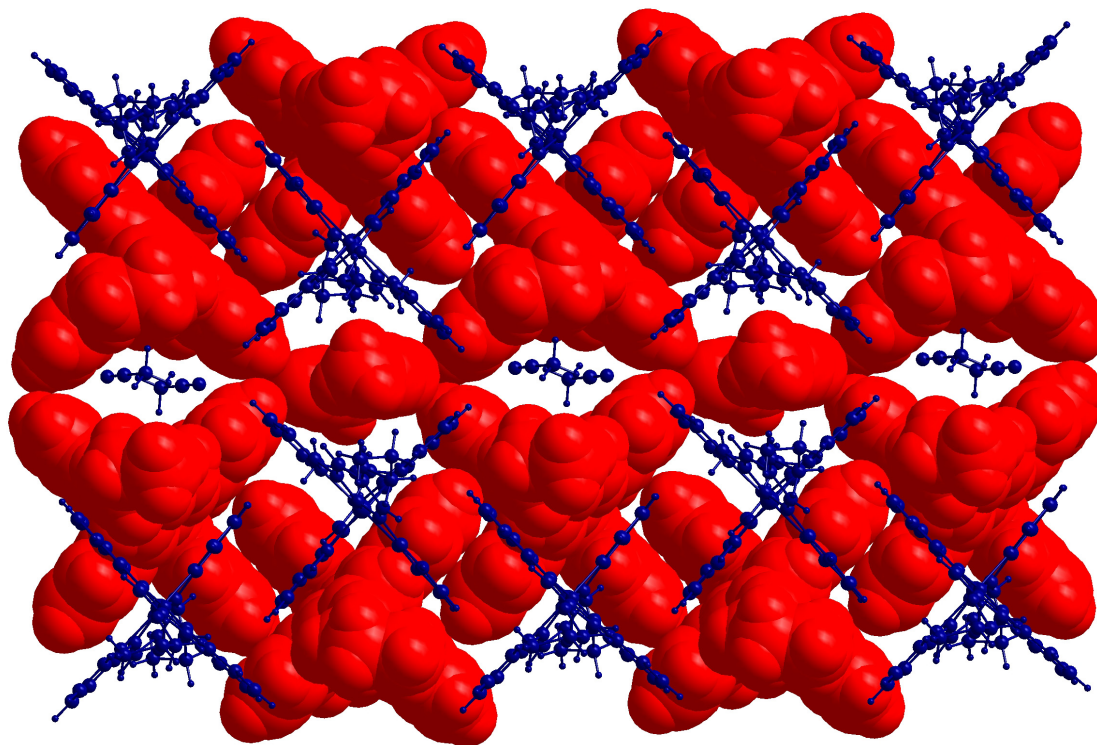
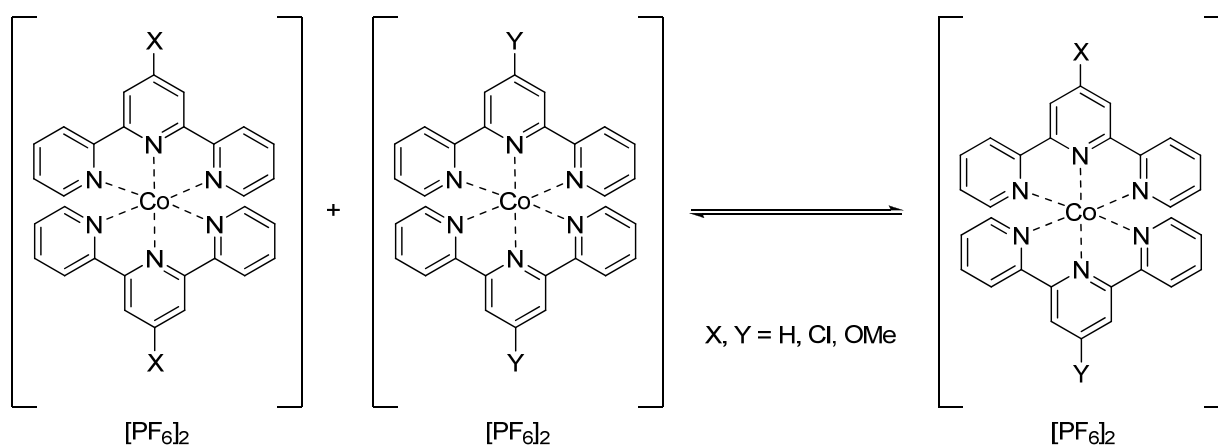


Figure 3.21 Packing of the layers in $[\text{Co}(\text{PrOtpy})_2][\text{PF}_6]_2 \cdot \text{MeCN} \cdot \text{Et}_2\text{O}$, showing only the cations and acetonitrile molecules.

In contrast, the bis(2,2':6',2''-terpyridine)cobalt(III) complexes show much less variation in their crystal packing. Previous crystallographic studies of bis(2,2':6',2''-terpyridine)cobalt(III) complexes^{145, 147, 161} have shown that the tpy embrace motif is disrupted by the increased number of anions and solvent molecules present in the structure. However, in both cases, π - π interactions were retained in one dimension. None of the cobalt(III) structures described in this chapter shows any π - π or $\text{C}-\text{H} \cdots \pi$ interactions, and the packing is primarily based on $\text{C}-\text{H} \cdots \text{F}$ cation-anion interactions. The structures of $2\{[\text{Co}(\text{tpy})_2][\text{PF}_6]_3\} \cdot 5\text{MeCN}$, $[\text{Co}(\text{Cltpy})_2][\text{PF}_6]_3 \cdot \text{MeCN}$ and $[\text{Co}(\text{EtOtpy})_2][\text{Br}]_3 \cdot \text{MeCN} \cdot \text{H}_2\text{O}$ show no cation-cation interactions. Cation-cation interactions in the structures $[\text{Co}(\text{MeOtpy})_2][\text{PF}_6]_3 \cdot \text{MeCN}$, $[\text{Co}(\text{EtOtpy})_2][\text{PF}_6]_3 \cdot \text{MeCN}$ and $2\{[\text{Co}(\text{PrOtpy})_2][\text{PF}_6]_3\} \cdot 5\text{MeCN}$ are exclusively weak $\text{C}-\text{H} \cdots \text{O}$ interactions between the alkoxy group and aromatic protons of adjacent molecules ($\text{C}-\text{H} \cdots \text{O}$ distances between 2.82 and 3.08 Å).

**3.4 Mononuclear cobalt(II) complexes as models for more complex systems:
How fast is the ligand exchange in bis(2,2':6',2''-terpyridine) cobalt(II)
hexafluorophosphate complexes?**

The rate of ligand exchange in bis(2,2':6',2''-terpyridine)cobalt(II) hexafluorophosphate complexes can be studied by ^1H NMR spectroscopy of a mixture of two homoleptic complexes. Ligand exchange between these complexes will give a heteroleptic species as shown in Scheme 3.5. The wide spectral width of ^1H NMR spectra of complexes containing the paramagnetic cobalt(II) ion (see Section 2.1) allows the separation of the signals corresponding to the three species. As a result, the reaction can be monitored more easily by ^1H NMR spectroscopy than for complexes with diamagnetic metal ions, where the signals corresponding to the terpyridine protons span a range of only approximately δ 2 ppm.



Scheme 3.5 Equilibration between two homoleptic bis(2,2':6',2''-terpyridine)cobalt(II) hexafluorophosphate complexes to give a heteroleptic complex.

Attempts have been made to isolate the heteroleptic species, but these have been unsuccessful due to fast ligand exchange,¹⁶² or characterisation of the final product is inconclusive (elemental analysis of the homoleptic complex is identical to that of a statistical mixture of the three complexes).¹⁶³⁻¹⁶⁵

Equimolar amounts of the complexes $[\text{Co}(\text{Xtpy})_2][\text{PF}_6]_2$ and $[\text{Co}(\text{Ytpy})_2][\text{PF}_6]_2$ (X, Y = H, Cl, OMe) were mixed in CD_3CN and the equilibration process was followed by ^1H NMR spectroscopy. The ^1H NMR spectra of equilibrium mixtures of each experiment contain sets of four resonances, corresponding to the two homoleptic complexes and the two ligands in the

heteroleptic complex. A representative example of the ^1H NMR spectrum of the equilibrium mixture of $[\text{Co}(\text{MeOtpy})_2][\text{PF}_6]_2$ and $[\text{Co}(\text{Cltpy})_2][\text{PF}_6]_2$ is given in Figure 3.22.

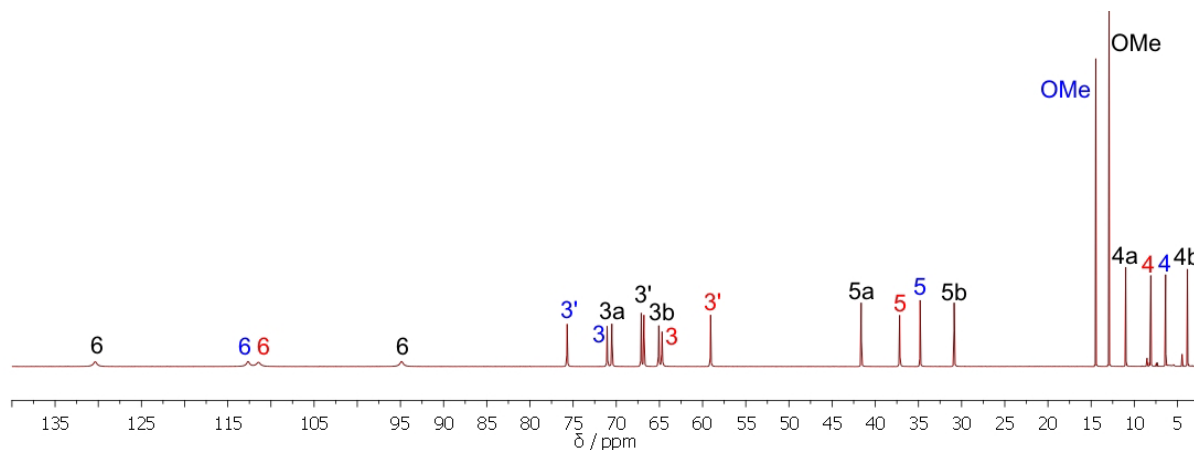


Figure 3.22 ^1H NMR spectrum of the equilibrium mixture of $[\text{Co}(\text{MeOtpy})_2][\text{PF}_6]_2$ (blue) $[\text{Co}(\text{Cltpy})_2][\text{PF}_6]_2$ (red) and $[\text{Co}(\text{MeOtpy})(\text{Cltpy})][\text{PF}_6]_2$ (black) (CD_3CN , 500 MHz, 295 K).

In all cases, the relative intensities of these signals are 1:1:1:1, corresponding to a statistical 1:2:1 distribution of the components in the mixture ($[\text{Co}(\text{Xtpy})_2][\text{PF}_6]_2$: $[\text{Co}(\text{Xtpy})(\text{Ytpy})][\text{PF}_6]_2$: $[\text{Co}(\text{Xtpy})_2][\text{PF}_6]_2$). One set of signals corresponds to each of the two homoleptic complexes and the heteroleptic complex shows a further two sets of signals in a 1:1 ratio corresponding to the two different ligands in the complex. The signals corresponding to the homoleptic complexes can be fully assigned by comparison with the spectra of the individual complexes. The signal corresponding to the methoxy group in the heteroleptic complexes containing 4'-methoxy-2,2':6',2''-terpyridine can be assigned on the basis of the integral (6 H). Similarly, the signal corresponding to $\text{H}^{4'}$ of the 2,2':6',2''-terpyridine ligand in the heteroleptic complexes can be assigned (2 H), and from the cross peak to this signal in the ^1H - ^1H COSY spectrum the $\text{H}^{3'}$ signal of this ligand can also be assigned. Consequently, the signal corresponding to $\text{H}^{3'}$ in the second ligand of the heteroleptic complexes containing 2,2':6',2''-terpyridine can also be assigned. Other terpyridine signals (H^3 , H^4 and H^5) from the heteroleptic complexes can be grouped together based on the cross peaks in the ^1H - ^1H COSY spectra, but it is not possible to determine which specific ligand these peaks belong to without a ^1H - ^1H NOE difference experiment of a mixture of the cobalt(II) and cobalt(III) complexes.⁹⁵

The equilibrium between $[\text{Co}(\text{tpy})_2][\text{PF}_6]_2$ and $[\text{Co}(\text{MeOtpy})_2][\text{PF}_6]_2$ was attained within 30 minutes of mixing the two components. In contrast, the equilibrium between $[\text{Co}(\text{tpy})_2][\text{PF}_6]_2$ and $[\text{Co}(\text{Cltpy})_2][\text{PF}_6]_2$ and between $[\text{Co}(\text{MeOtpy})_2][\text{PF}_6]_2$ and $[\text{Co}(\text{Cltpy})_2][\text{PF}_6]_2$ was reached only after approximately 8 hours. The progress of the reaction between $[\text{Co}(\text{MeOtpy})_2][\text{PF}_6]_2$ and $[\text{Co}(\text{Cltpy})_2][\text{PF}_6]_2$ as measured by ^1H NMR spectroscopy is shown in Figure 3.23.

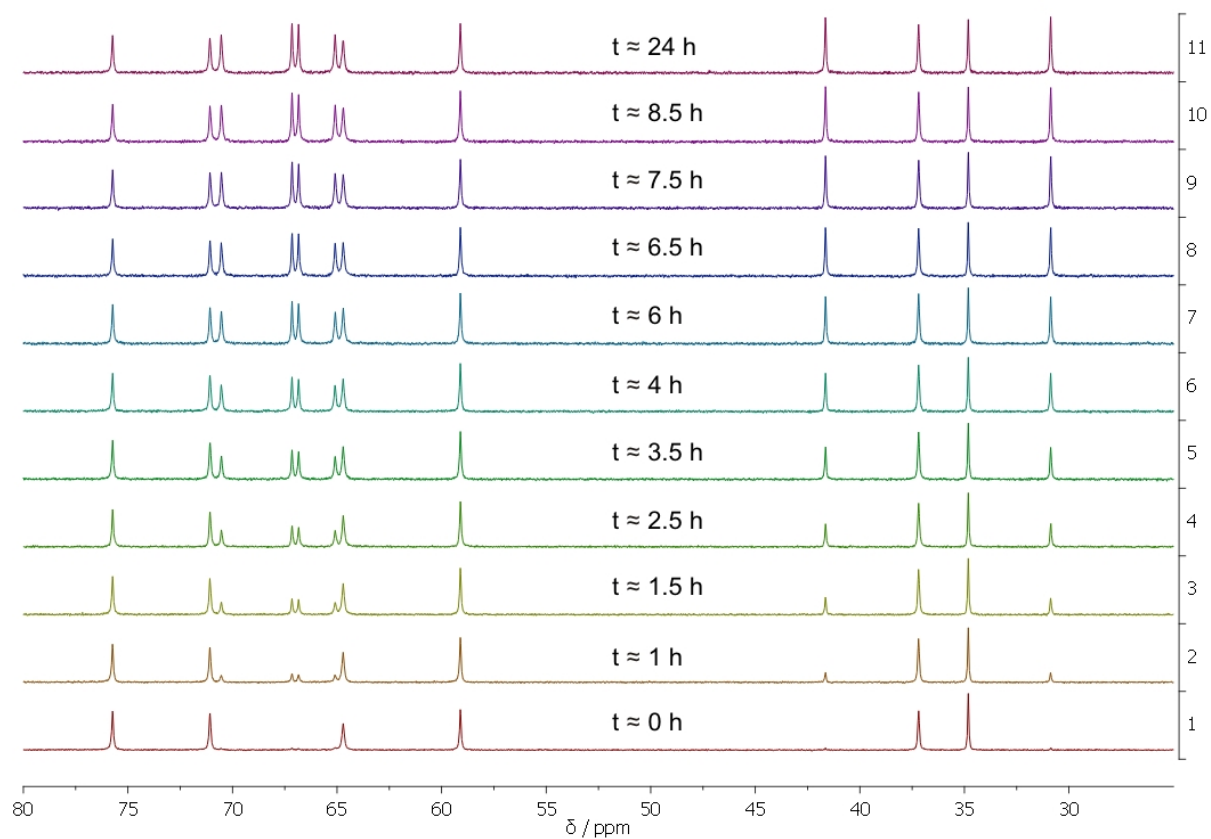


Figure 3.23 Stacked plot of the ^1H NMR spectra recorded during the equilibration of $[\text{Co}(\text{MeOtpy})_2][\text{PF}_6]_2$ and $[\text{Co}(\text{Cltpy})_2][\text{PF}_6]_2$ (CD_3CN , 250 MHz).

At first glance, it seems that the presence of the 4'-chloro-2,2':6',2''-terpyridine causes the rate of ligand exchange to slow down. However, previous studies of the rate of ligand exchange with 4'-substituted 2,2':6',2''-terpyridines^{90, 100, 162} suggest that the relationship between rate of ligand exchange and substituent is complicated and difficult to predict. Ligand exchange in cobalt(II) complexes of a set of 5,5''-substituted 2,2':6',2''-terpyridine ligands was found to be

extremely fast (equilibrium was attained within a few minutes of mixing).¹⁴³ However, the reactions were carried out in 30% acetonitrile in 0.01 M aqueous ammonium acetate. Addition of ammonium acetate to the reaction between $[\text{Co}(\text{MeOtpy})_2][\text{PF}_6]_2$ and $[\text{Co}(\text{Cltpy})_2][\text{PF}_6]_2$ caused the equilibrium to be established immediately after mixing the components instead of after approximately 8 hours without the added ammonium acetate. A similar accelerating effect has been found with addition of chloride ions.¹⁶² The effect of the anions on these complexes will be discussed further in Chapter 5. Ligand exchange in a 6-substituted 2,2':6',2''-terpyridine system was found to be slower than with either 5,5''- or 4'-substituted ligands.¹⁰⁰

In conclusion, the rate of ligand exchange appears to be dependent on a large number of variables and further studies under controlled conditions are needed in order to be able to compare rates of ligand exchange between different complexes.

3.5 Ligands and mononuclear cobalt(III) complexes as models for more complex systems: What size are the species in solution?

3.5.1 Measurement of diffusion coefficients using PGSE NMR spectroscopy

3.5.1.1 Mononuclear cobalt(III) complexes

Due to the short-spin lattice relaxation time (T_1) of the protons in cobalt(II) complexes, it is not possible to measure their diffusion coefficients using PGSE NMR spectroscopy. Diffusion coefficients for the homoleptic cobalt(III) complexes with 2,2':6',2''-terpyridine, 4'-chloro-2,2':6',2''-terpyridine, 4'-methoxy-2,2':6',2''-terpyridine and 4'-ethoxy-2,2':6',2''-terpyridine ligands were determined in DMSO- d_6 solution at a concentration of approximately 2 mM. Diffusion coefficients were measured for all signals and the average value over 4 experiments using different values for Δ and δ was taken. DOSY-type plots for all four complexes are shown in Figure 3.24. The viscosity of the solution was determined by the method described by Zuccaccia *et al.*¹¹⁹ The solvent viscosity (for DMSO- $d_6 = 2.195 \times 10^{-3} \text{ kg s}^{-1} \text{ m}^{-1}$)¹⁶⁶ was multiplied by a correction factor equal to the ratio of the diffusion coefficients of the residual solvent signal in the pure solvent and in the solution. The solution viscosity and averaged diffusion coefficients are shown in Table 3.3.

Complex	$\eta_{\text{solution}} / 10^{-3} \text{ kg s}^{-1} \text{ m}^{-1}$	$D_{\text{measured}} / 10^{-10} \text{ m}^2 \text{ s}^{-1}$
[Co(tpy) ₂][PF ₆] ₃	2.23	1.43±0.04
[Co(Cltpy) ₂][PF ₆] ₃	2.22	1.32±0.04
[Co(MeOtpy) ₂][PF ₆] ₃	2.24	1.33±0.04
[Co(EtOtpy) ₂][PF ₆] ₃	2.23	1.31±0.04

Table 3.3 Measured solution viscosity and diffusion coefficients for the mononuclear cobalt(III) complexes. Experimental error is *ca.* ±3%.

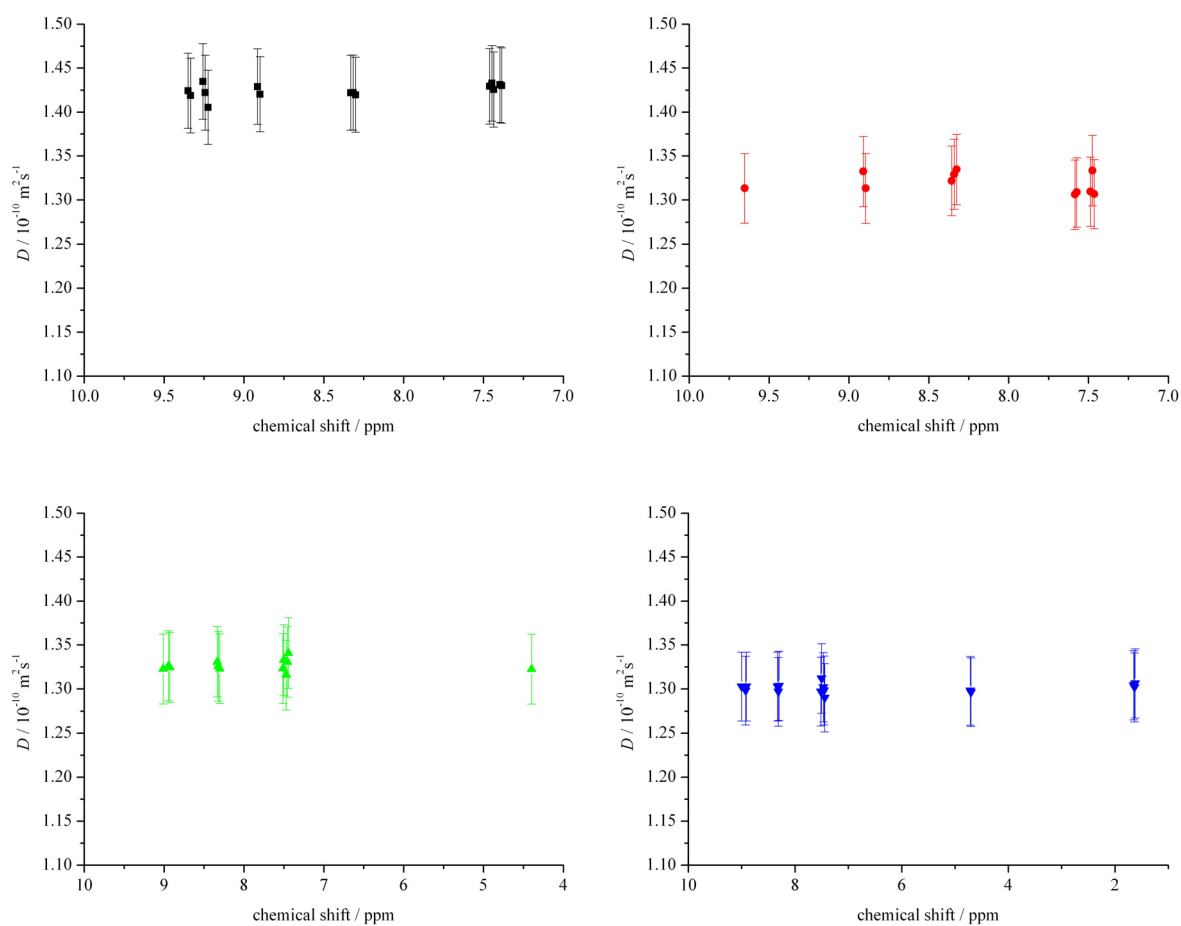


Figure 3.24 ¹H DOSY-type plots of [Co(tpy)₂][PF₆]₃ (black), [Co(Cltpy)₂][PF₆]₃ (red), [Co(MeOtpy)₂][PF₆]₃ (green), [Co(EtOtpy)₂][PF₆]₃ (blue) measured using $\Delta = 83.9$ ms and $\delta = 6.0$ ms (500 MHz, DMSO-d₆, 295 K).

3.5.1.2 Ligands

Diffusion coefficients for the ligands bis(terpyridyl)di(ethylene glycol), bis(terpyridyl)tri(ethylene glycol), bis(terpyridyl)tetra(ethylene glycol) and bis(terpyridyl)hexa(ethylene glycol) were determined in DMSO-d₆ at concentrations of less than 2 mM. Diffusion coefficients were measured only for the signals corresponding to the terpyridine protons and the average value over 4 experiments using different values for Δ and δ was taken. The viscosity of the solution was determined as described above.¹¹⁹ The solution viscosity and averaged diffusion coefficients are shown in Table 3.4.

Ligand	$\eta_{solution} / 10^{-3} \text{ kg s}^{-1} \text{ m}^{-1}$	$D_{measured} / 10^{-10} \text{ m}^2 \text{ s}^{-1}$
di	2.21	1.77±0.05
tri	2.20	1.73±0.05
tetra	2.22	1.68±0.05
hexa	2.20	1.59±0.05

Table 3.4 Measured solution viscosity and diffusion coefficients for the ligands (500 MHz, DMSO-d₆, 295 K). Experimental error is *ca.* ±3%.

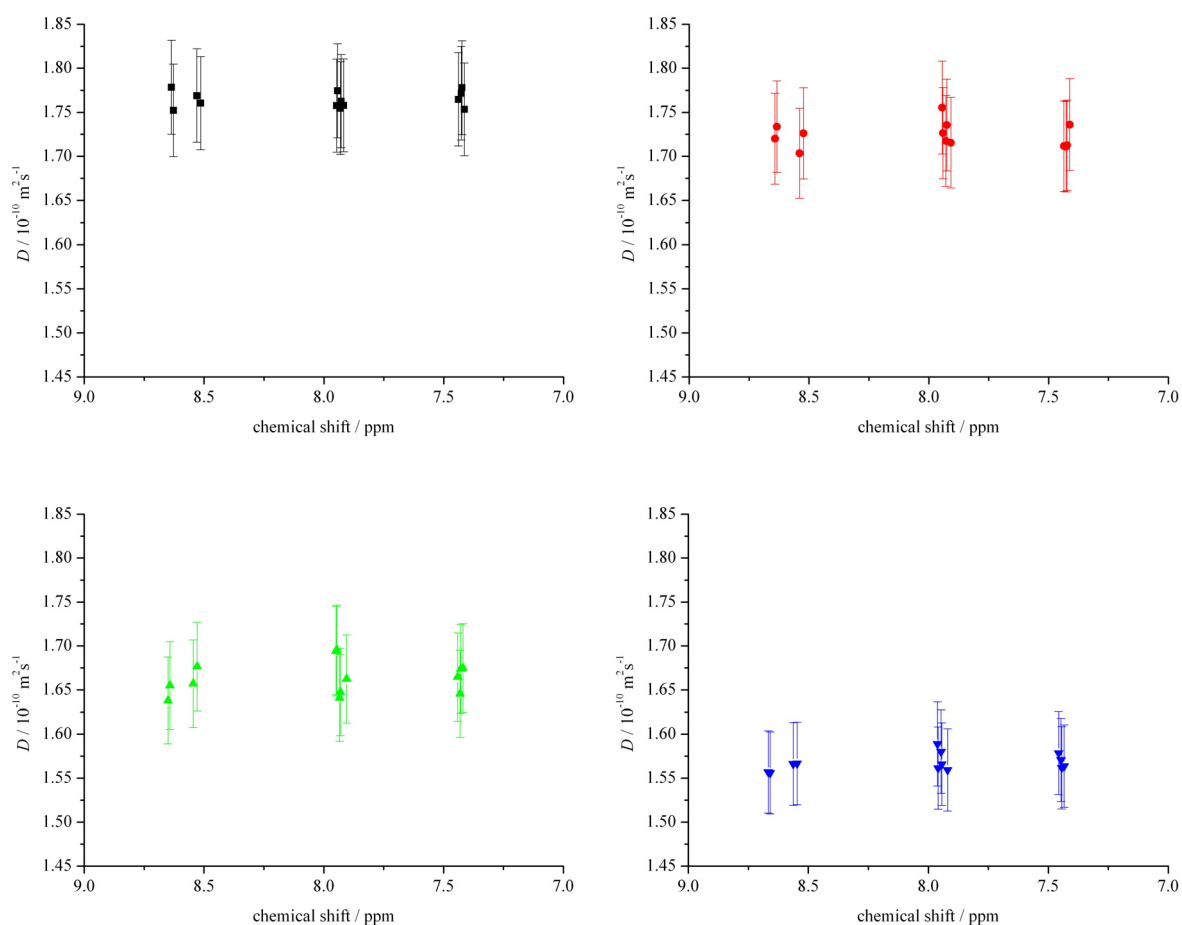


Figure 3.25 ^1H DOSY-type plots of bis(terpyridyl)di(ethylene glycol) (black), bis(terpyridyl)tri(ethylene glycol) (red), bis(terpyridyl)tetra(ethylene glycol) (green), and bis(terpyridyl)hexa(ethylene glycol) (blue) measured using $\Delta = 46.9$ ms and $\delta = 7.0$ ms (500 MHz, DMSO-d_6 , 295 K).

3.5.2 Models of the model compounds

3.5.2.1 Mononuclear cobalt(III) complexes

The crystal structures of the simple homoleptic cobalt(III) complexes with 2,2':6',2''-terpyridine, 4'-chloro-2,2':6',2''-terpyridine, 4'-methoxy-2,2':6',2''-terpyridine and 4'-ethoxy-2,2':6',2''-terpyridine ligands are described in section 3.3. As a first approximation, the shape of the cations could be considered to be spherical, however, a more accurate description of the cations with the substituted terpyridine ligands would be prolate ellipsoidal (see section 2.2.2). Considering the spherical model, the definition of the radius of the sphere remains ambiguous¹³⁵ and two models were used. Firstly, the average radius of each cation was

determined using equation 3.1 from its Connolly solvent excluded volume (calculated from the crystal structure data using ChemBio3D Ultra).

$$r = \sqrt[3]{\frac{3V}{4\pi}}$$

3.1

Secondly, as it has been suggested that disc-like crown ethers can be treated as spheres due to their rapid molecular motion,¹⁰⁹ the model sphere was considered to be tumbling rapidly in solution and the radius of the sphere to be equal to half the longest distance across the cation. The radii, r , of the spherical models and the calculated radii, r_e , of the prolate ellipsoid model (see Table 2.3) are shown in Table 3.5. The major axis of the prolate ellipsoid is considered to have a length, 2α , equal to the distance between the terminal atoms of the substituents in the 4'-position of the terpyridine (the longest distance across the cation in the crystal structure). The minor axis of length 2β is the width of a terpyridine unit. When the widths of the two terpyridine units in the complex were not equal, the longest distance was used. Of the two independent cations in the asymmetric unit in the crystal structure of $[\text{Co}(\text{tpy})_2][\text{PF}_6]_3$, the values for the largest cation were used.

Complex	$V / \text{\AA}^3$	$2\alpha / \text{\AA}$	$2\beta / \text{\AA}$	$r_{\text{volume}} / \text{\AA}$	$r_{\text{longest}} / \text{\AA}$	$r_{e, \text{prolate ellipsoid}} / \text{\AA}$
$[\text{Co}(\text{tpy})_2][\text{PF}_6]_3$	370	11.04	11.06	4.45	5.53	-- ^a
$[\text{Co}(\text{Cltpy})_2][\text{PF}_6]_3$	399	12.55	11.00	4.57	6.28	5.75
$[\text{Co}(\text{MeOtpy})_2][\text{PF}_6]_3$	413	15.32	11.03	4.62	7.66	6.15
$[\text{Co}(\text{EtOtpy})_2][\text{PF}_6]_3$	445	16.20	11.06	4.74	8.10	6.28

Table 3.5 Calculated volumes and radii for models of the complexes (a = The prolate ellipsoid model is not a suitable model for $[\text{Co}(\text{tpy})_2][\text{PF}_6]_3$ as the lengths of the two axes are equal).

As described in section 2.2.2, two corrections to the Stokes-Einstein equation need to be taken into account when dealing with non-spherical solutes of molecular size. These correction factors, ff_0 , for the shape of the molecule (see Table 2.3), and c , taking into account the size

of the molecule (see Equation 2.10), are given in Table 3.6. The Connolly solvent excluded volume (calculated from crystal structure data using ChemBio3D Ultra) of a molecule of DMSO is 65.3 \AA^3 . Assuming that the DMSO molecule is spherical, its radius can be calculated, using equation 3.1, to be 2.50 \AA .

Complex	$f/f_{0,prolate\ ellipsoid}$	C_{volume}	$C_{longest}$	$C_{prolate\ ellipsoid}$
[Co(tpy) ₂][PF ₆] ₃	-- ^a	0.840	0.895	-- ^a
[Co(Cltpy) ₂][PF ₆] ₃	1.00	0.847	0.918	0.903
[Co(MeOtpy) ₂][PF ₆] ₃	1.01	0.850	0.946	0.915
[Co(EtOtpy) ₂][PF ₆] ₃	1.01	0.857	0.952	0.919

Table 3.6 Correction factors for models of the complexes (a = The prolate ellipsoid model is not a suitable model for [Co(tpy)₂][PF₆]₃ as the lengths of the two axes are equal).

The calculated radii and correction factors for each model can then be substituted into the modified Stokes-Einstein equation (equation 2.11), to calculate a diffusion coefficient, D , for each model for comparison with the measured values. The measured and calculated diffusion coefficients are shown in Table 3.7.

Complex	$D_{measured}$ / $10^{-10} \text{ m}^2 \text{ s}^{-1}$	D_{volume} / $10^{-10} \text{ m}^2 \text{ s}^{-1}$	$D_{longest}$ / $10^{-10} \text{ m}^2 \text{ s}^{-1}$	$D_{prolate\ ellipsoid}$ / $10^{-10} \text{ m}^2 \text{ s}^{-1}$
[Co(tpy) ₂][PF ₆] ₃	1.43±0.04	2.60	1.96	-- ^a
[Co(Cltpy) ₂][PF ₆] ₃	1.32±0.04	2.51	1.69	1.87
[Co(MeOtpy) ₂][PF ₆] ₃	1.33±0.04	2.46	1.33	1.70
[Co(EtOtpy) ₂][PF ₆] ₃	1.31±0.04	2.39	1.26	1.66

Table 3.7 Measured (500 MHz, DMSO-d₆, 295 K) and calculated diffusion coefficients for the complexes (a = The prolate ellipsoid model is not a suitable model for [Co(tpy)₂][PF₆]₃ as the lengths of the two axes are equal).

From the data in Table 3.7, it is clear that the best fit to the measured diffusion coefficients is provided by the spherical model with the radius equal to half the longest distance across the molecule. Hence, it is reasonable to make the assumption that non-spherical molecules may be treated as spheres due to their rapid molecular motion in solution. However, for larger, more slowly tumbling molecules or particles (e.g. colloidal particles), or for molecules diffusing in more viscous solvents, this assumption may not be correct. The fit of the calculated data to the measured data is not perfect and there are several possible explanations for the deviations. The complexes with the 2,2':6',2''-terpyridine and the 4'-chloro-2,2':6',2''-terpyridine ligands appear larger than predicted by the modified Stokes-Einstein equation. As the anions were not considered when modelling the size of the complex, this could indicate that the anions are more tightly bound to the cation in these complexes, thus increasing the molecular size. Alternatively, although the experiments were carried out at low concentration, it is also possible that aggregation of the complexes occurs.

3.5.2.2 Ligands

The crystal structure of the ligand bis(terpyridyl)tri(ethylene glycol) is described in section 3.2.1. In the crystal structure, the ligand adopts a planar, extended conformation. At first glance, it does not appear that this family of ligands could be described using a spherical approximation, and that the long rod model (see Table 2.3) would be more appropriate. This would require the assumption that the rotation around the longest axis (along the length of the ethyleneoxy chain) was fast, leading to an averaged circular cross-section. The long-rod model may not be valid for small axial ratios (see section 2.2.2), so the prolate ellipsoid model was also tested. As mentioned above, it has been suggested that disc-like crown ethers can be treated as spheres due to their rapid molecular motion.¹⁰⁹ It is conceivable therefore, that the linear bis(terpyridyl)oligo(ethylene glycol)s could also be treated as spherical if they were considered to be rotating more freely. The radius of the resulting sphere would depend on the centre of rotation, with the smallest possible sphere resulting from rotation about the centre of the molecule, and the largest sphere from rotation around one of the terpyridine end units. These four models are shown in Figure 3.26 and were used to estimate diffusion coefficients for the four bis(terpyridyl)oligo(ethylene glycol) ligands for comparison with the measured values.

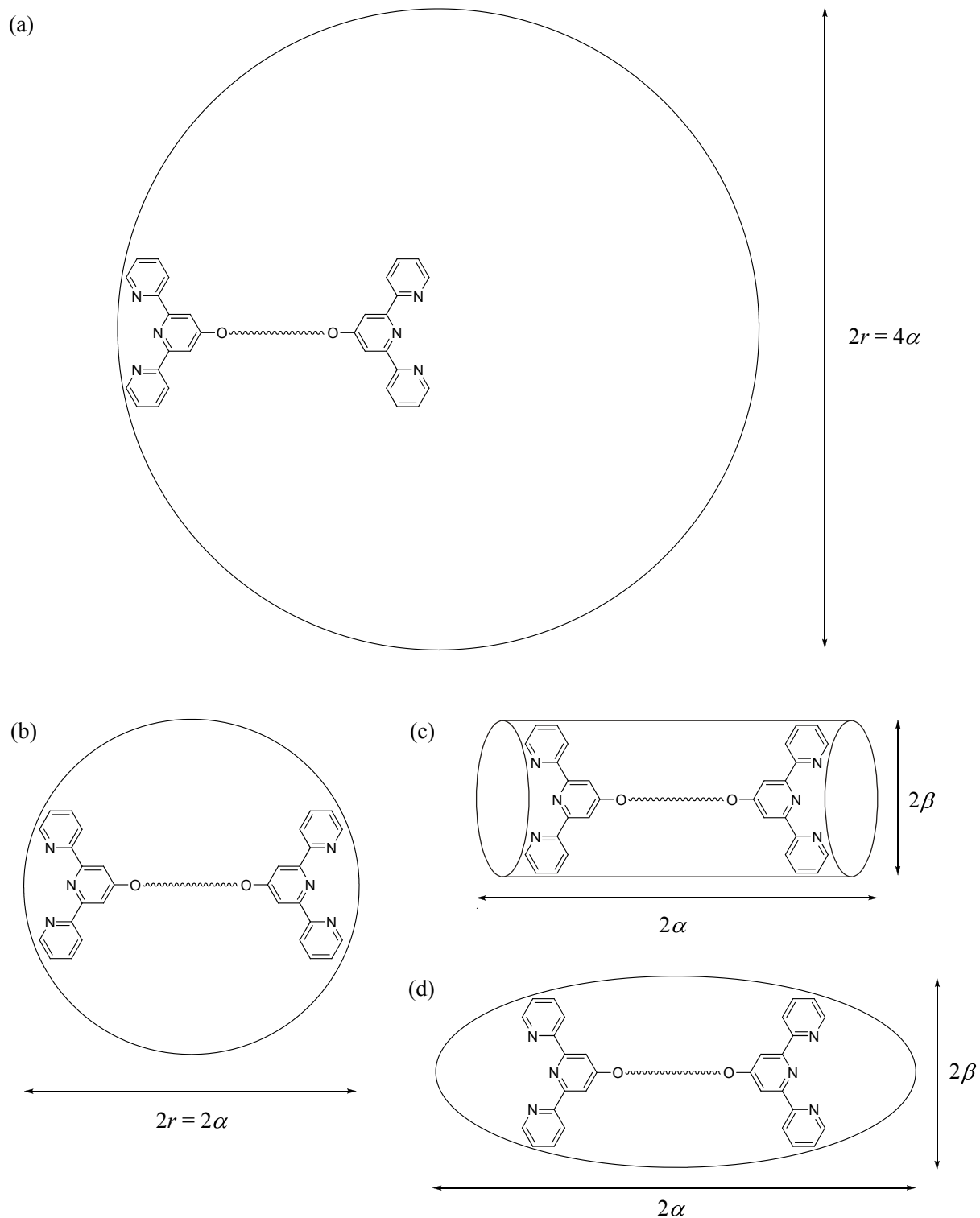


Figure 3.26 Models for determining the diffusion coefficients, D , of the bis(terpyridyl)oligo(ethylene glycol) ligands; (a) big sphere, (b) small sphere, (c) long rod and (d) prolate ellipsoid. 2α is the length of the ligand and 2β is the width of the terpyridine unit.

From the crystal structure, the length, 2α , of bis(terpyridyl)tri(ethylene glycol) (H31–H(131)^{iv}) is 24.3 Å. The length of the central ethyleneoxy unit (O2–O2^{iv}, symmetry code: iv = 2 – x, 1 – y, 2 – z) is 3.576(3) Å. The width of the terpyridine unit (H21–H141), 2β , is 11.3 Å. Assuming that all bond lengths and angles are equal, and the only difference between the fully extended conformation of all four ligands is the length of the ethyleneoxy chain, the length of each ligand in its planar, linear conformation can be calculated by simple addition or subtraction of the appropriate number of ethyleneoxy unit lengths from the total length of the tri(ethylene glycol)-based ligand and these values are given in Table 3.8. Also shown in Table 3.8 are the radii, r for the spherical models, or r_e for the non-spherical models (see Table 2.3). The correction factors to the Stokes-Einstein equation (see section 2.2.2), f/f_0 for the shape of the molecule and c for the size of the molecule are given in Table 3.9.

Ligand	2α / Å	$r_{big\ sphere}$ / Å	$r_{small\ sphere}$ / Å	$r_{e, long\ rod}$ / Å	$r_{e, prolate\ ellipsoid}$ / Å
di	20.69	20.69	10.34	7.90	6.91
tri	24.26	24.26	12.13	8.34	7.28
tetra	27.84	27.84	13.92	8.73	7.62
hexa	34.99	34.99	17.49	9.42	8.23

Table 3.8 Length, 2α , of the fully extended ligands and calculated radii for the models shown in Figure 3.26.

Ligand	$f/f_0, long\ rod$	$f/f_0, prolate\ ellipsoid$	$c_{big\ sphere}$	$c_{small\ sphere}$	$c_{long\ rod}$	$c_{prolate\ ellipsoid}$
di	1.31	1.03	0.994	0.972	0.950	0.933
tri	1.26	1.05	0.996	0.980	0.955	0.940
tetra	1.23	1.08	0.997	0.985	0.959	0.946
hexa	1.22	1.12	0.998	0.991	0.965	0.954

Table 3.9 Calculated shape (f/f_0) and size (c) correction factors for the models shown in Figure 3.26.

These values can then be substituted into the modified Stokes-Einstein equation (equation 2.11), to calculate a diffusion coefficient, D , for each model (shown in Table 3.10).

Ligand	$D_{measured}$ / $10^{-10} \text{ m}^2 \text{ s}^{-1}$	$D_{big \ sphere}$ / $10^{-10} \text{ m}^2 \text{ s}^{-1}$	$D_{small \ sphere}$ / $10^{-10} \text{ m}^2 \text{ s}^{-1}$	$D_{long \ rod}$ / $10^{-10} \text{ m}^2 \text{ s}^{-1}$	$D_{prolate \ ellipsoid}$ / $10^{-10} \text{ m}^2 \text{ s}^{-1}$
di	1.77±0.05	0.48	0.97	1.00	1.47
tri	1.73±0.05	0.41	0.83	0.98	1.36
tetra	1.68±0.05	0.35	0.71	0.95	1.26
hexa	1.59±0.05	0.28	0.57	0.89	1.12

Table 3.10 Measured (500 MHz, DMSO- d_6 , 295 K) and calculated diffusion coefficients, D , with correction for the shape and size of the molecule for the models shown in Figure 3.26.

As can be seen in Table 3.10, the diffusion coefficients calculated for models based on an extended conformation of the ligand do not fit the measured data well. The calculated diffusion coefficients based on the prolate ellipsoid model are most consistent with the measured data; however, this model does not adequately reflect the shape of the molecule.

Due to the flexibility of these ligands, it is unlikely that they adopt a rigid linear conformation in solution. Molecular modelling of these ligands (MMFF-level SPARTAN¹⁶⁷ calculations) suggested that the ethyleneoxy chain in each of the ligands is able to adopt a bent conformation such that the two terpyridine end units could undergo π -stacking interactions with each other. The energy minimised model of bis(terpyridyl)tri(ethylene glycol) is shown in Figure 3.27. This conformation could be envisaged in DMSO solution due to the lack of alternative favourable intermolecular interactions with the aromatic groups.

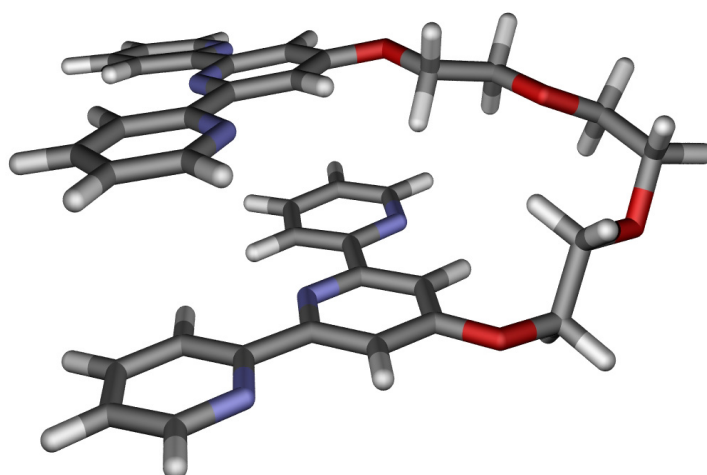


Figure 3.27 Molecular mechanics energy minimised model (MMFF, SPARTAN¹⁶⁷) of bis(terpyridyl)tri(ethylene glycol).

Based on molecular modelling of all four ligands, two further models for the estimation of the diffusion coefficients of these ligands were considered. In both cases, the ligand was assumed to be spherical. Firstly, the radius of the bent conformation was determined using equation 3.1 from the Connolly solvent excluded volume (calculated from the model using ChemBio3D Ultra). This would give the smallest possible radius based on this conformation of the ligand. Secondly it was assumed that due to rapid tumbling in solution, the molecule would behave as a sphere with a radius equal to half the longest distance across the molecule. These radii, r , and their associated size correction factors, c , are shown in Table 3.11, and the diffusion coefficients, D , calculated using equation 2.11, are shown in Table 3.12. A comparison of all calculated and measured diffusion coefficients is given in Figure 3.28.

Ligand	$V / \text{\AA}^3$	$r_{\text{volume}} / \text{\AA}$	$r_{\text{longest}} / \text{\AA}$	c_{volume}	c_{longest}
di	558	5.11	6.67	0.877	0.928
tri	594	5.21	7.44	0.882	0.943
tetra	650	5.37	7.65	0.888	0.946
hexa	758	5.66	8.76	0.899	0.960

Table 3.11 Calculated volumes, radii and correction factors for models based on the bent conformations of the ligands.

Ligand	$D_{measured}$ / $10^{-10} \text{ m}^2 \text{ s}^{-1}$	D_{volume} / $10^{-10} \text{ m}^2 \text{ s}^{-1}$	$D_{longest}$ / $10^{-10} \text{ m}^2 \text{ s}^{-1}$
di	1.77±0.05	2.19	1.58
tri	1.73±0.05	2.14	1.40
tetra	1.68±0.05	2.04	1.35
hexa	1.59±0.05	1.93	1.17

Table 3.12 Measured (500 MHz, DMSO-d₆, 295 K) and calculated diffusion coefficients, D , with correction for the size of the molecule for models based on the bent conformations of the ligands.

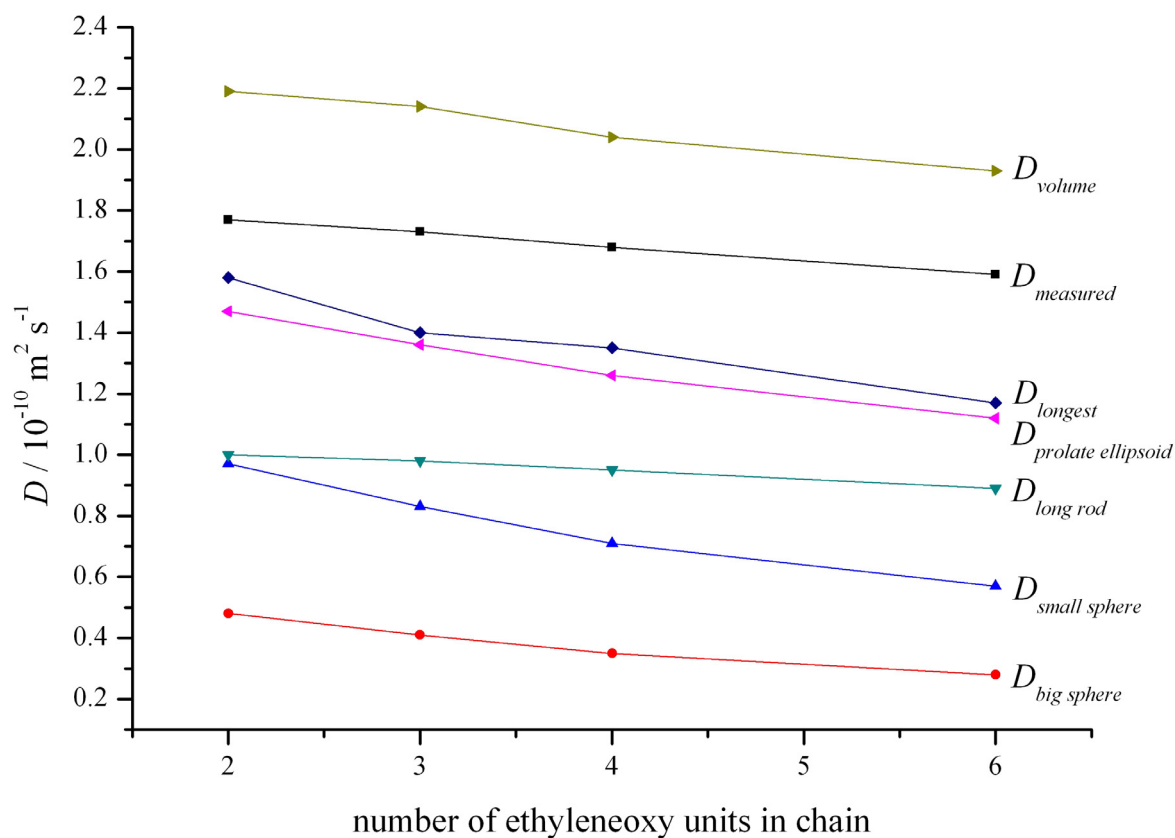


Figure 3.28 Graph of measured and calculated diffusion coefficients for all models of the ligands.

As shown in Table 3.10 and Table 3.12, and graphically in Figure 3.28, the best fit to the measured diffusion coefficients is given by the models which consider the ligands to have a

bent conformation. The radii used to calculate the diffusion coefficients for these models are only approximate due to the low level (MMFF) of the calculations used to model the ligands but it is clear that the measured diffusion coefficient lies between the largest possible diffusion coefficient (radius calculated from the volume) and the smallest possible calculated diffusion coefficient (longest radius of the molecule) based on the bent conformation of the ligands.

3.6 Conclusions

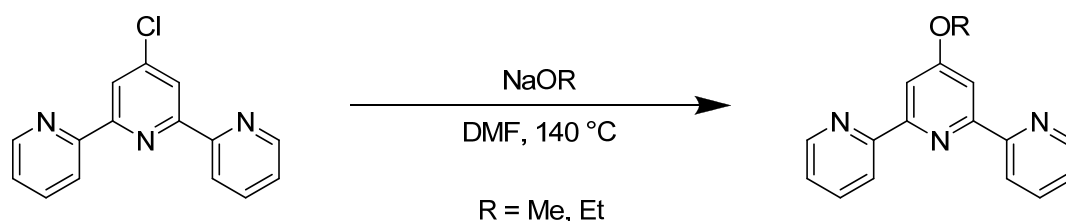
Two monotopic 4'-alkoxy-2,2':6',2"-terpyridine ligands, four ditopic bis(2,2':6',2"-terpyridine)oligo(ethylene glycol) ligands, and the homoleptic cobalt(II) and cobalt(III) complexes of four mononuclear 2,2':6',2"-terpyridine ligands were synthesised and fully characterised. Analysis of the X-ray crystal structures of these complexes revealed that the geometry around the cobalt(II) ion is highly dependent on many factors, including the substituent on the ligand and the presence of solvent molecules in the crystal structure. These complexes also displayed a wide variety of packing motifs in the crystal lattice, ranging from one-dimensional hydrogen-bonded and helical chains to several different two-dimensional layers of tpy embraces. The cobalt(III) complexes showed much less variation in both the geometry around the cobalt ion and the crystal packing. Attempts to examine the rate of ligand exchange in bis(2,2':6',2"-terpyridine)cobalt(II) hexafluorophosphate complexes were unfortunately not conclusive and further studies are needed to determine the effect of the substituent on the rate of ligand exchange. Finally, PGSE NMR spectroscopy was found to be a useful tool for determination of the size of both the homoleptic bis(2,2':6',2"-terpyridine)cobalt(III) hexafluorophosphate complexes and the bis(terpyridyl)oligo(ethylene glycol) ligands in DMSO-d₆ solution. Several models for calculating the diffusion coefficients of these model systems based on X-ray crystallographic data were tested, and it was found that both sets of compounds are best described using a spherical model, suggesting that the complexes are undergoing rapid rotation in solution. In addition, the ditopic ligands are proposed to have a bent structure in DMSO-d₆ solution.

3.7 Experimental

3.7.1 General ligand synthesis

2,2':6',2''-Terpyridine,¹⁶⁸ 4'-hydroxy-2,2':6',2''-terpyridine¹⁶⁹ and 4'-chloro-2,2':6',2''-terpyridine¹⁶⁹ were synthesised as previously described in the literature. 2,2':6',2''-Terpyridine was synthesised by Jörg Duschmalé and used as received.

3.7.2 Synthesis of 4'-alkoxy-2,2':6',2''-terpyridine ligands



3.7.2.1 Synthesis of 4'-methoxy-2,2':6',2''-terpyridine^{138, 139}

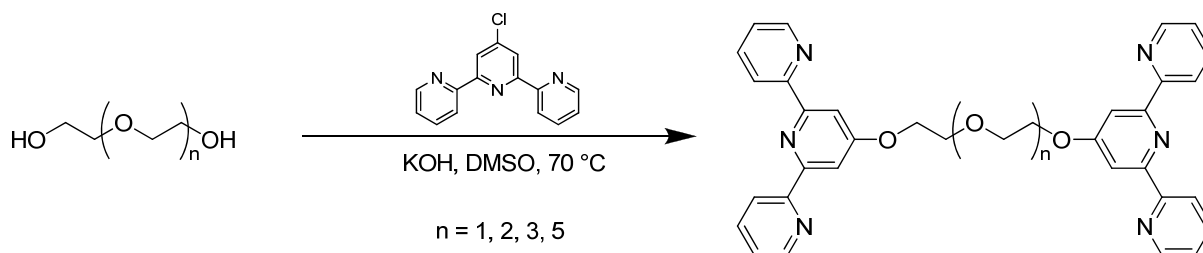
Sodium methoxide was prepared by slowly adding very small pieces of sodium (*ca.* 0.20 g, 4.3 mmol) to methanol (30 cm³) at room temperature. Once all the sodium had reacted, the solvent was removed *in vacuo* and the product was used without further purification. The sodium methoxide was suspended in dry DMF (20 cm³) and 4'-chloro-2,2':6',2''-terpyridine (1.0 g, 3.7 mmol) was added. The suspension was heated at 125 °C for 4 hours. After cooling to room temperature, the suspension was poured into water (100 cm³) and the off-white precipitate was collected by filtration, then purified by column chromatography (Al₂O₃, hexane-ethyl acetate (5:1)) and recrystallisation from hexane containing a few drops of chloroform (0.918 g, 93%). mp 112.1-113.9 °C (Lit.,¹³⁹ 56-57 °C; Lit.,¹³⁸ 212-213 °C); Found: C, 71.77; H, 4.93; N, 15.50%. C₁₆H₁₃N₄O·¼H₂O requires C, 71.76; H, 5.08; N, 15.50%; λ_{max}(CH₃CN)/nm (ε_{max}/M⁻¹cm⁻¹) 242 (31500), 276 (28100), 322 (4040); $\tilde{\nu}_{\text{max}}(\text{solid})/\text{cm}^{-1}$ 3101w, 3053w, 3005w, 2982w, 2939w, 2841w, 1601m, 1582s, 1560s, 1464m, 1429m, 1400m, 1358m, 1298w, 1252w, 1207s, 1175m, 1140w, 1115w, 1088m, 1063w, 1032s, 987m, 966w, 899m, 862m, 793s, 743m, 731m, 692m, 658m, 621m, 608m, 584m, 552w; δ_H(500 MHz, CDCl₃)/ppm 8.69 (d, *J* 4.6 Hz, 2 H, H⁶), 8.62 (d, *J* 7.9 Hz, 2 H, H³), 8.02 (s, 2 H, H^{3'}), 7.85 (td, *J* 1.5, 7.7 Hz, 2 H, H⁴), 7.33 (dd, *J* 5.3, 6.9 Hz, 2 H, H⁵), 4.03 (s, 3 H, OCH₃); δ_C(126 MHz, CDCl₃)/ppm 168.1 (C⁴), 157.3 (C^{2'}), 156.3 (C²), 149.3 (C⁶), 137.0 (C⁴), 124.1 (C⁵), 121.6 (C³), 107.2 (C^{3'}), 55.8 (OCH₃); *m/z* (MALDI-TOF, sinapinic acid) 264.2

($[M+H]^+$, 100%), 265.2 ($[M+2H]^+$, 50%). Crystals of MeOtpy suitable for X-ray diffraction were obtained by slow evaporation of a chloroform-hexane solution of the ligand at room temperature.

3.7.2.2 Synthesis of 4'-ethoxy-2,2':6',2''-terpyridine^{59, 139}

Sodium ethoxide (0.254 g, 3.74 mmol) was suspended in dry DMF (10 cm³). 4'-Chloro-2,2':6',2''-terpyridine (0.50 g, 1.8 mmol) was added and the pale orange suspension was heated at 125 °C for 3 hours. After cooling to room temperature, the suspension was poured into water (100 cm³) to give a white precipitate which was collected by filtration and recrystallised from hexane containing a few drops of chloroform (0.453 g, 88%). mp 116.3-117.5 °C (Lit.,¹³⁹ 85-86 °C); Found: C, 73.41; H, 5.57; N, 15.19%. C₁₇H₁₅N₃O requires C, 73.63; H, 5.45; N, 15.19%; $\lambda_{\max}(\text{CH}_3\text{CN})/\text{nm}$ ($\epsilon_{\max}/\text{M}^{-1}\text{cm}^{-1}$) 241 (37900), 277 (35200); $\tilde{\nu}_{\max}(\text{solid})/\text{cm}^{-1}$ 3030w, 3049w, 3005w, 2980w, 2935w, 2901w, 2883w, 1601m, 1582m, 1558s, 1470m, 1443m, 1393m, 1379m, 1350m, 1242w, 1198s, 1157w, 1146w, 1113w, 1094m, 1067w, 1040s, 991m, 164m, 881m, 864m, 844w, 793s, 743m, 733m, 698m, 658m, 619m, 569m; $\delta_{\text{H}}(500 \text{ MHz, CDCl}_3)/\text{ppm}$ 8.69 (d, J 4.5 Hz, 2 H, H⁶), 8.61 (d, J 7.9 Hz, 2 H, H³), 8.01 (s, 2 H, H^{3'}), 7.85 (td, J 1.5, 7.8 Hz, 2 H, H⁴), 7.32 (dd, J 5.2, 6.9 Hz, 2 H, H⁵), 4.30 (q, J 7.0 Hz, 2 H, tpyOCH₂CH₃), 1.49 (t, J 7.0 Hz, 3 H, tpyOCH₂CH₃); $\delta_{\text{C}}(126 \text{ MHz, CDCl}_3)/\text{ppm}$ 167.4 (C^{4'}), 157.3 (C^{2'}), 156.4 (C²), 149.3 (C⁶), 137.0 (C⁴), 124.0 (C⁵), 121.6 (C³), 107.6 (C^{3'}), 64.1 (tpyOCH₂CH₃), 14.8 (tpyOCH₂CH₃); m/z (MALDI-TOF, sinapinic acid) 278.3 ($[M+H]^+$, 100%).

3.7.3 Synthesis of bis(terpyridyl)oligo(ethylene glycol) ligands



3.7.3.1 General procedure

The glycol (1 eq) was dissolved in dry DMSO. Coarsely ground potassium hydroxide (10 eq) was added and the suspension was stirred at 70 °C for 1 hour. 4'-Chloro-2,2':6',2''-terpyridine (2.5 eq) was added and the brown suspension was stirred at 70 °C for a further 20-24 hours.

After cooling to room temperature, the pale orange suspension was poured into water (150 cm³) to give a white precipitate or emulsion which was extracted with chloroform (4 x 75 cm³). The combined organic fractions were washed with water, dried over anhydrous sodium sulfate and the solvent was removed *in vacuo*. If necessary, the product was purified by column chromatography (Al₂O₃, chloroform) and recrystallisation from chloroform-ethanol.

3.7.3.2 Synthesis of bis(terpyridyl)di(ethylene glycol)^{38, 39}

Reaction of di(ethylene glycol) (0.301 g, 2.84 mmol), potassium hydroxide (1.59 g, 28.4 mmol) and 4'-chloro-2,2':6',2''-terpyridine (1.90 g, 7.10 mmol) for 20 hours gave a white solid (1.42 g, 88%). mp 180.4-181.5 °C (Lit.,³⁹ 185 °C); Found: C, 70.33; H, 4.96; N, 14.34%. C₃₄H₂₈N₆O₃·³/₄H₂O requires C, 70.15; H, 5.11; N, 14.44%; λ_{max}(CH₂Cl₂)/nm (ε_{max}/M⁻¹cm⁻¹) 243 (62700), 278 (60400); ν̃_{max}(solid)/cm⁻¹ 2881w, 1582s, 1558s, 1470m, 1443m, 1404m, 1346m, 1315w, 1250w, 1200s, 1134m, 1092m, 1041m, 991m, 972m, 918w, 868m, 845w, 787s, 729s, 698m, 660m, 582s, 521s; δ_H(500 MHz, CDCl₃)/ppm 8.66 (d, *J* 4.0 Hz, 4 H, H⁶), 8.58 (d, *J* 7.9 Hz, 4 H, H³), 8.04 (s, 4 H, H^{3'}), 7.82 (td, *J* 1.7, 7.8 Hz, 4 H, H⁴), 7.30 (dd, *J* 5.3, 6.9 Hz, 4 H, H⁵), 4.44 (m, 4 H, tpyOCH₂CH₂), 4.05 (m, 4 H, tpyOCH₂CH₂); δ_C(126 MHz, CDCl₃)/ppm 167.2 (C^{4'}), 157.3 (C^{2'}), 156.3 (C²), 149.3 (C⁶), 136.9 (C⁴), 124.0 (C⁵), 121.5 (C³), 107.7 (C^{3'}), 70.0 (tpyOCH₂CH₂), 68.1 (tpyOCH₂CH₂); *m/z* (MALDI-TOF, sinapinic acid) 569.9 ([M+H]⁺, 100), 570.9 ([M+2H]⁺, 45).

3.7.3.3 Synthesis of bis(terpyridyl)tri(ethylene glycol)⁸²

Reaction of tri(ethylene glycol) (0.224 g, 1.49 mmol), potassium hydroxide (0.838 g, 14.9 mmol) and 4'-chloro-2,2':6',2''-terpyridine (1.00 g, 3.74 mmol) for 24 hours gave an off-white solid (0.805 g, 88%). mp 170.5-171.1 °C; Found: C, 69.02; H, 5.23; N, 13.59%. C₃₆H₃₂N₆O₄·³/₄H₂O requires C, 69.05; H, 5.39; N, 13.42%; λ_{max}(CH₂Cl₂)/nm (ε_{max}/M⁻¹cm⁻¹) 243 (55600), 278 (54000); ν̃_{max}(solid)/cm⁻¹ 2939w, 2905w, 2878w, 1562s, 1466m, 1447m, 1408s, 1369w, 1346w, 1312w, 1277w, 1254w, 1204s, 1142s, 1092w, 1057m, 1037m, 988m, 922m, 864m, 791s, 729m, 698m, 656m, 617s, 582s, 521s; δ_H(500 MHz, CDCl₃)/ppm 8.66 (d, *J* 4.6 Hz, 4 H, H⁶), 8.59 (d, *J* 7.9 Hz, 4 H, H³), 8.03 (s, 4 H, H^{3'}), 7.82 (td, *J* 1.6, 7.7 Hz, 4 H, H⁴), 7.30 (dd, *J* 5.0, 6.7 Hz, 4 H, H⁵), 4.39 (m, 4 H, tpyOCH₂CH₂), 3.95 (m, 4 H, tpyOCH₂CH₂), 3.79 (s, 4 H, tpyOCH₂CH₂OCH₂), 3.79 (s, 4 H, tpyOCH₂CH₂OCH₂); δ_C(126 MHz, CDCl₃)/ppm 167.2 (C^{4'}), 157.3 (C^{2'}), 156.3 (C²), 149.2 (C⁶), 136.9 (C⁴), 124.0 (C⁵), 121.5 (C³), 107.7 (C^{3'}), 71.3 (tpyOCH₂CH₂OCH₂), 69.8 (tpyOCH₂CH₂), 68.0 (tpyOCH₂CH₂); *m/z* (MALDI-TOF,

sinapinic acid) 613.7 ($[M+H]^+$, 100), 614.7 ($[M+2H]^+$, 45). Crystals of bis(terpyridyl)tri(ethylene glycol) suitable for X-ray diffraction were obtained by slow diffusion of diethyl ether into a solution of the ligand in THF at room temperature.

3.7.3.4 Synthesis of bis(terpyridyl)tetra(ethylene glycol)⁸³

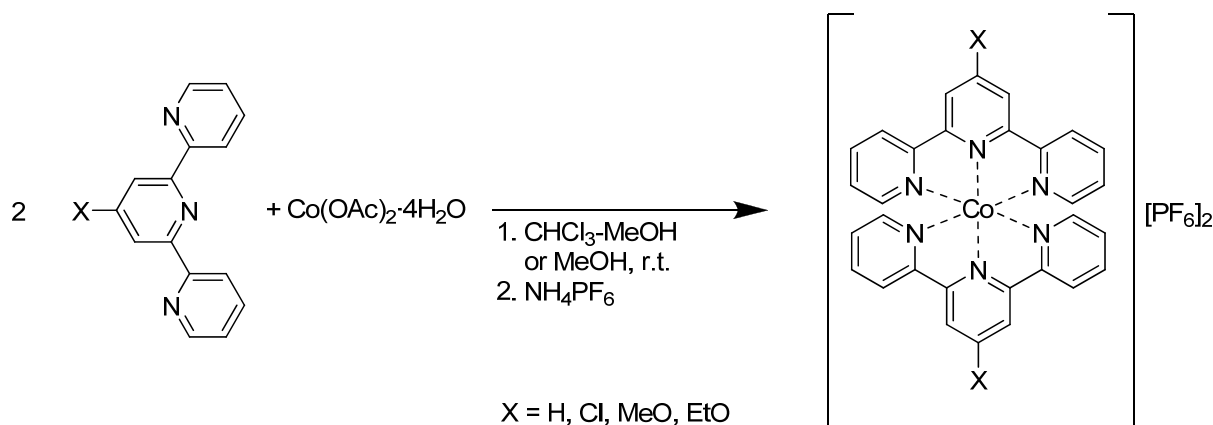
Reaction of tetra(ethylene glycol) (0.580 g, 2.99 mmol), potassium hydroxide (1.67 g, 29.9 mmol) and 4'-chloro-2,2':6',2''-terpyridine (2.00 g, 7.47 mmol) for 22 hours gave a white solid (1.59 g, 81%). mp 145.6-152.9 °C; Found: C, 68.96; H, 5.59; N, 12.70%. $C_{38}H_{36}N_6O_3 \cdot \frac{1}{4}H_2O$ requires C, 69.02; H, 5.59; N, 12.70%; $\lambda_{max}(CH_2Cl_2)/nm$ ($\epsilon_{max}/M^{-1}cm^{-1}$) 243 (53300), 278 (51900); $\tilde{\nu}_{max}(solid)/cm^{-1}$: 2943w, 2885w, 1582s, 1562s, 1466m, 1443m, 1404s, 1366w, 1350w, 1327m, 1250w, 1204s, 1146w, 1119m, 1092m, 1038m, 991m, 968w, 929w, 868s, 837w, 791s, 741 m, 729m, 698m, 660m, 644w, 575s, 521s; $\delta_H(500\text{ MHz, }CDCl_3)/ppm$ 8.66 (dd, J 0.8, 4.8 Hz, 4 H, H^6), 8.58 (d, J 7.9 Hz, 4 H, H^3), 8.02 (s, 4 H, H^3), 7.82 (td, J 1.7, 7.8 Hz, 4 H, H^4), 7.30 (ddd, J 1.0 Hz, 4.8 Hz, 7.4 Hz, 4 H, H^5), 4.38 (m, 4 H, tpyOCH₂CH₂), 3.93 (m, 4 H, tpyOCH₂CH₂), 3.74 (m, 4 H, tpyOCH₂CH₂OCH₂CH₂), 3.70 (m, 6 Hz 4 H, tpyOCH₂CH₂OCH₂CH₂); $\delta_C(126\text{ MHz, }CDCl_3)/ppm$ 167.2 (C^4), 157.3 (C^2), 156.3 (C^2), 149.2 (C^6), 137.0 (C^4), 124.0 (C^5), 121.5 (C^3), 107.7 (C^3), 71.2 (tpyOCH₂CH₂OCH₂CH₂), 71.0 (tpyOCH₂CH₂OCH₂CH₂), 69.7 (tpyOCH₂CH₂), 68.0 (tpyOCH₂CH₂); m/z (MALDI-TOF, α -cyano-3-hydroxycinnamic acid) 657.3 ($[M+H]^+$, 100).

3.7.3.5 Synthesis of bis(terpyridyl)hexa(ethylene glycol)⁸³

Reaction of hexa(ethylene glycol) (0.844 g, 2.99 mmol), potassium hydroxide (1.67 g, 29.9 mmol) and 4'-chloro-2,2':6',2''-terpyridine (2.00 g, 7.47 mmol) for 22 hours gave a yellow oil (2.18 g, 98%). Found: C, 65.48; H, 5.86; N, 10.80%. $C_{42}H_{44}N_6O_7 \cdot 1\frac{1}{2}H_2O$ requires C, 65.36; H, 6.14; N, 10.89%; $\lambda_{max}(CH_2Cl_2)/nm$ ($\epsilon_{max}/M^{-1}cm^{-1}$) 243 (50300), 278 (49100); $\tilde{\nu}_{max}(liquid)/cm^{-1}$: 2870m, 1600m 1582s, 1562s, 1468m, 1442m, 1406m, 1348m, 1297w, 1252w, 1204m, 1120m, 1093m, 1059m, 1040w, 991w, 969w, 869w, 794m, 745w, 699w, 632m, 622m, 542m; $\delta_H(500\text{ MHz, }CDCl_3)/ppm$ 8.66 (d, J 4.0 Hz, 4 H, H^6), 8.59 (d, J 7.9 Hz, 4 H, H^3), 8.02 (s, 4 H, H^3), 7.82 (t, J 7.7 Hz, 4 H, H^4), 7.30 (ddd, J 0.5, 5.6, 7.2 Hz, 4 H, H^5), 4.37 (m, 4 H, tpyOCH₂CH₂), 3.90 (m, 4 H, tpyOCH₂CH₂), 3.73 (m, 4 H, tpyOCH₂CH₂OCH₂CH₂), 3.66 (m, 4 H, tpyOCH₂CH₂OCH₂CH₂), 3.64 (s, 8 H, tpyOCH₂CH₂OCH₂CH₂OCH₂CH₂); $\delta_C(126\text{ MHz, }CDCl_3)/ppm$ 167.2 (C^4), 157.3 (C^2), 156.2 (C^2), 149.2 (C^6), 136.9 (C^4), 124.0 (C^5), 121.5 (C^3), 107.6 (C^3), 71.15

(tpyOCH₂CH₂OCH₂CH₂), 70.83 (tpyOCH₂CH₂OCH₂CH₂OCH₂CH₂), 70.75 (tpyOCH₂CH₂OCH₂CH₂), 69.59 (tpyOCH₂CH₂), 67.95 (tpyOCH₂CH₂); *m/z* (MALDI-TOF, sinapinic acid) 745.5 ([M+H]⁺, 100), 746.5 ([M+2H]⁺, 60).

3.7.4 Synthesis of mononuclear bis(terpyridine)cobalt(II) hexafluorophosphate complexes



3.7.4.1 General procedure

The ligand (2 eq) and cobalt(II) acetate tetrahydrate (1 eq) were dissolved in methanol or a chloroform-methanol solvent mixture (9:1) and the resulting orange solution was stirred at room temperature to give a dark brown solution. The product was precipitated by addition of excess ammonium hexafluorophosphate in methanol, collected by filtration through Celite, washed well with methanol and diethyl ether and redissolved in acetonitrile. The solvent was removed *in vacuo* to give a brown solid.

3.7.4.2 Synthesis of bis(2,2':6',2''-terpyridine)cobalt(II) hexafluorophosphate¹⁷⁰⁻¹⁷²

Reaction of 2,2':6',2''-terpyridine (0.100 g, 0.429 mmol) and cobalt(II) acetate tetrahydrate (0.053 g, 0.21 mmol) in the chloroform-methanol solvent mixture (20 cm³) for 20 minutes gave a brown solid (0.153 g, 88%). Found: C, 43.92; H, 2.70; N, 10.24%. C₃₀H₂₂N₆CoP₂F₁₂ requires C, 44.19; H, 2.72; N, 10.31%; $\tilde{\nu}_{\max}(\text{solid})/\text{cm}^{-1}$ 3130w, 3103w, 3061w, 1601m, 1578m, 1564m, 1502w, 1475m, 1452m, 1438m, 1402m, 1323m, 1298w, 1244m, 1194m, 1163m, 1107w, 1051m, 1030m, 1014m, 926w, 905w, 881w, 816s, 763s, 738s, 667m, 650m, 638m, 611m; $\delta_{\text{H}}(500 \text{ MHz, CD}_3\text{CN})/\text{ppm}$ 99.3 (s, br, 4 H, H⁶), 57.2 (s, 4 H, H³), 48.0 (s, 4 H, H^{3'}), 34.5 (s, 4 H, H⁵), 21.9 (s, 2 H, H^{4'}), 8.96 (s, 4 H, H⁴); *m/z* (ESI) 263.1 ([M-2PF₆]²⁺, 100), 669.7 ([M-PF₆]⁺, 20). Crystals of [Co(tpy)₂][PF₆]₂·2MeCN suitable for X-ray diffraction were

obtained by slow diffusion of diethyl ether into an acetonitrile solution of the complex at room temperature.

3.7.4.3 Synthesis of bis(4'-chloro-2,2':6',2''-terpyridine)cobalt(II) hexafluorophosphate¹³⁸

Reaction of 4'-chloro-2,2':6',2''-terpyridine (0.050 g, 0.19 mmol) and cobalt(II) acetate tetrahydrate (0.023 g, 0.094 mmol) in methanol (10 cm³) for 2 hours gave a brown solid (0.082 g, 99%). Found: C, 40.60; H, 2.44; N, 9.75%. C₃₀H₂₀N₆Cl₂CoP₂F₁₂ requires C, 40.75; H, 2.28; N, 9.50%; $\tilde{\nu}_{\max}(\text{solid})/\text{cm}^{-1}$ 3128w, 1601m, 1570m, 1558m, 1472m, 1425m, 1402m, 1344w, 1306w, 1292w, 1247m, 1159m, 1122m, 1097w, 1078m, 1053m, 1032w, 1014m, 976w, 912m, 881m, 818s, 789s, 744s, 727s, 690m, 654m, 640m, 611m; $\delta_{\text{H}}(500 \text{ MHz, CD}_3\text{CN})/\text{ppm}$ 111 (s, br, 4 H, H⁶), 64.7 (s, 4 H, H³), 59.1 (s, 4 H, H^{3'}), 37.2 (s, 4 H, H⁵), 8.08 (s, 4 H, H⁴); m/z (ESI) 297.0 ([M-2PF₆]²⁺, 100), 737.6 ([M-PF₆]⁺, 10). Crystals of [Co(Cltpy)₂][PF₆]₂ suitable for X-ray diffraction were obtained by slow evaporation of an acetonitrile solution of the complex at room temperature.

3.7.4.4 Synthesis of bis(4'-methoxy-2,2':6',2''-terpyridine)cobalt(II) hexafluorophosphate¹³⁸

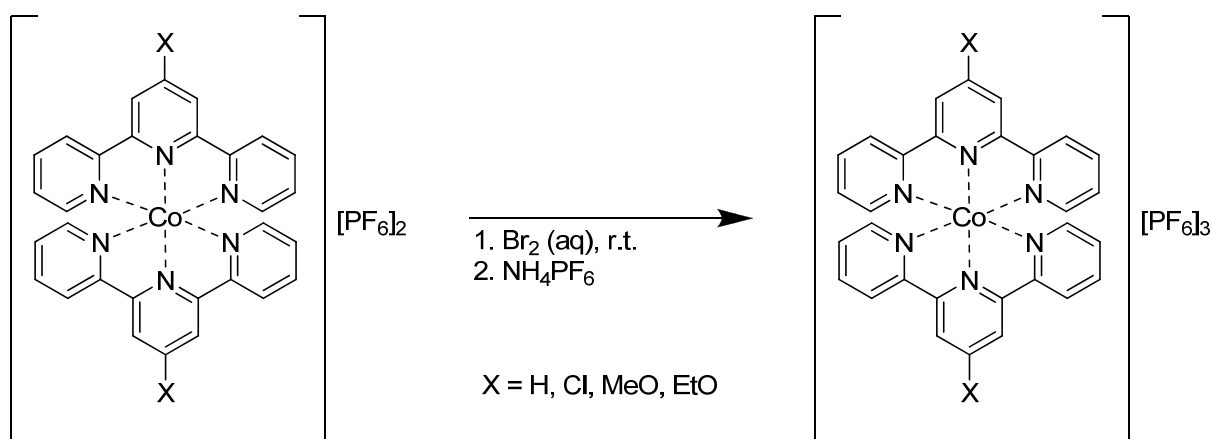
Reaction of 4'-methoxy-2,2':6',2''-terpyridine (0.100 g, 0.379 mmol) and cobalt(II) acetate tetrahydrate (0.047 g, 0.19 mmol) in the chloroform-methanol solvent mixture (20 cm³) for 45 minutes gave a brown solid (0.147 g, 89%). Found: C, 43.77; H, 2.90; N, 9.39%. C₃₂H₂₆N₆O₂CoP₂F₁₂ requires C, 43.90; H, 2.99; N, 9.60%; $\tilde{\nu}_{\max}(\text{solid})/\text{cm}^{-1}$ 1617m, 1601m, 1570m, 1560m, 1484m, 1439m, 1415m, 1367m, 1301w, 1232m, 1157m, 1059m, 1039m, 1014w, 908m, 825s, 793s, 746m, 727m, 696m, 660m, 553s, 547m; $\delta_{\text{H}}(500 \text{ MHz, CD}_3\text{CN})/\text{ppm}$ 113 (s, br, 4 H, H⁶), 75.8 (s, 4 H, H^{3'}), 71.1 (s, 4 H, H³), 34.8 (s, 4 H, H⁵), 14.5 (s, 6 H, OCH₃), 6.37 (s, 4 H, H⁴); m/z (ESI) 729.9 ([M-PF₆]⁺, 70), 292.7 ([M-2PF₆]²⁺, 100). Crystals of [Co(MeOtpy)₂][PF₆]₂ and [Co(MeOtpy)₂][PF₆]₂·MeCN suitable for X-ray diffraction were obtained by slow diffusion of diethyl ether into an acetonitrile solution of the complex at room temperature.

3.7.4.5 Synthesis of bis(4'-ethoxy-2,2':6',2''-terpyridine)cobalt(II) hexafluorophosphate

Reaction of 4'-ethoxy-2,2':6',2''-terpyridine (0.100 g, 0.361 mmol) and cobalt(II) acetate tetrahydrate (0.045 g, 0.18 mmol) in the chloroform-methanol solvent mixture (20 cm³) for 1 hour gave a brown solid (0.140 g, 86%). Found: C, 44.93; H, 3.50; N, 9.13%. C₃₄H₃₀N₆O₂CoP₂F₁₂ requires C, 45.20; H, 3.35; N, 9.30%; $\tilde{\nu}_{\max}(\text{solid})/\text{cm}^{-1}$ 1615m, 1603m,

1571m, 1558m, 1472m, 1440m, 1430m, 1398m, 1375m, 1359m, 1303w, 1254w, 1220m, 1160m, 1100w, 1092w, 1057m, 1040m, 1027m, 1016m, 966w, 904m, 867w, 819s, 789m, 748m, 728m, 700m, 661m, 640m, 618w; δ_{H} (500 MHz, CD_3CN)/ppm 112 (s, br, 4 H, H^6), 75.7 (s, 4 H, H^3), 70.9 (s, 4 H, H^3), 34.6 (s, 4 H, H^5), 15.2 (d, J 6 Hz, 4 H, $\text{tpyOCH}_2\text{CH}_3$), 7.27 (t, J 6 Hz, 6 H, $\text{tpyOCH}_2\text{CH}_3$), 6.38 (s, 4 H, H^4); m/z (ESI) 757.9 ($[\text{M}-\text{PF}_6]^+$, 80), 306.7 ($[\text{M}-2\text{PF}_6]^{2+}$, 100). Crystals of $[\text{Co}(\text{EtOtpy})_2][\text{PF}_6]_2 \cdot 2\text{MeCN}$ suitable for X-ray diffraction were obtained by slow diffusion of diethyl ether into an acetonitrile solution of the complex at room temperature.

3.7.5 Synthesis of mononuclear bis(terpyridine)cobalt(III) hexafluorophosphate complexes



3.7.5.1 General procedure

The cobalt(II) complex was suspended in water (5 cm^3). A saturated solution of bromine in water (*ca.* 5 drops in 5 cm^3) was added to give a bright orange suspension. This was stirred at room temperature for 20 hours, then excess ammonium hexafluorophosphate in water was added to give an orange precipitate. This was collected by filtration through Celite, washed well with water, ethanol and diethyl ether, then redissolved in acetonitrile. The solvent was removed *in vacuo* to give a yellow-orange solid.

3.7.5.2 Synthesis of bis(2,2':6',2''-terpyridine)cobalt(III) hexafluorophosphate

Reaction of bis(2,2':6',2''-terpyridine)cobalt(II) hexafluorophosphate (0.50 g, 0.061 mmol) gave a yellow-orange solid (0.032 g, 48%). Found: C, 37.43; H, 2.32; N, 8.75%. $\text{C}_{30}\text{H}_{22}\text{N}_6\text{CoP}_3\text{F}_{18}$ requires C, 37.52; H, 2.31; N, 8.75%; $\tilde{\nu}_{\text{max}}(\text{solid})/\text{cm}^{-1}$ 3096w, 3057w, 1609m, 1568m, 1558m, 1510w, 1485m, 1452s, 1408w, 1391w, 1332m, 1310w, 1248m,

1188w, 1177w, 1146w, 1124w, 1099m, 1056w, 1034m, 903w, 814s, 804s, 769s, 743s, 730s, 689m, 663m, 654m, 619m; δ_{H} (500 MHz, CD₃CN)/ppm 9.09 (A₂B, J 8.1 Hz, 2 H, H⁴), 9.00 (A₂B, J 8.0 Hz, 4 H, H³), 8.58 (d, J 8.0 Hz, 4 H, H³), 8.23 (t, J 7.8 Hz, 4 H, H⁴), 7.42 (t, J 6.8 Hz, 4 H, H⁵), 7.23 (d, J 5.8 Hz, 4 H, H⁶); δ_{C} (126 MHz, CD₃CN)/ppm 157.3 (C²), 157.0 (C²), 153.5 (C⁶), 146.8 (C⁴), 144.2 (C⁴), 132.1 (C⁵), 128.8 (C³), 128.4 (C³); m/z (ESI) 814.6 ([M-PF₆]⁺, 10), 669.7 ([M-2PF₆]⁺, 30), 335.0 ([M-2PF₆]²⁺, 20), 262.5 ([M-3PF₆]²⁺, 90), 175.2 ([M-3PF₆]³⁺, 100). Crystals of 2{[Co(tpy)₂][PF₆]₃}·5MeCN suitable for X-ray diffraction were obtained by slow diffusion of diethyl ether into an acetonitrile solution of the complex at room temperature.

3.7.5.3 Synthesis of bis(4'-chloro-2,2':6',2''-terpyridine)cobalt(III) hexafluorophosphate

Reaction of bis(4'-chloro-2,2':6',2''-terpyridine)cobalt(II) hexafluorophosphate (0.100 g, 0.113 mmol) gave a yellow-orange solid (0.094 g, 81%). Found: C, 35.98; H, 2.04; N, 8.99%. C₃₀H₂₀N₆Cl₂CoP₃F₁₈·CH₃CN requires C, 35.91; H, 2.17; N, 9.16%; $\tilde{\nu}_{\text{max}}$ (solid)/cm⁻¹ 3105w, 2257w 1684w, 1653w, 1603m, 1557m, 1485m, 1466w, 1427m, 1408w, 1348w, 1300w, 1248m, 1165w, 1117w, 1103w, 1080w, 1061w, 1032m, 908w, 897w, 879w 818s, 777s, 746s, 739s, 723s, 689m, 663m, 656m, 619m, 609w, 577m; δ_{H} (500 MHz, CD₃CN)/ppm 9.12 (s, 4 H, H³) 8.54 (dd, J 1.0 Hz, 8.0 Hz, 4 H, H³), 8.25 (td, J 1.2 Hz, 7.9 Hz, 4 H, H⁴), 7.47 (ddd, J 1.4 Hz, 5.9 Hz, 7.5 Hz, 4 H, H⁵), 7.35 (dd, J 0.8 Hz, 5.9 Hz, 4 H, H⁶); δ_{C} (126 MHz, CD₃CN)/ppm 157.8 (C⁴), 156.0 (C²), 155.4 (C²), 153.8 (C⁶), 144.4 (C⁴), 132.4 (C⁵), 129.2 (C³), 128.7 (C³); m/z (ESI) 883.1 ([M-PF₆]⁺, 70), 738.3 ([M-2PF₆]⁺, 100), 296.9 ([M-3PF₆]²⁺, 85). Crystals of [Co(Cltpy)₂][PF₆]₃·MeCN suitable for X-ray diffraction were obtained by slow diffusion of diethyl ether into an acetonitrile solution of the complex at room temperature.

3.7.5.4 Synthesis of bis(4'-methoxy-2,2':6',2''-terpyridine)cobalt(III) hexafluorophosphate

Reaction of bis(4'-methoxy-2,2':6',2''-terpyridine)cobalt(II) hexafluorophosphate (0.052 g, 0.059 mmol) gave a yellow-orange solid (0.045 g, 74 %). Found: C, 38.26; H, 2.85; N, 9.20%. C₃₂H₂₆N₆O₂CoP₃F₁₈·CH₃CN requires 38.47; H, 2.75; N, 9.24%; $\tilde{\nu}_{\text{max}}$ (solid)/cm⁻¹ 3120w, 3023w, 1619s, 1616s, 1569m, 1487s, 1444m, 1419m, 1371m, 1326w, 1311w, 1255w, 1230s, 1192w, 1163w, 1100m, 1101m, 1066m, 1042m, 1031m, 1013m, 901w, 882w, 820s, 808s, 779s, 750s, 740s, 719m, 698m, 663m, 656m; δ_{H} (500 MHz, CD₃CN)/ppm 8.61 (d, J 7.9 Hz, 4 H, H³), 8.57 (s, 4 H, H³), 8.21 (t, J 7.7 Hz, 4 H, H⁴), 7.44 (t, J 6.6 Hz, 4 H, H⁵), 7.36 (d, J 5.6 Hz, 4 H, H⁶), 4.47 (s, 6 H, OCH₃); δ_{C} (126 MHz, CD₃CN)/ppm 174.5 (C⁴), 157.9 (C²),

157.3 (C²), 153.4 (C⁶), 144.1 (C⁴), 131.9 (C⁵), 128.0 (C³), 115.7 (C^{3'}), 60.1 (OCH₃); *m/z* (ESI) 875.1 ([M-PF₆]⁺, 50), 730.3 ([M-2PF₆]⁺, 100), 365.2 ([M-2PF₆]²⁺, 10), 292.7 ([M-3PF₆]²⁺, 80). Crystals of [Co(MeOtpy)₂][PF₆]₃·MeCN suitable for X-ray diffraction were obtained by slow diffusion of diethyl ether into an acetonitrile solution of the complex at room temperature.

3.7.5.5 Synthesis of bis(4'-ethoxy-2,2':6',2''-terpyridine cobalt(III) hexafluorophosphate

Reaction of bis(4'-ethoxy-2,2':6',2''-terpyridine)cobalt(II) hexafluorophosphate (0.048 g, 0.053 mmol) gave a yellow-orange solid (0.051 g, 91%). Found: C, 39.08; H, 2.84; N, 8.87%. C₃₄H₃₀N₆O₂CoP₃F₁₈·½CH₃CN requires C, 39.32; H, 2.97; N, 8.52%; $\tilde{\nu}_{\max}(\text{solid})/\text{cm}^{-1}$ 3106w, 1616s, 1563m, 1484s, 1469m, 1435s, 1401w, 1379m, 1352m, 1324w, 1310w, 1254w, 1219s, 1164m, 1100m, 1101m, 1065m, 1041m, 1031m, 1022m, 965w, 819s, 816s, 814s, 808s, 780s, 778s, 750s, 740s, 718m, 698m, 663m; $\delta_{\text{H}}(500 \text{ MHz, CD}_3\text{CN})/\text{ppm}$ 8.58 (d, *J* 7.7 Hz, 4 H, H³), 8.51 (s, 4 H, H^{3'}), 8.21 (t, *J* 7.4 Hz, 4 H, H⁴), 7.43 (t, *J* 6.3 Hz, 4 H, H⁵), 7.36 (d, *J* 5.0 Hz, 4 H, H⁶), 4.78 (q, *J* 6.8 Hz, 4 H, tpyOCH₂CH₃), 1.71 (t, *J* 6.7 Hz, 6 H, tpyOCH₂CH₃); $\delta_{\text{C}}(126 \text{ MHz, CD}_3\text{CN})/\text{ppm}$ 173.7 (C⁴), 157.9 (C²), 157.3 (C²), 153.5 (C⁶), 144.1 (C⁴), 131.8 (C⁵), 128.0 (C³), 115.9 (C^{3'}), 69.4 (tpyOCH₂CH₃), 14.9 (tpyOCH₂CH₃); *m/z* (ESI) 903.1 ([M-PF₆]⁺, 10), 758.2 ([M-2PF₆]⁺, 60), 306.7 ([M-3PF₆]²⁺, 100). Crystals of [Co(EtOtpy)₂][PF₆]₃·MeCN suitable for X-ray diffraction were obtained by slow diffusion of diethyl ether into an acetonitrile solution of the complex at room temperature. Crystals of [Co(EtOtpy)₂][Br]₃·MeCN·H₂O were also obtained by slow diffusion of diethyl ether into an acetonitrile solution of the complex at room temperature.

3.7.6 Synthesis of mixtures of bis(terpyridine)cobalt(II) hexafluorophosphate complexes from two different complexes

3.7.6.1 General procedure

Solutions (0.5 cm³, 0.01 M) of [Co(tpy)₂][PF₆]₂, [Co(Cltpy)₂][PF₆]₂ and [Co(MeOtpy)₂][PF₆]₂ in CD₃CN were prepared, mixed (0.3 cm³ of each) and transferred immediately to an NMR tube. ¹H NMR spectra (250 MHz) were recorded as soon as possible after mixing and the reaction was monitored by ¹H NMR spectroscopy until equilibrium was established.

In the assignments, the homoleptic complexes are described as follows: T corresponds to bis(2,2':6',2''-terpyridine)cobalt(II) hexafluorophosphate, M corresponds to bis(4'-methoxy-2,2':6',2''-terpyridine)cobalt(II) hexafluorophosphate and Cl corresponds to bis(4'-chloro-

2,2':6',2''-terpyridine)cobalt(II) hexafluorophosphate. Groups of signals belonging to the same ligand in the heteroleptic complexes are designated A and B. If the signal could be assigned to a specific ligand in the heteroleptic complex, it is also denoted T, M or Cl.

3.7.6.2 Reaction of bis(2,2':6',2''-terpyridine)cobalt(II) hexafluorophosphate with bis(4'-methoxy-2,2':6',2''-terpyridine)cobalt(II) hexafluorophosphate

Equilibrium mixture: δ_{H} (500 MHz, CD_3CN)/ppm 130 (s, br, 4 H, $\text{H}^{6\text{A/B}}$), 113 (s, br, 4 H, $\text{H}^{6\text{M}}$), 111 (s, br, 4 H, $\text{H}^{6\text{Cl}}$), 94.9 (s, br, 4 H, $\text{H}^{6\text{A/B}}$), 75.7 (s, 4 H, $\text{H}^{3\text{M}}$), 71.1 (s, 4 H, $\text{H}^{3\text{M}}$), 70.5 (s, 4 H, $\text{H}^{3\text{A}}$), 67.1 (s, 4 H, $\text{H}^{3\text{A/B}}$), 66.8 (s, 4 H, $\text{H}^{3\text{A/B}}$), 65.1 (s, 4 H, $\text{H}^{3\text{B}}$), 64.7 (s, 4 H, $\text{H}^{3\text{Cl}}$), 59.1 (s, 4 H, $\text{H}^{3\text{Cl}}$), 41.6 (s, 4 H, $\text{H}^{5\text{A}}$), 37.2 (s, 4 H, $\text{H}^{5\text{Cl}}$), 34.8 (s, 4 H, $\text{H}^{5\text{M}}$), 30.9 (s, 4 H, $\text{H}^{5\text{B}}$), 14.5 (s, 6 H, $\text{OCH}_3(\text{M})$), 12.9 (s, 6 H, $\text{OCH}_3(\text{A/B})$), 11.0 (s, 4 H, $\text{H}^{4\text{A}}$), 8.09 (s, 4 H, $\text{H}^{4\text{Cl}}$), 6.37 (s, 4 H, $\text{H}^{4\text{M}}$), 3.84 (s, 4 H, $\text{H}^{4\text{B}}$).

3.7.6.3 Reaction of bis(2,2':6',2''-terpyridine)cobalt(II) hexafluorophosphate with bis(4'-chloro-2,2':6',2''-terpyridine)cobalt(II) hexafluorophosphate

Equilibrium mixture: δ_{H} (500 MHz, CD_3CN)/ppm 111 (s, br, 2 H, $\text{H}^{6\text{Cl}}$), 108 (s, br, 2 H, $\text{H}^{6\text{A/B}}$), 101 (s, br, 3 H, $\text{H}^{6\text{A/B}}$), 99.4 (s, br, 3 H, $\text{H}^{6\text{T}}$), 64.7 (s, 4 H, $\text{H}^{3\text{Cl}}$), 62.9 (s, 4 H, $\text{H}^{3\text{A}}$), 59.1 (s, 4 H, $\text{H}^{3\text{Cl}}$), 58.3 (s, 4 H, $\text{H}^{3\text{B}}$), 57.2 (s, 4 H, $\text{H}^{3\text{T}}$), 53.4 (s, 4 H, $\text{H}^{3\text{A/B(Cl)}}$), 53.1 (s, 4 H, $\text{H}^{3\text{A/B(T)}}$), 48.1 (s, 4 H, $\text{H}^{3\text{T}}$), 37.2 (s, 4 H, H^{Cl}), 37.0 (s, 4 H, $\text{H}^{5\text{B}}$), 34.5 (s, 4 H, $\text{H}^{5\text{A}}$), 34.3 (s, 4 H, $\text{H}^{5\text{T}}$), 22.0 (s, 2 H, $\text{H}^{4\text{T}}$), 21.9 (s, 2 H, $\text{H}^{4\text{A/B(T)}}$), 8.95 (s, 4 H, $\text{H}^{4\text{T}}$), 8.74 (s, 4 H, $\text{H}^{4\text{B}}$), 8.36 (s, 4 H, $\text{H}^{4\text{A}}$), 8.08 (s, 4 H, $\text{H}^{4\text{Cl}}$).

3.7.6.4 Reaction of bis(4'-chloro-2,2':6',2''-terpyridine)cobalt(II) hexafluorophosphate with bis(4'-methoxy-2,2':6',2''-terpyridine)cobalt(II) hexafluorophosphate

Equilibrium mixture: δ_{H} (500 MHz, CD_3CN)/ppm 120 (s, br, 4 H, $\text{H}^{6\text{A/B}}$), 113 (s, br, 4 H, $\text{H}^{6\text{M}}$), 99.4 (s, br, 4 H, $\text{H}^{6\text{T}}$), 93.8 (s, br, 4 H, $\text{H}^{6\text{A/B}}$), 75.7 (s, 4 H, $\text{H}^{3\text{M}}$), 71.1 (s, 4 H, $\text{H}^{3\text{M}}$), 64.5 (s, 4 H, $\text{H}^{3\text{A}}$), 63.6 (s, 4 H, $\text{H}^{3\text{B}}$), 61.8 (s, 4 H, $\text{H}^{3\text{A/B(T)}}$), 61.3 (s, 4 H, $\text{H}^{3\text{A/B(M)}}$), 57.2 (s, 4 H, $\text{H}^{3\text{T}}$), 48.1 (s, 4 H, $\text{H}^{3\text{T}}$), 38.7 (s, 4 H, $\text{H}^{5\text{A}}$), 34.8 (s, 4 H, $\text{H}^{5\text{M}}$), 34.5 (s, 4 H, $\text{H}^{5\text{T}}$), 31.4 (s, 4 H, $\text{H}^{5\text{B}}$), 27.5 (s, 2 H, $\text{H}^{4\text{A/B(T)}}$), 21.9 (s, 4 H, $\text{H}^{4\text{T}}$), 14.5 (s, 6 H, $\text{OCH}_3(\text{M})$), 12.0 (s, 6 H, $\text{OCH}_3(\text{A/B})$), 11.2 (s, 4 H, $\text{H}^{4\text{A}}$), 8.95 (s, 4 H, $\text{H}^{4\text{T}}$), 6.36 (s, 4 H, $\text{H}^{4\text{M}}$), 4.51 (s, 4 H, $\text{H}^{4\text{B}}$).

4 Solvent Effects

Reaction of 4'-Substituted-2,2':6',2''-Terpyridines with Alcohols

4.1 Introduction

To commence the investigation of the reaction of bis(terpyridyl)oligo(ethylene glycol)s with cobalt(II) salts, the shortest chain ligand, bis(terpyridyl)di(ethylene glycol) was chosen as an initial model. This ligand was considered to be a simpler analogue of the ligands with longer oligo(ethylene glycol) or poly(ethylene glycol) spacers. Attempts to simplify the system still further, by varying the reaction conditions, led to an unexpected reaction in which the glycol chain was cleaved, and this reaction was studied in more detail.

4.2 Alkoxy group exchange in cobalt(II) complexes of bis(terpyridyl)-oligo(ethylene glycol) ligands

At first, the complexation of bis(terpyridyl)di(ethylene glycol) with cobalt(II) salts was studied using 1:1 mixtures of the ligand and cobalt(II) acetate tetrahydrate in a chloroform-methanol (9:1) solvent mixture. This solvent mixture was chosen for solubility reasons as the ligand is only sparingly soluble in methanol, and has been used by Schubert for the synthesis of metallopolymers based on similar bis(terpyridyl)poly(ethylene glycol) ligands.³⁹⁻⁴¹ After one hour at reflux, excess ammonium hexafluorophosphate in methanol was added to precipitate the product(s) and the ¹H NMR spectrum was recorded in acetonitrile solution. The ¹H NMR spectrum showed a mixture of products, the composition of which changed with time. This behaviour will be discussed in Chapter 6. The reaction time, temperature and solvent mixture were varied in an attempt to alter the position of the polymer-macrocycle equilibrium and it became clear that the composition of the initial mixture of products from the reaction is very sensitive to the reaction conditions.

Using the chloroform-methanol solvent mixture, longer reaction times at higher temperatures gave rise to increased intensities of a peak in the ¹H NMR spectrum at δ 14.4 ppm. In the mixture of products obtained as described above, this peak was also present but only constituted a small proportion of the sample. Although the composition of the mixture

changed dramatically (see Chapter 6), the relative intensity of this signal remained constant for several months in acetonitrile solution.

Heating a 1:1 mixture of the ligand and cobalt(II) acetate tetrahydrate in methanol at reflux for 17 hours or at 125 °C for 15 minutes under microwave conditions gave a single cobalt(II)-containing species which exhibited the resonance at δ 14.4 ppm. This could be identified as bis(4'-methoxy-2,2':6',2''-terpyridine)cobalt(II) hexafluorophosphate by comparison of the ^1H NMR spectrum, shown in Figure 4.1, with that of an authentic sample (see section 3.7.4.4). Further confirmation of the formation of bis(4'-methoxy-2,2':6',2''-terpyridine)cobalt(II) hexafluorophosphate came from the electrospray mass spectrum, which showed a peak assigned to the species $[\text{Co}(\text{MeOtpy})_2\text{PF}_6]^+$ at $m/z = 730.0$ and determination of the solid state structures of $[\text{Co}(\text{MeOtpy})_2][\text{PF}_6]_2$ and $[\text{Co}(\text{MeOtpy})_2][\text{PF}_6]_2 \cdot \text{MeCN}$ (described in section 3.3).

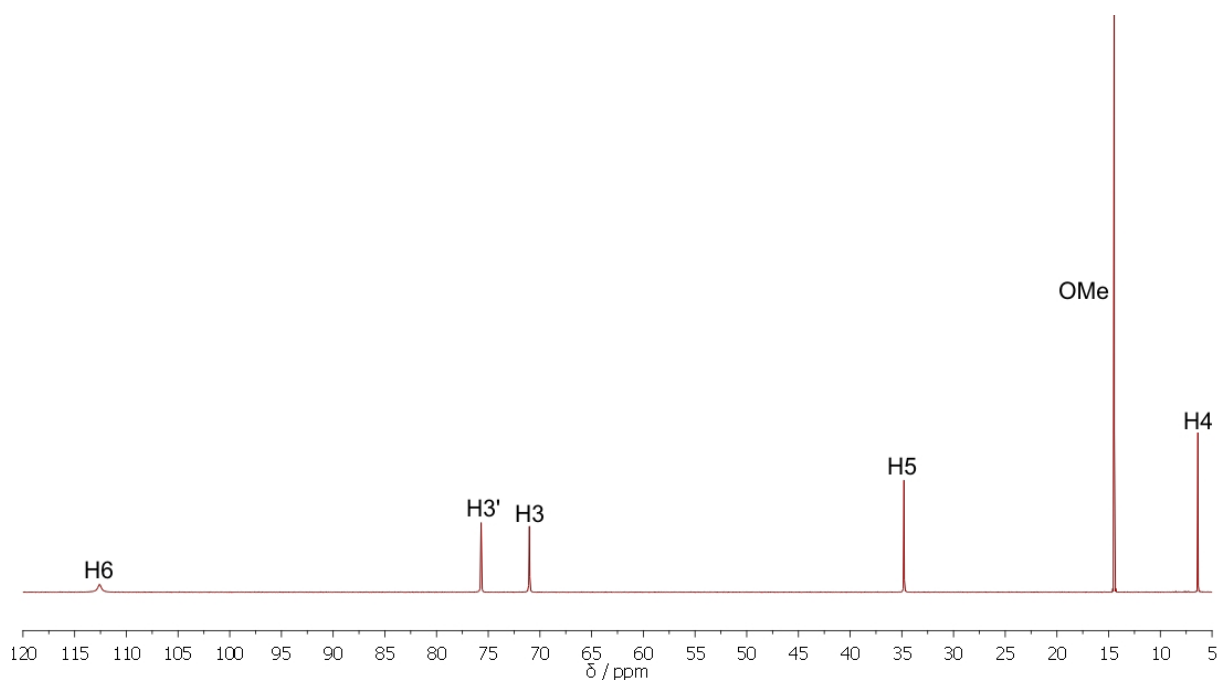
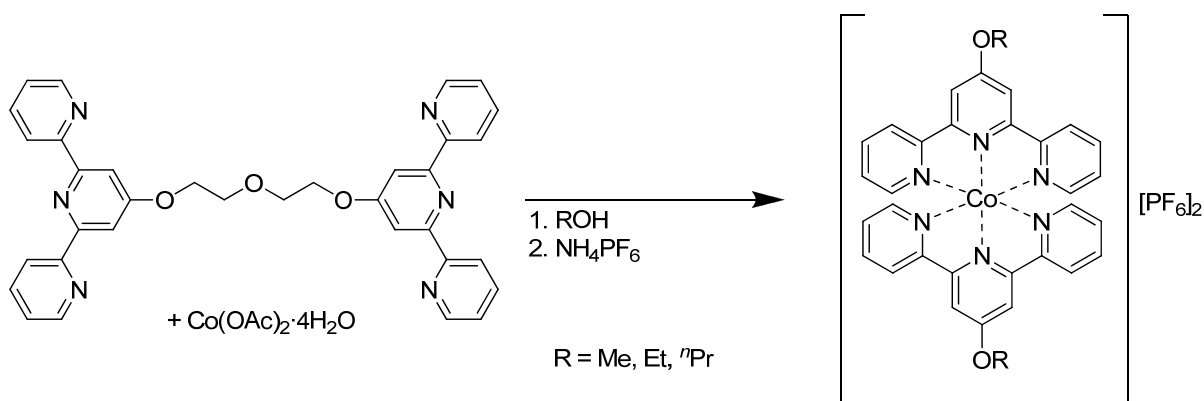


Figure 4.1 ^1H NMR spectrum of $[\text{Co}(\text{MeOtpy})_2][\text{PF}_6]_2$ (CD_3CN , 500 MHz, 295 K).

The methoxy group in the unexpected mononuclear product of this reaction could only have originated from the methanol solvent. This suggests that the reaction might be more general and that other bis(4'-alkoxy-2,2':6',2''-terpyridine)cobalt(II) complexes could be synthesised using a similar approach (Scheme 4.1).



Scheme 4.1 Reaction of bis(terpyridyl)di(ethylene glycol) with alcohols in the presence of cobalt(II) acetate tetrahydrate.

In order to verify the origin of the 4'-methoxy-2,2':6',2''-terpyridine ligand in the complex and to establish the generality of the reaction, two further experiments were performed. Using ethanol in place of methanol resulted in the formation of bis(4'-ethoxy-2,2':6',2''-terpyridine)cobalt(II) hexafluorophosphate when the reaction mixture was heated at reflux for 24 hours or under microwave conditions for 15 minutes. Similarly, heating the 1:1 mixture of the ditopic ligand and cobalt(II) acetate tetrahydrate in propan-1-ol under microwave conditions gave bis(4'-(1-propoxy)-2,2':6',2''-terpyridine)cobalt(II) hexafluorophosphate after addition of excess ammonium hexafluorophosphate. The formation of this complex was confirmed by standard characterisation techniques, as well as the determination of the solid-state structure, which is described in section 3.3.

The reaction of a 1:1 mixture of the bis(terpyridyl)di(ethylene glycol) and iron(II) chloride tetrahydrate under similar conditions has been reported to lead to the formation of metallopolymers.^{38, 39, 43} The ¹H NMR spectrum of the hexafluorophosphate salts of the products of this reaction after heating in methanol at reflux for 24 hours (see Figure 4.2) shows a mixture of products which clearly still contains the ditopic ligand (broad signals at δ 4.86 and 4.32 ppm). The exchange product, 4'-methoxy-2,2':6',2''-terpyridine, was also not observed when the ditopic ligand was heated in the absence of cobalt(II) salts in methanol or methanol containing hydrochloric acid. This suggests that the role of the cobalt(II) ion was not as a general Lewis acid activating the ligand to nucleophilic attack, as in this case protonation of the ligand should have the same effect.

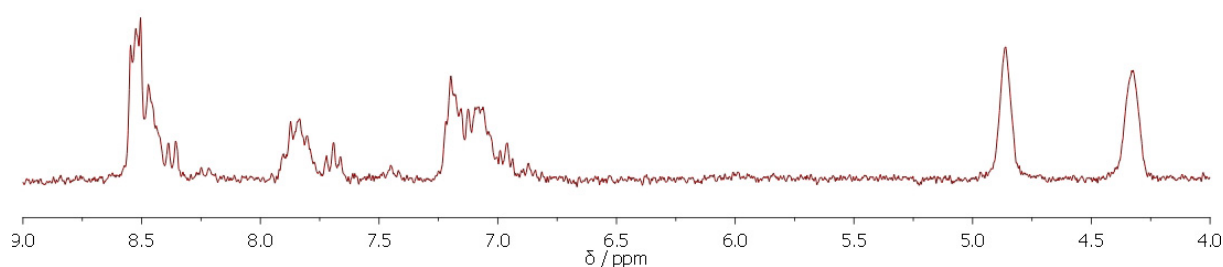
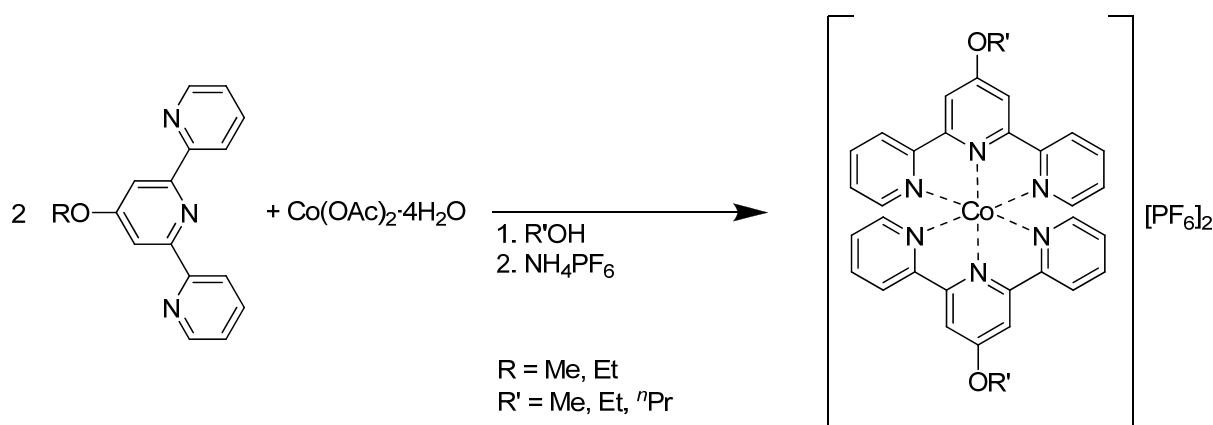


Figure 4.2 ^1H NMR spectrum of the product mixture obtained from the reaction of bis(2,2':6',2''-terpyridyl)di(ethylene glycol) with iron(II) chloride tetrahydrate in methanol (CD_3CN , 250 MHz).

4.3 Alkoxy group exchange in cobalt(II) complexes of 4'-alkoxy-2,2':6',2''-terpyridine ligands

It was anticipated that this alkoxy exchange reaction might be extended to other 4'-substituted-2,2':6',2''-terpyridine ligands. Firstly, the reaction of monotopic 4'-alkoxy-2,2':6',2''-terpyridine ligands with alcohols in the presence of cobalt(II) acetate tetrahydrate (Scheme 4.2) was investigated.



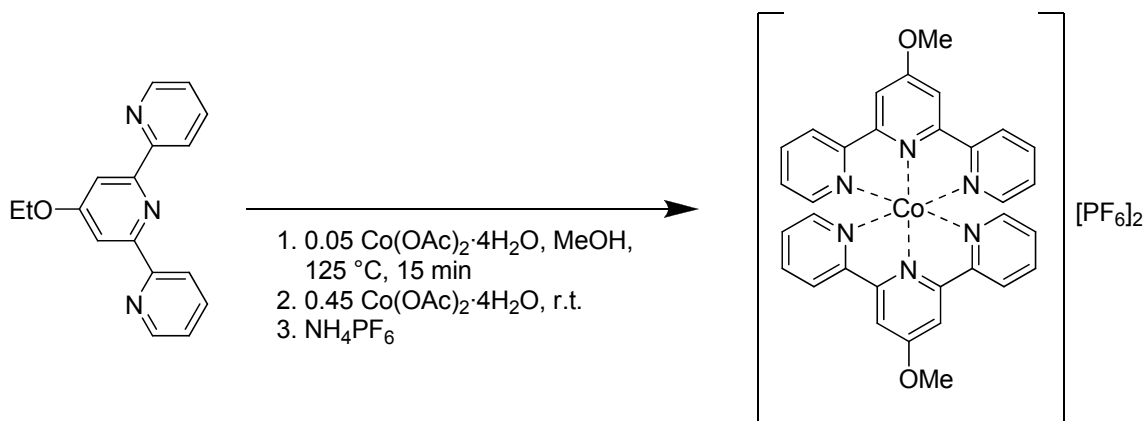
Scheme 4.2 Reaction of 4'-alkoxy-2,2':6',2''-terpyridine ligands with alcohols in the presence of cobalt(II) acetate tetrahydrate.

Two equivalents of 4'-methoxy-2,2':6',2''-terpyridine were heated to reflux with one equivalent of cobalt(II) acetate tetrahydrate in ethanol for twelve days, then the products were precipitated as the hexafluorophosphate salts by addition of excess ammonium

hexafluorophosphate. The ^1H NMR spectrum of the product showed that the 4'-methoxy-2,2':6',2''-terpyridine ligand was completely converted to the 4'-ethoxy-substituted ligand in the final complex. Further reactions showed that 4'-methoxy-2,2':6',2''-terpyridine could be quantitatively converted to the cobalt(II) complex of 4'-(1-propoxy)-2,2':6',2''-terpyridine by heating with one equivalent of cobalt(II) acetate tetrahydrate in propan-1-ol under microwave conditions. Similarly, 4'-ethoxy-2,2':6',2''-terpyridine was cleanly converted to the cobalt(II) complexes of 4'-methoxy-2,2':6',2''-terpyridine or 4'-(1-propoxy)-2,2':6',2''-terpyridine by heating under microwave conditions in the appropriate solvent.

As with the ditopic bis(terpyridyl)oligo(ethylene glycol) ligands, none of the exchange product was observed when the monotopic 4'-alkoxy-2,2':6',2''-terpyridine ligands were heated in alcohol under acidic conditions. It was also found that the alkoxy exchange reaction did not occur when cobalt(II) chloride hexahydrate was used in place of cobalt(II) acetate tetrahydrate. Possible reasons for this will be discussed in section 4.5.

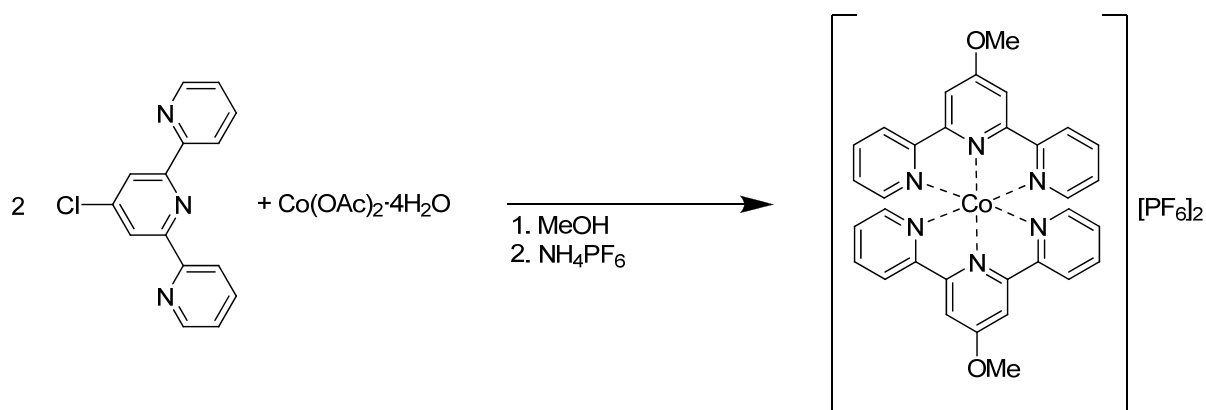
The coordination of oligopyridine ligands to high-spin $[\text{Co}(\text{ROH})_6]^{2+}$ cations ($\text{R} = \text{H}$ or alkyl) is fast,^{173, 174} although the exchange of 2,2':6',2''-terpyridine ligands between complexes can be much slower (see section 3.4). As the alkoxy exchange reaction does not occur in the absence of the cobalt(II) ion, the hypothesis was made that the reaction only takes place when the ligand is coordinated to the cobalt(II) metal centre. At the high temperatures attained under microwave conditions, it was expected that the rate of ligand exchange should be fast enough that only a catalytic amount of cobalt(II) acetate tetrahydrate would be required to cleanly convert one 4'-alkoxy-2,2':6',2''-terpyridine ligand to another. A solution of 4'-ethoxy-2,2':6',2''-terpyridine and 0.05 equivalents of cobalt(II) acetate tetrahydrate in methanol was heated at 125 °C for 15 minutes under microwave conditions. After the mixture had cooled to room temperature, another 0.45 equivalents of cobalt(II) acetate tetrahydrate were added and the product was precipitated as the hexafluorophosphate salt by addition of excess ammonium hexafluorophosphate (see Scheme 4.3). The ^1H NMR spectrum of the product indicated that the 4'-ethoxy-2,2':6',2''-terpyridine ligand had been cleanly converted to the 4'-methoxy-2,2':6',2''-terpyridine ligand in the resulting complex.



Scheme 4.3 Reaction of 4'-ethoxy-2,2':6',2''-terpyridine with methanol in the presence of a catalytic amount of cobalt(II) acetate tetrahydrate.

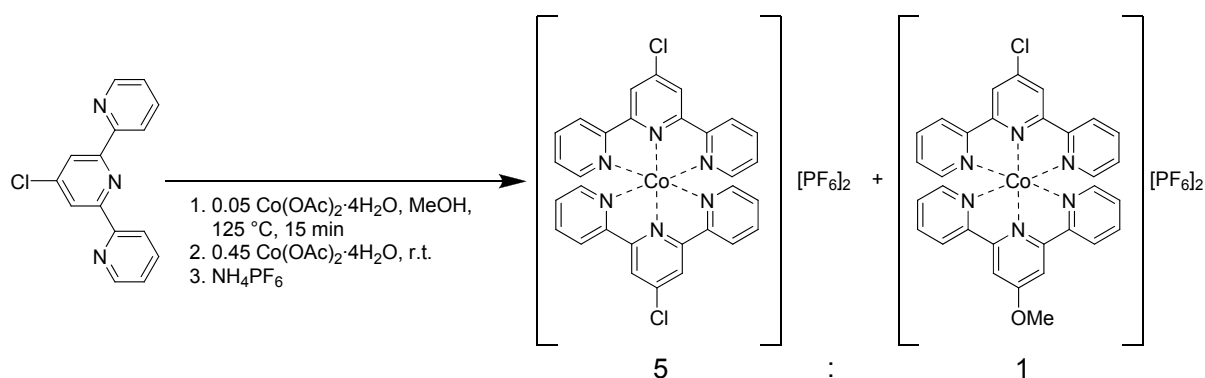
4.4 Substituent exchange in cobalt(II) complexes of 4'-chloro-2,2':6',2''-terpyridine

As 4-halopyridines are known to be activated towards nucleophilic substitution by coordination to ruthenium,^{59, 175, 176} the investigation was extended further to include the reaction of 4'-chloro-2,2':6',2''-terpyridine with methanol in the presence of the cobalt(II) ion (Scheme 4.4).



Scheme 4.4 Reaction of 4'-chloro-2,2':6',2''-terpyridine ligands with methanol in the presence of cobalt(II) acetate tetrahydrate.

Complete conversion of the 4'-chloro-2,2':6',2''-terpyridine ligand to the cobalt(II) complex of 4'-methoxy-2,2':6',2''-terpyridine was observed when a solution of two equivalents of the ligand and one equivalent of cobalt(II) acetate tetrahydrate was heated in methanol at 125 °C for 10 minutes under microwave conditions. In this case, the alkoxy exchange reaction is not catalytic, as was observed for the same reaction with the 4'-alkoxy-2,2':6',2''-terpyridine ligands. Using 0.05 equivalents of cobalt(II) acetate tetrahydrate to one equivalent of 4'-chloro-2,2':6',2''-terpyridine under the conditions described above resulted in only 10% conversion to the 4'-methoxy-substituted ligand. The ^1H NMR spectrum of the product mixture of this reaction after addition of a further 0.45 equivalents of cobalt(II) acetate tetrahydrate and immediate precipitation as the hexafluorophosphate salts showed a mixture of $[\text{Co}(\text{Cltpy})_2][\text{PF}_6]_2$ (see section 3.7.4.3) and $[\text{Co}(\text{MeOtpy})(\text{Cltpy})][\text{PF}_6]_2$ (see section 3.7.6.4) in a ratio of approximately 5:1, as shown in Scheme 4.5.



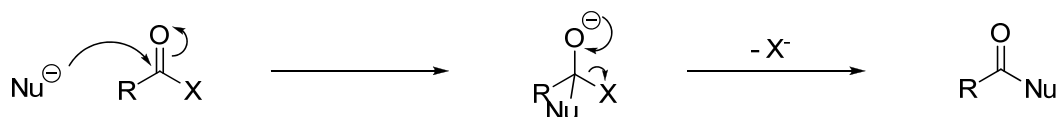
Scheme 4.5 Reaction of 4'-chloro-2,2':6',2''-terpyridine with methanol in the presence of a catalytic amount of cobalt(II) acetate tetrahydrate.

Following the observation that the exchange reaction did not occur in 4'-alkoxy-2,2':6',2''-terpyridines when cobalt(II) chloride hexahydrate was used in place of cobalt(II) acetate tetrahydrate, the effect of the anion was also investigated for the 4'-chloro-2,2':6',2''-terpyridine system. Again, the use of cobalt(II) chloride hexahydrate did not lead to the formation of 4'-methoxy-2,2':6',2''-terpyridine after reaction in methanol under microwave conditions, and the only species observed in the ^1H NMR spectrum was the bis(4'-chloro-2,2':6',2''-terpyridine)cobalt(II) complex. Similarly, no reaction (apart from the complexation) occurred when iron(II) chloride tetrahydrate was used under the same conditions. Finally, no

exchange of the substituent occurred when 4'-chloro-2,2':6',2''-terpyridine was heated under microwave conditions in methanol or methanol containing hydrochloric or sulfuric acid.

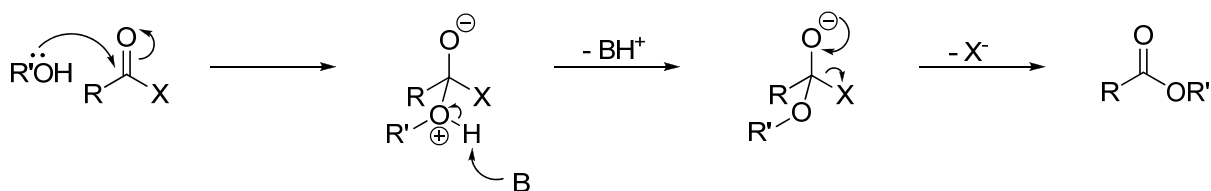
4.5 Proposed mechanism for the substituent exchange in cobalt(II) complexes of 4'-substituted-2,2':6',2''-terpyridine ligands

The behaviour of pyridines towards nucleophiles resembles that of carbonyl groups, and pyridines commonly undergo nucleophilic substitution reactions. A general nucleophilic substitution reaction at a carbonyl group is shown in Scheme 4.6. The first step of the reaction involves the addition of the nucleophile, Nu^- , to the carbonyl group, where the nucleophile attacks the carbonyl group at the carbon atom and an unstable tetrahedral intermediate is formed. This collapses with the loss of the leaving group, X^- , giving the product in which the carbonyl group is reformed.¹⁷⁷



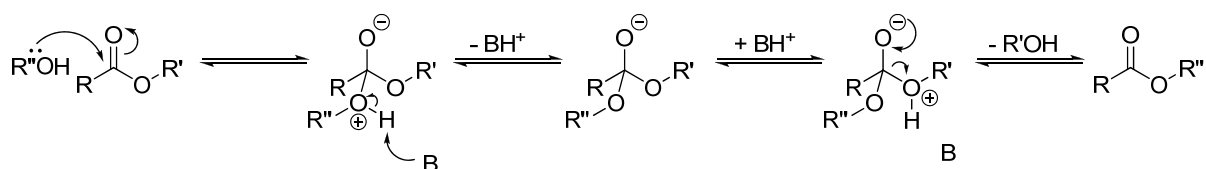
Scheme 4.6 Nucleophilic substitution at a carbonyl group.

The reaction of carboxylic acid derivatives (acyl chlorides and acid anhydrides) with an alcohol in the presence of a weak base, B, is shown in Scheme 4.7. Again, the first step is the nucleophilic addition of the alcohol to the carbonyl group. The base deprotonates the alcohol as it attacks the carbonyl group, then the tetrahedral intermediate collapses to give the ester product. Pyridine is often used as the base in these reactions and is required in stoichiometric amounts as the base is consumed during the reaction.¹⁷⁷



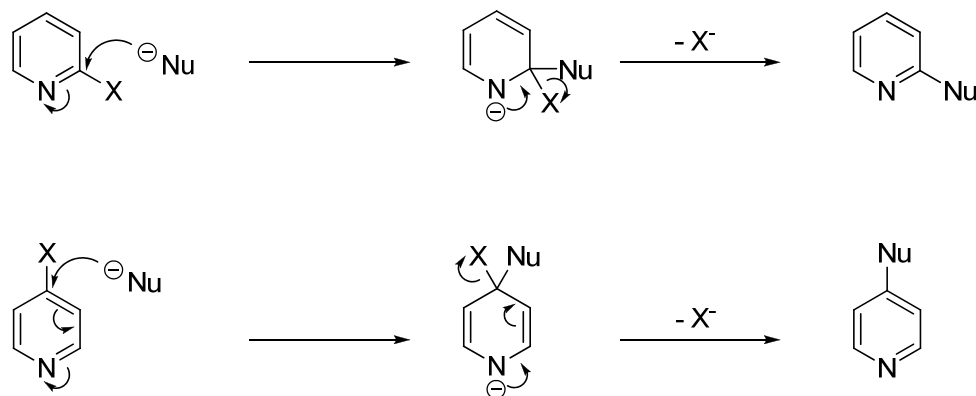
Scheme 4.7 Reaction of a carboxylic acid derivative ($\text{X} = \text{Cl}, \text{CO}_2\text{R}$) with an alcohol in the presence of a base, B.

The reaction of an ester with an alcohol in the presence of a base is shown in Scheme 4.8. The mechanism is similar to that of the reaction shown in Scheme 4.7, however in this case all the reaction steps are reversible as the bond energies (C–O) in the products and reactants of each step are very similar. The reaction can be driven in the forward direction by using a large excess of the reacting alcohol, for example as the solvent for the reaction. After nucleophilic attack at the carbon atom, protonation of one of the alkoxy groups in the acetal intermediate and elimination of the alcohol leads to the collapse of the tetrahedral intermediate and formation of the ester product. This protonation step regenerates the base required for the initial deprotonation of the alcohol as it attacks the carbonyl group, so in this case only a catalytic amount of base is required.¹⁷⁸



Scheme 4.8 Mechanism of base-catalysed transesterification.

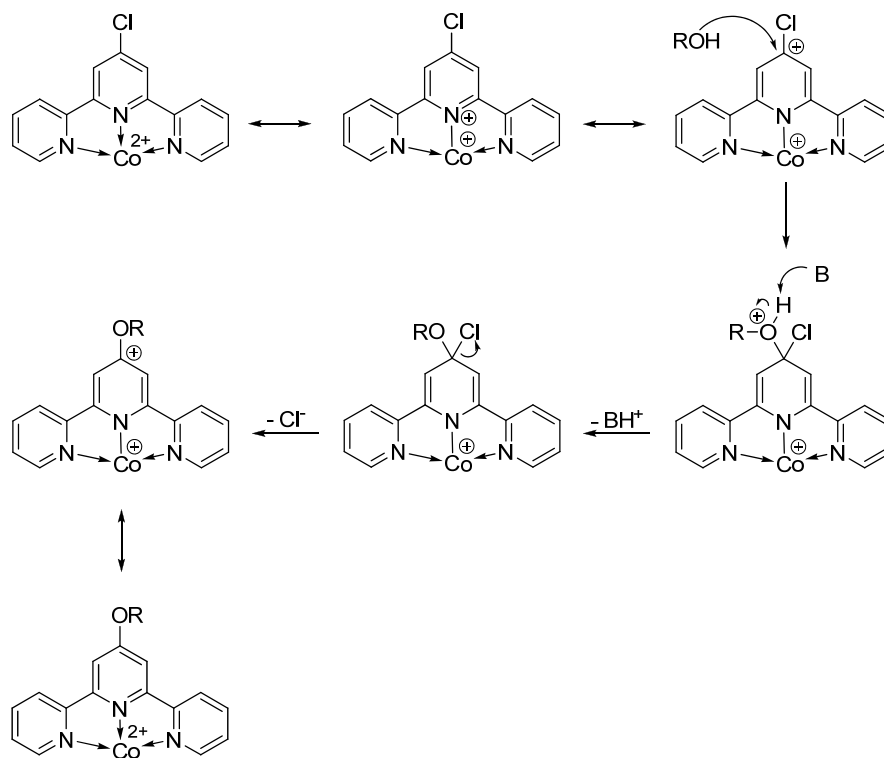
As mentioned above, pyridines are also reactive towards nucleophilic substitution and undergo similar reactions to the carboxylic acid derivatives (Scheme 4.9). The 2- and 4-positions of the pyridine are activated towards nucleophilic attack due to stabilisation of the intermediate anion by delocalisation of the negative charge around the aromatic ring.¹⁷⁷



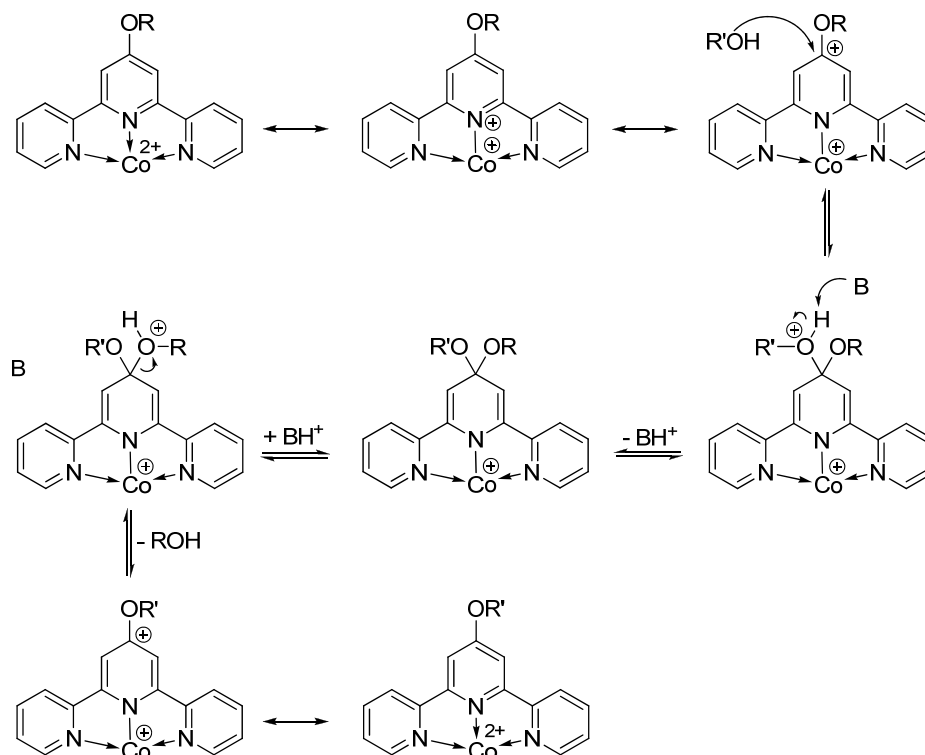
Scheme 4.9 Nucleophilic substitution of 2- and 4-substituted pyridines.

Protonation or alkylation of the pyridine at the nitrogen atom activates the pyridine towards nucleophilic attack and stabilises the intermediate still further due to the positively charged nitrogen atom, so nucleophilic substitution in these molecules is particularly easy.¹⁷⁹ Also, as mentioned above, coordination to a metal centre is known to activate 4-halopyridines towards nucleophilic substitution.^{59, 175, 176}

The reaction of a 4'-substituted-2,2':6',2''-terpyridine with an alcohol is therefore expected to be analogous to a nucleophilic substitution reaction at a carbonyl group, and the proposed mechanisms are shown in Scheme 4.10 (for 4'-chloro-2,2':6',2''-terpyridine) and Scheme 4.11 (for 4'-alkoxy-2,2':6',2''-terpyridines). Coordination of the 4'-substituted-2,2':6',2''-terpyridine to the cobalt(II) cation activates the 4'-position towards nucleophilic attack as the positive charge on the metal can be delocalised around the central pyridine ring. The 2'-positions, which should also be activated due to delocalisation of the positive charge, are occupied by electron-withdrawing pyridine rings, increasing the positive charge at the 4'-position. In both cases, the alcohol attacks the terpyridine at the positively charged carbon atom and is deprotonated by a base, B. In the case of 4'-chloro-2,2':6',2''-terpyridine, the chloro substituent is eliminated as a chloride ion giving the final alkoxy-substituted product by analogy with nucleophilic substitution of acyl chlorides. In the case of the 4'-alkoxy-2,2':6',2''-terpyridines, one of the alkoxy groups in the acetal intermediate must first be protonated, then the alcohol is eliminated to give the final product in a process similar to base-catalysed transesterification. This step is not favoured for one alcohol over the other, but use of a large excess of one of the alcohols (i.e. as the solvent) drives the reaction in the appropriate direction.



Scheme 4.10 Proposed mechanism for the reaction of 4'-chloro-2,2':6,2''-terpyridine with alcohols.



Scheme 4.11 Proposed mechanism for the reaction of 4'-alkoxy-2,2':6,2''-terpyridines with alcohols.

As described above, the exchange reaction does not occur in either the alkoxy-substituted or the chloro-substituted terpyridines when cobalt(II) chloride hexahydrate or iron(II) chloride tetrahydrate is used in place of cobalt(II) acetate tetrahydrate. Similarly, no reaction is observed when the ligands are heated in methanol in the absence of metal salts. Based on these observations, the base required for the deprotonation of the alcohol as it attacks the ligand is proposed to be the acetate anion. The chloride anion is a much weaker base than the acetate anion and cannot deprotonate the alcohol ($\text{pK}_a(\text{HCl})^{177} = -7$, $\text{pK}_a(\text{HOAc})^{177} = 4.8$).

This mechanism would also explain the observation that the reaction of 4'-alkoxy-2,2':6',2''-terpyridines with alcohols requires only a catalytic amount of cobalt(II) acetate tetrahydrate, whereas the reaction of 4'-chloro-2,2':6',2''-terpyridine requires one equivalent of cobalt(II) acetate tetrahydrate to two equivalents of the ligand. The base is regenerated in the reaction of 4'-alkoxy-2,2':6',2''-terpyridines by the protonation of the acetal intermediate but is consumed in the reaction of 4'-chloro-2,2':6',2''-terpyridine.

Use of an acid to protonate the nitrogen atom of the terpyridine should activate the terpyridine towards nucleophilic attack in a similar manner to the coordination to the cobalt(II) cation. However, under acidic conditions the deprotonation of the attacking alcohol is not favoured, and the tetrahedral intermediate collapses to reform the starting materials.

In order to confirm the role of the base in the reaction, further experiments were carried out. Firstly, a solution of 4'-chloro-2,2':6',2''-terpyridine and excess sodium acetate in methanol was heated at 125 °C for 10 minutes under microwave conditions. The ^1H NMR spectrum of the product showed that approximately 5% of the 4'-chloro-2,2':6',2''-terpyridine had been converted to 4'-methoxy-2,2':6',2''-terpyridine. In the absence of a metal ion, the terpyridine is not particularly activated towards nucleophilic attack, so while the substituent exchange reaction is possible, the rate of the reaction is slow. Longer reaction times should lead to higher conversion to the methoxy-substituted product.

Heating a solution of two equivalents of 4'-chloro-2,2':6',2''-terpyridine, one equivalent of cobalt(II) chloride hexahydrate and excess sodium acetate in methanol under microwave conditions resulted in complete conversion to the bis(4'-methoxy-2,2':6',2''-terpyridine)cobalt(II) complex. Several experiments were carried out to test the reaction of 4'-chloro-2,2':6',2''-terpyridine with methanol using catalytic amounts of cobalt(II) chloride hexahydrate or cobalt(II) acetate tetrahydrate and excess sodium acetate. None of these

reactions resulted in complete conversion of the chloro substituent to the methoxy substituent, and mixtures of $[\text{Co}(\text{MeOtpy})_2]^{2+}$, $[\text{Co}(\text{MeOtpy})(\text{Cltpy})]^{2+}$ and $[\text{Co}(\text{Cltpy})_2]^{2+}$ in various ratios were observed (see sections 4.7.3.6 and 4.7.3.7). Increasing the reaction time or the amount of the cobalt(II) salt present in the reaction mixture led to higher proportions of the bis(4'-methoxy-2,2':6',2''-terpyridine)cobalt(II) complex, which suggests that the reaction will go to completion if the reaction time is long enough.

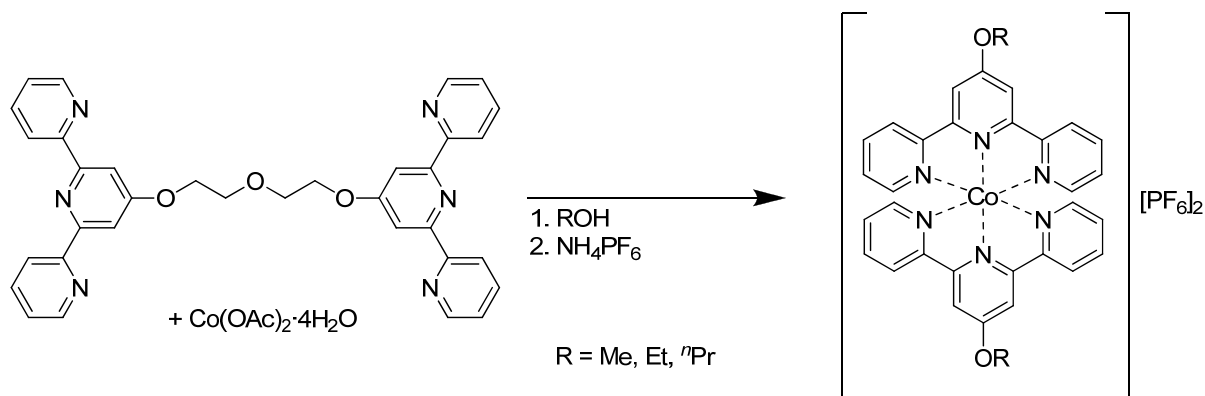
Finally, an alternative base (sodium hydrogen carbonate) was used in place of sodium acetate. Heating a solution of two equivalents of 4'-chloro-2,2':6',2''-terpyridine with one equivalent or a catalytic amount of cobalt(II) chloride hexahydrate and excess sodium hydrogen carbonate in methanol under microwave conditions gave a clean sample of bis(4'-methoxy-2,2':6',2''-terpyridine)cobalt(II) hexafluorophosphate after anion exchange with ammonium hexafluorophosphate. The hydrogen carbonate anion is a stronger base than the acetate anion ($\text{pK}_a(\text{H}_2\text{CO}_3)^{180} = 6.35$), which may explain the increased rate of this reaction compared to the same reaction with sodium acetate.

4.6 Conclusions

It was found that in alcohol-containing solvents and in the presence of a base, cobalt(II) complexes of 4'-substituted-2,2':6',2''-terpyridine ligands are unstable with respect to a reaction in which the substituent is exchanged for an alkoxy group from the solvent. A potential mechanism for this reaction was proposed, based on a general nucleophilic substitution reaction at a carbonyl group. The acetate counterion was proposed to act as the base in this mechanism. In the case of the ditopic ligand, bis(terpyridyl)di(ethylene glycol), this results in the cleavage of the spacer unit and the formation of mononuclear complexes. This observation imposes severe limitations on the stability and application of metallosupramolecular polymers based on bis(terpyridyl)oligo- or -poly(ethylene glycol)s in alcohol solutions. In addition, the *in situ* formation of monotopic 2,2':6',2''-terpyridine ligands gives rise to end-capping units which can influence the position of the equilibrium between polymeric and macrocyclic species.

4.7 Experimental

4.7.1 Alkoxy group exchange with bis(terpyridyl)oligo(ethylene glycol) ligands



4.7.1.1 Method 1 (reflux)

Bis(terpyridyl)di(ethylene glycol) (0.050 g, 0.088 mmol) and cobalt(II) acetate tetrahydrate (0.022 g, 0.088 mmol) were suspended in alcohol (10 cm³) and heated under reflux to give a brown solution. After cooling to room temperature, the product was precipitated by addition of excess ammonium hexafluorophosphate in the appropriate alcohol, collected by filtration through Celite, washed well with the alcohol and diethyl ether and redissolved in acetonitrile. The solvent was removed *in vacuo* to give a brown solid.

Reaction in methanol at for 17 hours gave bis(4'-methoxy-2,2':6',2''-terpyridine)cobalt(II) hexafluorophosphate as identified by ¹H NMR spectroscopy (see section 3.7.4.4). No yield was determined. Crystals of [Co(MeOtpy)₂][PF₆]₂ and [Co(MeOtpy)₂][PF₆]₂·MeCN suitable for X-ray diffraction were obtained by slow diffusion of diethyl ether into an acetonitrile solution of the complex at room temperature.

Reaction in ethanol for 24 hours gave bis(4'-ethoxy-2,2':6',2''-terpyridine)cobalt(II) hexafluorophosphate as identified by ¹H NMR spectroscopy (see section 3.7.4.5) (0.063 g, 79%). Crystals of [Co(EtOtpy)₂][PF₆]₂·2MeCN suitable for X-ray diffraction were obtained by slow diffusion of diethyl ether into an acetonitrile solution of the complex at room temperature.

4.7.1.2 Method 2 (microwave)

Bis(terpyridyl)di(ethylene glycol) (0.050 g, 0.088 mmol) and cobalt(II) acetate tetrahydrate (0.022 g, 0.088 mmol) were dissolved or suspended in alcohol (15 cm³). After 30 seconds pre-stirring, the mixture was heated for 15 minutes in the microwave reactor to give a red-brown solution. After cooling to room temperature, the product was precipitated by addition of excess ammonium hexafluorophosphate in methanol, collected by filtration through Celite, washed well with methanol and diethyl ether and redissolved in acetonitrile. The solvent was removed *in vacuo* to give a brown solid.

Reaction in methanol at 125 °C gave bis(4'-methoxy-2,2':6',2''-terpyridine)cobalt(II) hexafluorophosphate as identified by ¹H NMR spectroscopy (see section 3.7.4.4) (0.054 g, 71%).

Reaction in propan-1-ol at 150 °C gave bis(4'-propoxy-2,2':6',2''-terpyridine)cobalt(II) hexafluorophosphate (0.060 g, 73%). Found: C, 45.18; H, 3.76; N, 8.74%. C₃₆H₃₄N₆O₂CoP₂F₁₂·1½H₂O requires C, 45.11; H, 3.89; N, 8.77%; $\tilde{\nu}_{\max}(\text{solid})/\text{cm}^{-1}$ 1615m, 1603m, 1573m, 1558m, 1471m, 1456w, 1441m, 1436m, 1404w, 1370m, 1350w, 1324w, 1303w, 1256w, 1225m, 1163w, 1099w, 1061m, 1054m, 1030m, 1014w, 987m, 931w, 911m, 903w, 887w, 866w, 824s, 793s, 750m, 743w, 729m, 700w, 661m, 639w, 623w; $\delta_{\text{H}}(500 \text{ MHz, CD}_3\text{CN})/\text{ppm}$ 112 (br, 4 H, H⁶), 75.7 (s, 4 H, H^{3'}), 70.9 (s, 4 H, H³), 34.6 (s, 4 H, H⁵), 15.1 (s, 4 H, OCH₂CH₂CH₃), 7.76 (d, *J* 6 Hz, 4 H, OCH₂CH₂CH₃), 6.38 (s, 4 H, H⁴), 5.57 (t, *J* 6 Hz, 6 H, OCH₂CH₂CH₃); *m/z*(ESI) 786.0 ([M-PF₆]⁺, 100). Crystals of [Co(PrOtpy)₂][PF₆]₂·MeCN and [Co(PrOtpy)₂][PF₆]₂·MeCN·Et₂O suitable for X-ray diffraction were obtained by slow diffusion of diethyl ether into an acetonitrile solution of the complex at room temperature. Crystals of the cobalt(III) complex, 2{[Co(PrOtpy)₂][PF₆]₃}·5MeCN, were also obtained by slow diffusion of diethyl ether into an acetonitrile solution of the cobalt(II) complex at room temperature.

4.7.1.3 Attempted reaction of bis(terpyridyl)di(ethylene glycol) with methanol

Bis(terpyridyl)di(ethylene glycol) (0.050 g, 0.088 mmol) was suspended in methanol (15 cm³). After 30 seconds pre-stirring, the suspension was heated to 125 °C for 15 minutes in the microwave reactor to give a colourless solution. The solvent was removed *in vacuo* to give a white solid which was identified as bis(terpyridyl)di(ethylene glycol) by ¹H NMR spectroscopy (see section 3.7.3.2). No yield was determined.

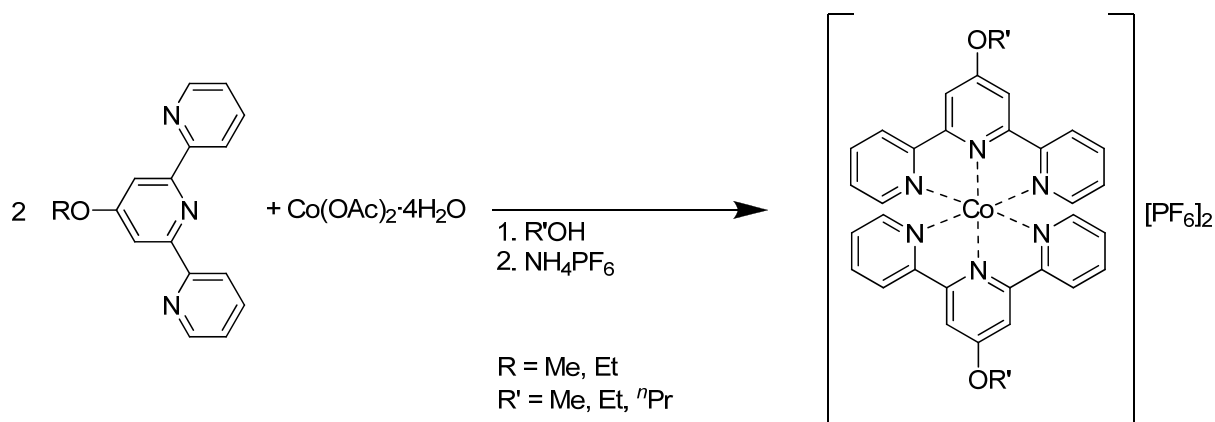
4.7.1.4 Attempted reaction of bis(terpyridyl)di(ethylene glycol) with hydrochloric acid in methanol

Bis(terpyridyl)di(ethylene glycol) (0.050 g, 0.088 mmol) was suspended in methanol (15 cm³) to which 5 drops of concentrated hydrochloric acid had been added. After 30 seconds pre-stirring, the mixture was heated at 125 °C for 15 minutes in the microwave reactor to give a pale pink solution. The solvent was removed *in vacuo* to give a pale pink solid. This was dissolved in chloroform (20 cm³) and washed with aqueous sodium hydrogen carbonate solution (2 x 20 cm³). The organic layer was dried over anhydrous sodium sulfate, filtered and the solvent was removed *in vacuo* to give a white solid which was identified as bis(terpyridyl)di(ethylene glycol) by ¹H NMR spectroscopy see section 3.7.3.2). No yield was determined.

4.7.1.5 Reaction of bis(terpyridyl)di(ethylene glycol) with iron(II) chloride tetrahydrate in methanol

Bis(terpyridyl)di(ethylene glycol) (0.050 g, 0.088 mmol) and iron(II) chloride tetrahydrate (0.018 g, 0.088 mmol) were dissolved in methanol (10 cm³) and heated under reflux for 17 hours to give a purple solution. After cooling to room temperature, the product was precipitated by addition of excess ammonium hexafluorophosphate in ethanol, collected by filtration through Celite, washed well with methanol and diethyl ether and redissolved in acetonitrile. The solvent was removed *in vacuo* to give a dark purple solid (0.074 g). The ¹H NMR spectrum shows a complex mixture of products (see the discussion in section 4.2).

4.7.2 Alkoxy group exchange with 4'-alkoxy-2,2':6',2''-terpyridines



4.7.2.1 Method 1 (reflux)

4'-Methoxy-2,2':6',2''-terpyridine (0.050 g, 0.19 mmol) and cobalt(II) acetate tetrahydrate (0.024 g, 0.095 mmol) were suspended in ethanol (10 cm³) and heated under reflux for 12 days to give a dark red-brown solution. After cooling to room temperature, the product was precipitated by addition of excess ammonium hexafluorophosphate in ethanol, collected by filtration through Celite, washed with ethanol and diethyl ether and redissolved in acetonitrile. The solvent was removed *in vacuo* to give a brown solid which was identified as bis(4'-ethoxy-2,2':6',2''-terpyridine)cobalt(II) hexafluorophosphate by ¹H NMR spectroscopy (see section 3.7.4.5) (0.064 g, 75%).

4.7.2.2 Method 2 (microwave)

The 4'-alkoxy-2,2':6',2''-terpyridine (0.050 g, 2 eq) and cobalt(II) acetate tetrahydrate (1 eq) were suspended in alcohol (15 cm³). After 30 seconds pre-stirring, the mixture was heated for 15 minutes in the microwave reactor to give a red-brown solution. After cooling to room temperature, the product was precipitated by addition of excess ammonium hexafluorophosphate in ethanol or in methanol, collected by filtration through Celite, washed well with ethanol or methanol and diethyl ether and redissolved in acetonitrile. The solvent was removed *in vacuo* to give a brown solid.

Reaction of 4'-methoxy-2,2':6',2''-terpyridine in propan-1-ol at 150 °C gave bis(4'-propoxy-2,2':6',2''-terpyridine)cobalt(II) hexafluorophosphate as identified by ¹H NMR spectroscopy (see section 4.7.1.2) (0.077 g, 87%).

Reaction of 4'-ethoxy-2,2':6',2''-terpyridine in propan-1-ol at 150 °C gave bis(4'-propoxy-2,2':6',2''-terpyridine)cobalt(II) hexafluorophosphate as identified by ¹H NMR spectroscopy (see section 4.7.1.2) (0.067 g, 79%).

Reaction of 4'-ethoxy-2,2':6',2''-terpyridine in methanol at 125 °C gave bis(4'-methoxy-2,2':6',2''-terpyridine)cobalt(II) hexafluorophosphate as identified by ¹H NMR spectroscopy (see section 3.7.4.4) (0.066 g, 83%).

4.7.2.3 Method 3 (catalytic)

4'-Ethoxy-2,2':6',2''-terpyridine (0.050 g, 0.18 mmol) and cobalt(II) acetate tetrahydrate (0.002 g, 0.008 mmol) were dissolved in methanol (15 cm³). After 30 seconds pre-stirring, the pale orange solution was heated to 125 °C for 15 minutes in the microwave reactor. After

cooling to room temperature, a second portion of cobalt(II) acetate tetrahydrate (0.023 g, 0.093 mmol) was added and the brown solution was stirred at room temperature for 20 minutes. The product was precipitated by addition of excess ammonium hexafluorophosphate in methanol, collected by filtration through Celite, washed well with methanol and diethyl ether and redissolved in acetonitrile. The solvent was removed *in vacuo* to give a brown solid which was identified as bis(4'-methoxy-2,2':6',2''-terpyridine)cobalt(II) hexafluorophosphate by ¹H NMR spectroscopy (see section 3.7.4.4) (0.065 g, 79%).

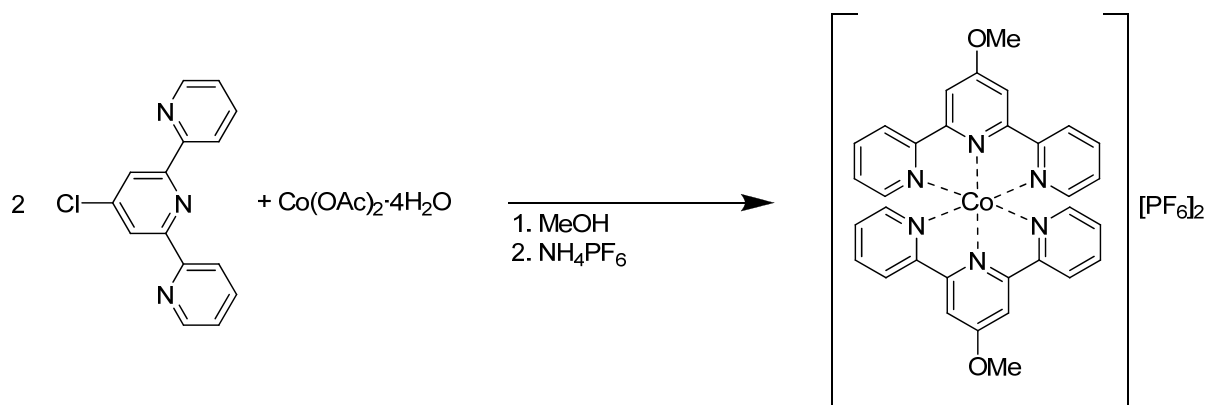
4.7.2.4 Attempted reaction of 4'-methoxy-2,2':6',2''-terpyridine with cobalt(II) chloride hexahydrate in ethanol

4'-Methoxy-2,2':6',2''-terpyridine (0.050 g, 0.19 mmol) and cobalt(II) chloride hexahydrate (0.023 g, 0.095 mmol) were suspended in ethanol (15 cm³). After 30 seconds pre-stirring, the mixture was heated at 125 °C for 15 minutes in the microwave reactor to give a brown solution. After cooling to room temperature, the product was precipitated by addition of excess ammonium hexafluorophosphate in ethanol, collected by filtration through Celite, washed well with ethanol and diethyl ether and redissolved in acetonitrile. The solvent was removed *in vacuo* to give a brown solid which was identified as bis(4'-methoxy-2,2':6',2''-terpyridine)cobalt(II) hexafluorophosphate by ¹H NMR spectroscopy (see section 3.7.4.4) (0.074 g, 89%).

4.7.2.5 Attempted reaction of 4'-methoxy-2,2':6',2''-terpyridine with acetic acid in ethanol

4'-Methoxy-2,2':6',2''-terpyridine (0.050 g, 0.19 mmol) was suspended in ethanol (15 cm³). Glacial acetic acid (0.1 cm³) was added to give a clear colourless solution. After 30 seconds pre-stirring, the solution was heated at 125 °C for 15 minutes in the microwave reactor. The solvent was removed *in vacuo* to give a colourless oil. This was dissolved in chloroform (20 cm³) and washed with aqueous sodium hydrogen carbonate solution (2 x 20 cm³). The organic layer was dried over anhydrous sodium sulfate, filtered and the solvent removed *in vacuo* to give an off white solid which was identified as 4'-methoxy-2,2':6',2''-terpyridine by ¹H NMR spectroscopy (see section 3.7.2.1). No yield was determined.

4.7.3 Substituent exchange with 4'-chloro-2,2':6,2''-terpyridine



4.7.3.1 Reaction with cobalt(II) acetate tetrahydrate in methanol

4'-Chloro-2,2':6,2''-terpyridine (0.050 g, 0.19 mmol) and cobalt(II) acetate tetrahydrate (0.023 g, 0.093 mmol) were suspended in methanol (15 cm³). After 30 seconds pre-stirring, the mixture was heated at 125 °C for 10 minutes in the microwave reactor to give a red-brown solution. After cooling to room temperature, the product was precipitated by addition of excess ammonium hexafluorophosphate in methanol, collected by filtration through Celite, washed well with methanol and diethyl ether and redissolved in acetonitrile. The solvent was removed *in vacuo* to give a brown solid which was identified as bis(4'-methoxy-2,2':6,2''-terpyridine)cobalt(II) hexafluorophosphate by ¹H NMR spectroscopy (see section 3.7.4.4) (0.064 g, 78%).

4.7.3.2 Attempted reaction with cobalt(II) acetate tetrahydrate (catalytic) in methanol

4'-Chloro-2,2':6,2''-terpyridine (0.050 g, 0.19 mmol) and cobalt(II) acetate tetrahydrate (0.002 g, 0.009 mmol) were suspended in methanol (15 cm³). After 30 seconds pre-stirring, the mixture was heated at 125 °C for 10 minutes in the microwave reactor to give a pale orange solution. After cooling to room temperature, a second portion of cobalt(II) acetate tetrahydrate (0.020 g, 0.080 mmol) was added and the brown solution was stirred at room temperature for 2 hours. The product was precipitated by addition of excess ammonium hexafluorophosphate in methanol, collected by filtration through Celite, washed well with methanol and diethyl ether and redissolved in acetonitrile. The solvent was removed *in vacuo* to give a brown solid which was identified as a mixture of bis(4'-chloro-2,2':6,2''-terpyridine)cobalt(II) hexafluorophosphate and (4'-chloro-2,2':6,2''-terpyridine)(4'-methoxy-

2,2':6',2''-terpyridine)cobalt(II) hexafluorophosphate (*ca.* 5:1) by ^1H NMR spectroscopy (see sections 3.7.4.3 and 3.7.6.4) (total mass of products was 0.076 g).

4.7.3.3 Attempted reaction with cobalt(II) chloride hexahydrate in methanol

4'-Chloro-2,2':6',2''-terpyridine (0.050 g, 0.19 mmol) and cobalt(II) chloride hexahydrate (0.022 g, 0.093 mmol) were suspended in methanol (15 cm³). After 30 seconds pre-stirring, the mixture was heated at 125 °C for 10 minutes in the microwave reactor to give a red-brown solution. After cooling to room temperature, the product was precipitated by addition of excess ammonium hexafluorophosphate in methanol, collected by filtration through Celite, washed well with methanol and diethyl ether and redissolved in acetonitrile. The solvent was removed *in vacuo* to give a brown solid which was identified as bis(4'-chloro-2,2':6',2''-terpyridine)cobalt(II) hexafluorophosphate by ^1H NMR spectroscopy (see section 3.7.4.3) (0.080 g, 96%).

4.7.3.4 Attempted reaction with sodium acetate in methanol

4'-Chloro-2,2':6',2''-terpyridine (0.050 g, 0.19 mmol) and sodium acetate (0.153 g, 1.87 mmol) were suspended in methanol (15 cm³). After 30 seconds pre-stirring, the mixture was heated at 125 °C for 10 minutes in the microwave reactor to give a colourless solution. After cooling to room temperature, approximately half the solvent was removed *in vacuo*. Water was added and a white precipitate was formed, which was collected by filtration and washed with water. The solid was identified as a mixture of 4'-chloro-2,2':6',2''-terpyridine and 4'-methoxy-2,2':6',2''-terpyridine (*ca.* 20:1) by ^1H NMR spectroscopy (see Ref.¹⁶⁹ and section 3.7.2.1) (total mass of products was 0.034 g).

4.7.3.5 Reaction with cobalt(II) chloride hexahydrate and sodium acetate in methanol

4'-Chloro-2,2':6',2''-terpyridine (0.050 g, 0.19 mmol), cobalt(II) chloride hexahydrate (0.023 g, 0.093 mmol) and sodium acetate (0.153 g, 1.87 mmol) were suspended in methanol (15 cm³). After 30 seconds pre-stirring, the mixture was heated at 125 °C for 10 minutes in the microwave reactor to give a red-brown solution. After cooling to room temperature, the product was precipitated by addition of excess ammonium hexafluorophosphate in methanol, collected by filtration through Celite, washed well with methanol and diethyl ether and redissolved in acetonitrile. The solvent was removed *in vacuo* to give a brown solid which

was identified as bis(4'-methoxy-2,2':6',2''-terpyridine)cobalt(II) hexafluorophosphate by ^1H NMR spectroscopy (see section 3.7.4.4) (0.074 g, 90%).

4.7.3.6 Attempted reaction with cobalt(II) chloride hexahydrate (catalytic) and sodium acetate in methanol

4'-Chloro-2,2':6',2''-terpyridine (0.050 g, 0.19 mmol), a catalytic amount of cobalt(II) chloride hexahydrate and sodium acetate (0.153 g, 1.87 mmol) were dissolved in methanol (15 cm³). After 30 seconds pre-stirring, the pale orange solution was heated at 125 °C in the microwave reactor. After cooling to room temperature, a second portion of cobalt(II) chloride hexahydrate (0.020 g, 0.080 mmol) was added and the brown solution was stirred at room temperature for 15 minutes. The product was precipitated by addition of excess ammonium hexafluorophosphate in methanol, collected by filtration through Celite, washed well with methanol and diethyl ether and redissolved in acetonitrile. The solvent was removed *in vacuo* to give a brown solid which was identified as a mixture of bis(4'-chloro-2,2':6',2''-terpyridine)cobalt(II) hexafluorophosphate, bis(4'-methoxy-2,2':6',2''-terpyridine)cobalt(II) hexafluorophosphate and (4'-chloro-2,2':6',2''-terpyridine)(4'-methoxy-2,2':6',2''-terpyridine)cobalt(II) hexafluorophosphate by ^1H NMR spectroscopy (see sections 3.7.4.3, 3.7.4.4 and 3.7.6.4).

Reaction with cobalt(II) chloride hexahydrate (0.002 g, 0.009 mmol) for 10 minutes gave a mixture of bis(4'-chloro-2,2':6',2''-terpyridine)cobalt(II) hexafluorophosphate, bis(4'-methoxy-2,2':6',2''-terpyridine)cobalt(II) hexafluorophosphate and (4'-chloro-2,2':6',2''-terpyridine)(4'-methoxy-2,2':6',2''-terpyridine)cobalt(II) hexafluorophosphate (*ca.* 3:5:8) as identified by ^1H NMR spectroscopy (see sections 3.7.4.3, 3.7.4.4 and 3.7.6.4) (total mass of products was 0.085 g).

Reaction with cobalt(II) chloride hexahydrate (0.002 g, 0.009 mmol) for 30 minutes gave a mixture of bis(4'-chloro-2,2':6',2''-terpyridine)cobalt(II) hexafluorophosphate, bis(4'-methoxy-2,2':6',2''-terpyridine)cobalt(II) hexafluorophosphate and (4'-chloro-2,2':6',2''-terpyridine)(4'-methoxy-2,2':6',2''-terpyridine)cobalt(II) hexafluorophosphate (*ca.* 1:7:6) as identified by ^1H NMR spectroscopy (see sections 3.7.4.3, 3.7.4.4 and 3.7.6.4) (total mass of products was 0.084 g).

Reaction with cobalt(II) chloride hexahydrate (0.005 g, 0.02 mmol) for 10 minutes gave a mixture of bis(4'-chloro-2,2':6',2''-terpyridine)cobalt(II) hexafluorophosphate, bis(4'-methoxy-

2,2':6',2''-terpyridine)cobalt(II) hexafluorophosphate and (4'-chloro-2,2':6',2''-terpyridine)(4'-methoxy-2,2':6',2''-terpyridine)cobalt(II) hexafluorophosphate (*ca.* 1:6:6) as identified by ¹H NMR spectroscopy (see sections 3.7.4.3, 3.7.4.4 and 3.7.6.4) (total mass of products was 0.069 g).

4.7.3.7 Attempted reaction with cobalt(II) acetate tetrahydrate (catalytic) and sodium acetate in methanol

4'-Chloro-2,2':6',2''-terpyridine (0.050 g, 0.19 mmol), cobalt(II) acetate tetrahydrate (0.002 g, 0.009 mmol) and sodium acetate (0.153 g, 1.87 mmol) were dissolved in methanol (15 cm³). After 30 seconds pre-stirring, the pale orange solution was heated at 125 °C for 10 minutes in the microwave reactor. After cooling to room temperature, a second portion of cobalt(II) acetate tetrahydrate (0.020 g, 0.080 mmol) was added and the brown solution was stirred at room temperature for 30 minutes. The product was precipitated by addition of excess ammonium hexafluorophosphate in methanol, collected by filtration through Celite, washed well with methanol and diethyl ether and redissolved in acetonitrile. The solvent was removed *in vacuo* to give a brown solid which was identified as a mixture of bis(4'-chloro-2,2':6',2''-terpyridine)cobalt(II) hexafluorophosphate, bis(4'-methoxy-2,2':6',2''-terpyridine)cobalt(II) hexafluorophosphate and (4'-chloro-2,2':6',2''-terpyridine)(4'-methoxy-2,2':6',2''-terpyridine)cobalt(II) hexafluorophosphate (*ca.* 1:3:4) by ¹H NMR spectroscopy (see sections 3.7.4.3, 3.7.4.4 and 3.7.6.4) (total mass of products was 0.076 g).

4.7.3.8 Reaction with cobalt(II) chloride hexahydrate and sodium hydrogen carbonate in methanol

4'-Chloro-2,2':6',2''-terpyridine (0.050 g, 0.19 mmol), cobalt(II) chloride hexahydrate (0.022 g, 0.093 mmol) and sodium hydrogen carbonate (0.157 g, 1.87 mmol) were suspended in methanol (15 cm³). After 30 seconds pre-stirring, the mixture was heated at 125 °C for 10 minutes in the microwave reactor to give a brown solution. After cooling to room temperature, the product was precipitated by addition of excess ammonium hexafluorophosphate in methanol, collected by filtration through Celite, washed well with methanol and diethyl ether and redissolved in acetonitrile. The solvent was removed *in vacuo* to give a brown solid which was identified as bis(4'-methoxy-2,2':6',2''-terpyridine)cobalt(II) hexafluorophosphate by ¹H NMR spectroscopy (see section 3.7.4.4) (0.076 g, 93%).

4.7.3.9 Reaction with cobalt(II) chloride hexahydrate (catalytic) and sodium hydrogen carbonate in methanol

4'-Chloro-2,2':6',2''-terpyridine (0.050 g, 0.19 mmol), cobalt(II) chloride hexahydrate (0.003 g, 0.013 mmol) and sodium hydrogen carbonate (0.157 g, 1.87 mmol) were suspended in methanol (15 cm³). After 30 seconds pre-stirring, the pale orange solution was heated at 125 °C for 10 minutes in the microwave reactor. After cooling to room temperature, a second portion of cobalt(II) chloride hexahydrate (0.020 g, 0.084 mmol) was added and the brown solution was stirred at room temperature for 20 minutes. The product was precipitated by addition of excess ammonium hexafluorophosphate in methanol, collected by filtration through Celite, washed well with methanol and diethyl ether and redissolved in acetonitrile. The solvent was removed *in vacuo* to give a brown solid which was identified as bis(4'-methoxy-2,2':6',2''-terpyridine)cobalt(II) hexafluorophosphate by ¹H NMR spectroscopy (see section 3.7.4.4) (0.069 g, 84%).

4.7.3.10 Attempted reaction with methanol

4'-Chloro-2,2':6',2''-terpyridine (0.050 g, 0.187 mmol) was suspended in methanol (15 cm³). After 30 seconds pre-stirring, the mixture was heated at 125 °C for 10 minutes in the microwave reactor to give a colourless solution. The solvent was removed *in vacuo* to give a white solid which was identified as 4'-chloro-2,2':6',2''-terpyridine by ¹H NMR spectroscopy.¹⁶⁹ No yield was determined.

4.7.3.11 Attempted reaction with hydrochloric acid in methanol

4'-Chloro-2,2':6',2''-terpyridine (0.050 g, 0.187 mmol) was suspended in methanol (15 cm³). Concentrated hydrochloric acid (*ca.* 0.2 cm³) was added. After 30 seconds pre-stirring, the mixture was heated at 125 °C for 10 minutes in the microwave reactor to give a colourless solution. The solvent was removed *in vacuo* to give a white solid which was identified as 4'-chloro-2,2':6',2''-terpyridine by ¹H NMR spectroscopy.¹⁶⁹ No yield was determined.

4.7.3.12 Attempted reaction with sulfuric acid in methanol

4'-Chloro-2,2':6',2''-terpyridine (0.020 g, 0.075 mmol) was suspended in methanol (5 cm³). Concentrated sulfuric acid (*ca.* 0.2 cm³) was added. After 30 seconds pre-stirring, the mixture was heated at 125 °C for 10 minutes in the microwave reactor to give a colourless solution. The solvent was removed *in vacuo* to give a colourless oil. This was dissolved in

dichloromethane (10 cm³) and washed with aqueous sodium hydrogen carbonate (2 x 20 cm³). The organic layer was dried over magnesium sulfate dihydrate, filtered and the solvent removed *in vacuo* to give a white solid which was identified as 4'-chloro-2,2':6',2''-terpyridine by ¹H NMR spectroscopy.¹⁶⁹ No yield was determined.

4.7.3.13 Attempted reaction with iron(II) chloride tetrahydrate in methanol

4'-Chloro-2,2':6',2''-terpyridine (0.050 g, 0.19 mmol) and iron(II) chloride tetrahydrate (0.019 g, 0.093 mmol) were suspended in methanol (15 cm³). After 30 seconds pre-stirring, the mixture was heated at 125 °C for 10 minutes in the microwave reactor to give a dark purple solution. After cooling to room temperature, the product was precipitated by addition of excess ammonium hexafluorophosphate in methanol, collected by filtration through Celite, washed well with methanol and diethyl ether and redissolved in acetonitrile. The solvent was removed *in vacuo* to give a purple solid which was identified as bis(4'-chloro-2,2':6',2''-terpyridine) iron(II) hexafluorophosphate by ¹H NMR spectroscopy¹⁸¹ (0.082 g, 100%).

5 Anion Effects

Formation of Mono(2,2':6',2''-terpyridine)cobalt(II) Complexes

5.1 Introduction

After the unexpected consequences of choosing an inappropriate anion for the reaction of bis(terpyridyl)oligo(ethylene glycol)s with cobalt(II) ions in alcohol solutions, the choice of anion for these systems was considered in more detail. Mono(2,2':6',2''-terpyridine)cobalt(II) complexes with coordinated anions are known,^{48, 182-187} and the presence of these complexes within a system containing the ditopic ligands would provide end units for any polymeric species formed, thus influencing the position of the equilibrium between polymers and discrete molecular species.

5.2 Initial observations

As mentioned in Chapter 4, the composition of the mixture of products obtained from the reaction of the ditopic bis(terpyridyl)oligo(ethylene glycol) ligands appears to be very sensitive to the reaction conditions. In an attempt to follow the reaction from the initial mixing of the ligand with the cobalt(II) salt to an equilibrium point (ideally a macrocyclic product), the reaction of a 1:1 mixture of bis(terpyridyl)hexa(ethylene glycol) with cobalt(II) acetate tetrahydrate in a CDCl₃-CD₃OD solvent mixture (9:1) was followed by ¹H NMR spectroscopy. A stacked plot of the spectra is shown in Figure 5.1.

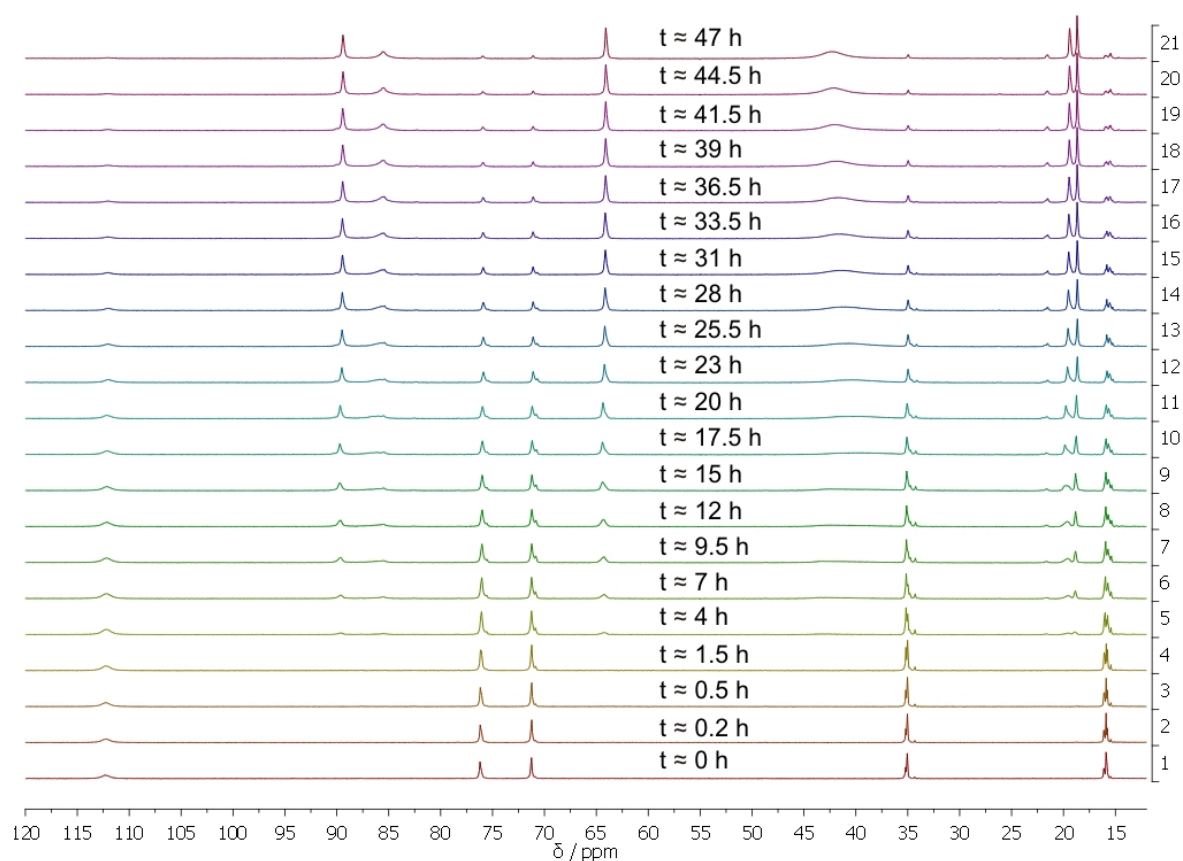


Figure 5.1 Stacked plot of the ^1H NMR spectra (δ 12 – 120 ppm) recorded during the reaction of bis(terpyridyl)hexa(ethylene glycol) with cobalt(II) acetate tetrahydrate (1:1) ($\text{CDCl}_3\text{-CD}_3\text{OD}$ (9:1), 500 MHz, 295 K).

A bis(2,2':6',2''-terpyridine)cobalt(II) complex formed immediately on mixing the two components – this is clear from both the colour of the resulting solution (brown) and the first ^1H NMR spectrum (measured *ca.* 10 minutes after mixing), which displays the paramagnetically shifted peaks characteristic of a low-spin bis(2,2':6',2''-terpyridine)cobalt(II) complex (see Chapter 2). After approximately 2.5 hours, a new species started to form with peaks at δ 89.4, 85.6, 64.1, 19.4, 18.7, 9.25, 7.17, 6.37, 5.84, 5.44 and -2.87 ppm. In addition, a broad peak between δ 35 and 45 ppm appeared, the position of which varied with time (or depending on the ratio of the species). The intensities of these new signals slowly increased at the expense of the original bis(2,2':6',2''-terpyridine)cobalt(II) complex until, after two days, this species was the major component of the mixture. On removing the sample from the spectrometer after two days, it was observed that the originally brown solution had started to form two layers, the lower one pale pink and the upper one brown. Shaking the NMR tube

caused them to mix giving a homogenous brown solution. The ^1H NMR spectrum was measured again and it was found that the ratios of the two species had altered and the original bis(2,2':6',2''-terpyridine)cobalt(II) complex had again become the major component of the mixture, although the new species was still present in appreciable amounts (see Figure 5.2).

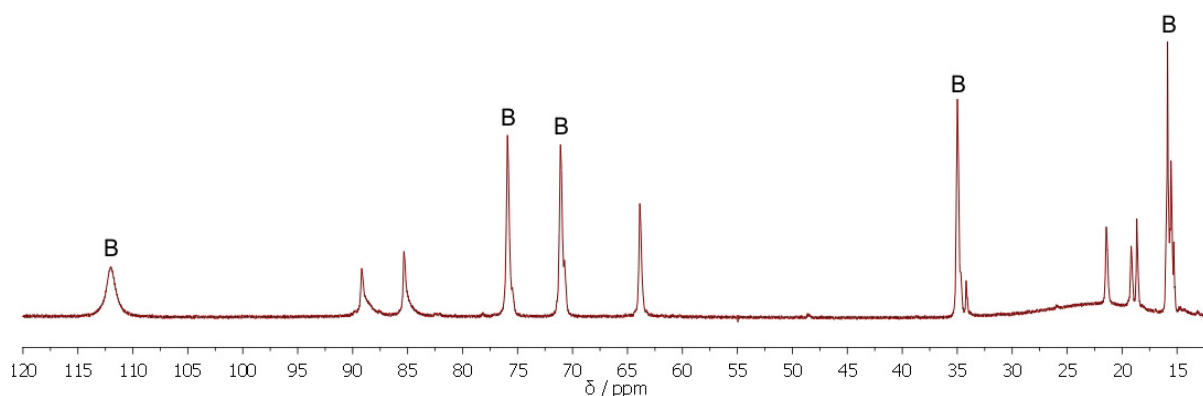


Figure 5.2 ^1H NMR spectrum (δ 12 – 120 ppm) of the reaction of bis(terpyridyl)hexa(ethylene glycol) with cobalt(II) acetate tetrahydrate (1:1) after shaking the NMR tube (CDCl_3 - CD_3OD (9:1), 500 MHz, 295 K). Signals corresponding to the original bis(2,2':6',2''-terpyridine)cobalt(II) complex are labelled B.

The known neutral mono(2,2':6',2''-terpyridine)cobalt(II) complex (Figure 5.3) with two coordinated acetate anions,¹⁸⁷ exhibits signals at δ 92.9, 82.7, 62.3, 24.9, 13.5, 7.62 and 2.73 ppm in CD_3CN - CDCl_3 (1:1) solution containing one drop of CD_3OD .

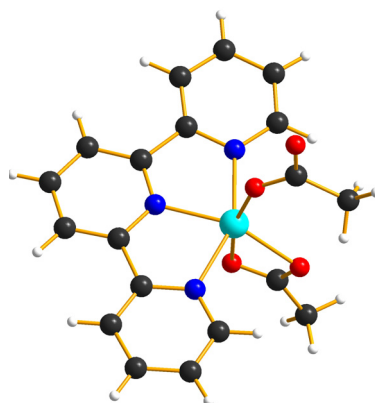
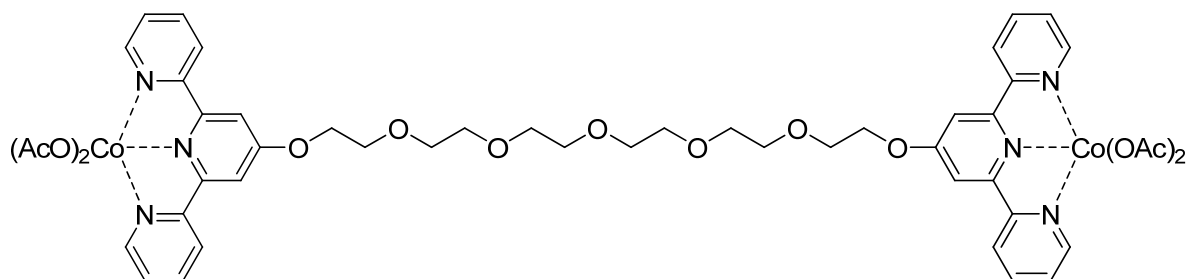


Figure 5.3 X-ray crystal structure of the mono(2,2':6',2''-terpyridine)cobalt(II) complex with two coordinated acetate anions.¹⁸⁷

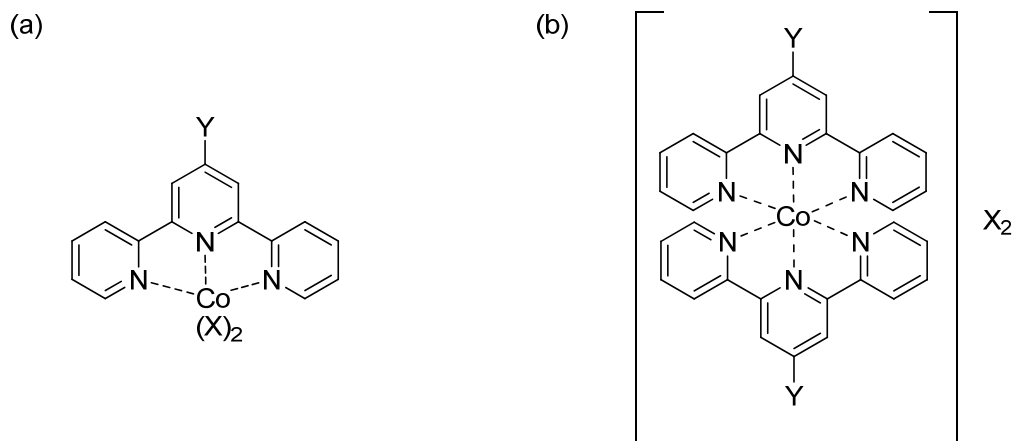
The formation of a similar species in the mixture of bis(terpyridyl)hexa(ethylene glycol) and cobalt(II) acetate tetrahydrate with acetate anions coordinated to the two cobalt(II) centres (see Scheme 5.1) was postulated. Alternatively, oligomers containing one or more bis(2,2':6',2''-terpyridine)cobalt(II) moieties could form with their ends capped with mono(2,2':6',2''-terpyridine)cobalt(II) units with coordinated acetate anions.



Scheme 5.1 Potential structure of the new species formed in the reaction of bis(terpyridyl)hexa(ethylene glycol) with cobalt(II) acetate tetrahydrate (1:1) in CDCl_3 - CD_3OD (9:1).

5.3 Monotopic 2,2':6',2''-terpyridine ligands as model systems

Since a large number of species are likely to be present in any reaction involving the ditopic ligands (macrocycles of different nuclearities, polymers and oligomers of different lengths), investigation of the effect of the anion was first carried out using simpler monotopic 2,2':6',2''-terpyridine ligands. Theoretically, only two (2,2':6',2''-terpyridine)cobalt(II) species are possible in these systems: the bis(2,2':6',2''-terpyridine)cobalt(II) complex or the mono(2,2':6',2''-terpyridine)cobalt(II) species with coordinated anions (see Scheme 5.2), although what exactly is coordinated to the metal ion in the mono(2,2':6',2''-terpyridine)cobalt(II) complex is debatable.

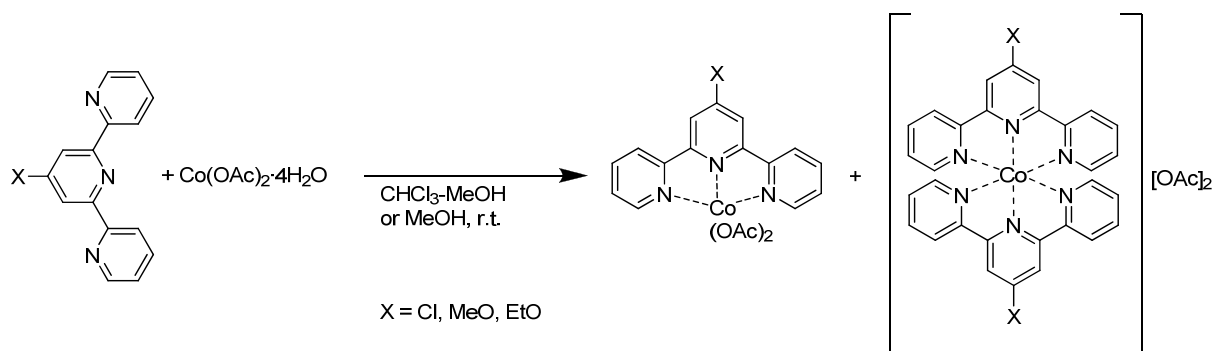


Scheme 5.2 Possible cobalt(II) complexes with monotopic 2,2':6',2''-terpyridine ligands: (a) mono(2,2':6',2''-terpyridine)cobalt(II) complex with coordinated anions and (b) bis(2,2':6',2''-terpyridine)cobalt(II) complex.

5.3.1 Coordinated acetate anions

To investigate the possibility that acetate anions were coordinated to the cobalt(II) metal centre in the complex described in section 5.2, three monotopic 4'-substituted-2,2':6',2''-terpyridine ligands, 4'-chloro-2,2':6',2''-terpyridine, 4'-methoxy-2,2':6',2''-terpyridine and 4'-ethoxy-2,2':6',2''-terpyridine, were mixed with cobalt(II) acetate tetrahydrate in a chloroform-methanol solvent mixture (9:1). After reaction at room temperature, the solvent was removed *in vacuo* and the resulting lilac solid was analysed by ¹H NMR spectroscopy (measured immediately after dissolving the solid in the deuterated solvent). Initially, similar conditions to those described above were used (2L:1M, NMR spectrum measured in CDCl₃ containing one drop of CD₃OD), however, different solvent systems (CD₃OD, CDCl₃-CD₃OD (1:1)) and metal to ligand ratios (1L:1M, 1L:2M) were also considered.

The reaction of monotopic 4'-substituted-2,2':6',2''-terpyridines with cobalt(II) acetate tetrahydrate can give mixtures of bis- and mono(2,2':6',2''-terpyridine)cobalt(II) complexes as shown in Scheme 5.3. The compositions of these mixtures were found to be dependent on various factors which will be discussed below.



Scheme 5.3 Reaction of a monotopic 4'-substituted-2,2':6',2''-terpyridine ligand with cobalt(II) acetate.

The ^1H NMR spectrum in CDCl_3 containing one drop of CD_3OD of the product from the reaction of two equivalents of 4'-methoxy-2,2':6',2''-terpyridine with one equivalent of cobalt(II) acetate tetrahydrate is shown in Figure 5.4. There is clearly only one cobalt(II) containing species present. It is difficult to compare the ^1H NMR spectrum of this species with the known bis(4'-methoxy-2,2':6',2''-terpyridine)cobalt(II) hexafluorophosphate complex as the latter is insoluble in the solvent mixture used here. However, the presence of uncoordinated ligand (signals between δ 7 – 9 ppm) suggests that this species is a mono(2,2':6',2''-terpyridine)cobalt(II) complex.

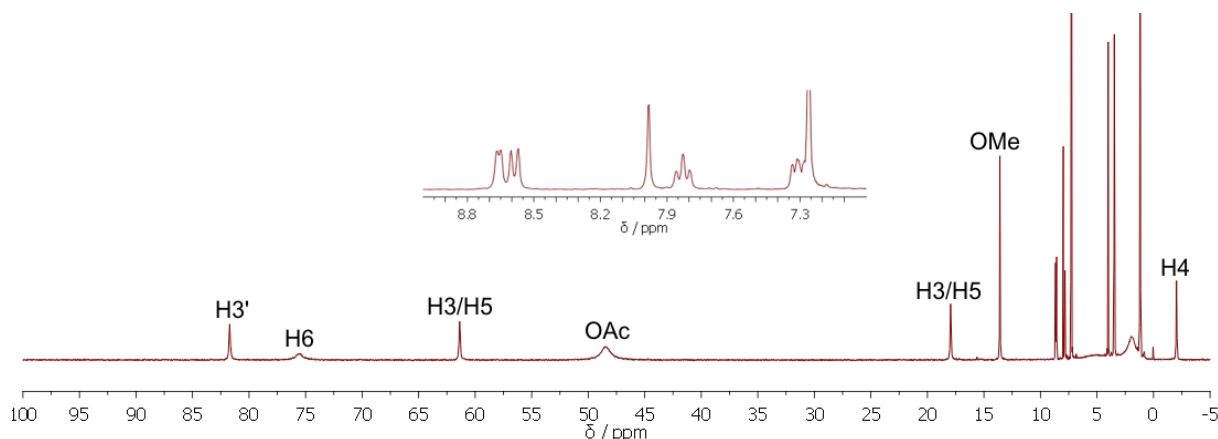


Figure 5.4 Full ^1H NMR spectrum of the product from the reaction of two equivalents of 4'-methoxy-2,2':6',2''-terpyridine with one equivalent of cobalt(II) acetate tetrahydrate (CDCl_3 containing one drop of CD_3OD , 250 MHz). The inset (δ 7 – 9 ppm) shows the presence of uncoordinated ligand.

Assignment of the signals was based on comparison of the integrals of the peaks and on a ^1H - ^1H COSY experiment. The signal at δ 13.6 ppm can be unambiguously assigned to the protons from the methoxy group of the coordinated ligand on the basis of the integral (3 H compared to 2 H for the other sharp paramagnetically shifted signals). The broad signal at δ 48.5 ppm (6 H) is assigned to the coordinated acetate anions. Other signals were assigned based on the ^1H - ^1H COSY experiment as described in Chapters 2 and 3. Unambiguous assignment of the signals corresponding to H^3 and H^5 was not possible as both signals show a cross peak to H^4 only.

Comparison of this spectrum with the spectrum of the reaction product of bis(terpyridyl)hexa(ethylene glycol) with cobalt(II) acetate measured after 47 hours (Figure 5.1) suggests the presence of similar species in the two solutions, supporting the formation of a species with coordinated acetate anions with the ditopic ligand.

The ^1H NMR spectrum of the same solid product from the reaction of two equivalents of 4'-methoxy-2,2':6',2''-terpyridine with one equivalent of cobalt(II) acetate tetrahydrate was also measured in CD_3OD and is shown in Figure 5.5. In this case, it is clear that there are two cobalt(II)-containing species present in solution with an integral ratio of approximately 5:1. The major component exhibits peaks at δ 110, 74.1, 70.0, 34.3, 14.4 and 6.63 ppm and, by comparison with the ^1H NMR spectrum of a sample of bis(4'-methoxy-2,2':6',2''-terpyridine)cobalt(II) hexafluorophosphate in CD_3CN (Figure 5.6(a)), can be identified as the bis(4'-methoxy-2,2':6',2''-terpyridine)cobalt(II) acetate complex. The effect of the anion and the solvent on the ^1H NMR spectrum of the bis(2,2':6',2''-terpyridine)cobalt(II) complex appears to be minimal.

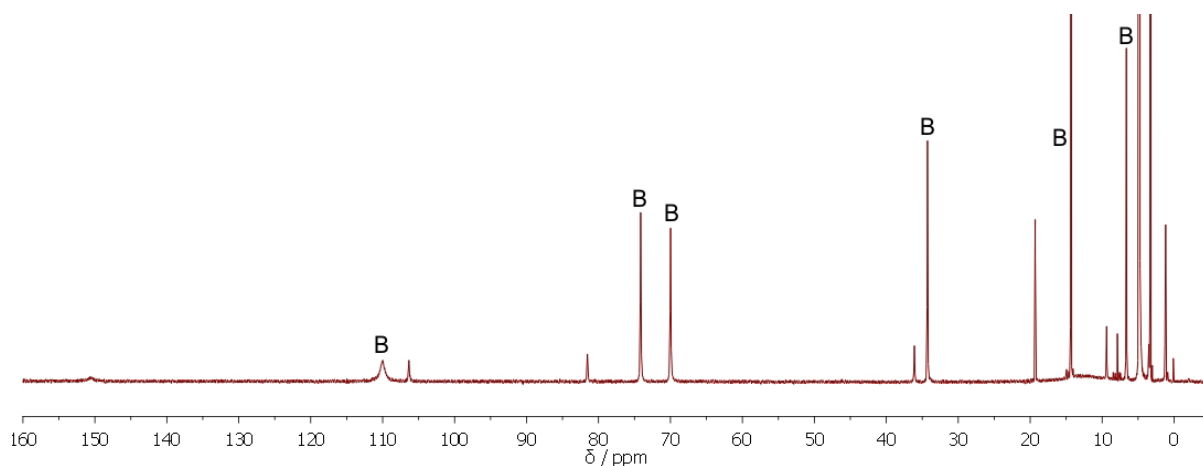


Figure 5.5 Full ^1H NMR spectrum of the product from the reaction of two equivalents of 4'-methoxy-2,2':6',2''-terpyridine with one equivalent of cobalt(II) acetate tetrahydrate (CD_3OD , 250 MHz). Signals corresponding to the bis(4'-methoxy-2,2':6',2''-terpyridine)cobalt(II) complex are labelled B.

The minor component of the mixture can therefore be assumed to be the mono(4'-methoxy-2,2':6',2''-terpyridine)cobalt(II) acetate complex, and the 5:1 integral ratio thus corresponds to a 5:2 ratio of the two complexes in CD_3OD solution. The mono(4'-methoxy-2,2':6',2''-terpyridine)cobalt(II) acetate complex exhibits signals at δ 151, 106, 81.5, 36.1, 19.3 and 9.39 ppm. The position of the highest frequency resonance at δ 151 ppm suggests that the complex has some high-spin character in solution (see Chapter 2).¹⁰⁰ In this sample, the very broad peak at δ 4 – 20 ppm is assigned to the acetate protons. In the case of slow exchange between coordinated and ionic acetate anions, the peak will be broad and represent the average environment of the acetate anion. The signal can therefore be expected to move depending on the relative amounts of the two species.

Using a 1:1 mixture of 4'-methoxy-2,2':6',2''-terpyridine and cobalt(II) acetate tetrahydrate gives almost identical ^1H NMR spectra (Figure 5.6). The only difference in the spectra of 1L:1M and 2L:1M mixtures recorded in CDCl_3 containing one drop of CD_3OD is the absence of the uncoordinated ligand signals in the 1:1 mixture. In CD_3OD solution, the relative amount of the mono(4'-methoxy-2,2':6',2''-terpyridine)cobalt(II) complex increases for the 1L:1M mixture, giving a mono:bis ratio of 2:1 (integral ratio of 1:1). In addition, the broad acetate signal moves from δ 4 – 20 ppm in the 2L:1M system (Figure 5.5) to δ 21 – 33 ppm in the 1L:1M system (Figure 5.6(b)).

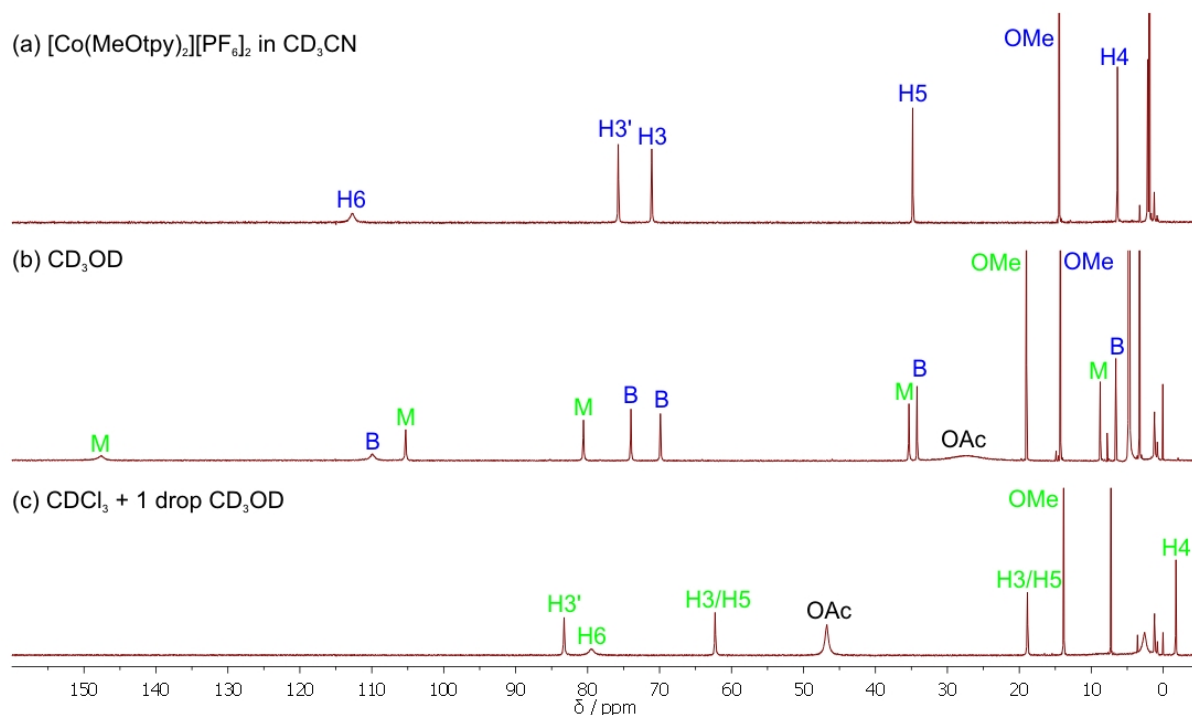


Figure 5.6 Comparison of the full ^1H NMR spectra of (a) $[\text{Co}(\text{MeOtpy})_2][\text{PF}_6]_2$ (CD_3CN , 250 MHz) and the product from the reaction of one equivalent of 4'-methoxy-2,2':6',2''-terpyridine with one equivalent of cobalt(II) acetate tetrahydrate in (b) CD_3OD and (c) CDCl_3 containing 1 drop of CD_3OD (250 MHz). Assignments given in blue correspond to $[\text{Co}(\text{MeOtpy})_2]^{2+}$ (B), assignments given in green correspond to $[\text{Co}(\text{MeOtpy})(\text{OAc})_2]$ (M).

These experiments were repeated using 4'-chloro-2,2':6',2''-terpyridine and 4'-ethoxy-2,2':6',2''-terpyridine in place of 4'-methoxy-2,2':6',2''-terpyridine and similar behaviour was observed. The signals in the ^1H NMR spectra of the 4'-ethoxy-2,2':6',2''-terpyridine complexes are in essentially identical positions as in the spectra of the complexes with the 4'-methoxy-substituted ligand. The ^1H NMR spectra of the complexes of 4'-chloro-2,2':6',2''-terpyridine are shown in Figure 5.7 and the results of all experiments are summarised in Table 5.1.

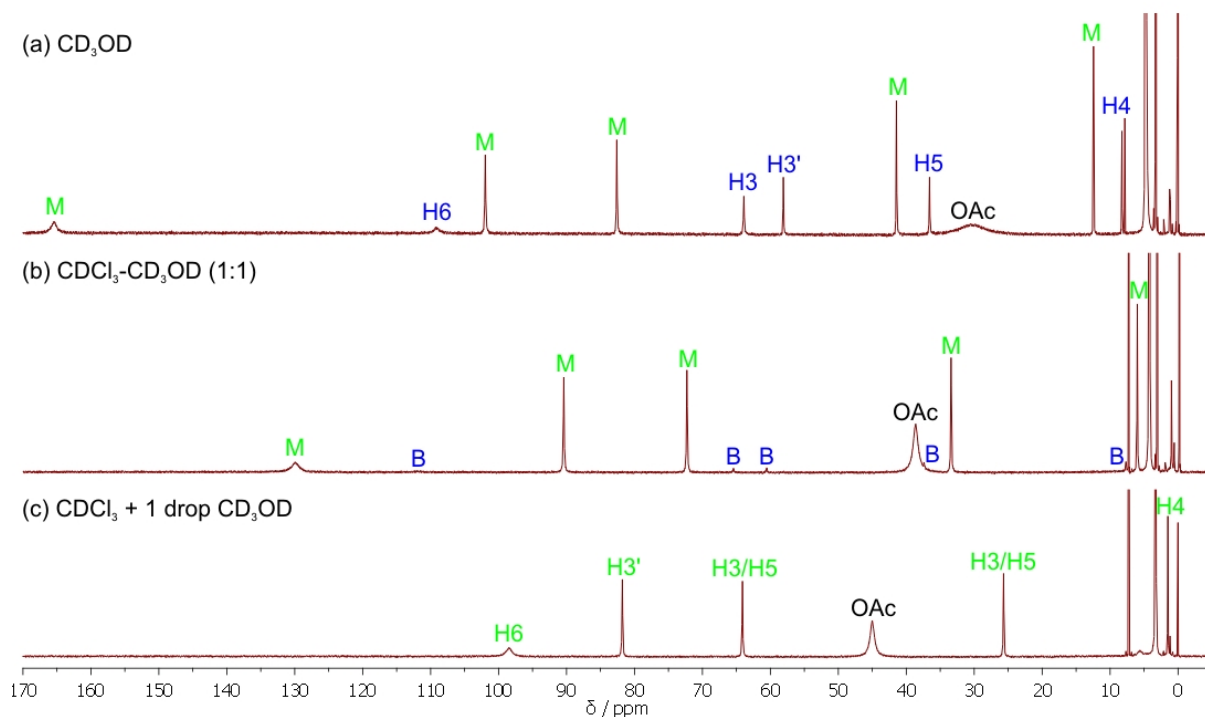


Figure 5.7 Full ^1H NMR spectra of the product from the reaction of a 1:1 mixture of 4'-chloro-2,2':6',2''-terpyridine and cobalt(II) acetate tetrahydrate in (a) CD_3OD , (b) $\text{CDCl}_3\text{-CD}_3\text{OD}$ (1:1) and (c) CDCl_3 containing one drop of CD_3OD (250 MHz). Assignments given in blue correspond to $[\text{Co}(\text{Cltpy})_2][\text{OAc}]_2$ (B), assignments given in green correspond to $[\text{Co}(\text{Cltpy})(\text{OAc})_2]$ (M).

The ratios of mono- to bis(2,2':6',2''-terpyridine)cobalt(II) complexes shown in Table 5.1 cannot be compared between experiments as the ^1H NMR spectra of all of the mixtures were measured immediately after dissolving the solid product in the deuterated solvent, and no attempt was made to establish whether or not the system had reached equilibrium. This issue is considered in section 5.3.2 in a more controlled study of the reaction of 4'-methoxy-2,2':6',2''-terpyridine with several cobalt(II) salts. However, the effect of the composition of the mixture on the broad signal corresponding to the acetate protons is evident from Table 5.1.

Ligand	L:M ratio	Solvent	% Mono	% Bis	Acetate signal / ppm
MeOtpy	2:1	CDCl ₃ + 1 drop CD ₃ OD	100%	0%	45 – 51
		CD ₃ OD	28%	72%	4 – 20
	1:1	CDCl ₃ + 1 drop CD ₃ OD	100%	0%	45 – 48
		CD ₃ OD	65%	35%	21 – 33
EtOtpy	2:1	CDCl ₃ + 1 drop CD ₃ OD	100%	0%	44 – 51
		CD ₃ OD	19%	81%	4 – 14
	1:1	CDCl ₃ + 1 drop CD ₃ OD	100%	0%	45 – 49
		CD ₃ OD	68%	32%	19 – 37
Cltpy	2:1	CDCl ₃ + 1 drop CD ₃ OD	100%	0%	42 – 46
		CDCl ₃ -CD ₃ OD (1:1)	44%	56%	17 – 21
		CD ₃ OD	40%	60%	10 – 22
	1:1	CDCl ₃ + 1 drop CD ₃ OD	100%	0%	43 – 47
		CDCl ₃ -CD ₃ OD (1:1)	99%	1%	36 – 41
		CD ₃ OD	83%	17%	24 – 36
	1:2	CDCl ₃ + 1 drop CD ₃ OD	100%	0%	41 – 47
CD ₃ OD		96%	4%	27 – 38	

Table 5.1 Ratios of mono- to bis(2,2':6',2''-terpyridine)cobalt(II) complexes and position of the signal in the ¹H NMR spectrum corresponding to the acetate protons. Percentages are based on integrals of the peaks corresponding to H3 and H3' (bis) and the two highest frequency sharp singlets (mono).

The paramagnetic shift of the signal corresponding to the acetate protons is expected to increase on coordination of the acetate anion to the cobalt(II) centre. The position of the acetate signal is therefore indicative of the proportion of the mono(2,2':6',2''-terpyridine)cobalt(II) acetate complex present in the solution with a signal at higher frequency indicating a higher proportion of the mono(2,2':6',2''-terpyridine)cobalt(II) complex. The

position of this signal is also solvent dependent, but by comparison of the values from the ^1H NMR spectra measured in CD_3OD solution it is clear that this peak moves to higher frequency as the proportion of the mono(2,2':6',2''-terpyridine)cobalt(II) complex increases.

Addition of excess sodium acetate to a CD_3OD solution of the product from the reaction of two equivalents of 4'-chloro-2,2':6',2''-terpyridine with one equivalent of cobalt(II) acetate tetrahydrate resulted in an increase in the intensity of the signals corresponding to the mono(4'-chloro-2,2':6',2''-terpyridine)cobalt(II) acetate complex, further supporting the formation of a complex with coordinated acetate anions.

MALDI-TOF mass spectra of the products from reactions of mixtures of 4'-chloro-2,2':6',2''-terpyridine with cobalt(II) acetate tetrahydrate (1L:1M and 2L:1M) were measured using sinapinic acid ($M = 224 \text{ g mol}^{-1}$) as a matrix and all samples were transferred to the mass spectrometer plate as both chloroform and methanol solutions. In all cases the following peaks were observed: $m/z = 268 [\text{Cltpy} + \text{H}]^+$, $290 [\text{Cltpy} + \text{Na}]^+$, $306 [\text{Cltpy} + \text{K}]^+$, $549 [\text{Co}(\text{Cltpy}) + \text{matrix}]^+$, $593 [\text{Co}(\text{Cltpy})_2]^+$, $774 [\text{Co}(\text{Cltpy}) + 2\text{matrix}]^+$. The intensities of the signals did not correspond to the composition of the mixtures as determined by ^1H NMR spectroscopy, so this method of characterisation was not employed further.

The advantage of using paramagnetic cobalt(II) salts for these investigations became clear when attempting an equivalent reaction with a 1:1 mixture of 4'-chloro-2,2':6',2''-terpyridine and iron(II) chloride tetrahydrate. Very little information could be gained from the ^1H NMR spectrum due to the overlap of the signals corresponding to the two (4'-chloro-2,2':6',2''-terpyridine)iron(II) species present in solution.

5.3.2 NMR spectroscopic studies with other anions

The monotopic ligand 4'-methoxy-2,2':6',2''-terpyridine was mixed with cobalt(II) acetate tetrahydrate, cobalt(II) chloride hexahydrate, cobalt(II) nitrate hexahydrate or cobalt(II) tetrafluoroborate hexahydrate at room temperature in the ratios and solvents given in Table 5.2. In all experiments the concentration of cobalt(II) was 0.030 M. The reaction mixtures with a 2L:1M ratio were then diluted with the same solvent mixture to give three samples with concentrations of 0.030 M, 0.015 M and 0.0076 M, and all samples were characterised by ^1H NMR spectroscopy. Also shown in Table 5.2 are the ratios of mono- to bis(4'-methoxy-2,2':6',2''-terpyridine)cobalt(II) complexes as determined from the ^1H NMR spectra and these results are discussed below.

CoX ₂ ·nH ₂ O	L:M ratio	Solvent	% Mono	% Bis
Co(OAc) ₂ ·4H ₂ O	2:1	CDCl ₃ -CD ₃ OD (9:1)	15 – 22% ^a	78 – 85% ^a
		CD ₃ OD	11 – 13% ^a	87 – 89% ^a
	1:1	CDCl ₃ -CD ₃ OD (9:1)	100%	0%
		CD ₃ OD	61%	39%
CoCl ₂ ·6H ₂ O	2:1	CDCl ₃ -CD ₃ OD (9:1)	0%	100%
		CD ₃ OD	0%	100%
	1:1	CDCl ₃ -CD ₃ OD (9:1)	insoluble	insoluble
		CD ₃ OD	precipitate ^b	precipitate ^b
Co(NO ₃) ₂ ·6H ₂ O	2:1	CDCl ₃ -CD ₃ OD (9:1)	14 – 15% ^a	84 – 85% ^a
		CD ₃ OD	5 – 6% ^a	94 – 95% ^a
	1:1	CDCl ₃ -CD ₃ OD (9:1)	precipitate ^b	precipitate ^b
		CD ₃ OD	43%	57%
Co(BF ₄) ₂ ·6H ₂ O	2:1	CD ₃ CN	0%	100%
	1:1	CD ₃ CN	57%	43%

Table 5.2 Ratios of mono- to bis(4'-methoxy-2,2':6',2''-terpyridine)cobalt(II) complexes. Percentages are based on integrals of the peaks corresponding to H3 and H3' (bis) and two highest frequency sharp singlets (mono). a = ratios depend slightly on concentration, with more of the mono(4'-methoxy-2,2':6',2''-terpyridine)cobalt(II) complex at lower concentrations. b = a precipitate formed during the reaction so the ratios measured from the ¹H NMR spectrum do not correspond to an equilibrium position.

The compositions of the mixtures of products from the reaction of 4'-methoxy-2,2':6',2''-terpyridine with cobalt(II) salts are clearly dependent on several factors including the initial ratio of ligand to metal, the solvent and the anion. In all cases, the bis(4'-methoxy-2,2':6',2''-terpyridine)cobalt(II) complex is favoured by using ratios of 2L:1M, and using a 1:1 ratio of the ligand to the cobalt(II) salt gives a greater proportion of the mono(4'-methoxy-2,2':6',2''-terpyridine)cobalt(II) complex. With acetate and nitrate, the proportion of the mono(4'-methoxy-2,2':6',2''-terpyridine)cobalt(II) complex is increased by using CDCl₃-CD₃OD (9:1)

as a solvent. The more polar methanol solvent solubilises and stabilises the ionic bis(4'-methoxy-2,2':6',2''-terpyridine)cobalt(II) complex. Conversely, the neutral mono(4'-methoxy-2,2':6',2''-terpyridine)cobalt(II) complex should be more soluble in the less polar chloroform solvent. The green mono(4'-methoxy-2,2':6',2''-terpyridine)cobalt(II) chloride is particularly insoluble in both CDCl₃-CD₃OD (9:1) and CD₃OD and the ¹H NMR spectrum could only be measured in CD₃OD solution shortly after mixing one equivalent of the ligand with one equivalent of cobalt(II) chloride hexahydrate before precipitation of the complex occurred. The pink mono(4'-methoxy-2,2':6',2''-terpyridine)cobalt(II) nitrate is also only sparingly soluble in the CDCl₃-CD₃OD (9:1) solvent mixture. Systems involving these species in the solvents specified above cannot be considered to be at equilibrium. Considering only those systems at equilibrium, the proportion of the mono(4'-methoxy-2,2':6',2''-terpyridine)cobalt(II) species decreases in the order OAc⁻ > [NO₃]⁻ > Cl⁻, with only the bis(4'-methoxy-2,2':6',2''-terpyridine)cobalt(II) species present in solution when the chloride anion is used. The acetate anion can coordinate to a metal centre as a bidentate ligand, stabilising the complex by the chelate effect. The negative charge on the anion is also delocalised making the complex relatively non-polar, and the methyl group of the anion further helps to solubilise the complex in organic solvents. The nitrate anion could also potentially act as a chelating ligand and has a delocalised negative charge, leading to similar equilibrium mixtures to the acetate system. Finally, the chloride anion is a hard spherical monodentate anion, which gives the most polar and least soluble mono(4'-methoxy-2,2':6',2''-terpyridine)cobalt(II) complexes. The ¹H NMR spectra of the acetate, chloride and nitrate systems are shown in Figure 5.8, Figure 5.9 and Figure 5.10, respectively.

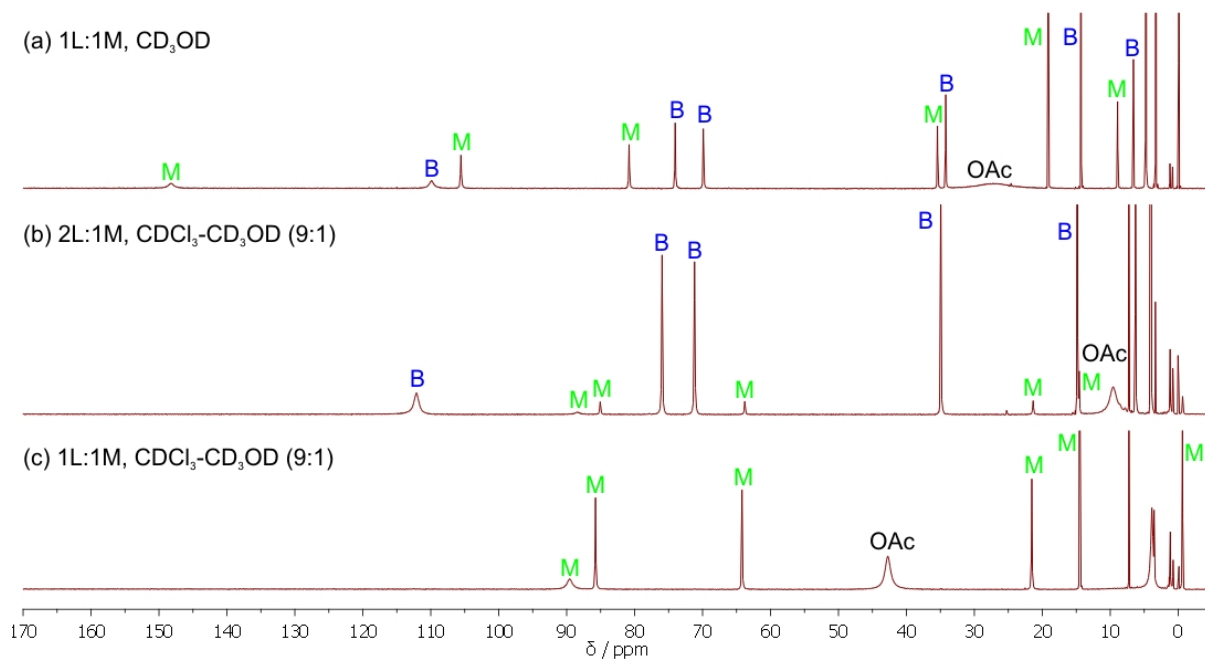


Figure 5.8 Full ^1H NMR spectra of mixtures of 4'-methoxy-2,2':6,2''-terpyridine and cobalt(II) acetate tetrahydrate (250 MHz). (a) 1L:1M in CD_3OD , (b) 2L:1M in $\text{CDCl}_3\text{-CD}_3\text{OD}$ (9:1), (c) 1L:1M in $\text{CDCl}_3\text{-CD}_3\text{OD}$ (9:1). The spectrum of 2L:1M in CD_3OD is identical to that of 1L:1M in CD_3OD except for the intensities of the peaks. Signals corresponding to the bis(2,2':6,2''-terpyridine)cobalt(II) complex are labelled B and those corresponding to the mono(2,2':6,2''-terpyridine)cobalt(II) complex are labelled M.

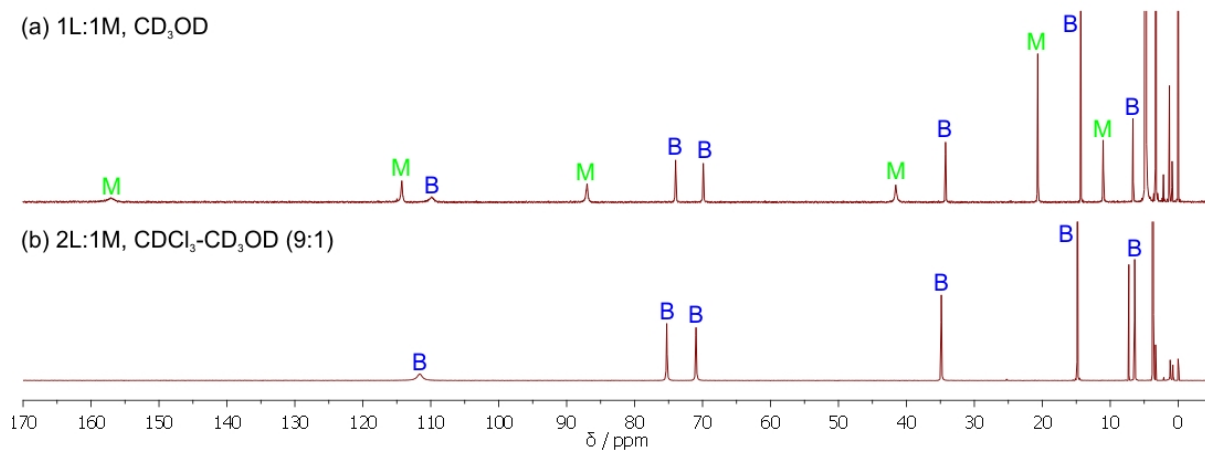


Figure 5.9 Full ^1H NMR spectra of mixtures of 4'-methoxy-2,2':6,2''-terpyridine and cobalt(II) chloride hexahydrate (250 MHz). (a) 1L:1M in CD_3OD (not at equilibrium), (b) 2L:1M in $\text{CDCl}_3\text{-CD}_3\text{OD}$ (9:1). The spectrum of 2L:1M in CD_3OD shows only the bis(4'-methoxy-2,2':6,2''-terpyridine)cobalt(II) complex. The product of 1L:1M is insoluble in the $\text{CDCl}_3\text{-CD}_3\text{OD}$ (9:1) solvent mixture. Signals corresponding to the bis(2,2':6,2''-terpyridine)cobalt(II) complex are labelled B and those corresponding to the mono(2,2':6,2''-terpyridine)cobalt(II) complex are labelled M.

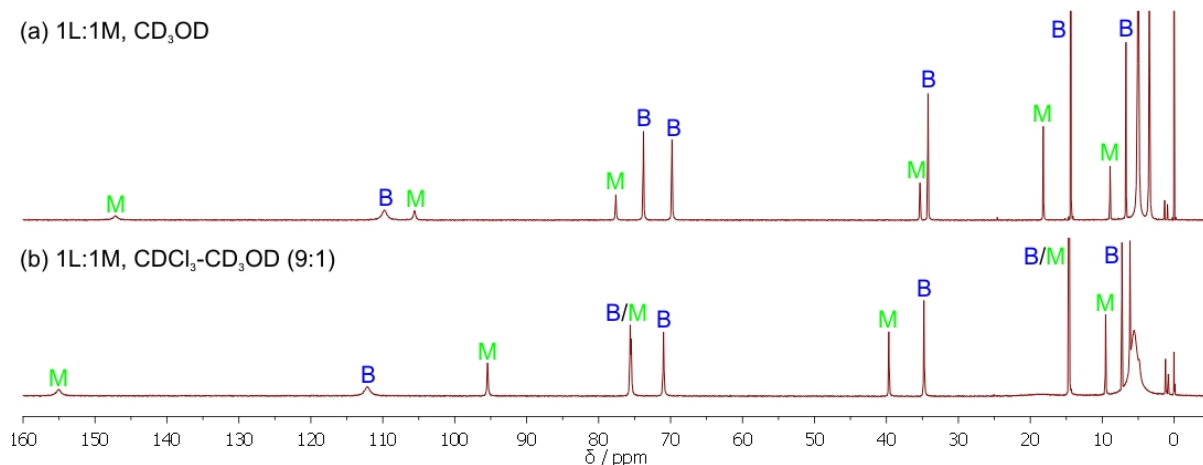


Figure 5.10 Full ^1H NMR spectra of 1:1 mixtures of 4'-methoxy-2,2':6',2''-terpyridine and cobalt(II) nitrate hexahydrate in (a) CD_3OD , (b) CDCl_3 - CD_3OD (9:1) (not at equilibrium) (250 MHz). The spectra of 2L:1M are identical to those of 1L:1M in the same solvent except for the intensities of the peaks. Signals corresponding to the bis(2,2':6',2''-terpyridine)cobalt(II) complex are labelled B and those corresponding to the mono(2,2':6',2''-terpyridine)cobalt(II) complex are labelled M.

By comparison of the ^1H NMR spectra of the systems described above, it is clear that while the ^1H NMR spectrum of the bis(2,2':6',2''-terpyridine)cobalt(II) complex is largely independent of the solvent, the ^1H NMR spectra of the mono(2,2':6',2''-terpyridine)cobalt(II) complexes are highly dependent on both the solvent and the anion.

As mentioned in Chapter 2, the appearance of the ^1H NMR spectrum of bis(2,2':6',2''-terpyridine)cobalt(II) complexes is indicative of the spin state of the complex in solution.¹⁰⁰ In CD_3CN solution bis(2,2':6',2''-terpyridine)cobalt(II) hexafluorophosphate complexes are low-spin and the highest frequency resonance (corresponding to H^6) is observed at approximately δ 100 ppm. High-spin complexes, such as the cobalt(II) complex of 6-bromo-2,2':6',2''-terpyridine, exhibit high frequency resonances up to δ 260 ppm.¹⁰⁰ In the solid state, the spin state of bis(4'-substituted-2,2':6',2''-terpyridine)cobalt(II) complexes is temperature dependent and highly influenced by the substituent, the anion and the presence of solvate molecules in the crystal structure (see Chapter 3). Mono(2,2':6',2''-terpyridine)cobalt(II) complexes with halide, nitrate and isothiocyanate (NCS^-) anions are high-spin in the solid state.^{48, 182, 184, 185}

The magnetic susceptibilities of cobalt(II) chloride hexahydrate and cobalt(II) nitrate hexahydrate have been determined in water, ethanol and acetone solution,¹⁸⁸ and found to be

significantly influenced by the solvent. Based on the chemical shifts of the highest frequency signals in the ^1H NMR spectra shown in Figure 5.8 to Figure 5.10, the spin state in the mono(4'-methoxy-2,2':6',2''-terpyridine)cobalt(II) complexes also seems to be highly dependent on the solvent, and could be a result of coordination of one or more solvent molecules to the cobalt(II) centre in place of one or both of the coordinated anions or as a sixth ligand. However, the fact that the ^1H NMR spectra differ for the mono(4'-methoxy-2,2':6',2''-terpyridine)cobalt(II) species with different anions suggests that one or more of the anions must remain coordinated.

The behaviour of a non-coordinating anion ($[\text{BF}_4]^-$) was also studied and was anticipated to form the bis(4'-methoxy-2,2':6',2''-terpyridine)cobalt(II) complex irrespective of the initial ratio of ligand to metal salt. Using an initial ligand to cobalt(II) tetrafluoroborate hexahydrate ratio of 2:1 resulted in the expected formation of only bis(4'-methoxy-2,2':6',2''-terpyridine)cobalt(II) tetrafluoroborate. The ^1H NMR spectrum of a 1:1 mixture in CD_3CN is shown in Figure 5.11 and it is clear that two cobalt(II) species are present in solution.

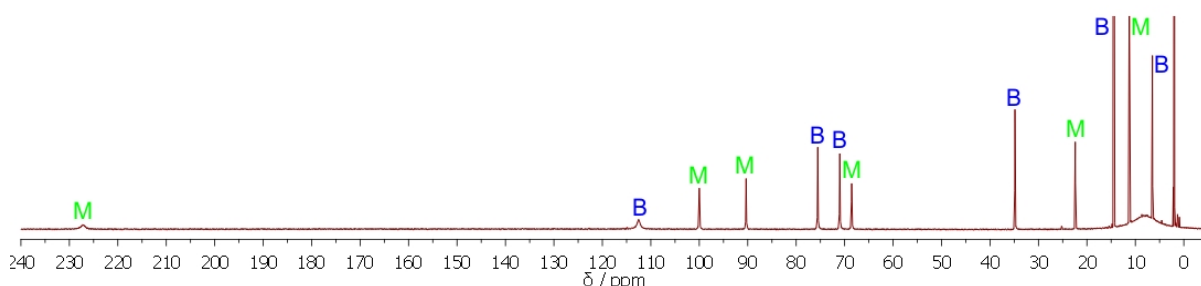
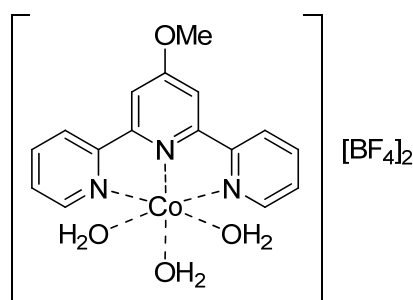


Figure 5.11 Full ^1H NMR spectra of a 1:1 mixture of 4'-methoxy-2,2':6',2''-terpyridine and cobalt(II) tetrafluoroborate hexahydrate in CD_3CN (250 MHz). Signals corresponding to the bis(2,2':6',2''-terpyridine)cobalt(II) complex are labelled B and those corresponding to the mono(2,2':6',2''-terpyridine)cobalt(II) complex are labelled M.

The broad peak at δ -3 – 19 ppm is assigned to the water protons as the normal signal for water in CD_3CN at δ 2.13 ppm is missing. It is proposed that the mono(4'-methoxy-2,2':6',2''-terpyridine)cobalt(II) species has a structure as shown in Scheme 5.4, with up to three coordinated water molecules. These water molecules would be in equilibrium with the free water molecules in the solvent, giving rise to the broadened signal in the ^1H NMR spectrum. The proposed mono(4'-methoxy-2,2':6',2''-terpyridine)cobalt(II) complex appears to be high-

spin in solution due to the position of the highest frequency resonance at δ 227 ppm (see Chapter 2).¹⁰⁰



Scheme 5.4 Proposed structure for the mono(4'-methoxy-2,2':6',2''-terpyridine)cobalt(II) tetrafluoroborate species.

5.3.3 Crystal structures of mono(4'-substituted-2,2':6',2''-terpyridine)cobalt complexes

Further confirmation for the formation of mono(4'-substituted-2,2':6',2''-terpyridine)cobalt(II) complexes came from the determination of the single crystal X-ray structures of $[\text{Co}(\text{Cltpy})(\text{OAc})_2]$, $[\text{Co}(\text{MeOtpy})(\text{OAc})_2]$, $[\text{Co}(\text{MeOtpy})(\text{NO}_3)_2(\text{OH}_2)]$ and $[\text{Co}(\text{MeOtpy})\text{Cl}_2]$. Diffusion of diethyl ether into a chloroform-methanol solution of the product from the reaction of a 1:1 mixture of 4'-chloro-2,2':6',2''-terpyridine and cobalt(II) acetate tetrahydrate gave green crystals of $[\text{Co}(\text{Cltpy})\text{Cl}_3]\cdot\text{CHCl}_3$ after several weeks. Yellow X-ray quality crystals of $[\text{Fe}(\text{Cltpy})\text{Cl}_3]\cdot\text{CHCl}_3$ were obtained by slow evaporation of a purple solution of the product from the reaction of one equivalent of 4'-chloro-2,2':6',2''-terpyridine with one equivalent of iron(II) chloride tetrahydrate in CDCl_3 containing a few drops of CD_3OD . The X-ray crystal structure determinations of these trivalent complexes are also discussed below. Cobalt–nitrogen bond lengths, $\text{N}_{\text{terminal}}\text{--Co--N}_{\text{terminal}}$ bond angles and angles between the least-squared planes of the pyridine rings are given in Table 5.3.

Complex	M–N1	M–N2	M–N3	N1–M–N3	angle between least-squared planes containing:	
					N1 and N2	N2 and N3
[Co(MeOtpy)(OAc) ₂]	2.1343(13)	2.0378(11)	2.1617(13)	152.16(4)	5.08(4)	3.53(4)
[Co(MeOtpy)Cl ₂] ^a	2.1636(6)	2.0365(6)	2.1573(6)	151.17(2)	6.44(1)	7.39(2)
	2.1527(6)	2.0466(6)	2.1440(6)	148.38(2)	5.95(2)	3.00(2)
[Co(MeOtpy)(NO ₃) ₂ (OH ₂)]	2.1465(13)	2.0699(12)	2.1256(13)	151.40(5)	2.20(5)	3.02(5)
[Co(Cltpy)(OAc) ₂]	2.1430(16)	2.0433(15)	2.1567(16)	152.95(6)	5.79(6)	10.11(7)
[Co(Cltpy)Cl ₃]·CHCl ₃	1.952(2)	1.8582(19)	1.9363(19)	165.39(8)	8.10(6)	0.65(7)
[Fe(Cltpy)Cl ₃]·CHCl ₃ ^b	2.148(3)	2.125(3)	2.130(3)	148.93(11)	2.20(10)	1.48(9)

Table 5.3 Cobalt–nitrogen bond lengths (Å) and selected bond angles and angles between least-squared planes (°) in mono(2,2':6',2''-terpyridine)cobalt(II) (white), cobalt(III) (green) and iron(III) (yellow) complexes. N2 is the nitrogen atom in the central pyridine ring. The numbering of the atoms in the table does not always correspond to the numbering of the atoms in the cif file. (a = The numbering of the second cation in the asymmetric unit uses the labels N4–6 in the cif file, b = N2 is labelled N1' and N3 is labelled N1'' in the cif file.)

As described in section 3.3, the length of the cobalt–nitrogen bonds in bis(2,2':6',2''-terpyridine)cobalt(II) salts is indicative of the spin state of the complex, with high-spin species having significantly longer cobalt–nitrogen bond lengths than low-spin species. The Co–N_{central} bond length in bis(2,2':6',2''-terpyridine)cobalt(II) iodide dihydrate, which has a magnetic moment of 2.2 μ_B is 1.912(5) Å and this value can be considered typical for a fully low-spin species.¹⁵² A representative value for a high-spin species comes from the structure of the perchlorate salt with 1.3 water molecules at 295 K. This species has a magnetic moment of 4.2 μ_B and Co–N_{central} bond lengths of 2.030(6) and 2.026(6) Å.¹⁵¹ Longer bond lengths were measured for bis(2,2':6',2''-terpyridine)cobalt(II) nitrate dihydrate (Co–N_{central} = 2.101(4) and 2.075(3) Å), but no magnetic data are available for this complex.¹⁵³

Inspection of the cobalt–nitrogen bond lengths in Table 5.3 suggests that all the mono(4'-substituted-2,2':6',2''-terpyridine)cobalt(II) complexes are in the high-spin state in the solid state, irrespective of the coordinated anion. This is in agreement with published magnetic data for the mono(2,2':6',2''-terpyridine)cobalt(II) halide, nitrate and isothiocyanate (NCS) species.^{48, 182, 184, 185} The cobalt–nitrogen bond lengths for the cobalt(III) complex, [Co(Cltpy)Cl₃]·CHCl₃, are significantly shorter than for the cobalt(II) complexes and within the ranges found for the bis(2,2':6',2''-terpyridine)cobalt(III) complexes described in section 3.3. The iron–nitrogen bond lengths in [Fe(Cltpy)Cl₃]·CHCl₃ are considerably longer (0.19 Å) than the cobalt–nitrogen bonds in the analogous cobalt(III) complex. Probably also due to the smaller variation in spin state, the N_{terminal}–Co–N_{terminal} bite angles for the mono(2,2':6',2''-terpyridine)cobalt(II) complexes span a much smaller range than for the bis(2,2':6',2''-terpyridine)cobalt(II) complexes (Section 3.3) and these angles are at the lower end of the range seen for the bis(2,2':6',2''-terpyridine) complexes. Again, the cobalt(III) species shows a larger (12 – 17°) bite angle than the cobalt(II) complexes, and the same angle in the analogous iron(III) complex is of a similar size (as are the M–N bond lengths) to the cobalt(II) species.

The molecular structures of [Co(MeOtpy)(OAc)₂] and [Co(Cltpy)(OAc)₂] are shown in Figure 5.12 and Figure 5.13, respectively. Both have a similar structure in which the cobalt(II) ion is six-coordinate with one monodentate (MeOtpy: Co–O = 1.9926(11) Å, Cltpy: Co–O = 1.9957(14) Å) and one bidentate (MeOtpy: Co–O = 2.1240(11) Å and 2.2256(11) Å, Cltpy: Co–O = 2.0454(14) Å and 2.3790(15) Å) acetate ligand. The geometry around the cobalt(II) centre is distorted from the ideal octahedral arrangement due to the restricted bite angle of the

bidentate acetate ligand (MeOtpy, O–Co–O = 60.28(4)°, Cltpy, O–Co–O = 58.69(6)°) resulting in $N_{\text{central}}\text{--Co--}O_{\text{monodentate}}$ angles of 97.77(4)° (MeOtpy) and 92.85(6)° (Cltpy) and $N_{\text{central}}\text{--Co--}O_{\text{bidentate}}$ angles of 104.99(5)° (MeOtpy) and 111.84(6)° (Cltpy).

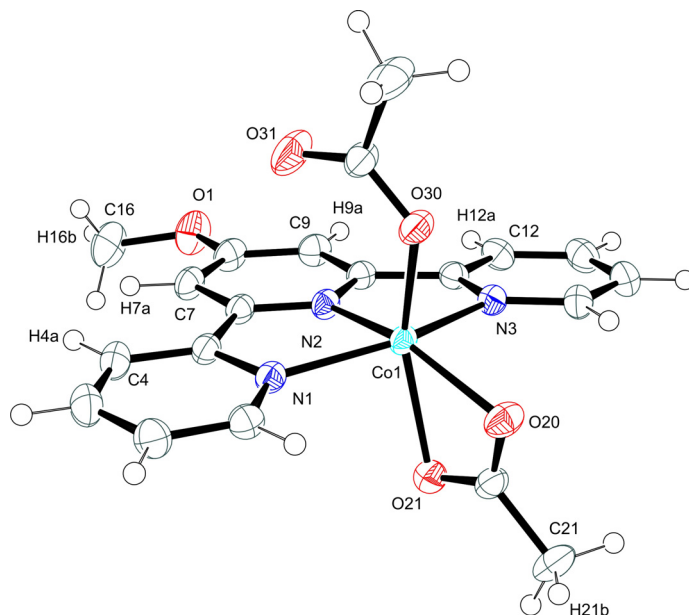


Figure 5.12 Molecular structure of $[\text{Co}(\text{MeOtpy})(\text{OAc})_2]$ with anisotropic displacement ellipsoids drawn at the 50% probability level. Hydrogen atoms are shown as spheres of arbitrary radius.

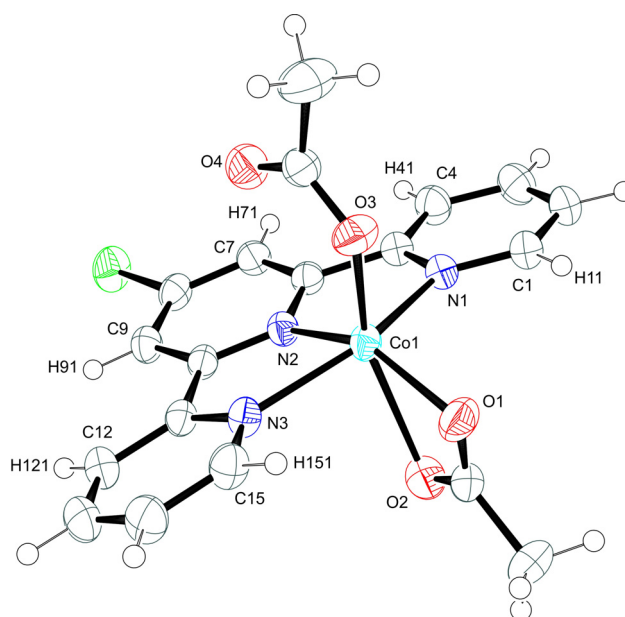


Figure 5.13 Molecular structure of $[\text{Co}(\text{Cltpy})(\text{OAc})_2]$ with anisotropic displacement ellipsoids drawn at the 50% probability level. Hydrogen atoms are shown as spheres of arbitrary radius.

In both structures, the non-coordinated oxygen atom of the monodentate acetate ligand sits approximately over the Co–N_{central} bond, and a hydrogen-bonded dimer featuring non-classical C–H···O interactions is formed by the interaction of this oxygen atom with the protons in the 3- and 3'-positions of an adjacent terpyridine (MeOtpy, C4ⁱ–H4Aⁱ···O31 = 2.37 Å, C7ⁱ–H7Aⁱ···O31 = 2.40 Å; Cltpy, C4ⁱ–H41ⁱ···O4 = 2.64 Å, C7ⁱⁱ–H71ⁱⁱ···O4 = 2.27 Å; symmetry codes i = 2 – x, 1 – y, 2 – z, ii = 1 – x, 1 – y, 1 – z) (Figure 5.14). This packing motif is in contrast with the structure of [Co(tpy)(OAc)₂] \cdot 0.5H₂O, which shows a similar arrangement of ligands around the cobalt(II) centre. In this structure, the non-coordinated oxygen atoms of two monodentate acetate ligands form hydrogen-bonds to the water molecule, forming dinuclear [Co(tpy)(OAc)₂](H₂O)[Co(tpy)(OAc)₂] units, which pack via π -stacking interactions.¹⁸⁷

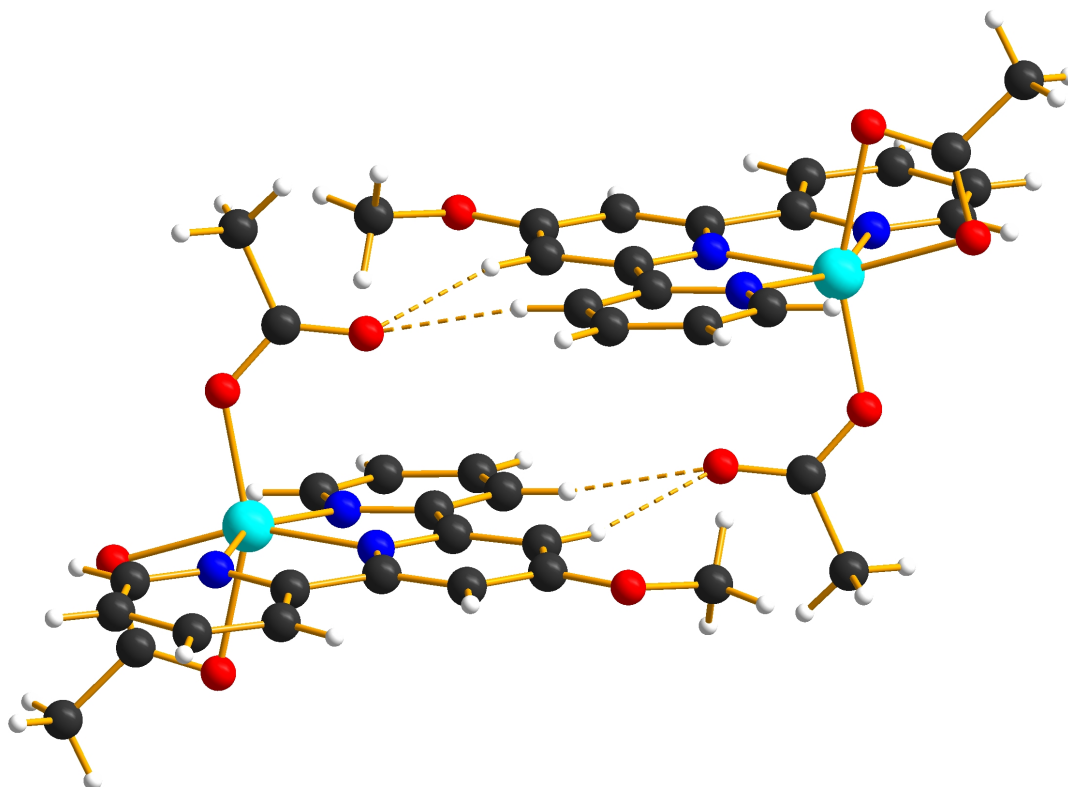


Figure 5.14 Non-classical hydrogen-bonded centrosymmetric dimer in [Co(MeOtpy)OAc₂].

The two structures, [Co(MeOtpy)(OAc)₂] and [Co(Cltpy)(OAc)₂], with coordinated acetates differ in the packing of the dimeric units. In the structure of [Co(MeOtpy)(OAc)₂], the coordinated oxygen atoms of the acetate ligands form hydrogen bonds with the protons from

the methoxy groups ($C16^{iii}-H16B^{iii}\cdots O30 = 2.40 \text{ \AA}$; symmetry code, $iii = x, 1 + y, z$), the protons from the methyl group of the bidentate acetate ($C21^{iv}-H21B^{iv}\cdots O20 = 2.62 \text{ \AA}$; symmetry code $iv = 2 - x, 2 - y, 1 - z$), or the protons in the 3- and 3'-positions on the other side of the terpyridine ligand ($C9^{ii}-H9A^{ii}\cdots O21 = 2.55 \text{ \AA}$, $C12^{ii}-H12A^{ii}\cdots O21 = 2.43 \text{ \AA}$; symmetry code $ii = 1 - x, 1 - y, 1 - z$), forming a three-dimensional network of dimers. In the structure of $[Co(Cltpy)(OAc)_2]$ with no methoxy groups, the hydrogen bonds are formed between the oxygen atoms and the protons in the 6-positions of the terpyridine ($C1^v-H11^v\cdots O1 = 2.44 \text{ \AA}$, $C15^{vi}-H151^{vi}\cdots O3 = 2.59 \text{ \AA}$; symmetry codes $v = -x, -y, -z$, $vi = 1 - x, -y, -z$). Similar hydrogen bonds as in the structure of $[Co(MeOtpy)(OAc)_2]$ are formed between the remaining oxygen atom and the protons in the 3- and 3'-positions of the terpyridine ($C9^{vii}-H91^{vii}\cdots O2 = 2.43 \text{ \AA}$, $C12^{vii}-H121^{vii}\cdots O2 = 2.57 \text{ \AA}$; symmetry code $vii = 1 - x, -y, 1 - z$), also resulting in a three-dimensional network of dimers. The three-dimensional networks are further supported by offset face-to-face $\pi-\pi$ interactions between adjacent dimeric units (distance between the planes = 3.5 \AA).

The molecular structure of $[Co(MeOtpy)(NO_3)_2(OH_2)]$ is shown in Figure 5.15. The cobalt(II) centre is again six-coordinate with two monodentate nitrate ligands ($Co-O = 2.1445(12)$ and $2.1513(12) \text{ \AA}$) and one coordinated water molecule ($Co-O8 = 2.0246(12) \text{ \AA}$). The two nitrate ligands lie *trans* to one another with the oxygen of the coordinated water in the same plane as the 4'-methoxy-2,2':6',2''-terpyridine ligand.

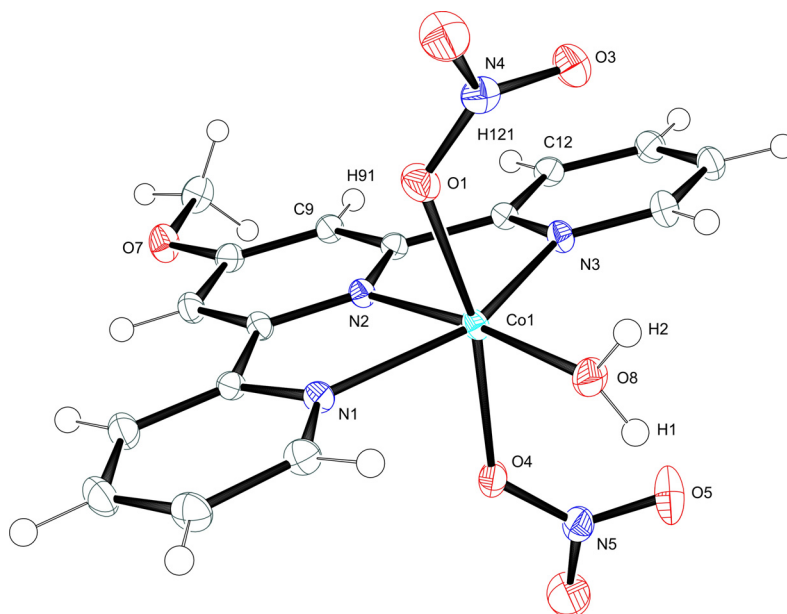


Figure 5.15 Molecular structure of $[\text{Co}(\text{MeOtpy})(\text{NO}_3)_2(\text{OH}_2)]$ with anisotropic displacement ellipsoids drawn at the 50% probability level. Hydrogen atoms are shown as spheres of arbitrary radius.

The molecules form hydrogen-bonded chains as shown in Figure 5.16 through the interaction of the water protons with the nitrate oxygen atoms on an adjacent molecule ($\text{O8}^{\text{viii}}-\text{H2}^{\text{viii}}\cdots\text{O3} = 1.95 \text{ \AA}$, $\text{O8}^{\text{ii}}-\text{H1}^{\text{ii}}\cdots\text{O5} = 2.27 \text{ \AA}$; symmetry codes $\text{viii} = 1 - x, 1 - y, -z$; $\text{ii} = 1 - x, 1 - y, 1 - z$). Interaction between the chains is via hydrogen bonding between one of the coordinated oxygen atoms of one of the nitrate groups and the protons in the 3- and 3'-positions of the terpyridine ligand ($\text{C9}^{\text{ix}}-\text{H91}^{\text{ix}}\cdots\text{O4} = 2.52 \text{ \AA}$, $\text{C12}^{\text{ix}}-\text{H121}^{\text{ix}}\cdots\text{O4} = 2.53 \text{ \AA}$; symmetry code $\text{ix} = 0.5 + x, 1.5 - y, 0.5 + z$), and the chains are arranged such that each terminal pyridine ring participates in an offset face-to-face π - π interaction with the central pyridine ring of an adjacent molecule (distance between the planes = 3.4 \AA) as shown in Figure 5.17.

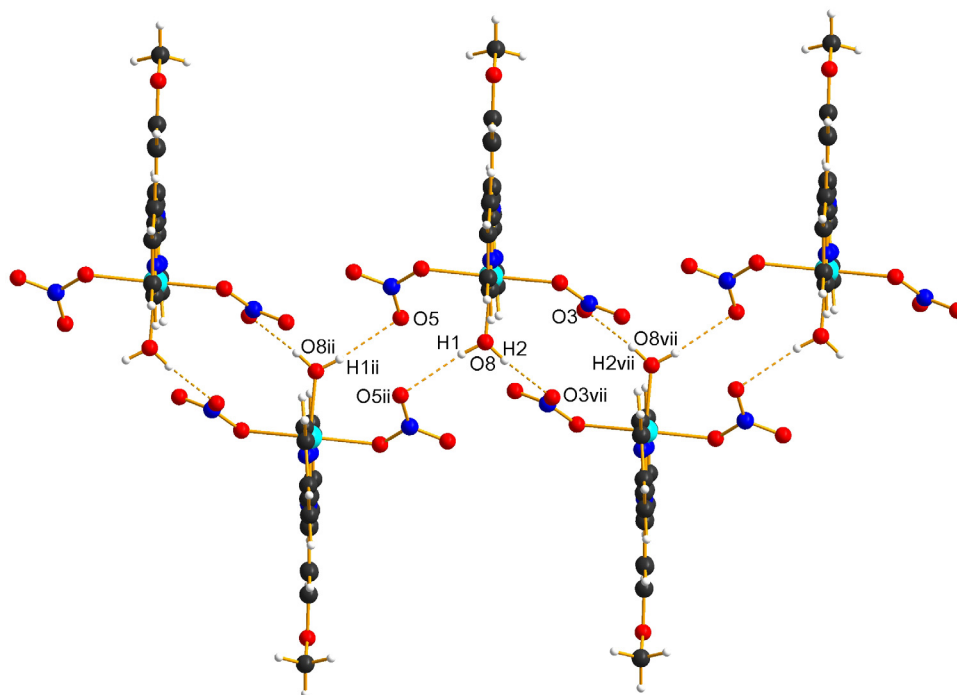


Figure 5.16 Hydrogen-bonded chains of $[\text{Co}(\text{MeOtpy})(\text{NO}_3)_2(\text{OH}_2)]$ (symmetry codes: viii = $1 - x, 1 - y, -z$; ii = $1 - x, 1 - y, 1 - z$).

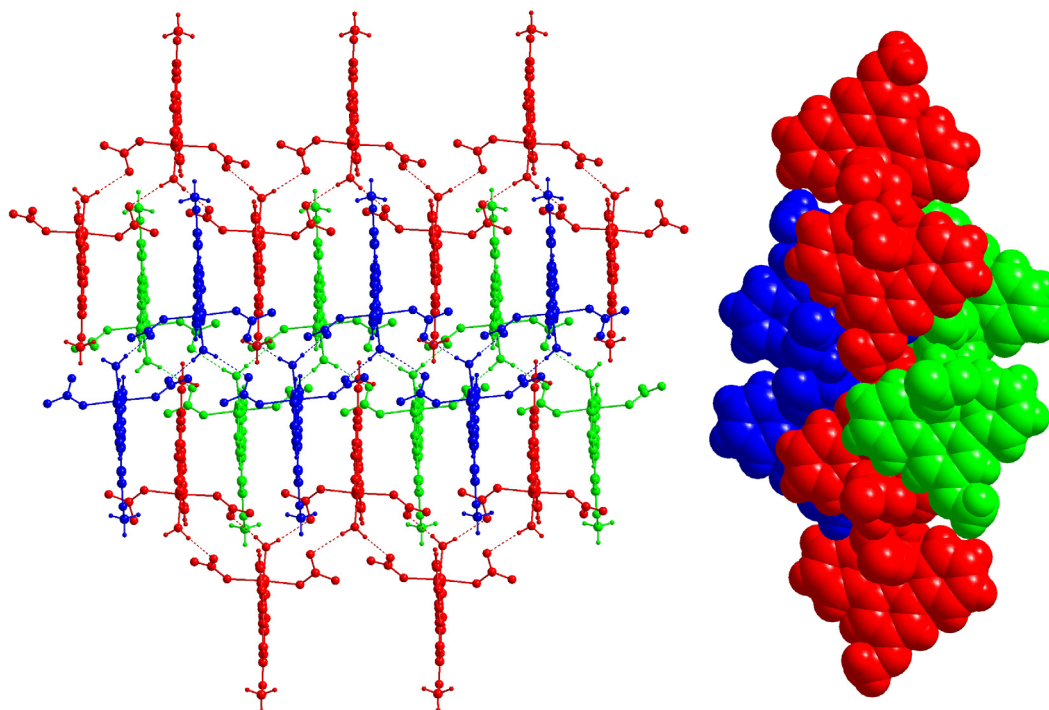


Figure 5.17 Packing of the hydrogen-bonded chains in the structure of $[\text{Co}(\text{MeOtpy})(\text{NO}_3)_2(\text{OH}_2)]$.

It is worth noting that the compound $[\text{Co}(\text{tpy})(\text{NO}_3)][\text{NO}_3]$ has been previously reported, and was proposed to contain one coordinated and one ionic nitrate anion based on infrared spectroscopic data. The complex was proposed to be either four- or five-coordinate, depending on the denticity of the coordinated nitrate ligand.¹⁸²

The molecular structure of $[\text{Co}(\text{MeOtpy})\text{Cl}_2]$ is shown in Figure 5.18. The asymmetric unit contains two independent molecules. In both of these, the cobalt(II) centre is five-coordinate, with the two chloride anions coordinated to the metal centre ($\text{Co1}-\text{Cl1} = 2.28917(19) \text{ \AA}$, $\text{Co1}-\text{Cl2} = 2.30895(19) \text{ \AA}$, $\text{Co2}-\text{Cl3} = 2.32461(19) \text{ \AA}$, $\text{Co2}-\text{Cl4} = 2.2771(2) \text{ \AA}$). While the 4'-methoxy-2,2':6',2''-terpyridine ligands are essentially planar, the cobalt(II) ion is pushed out of the plane of the terpyridine ligand (distance from plane, $\text{Co1} = 0.32 \text{ \AA}$, $\text{Co2} = 0.41 \text{ \AA}$) and the geometry around the metal centre is neither trigonal bipyramidal or square-based pyramidal. One of the independent molecules in the asymmetric unit has a $\text{Cl1}-\text{Co1}-\text{Cl2}$ bond angle of $115.972(7)^\circ$ and in this molecule the $\text{N}_{\text{central}}-\text{Co1}-\text{Cl}$ bond angles are $137.642(16)$ and $106.265(17)^\circ$. The geometry of the other molecule could be considered closer to square-based pyramidal with a $\text{Cl3}-\text{Co2}-\text{Cl4}$ bond angle of $110.817(7)^\circ$ and $\text{N}_{\text{central}}-\text{Co2}-\text{Cl}$ angles of $147.532(16)$ and $101.611(16)^\circ$. The structure of $[\text{Co}(\text{tpy})\text{Cl}_2]$ has previously been reported¹⁸⁶ and has a similar structure to the second molecule in the asymmetric unit described here. The geometric data are reported as: $\text{Cl}-\text{Co}-\text{Cl} = 111 \pm 0.5^\circ$, $\text{N}_{\text{central}}-\text{Co}-\text{Cl} = 99 \pm 0.7$ and $150 \pm 0.5^\circ$.

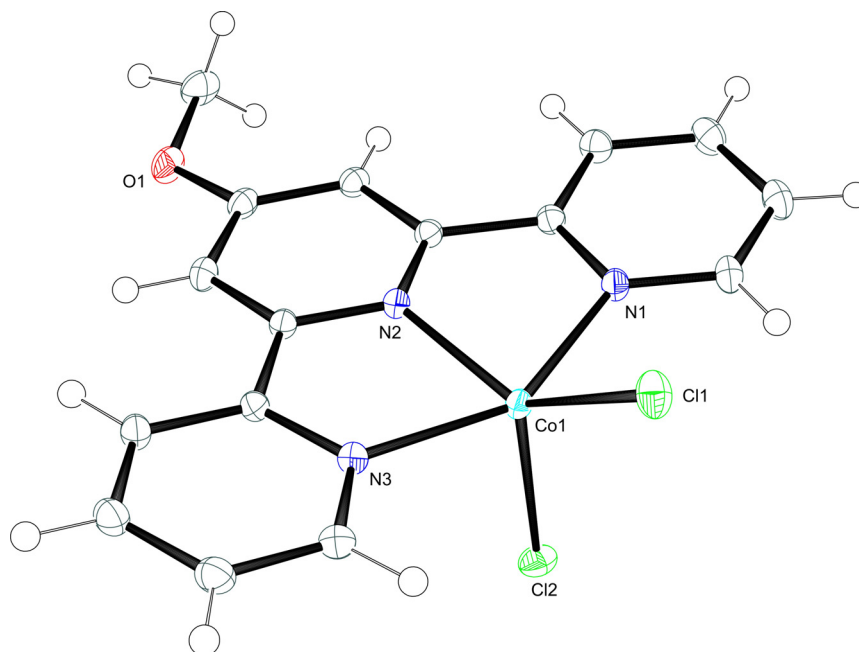


Figure 5.18 Molecular structure of one of the independent molecules in the asymmetric unit of $[\text{Co}(\text{MeOtpy})\text{Cl}_2]$ with anisotropic displacement ellipsoids drawn at the 50% probability level. Hydrogen atoms are shown as spheres of arbitrary radius.

The molecules are arranged in a two-dimensional π -stacked layer structure (distance between the planes = 3.4 Å) as shown in Figure 5.19. Layers of π -stacked molecules are arranged at approximately 90° to one another.

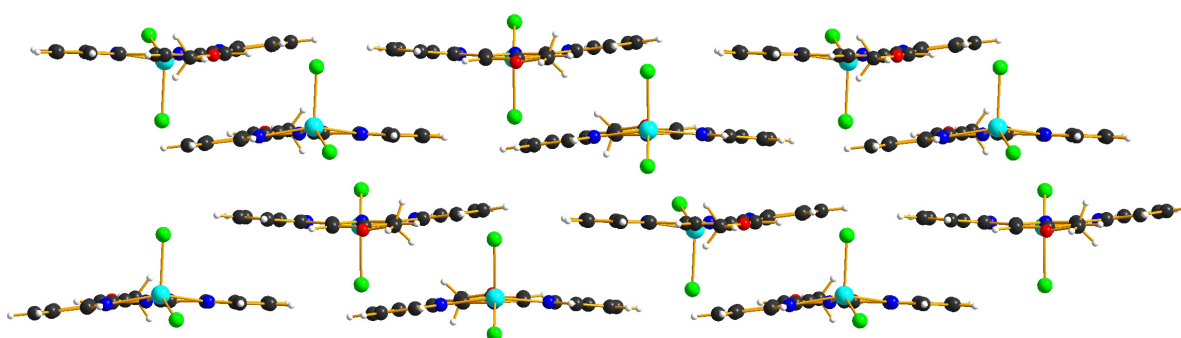


Figure 5.19 π -Stacked layer structure in $[\text{Co}(\text{MeOtpy})\text{Cl}_2]$.

The two trivalent complexes $[\text{Co}(\text{Cltpy})\text{Cl}_3]\cdot\text{CHCl}_3$ and $[\text{Fe}(\text{Cltpy})\text{Cl}_3]\cdot\text{CHCl}_3$ have similar molecular structures (shown in Figure 5.20 and Figure 5.21), but differ greatly in the packing

of the molecules in the lattice. Both metal centres are six-coordinate with three coordinated chloride ligands (Co–Cl2 = 2.2696(7) Å, Co–Cl3 = 2.2391(7) Å, Co–Cl4 = 2.2535(7) Å, Fe–Cl2 = 2.2403(12) Å, Fe–Cl3 = 2.3244(11) Å, Fe–Cl4 = 2.3821(10) Å) arranged at approximately 90° to each other. The molecular structure of the iron(III) complex is similar to that of mono(2,2':6',2''-terpyridine)iron(III) chloride published previously.¹⁸⁹

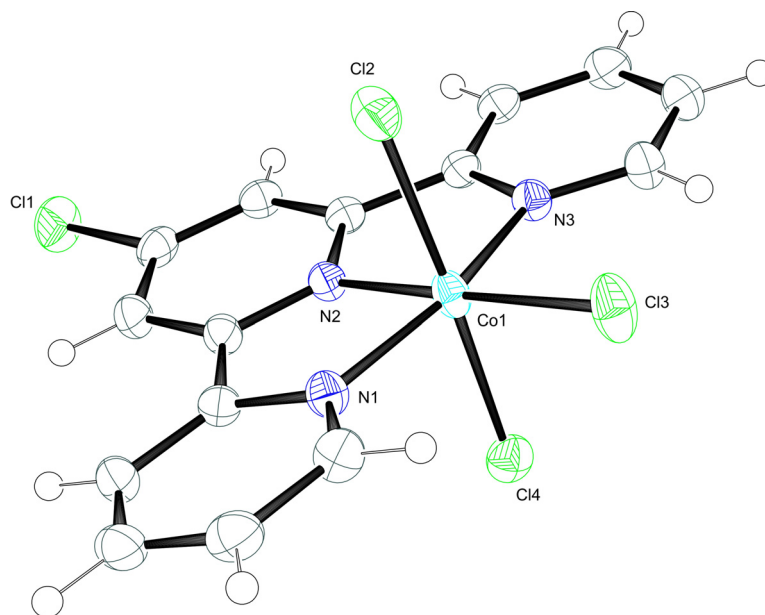


Figure 5.20 Molecular structure of the complex in $[\text{Co}(\text{Cltpy})\text{Cl}_3]\cdot\text{CHCl}_3$ with anisotropic displacement ellipsoids drawn at the 50% probability level. Hydrogen atoms are shown as spheres of arbitrary radius.

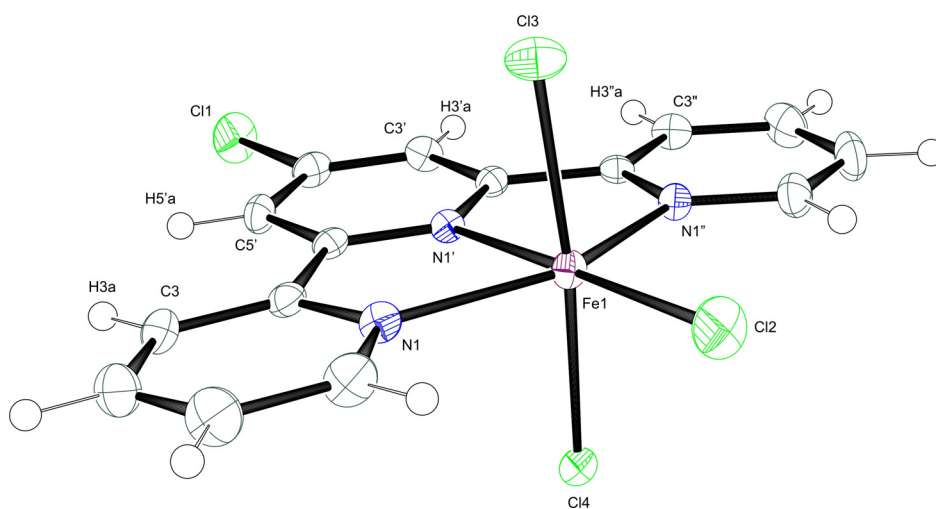


Figure 5.21 Molecular structure of the complex in $[\text{Fe}(\text{Cltpy})\text{Cl}_3]\cdot\text{CHCl}_3$ with anisotropic displacement ellipsoids drawn at the 50% probability level. Hydrogen atoms are shown as spheres of arbitrary radius.

The molecules in $[\text{Co}(\text{Cltpy})\text{Cl}_3]\cdot\text{CHCl}_3$ are arranged in two-dimensional π -stacked layers (distance between the planes = 3.3 Å) as shown in Figure 5.22. Interaction between layers of π -stacked molecules is via multiple C–H \cdots Cl interactions between the 4'-methoxy-2,2':6',2''-terpyridine ligand and the chloroform molecules.

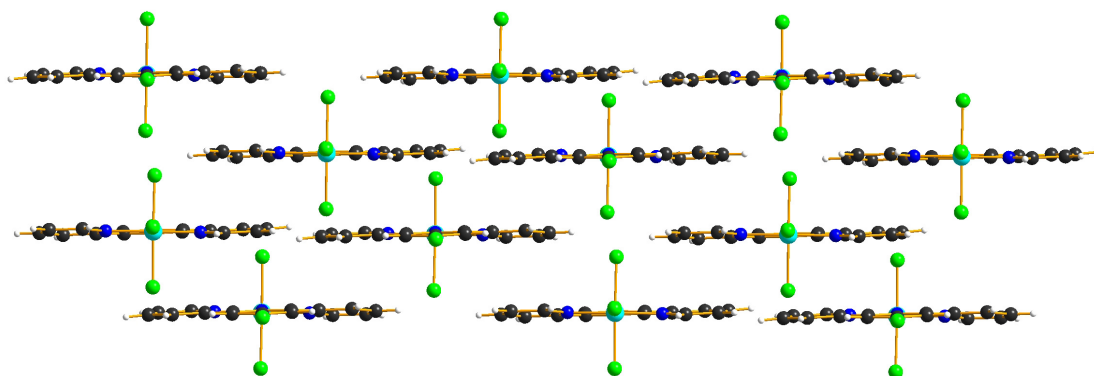


Figure 5.22 π -Stacked layer structure in $[\text{Co}(\text{Cltpy})\text{Cl}_3]\cdot\text{CHCl}_3$.

In contrast, the molecules in $[\text{Fe}(\text{Cltpy})\text{Cl}_3]\cdot\text{CHCl}_3$ are arranged into chains held together by weak hydrogen bonds between the two coordinated chloride ligands arranged *trans* to each other and the protons in the 3- and 3'-positions of a 4'-chloro-2,2':6',2''-terpyridine ($\text{C3}^{\text{viii}}-\text{H3}^{\text{vii}}\cdots\text{Cl3} = 2.80$ Å, $\text{C3}^{\text{vii}}-\text{H3}'\text{A}^{\text{vii}}\cdots\text{Cl3} = 2.88$ Å, $\text{C3}^{\text{x}}-\text{H3}\text{A}^{\text{x}}\cdots\text{Cl4} = 2.79$ Å, $\text{C5}^{\text{x}}-\text{H5}'\text{A}^{\text{x}}\cdots\text{Cl4} = 2.65$ Å; symmetry codes $\text{vii} = 1 - x, 1 - y, -z$, $\text{x} = -x, 1 - y, -z$) in an adjacent molecule as shown in Figure 5.23. These weak interactions are supported by offset face-to-face π - π interactions between the terpyridine rings (distance between the planes = 3.6 Å). These chains interact via the chloroform molecules to form two-dimensional layers, which then pack, again via interactions with the chloroform molecules, with adjacent layers in which the molecules are rotated by 90°.

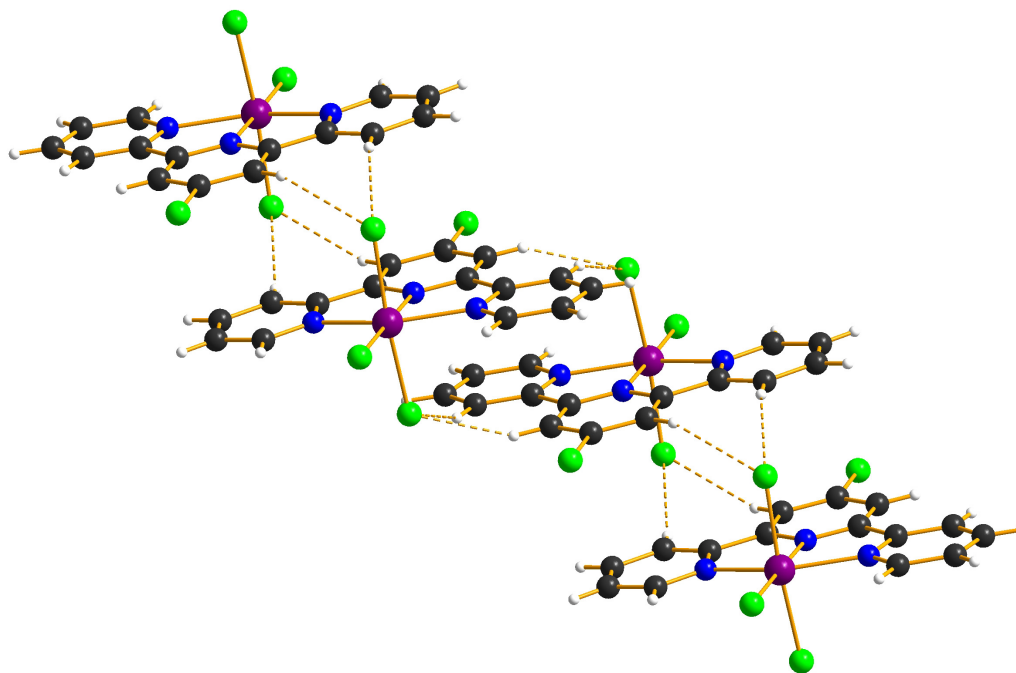


Figure 5.23 Weakly hydrogen-bonded (non-classical C–H···Cl) chain in the structure of $[\text{Fe}(\text{Cltpy})\text{Cl}_3]\cdot\text{CHCl}_3$.

5.4 NMR spectroscopic studies with bis(terpyridyl)tetra(ethylene glycol)

After studying the effect of the anion on the mononuclear systems, the investigation was extended to the ditopic ligands. Bis(terpyridyl)tetra(ethylene glycol) was chosen as a model system as the speciation of cobalt(II) salts of this ligand was best understood and the polymer-macrocycle equilibrium with the $[\text{PF}_6]^-$ anion tends to form a single macrocyclic product with well-separated signals in the ^1H NMR spectrum (see Chapter 6), simplifying the characterisation of the mixtures. As mentioned above, a large number of species are present in the equilibrium mixtures of the cobalt(II) salts of the ditopic bis(terpyridyl)oligo(ethylene glycol) ligands. In this section, only the equilibrium between the mono- and the bis(2,2':6',2''-terpyridine)cobalt(II) units will be considered. These moieties are not necessarily independent species and could coexist within the same oligomer or polymer. The anion also has an effect on the equilibrium between the polymeric, oligomeric and macrocyclic species and on the time taken to reach this equilibrium position. This behaviour will be discussed in Chapter 6.

The ditopic ligand bis(terpyridyl)tetra(ethylene glycol) was mixed with cobalt(II) acetate tetrahydrate, cobalt(II) chloride hexahydrate or cobalt(II) tetrafluoroborate hexahydrate at

room temperature in the ratios and solvents given in Table 5.4. As the ligand contains two 2,2':6',2''-terpyridine units, the ligand to metal ratios were altered with respect to the study of 4'-methoxy-2,2':6',2''-terpyridine. With the ditopic ligand, a ligand to metal ratio of 1:1 corresponds to a 2:1 ratio of 2,2':6',2''-terpyridine units to metal salt and a ratio of 1L:2M is the same as a 1:1 ratio of 2,2':6',2''-terpyridine units to metal salt. In all experiments the concentration of cobalt(II) was 0.030 M. The reaction mixtures with a 1L:1M ratio were then diluted with the same solvent mixture to give three samples with concentrations of 0.030 M, 0.015 M and 0.0076 M, and all samples were characterised by ^1H NMR spectroscopy. Also shown in Table 5.4 are the ratios of mono- to bis(2,2':6',2''-terpyridine)cobalt(II) units as determined from the ^1H NMR spectra and these results are discussed below.

$\text{CoX}_2 \cdot n\text{H}_2\text{O}$	L:M ratio	Solvent	% Mono	% Bis
$\text{Co(OAc)}_2 \cdot 4\text{H}_2\text{O}$	1:1	$\text{CDCl}_3\text{-CD}_3\text{OD}$ (9:1)	17 – 22% ^a	78 – 83% ^a
		CD_3OD	11 – 14% ^b	86 – 89% ^b
	1:2	$\text{CDCl}_3\text{-CD}_3\text{OD}$ (9:1)	100%	0%
		CD_3OD	80% ^c	20% ^c
$\text{CoCl}_2 \cdot 6\text{H}_2\text{O}$	1:1	$\text{CDCl}_3\text{-CD}_3\text{OD}$ (9:1)	0%	100%
		CD_3OD	0%	100%
	1:2	$\text{CDCl}_3\text{-CD}_3\text{OD}$ (9:1)	100% ^d	0% ^d
		CD_3OD	90%	10%
$\text{Co(BF}_4)_2 \cdot 6\text{H}_2\text{O}$	1:1	CD_3CN	0%	100%
	1:2	CD_3CN	45%	55%

Table 5.4 Ratios of mono- to bis(2,2':6',2''-terpyridine)cobalt(II) units in mixtures of bis(terpyridyl)tetra(ethylene glycol) and cobalt(II) salts. Percentages are based on integrals of the peaks corresponding to H3 and H3' (bis) and the two highest frequency sharp singlets (mono). a = ratios depend slightly on concentration, with more of the mono(2,2':6',2''-terpyridine)cobalt(II) unit at lower concentrations. b = ratios depend slightly on concentration, with more of the bis(2,2':6',2''-terpyridine)cobalt(II) unit at lower concentrations. c = three species are present in solution; the percentages are based on integrals of peaks corresponding to H6. d = a precipitate formed during the reaction so the system cannot be considered to be at equilibrium.

The compositions of the mixtures of products from the reaction of bis(terpyridyl)tetra(ethylene glycol) with cobalt(II) salts with regard to the proportions of mono- and bis(2,2':6',2''-terpyridine)cobalt(II) units are very similar to those from the reaction of 4'-methoxy-2,2':6',2''-terpyridine with the same cobalt(II) salts. The ^1H NMR spectra of the equilibrium mixtures of these reactions are shown in Figure 5.24 to Figure 5.28. Each figure also includes the ^1H NMR spectrum of a 1:1 mixture of 4'-methoxy-2,2':6',2''-terpyridine and the appropriate cobalt(II) salt in the same solvent mixture for comparison and the concentration of cobalt(II) in all samples was 0.030 M. The appearance of the ^1H NMR spectrum is in some cases highly dependent on the concentration due to variations in the proportions of different bis(2,2':6',2''-terpyridine)cobalt(II) units. However, the ratio of mono- to bis(2,2':6',2''-terpyridine)cobalt(II) units is relatively independent of the concentration. This is interesting as similar metallosupramolecular polymers are often synthesised in highly concentrated solutions which is believed to favour polymer formation over the formation of discrete macrocycles.^{40, 41, 43}

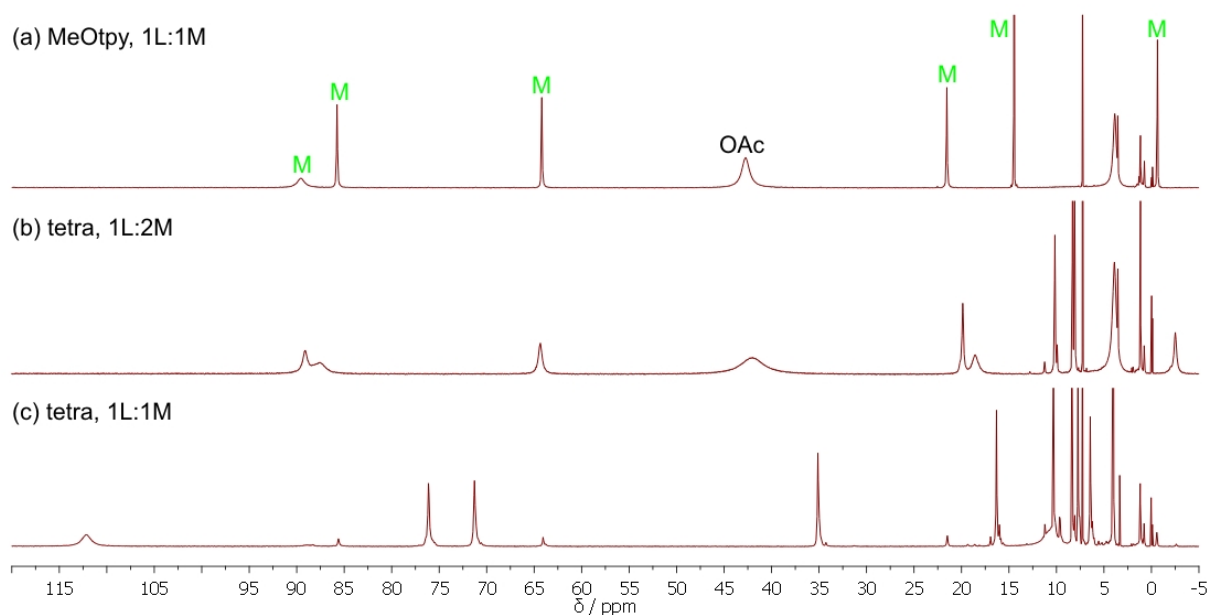


Figure 5.24 Full ^1H NMR spectra of mixtures of 4'-methoxy-2,2':6',2''-terpyridine (a) or bis(terpyridyl)tetra(ethylene glycol) (b and c) and cobalt(II) acetate tetrahydrate (CDCl_3 - CD_3OD (9:1), 250 MHz). All samples have a concentration of cobalt(II) of 0.030 M. M = mono(4'-methoxy-2,2':6',2''-terpyridine)cobalt(II) complex.

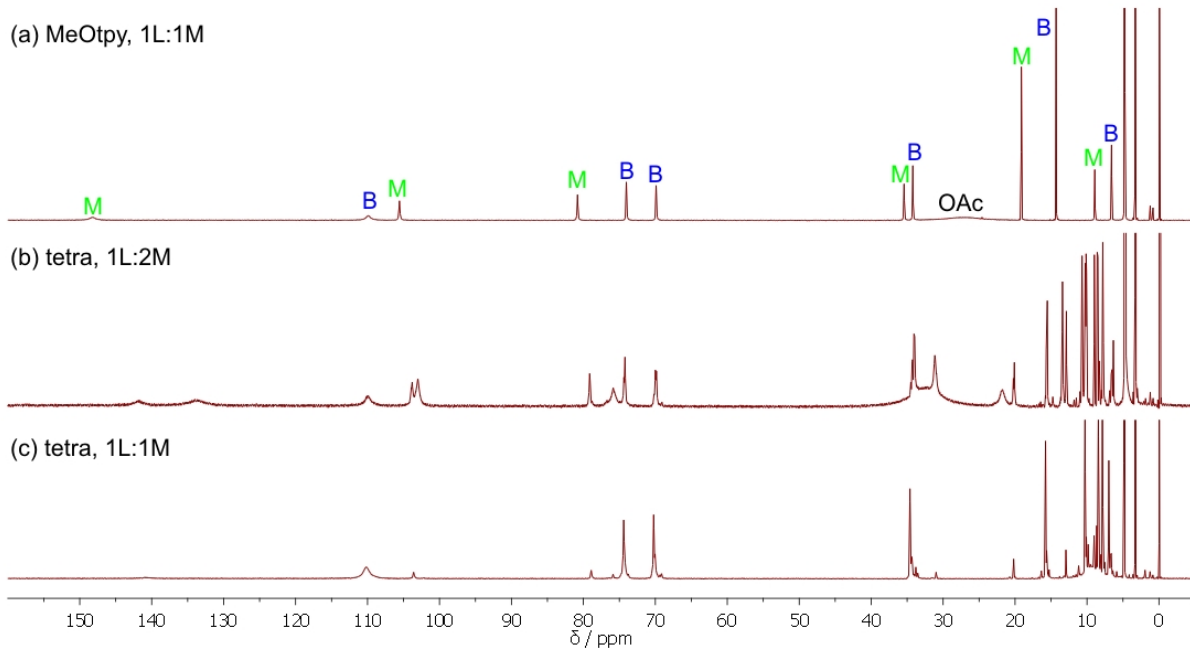


Figure 5.25 Full ¹H NMR spectra of mixtures of 4'-methoxy-2,2':6',2''-terpyridine (a) or bis(terpyridyl)tetra(ethylene glycol) (b and c) and cobalt(II) acetate tetrahydrate (CD₃OD, 250 MHz). All samples have a concentration of cobalt(II) of 0.030 M. B = bis(4'-methoxy-2,2':6',2''-terpyridine)cobalt(II) complex, M = mono(4'-methoxy-2,2':6',2''-terpyridine)cobalt(II) complex.

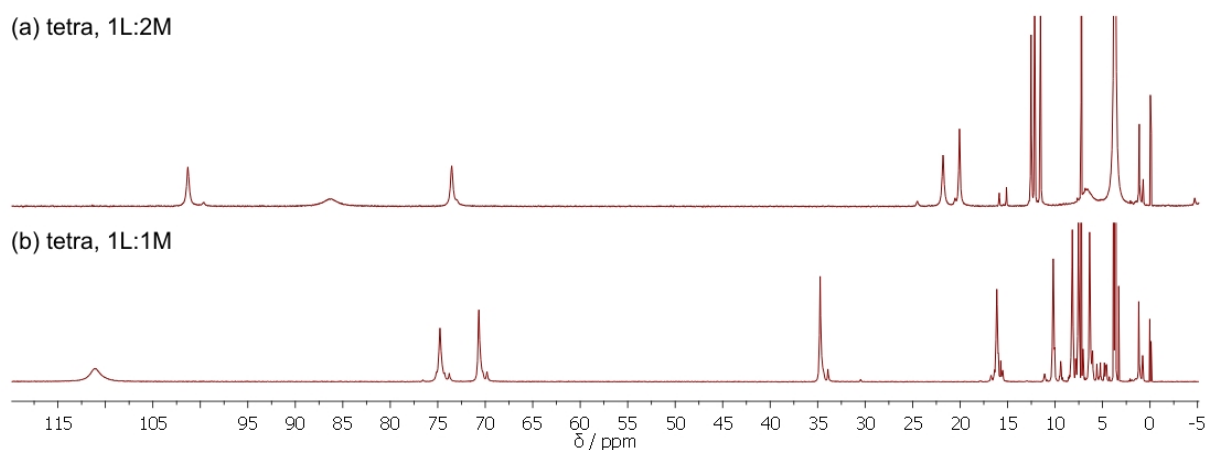


Figure 5.26 Full ¹H NMR spectra of mixtures of bis(terpyridyl)tetra(ethylene glycol) and cobalt(II) chloride hexahydrate (CDCl₃-CD₃OD (9:1), 250 MHz). All samples have a concentration of cobalt(II) of 0.030 M. The 1L:1M mixture of 4'-methoxy-2,2':6',2''-terpyridine and cobalt(II) chloride hexahydrate is insoluble in this solvent mixture.

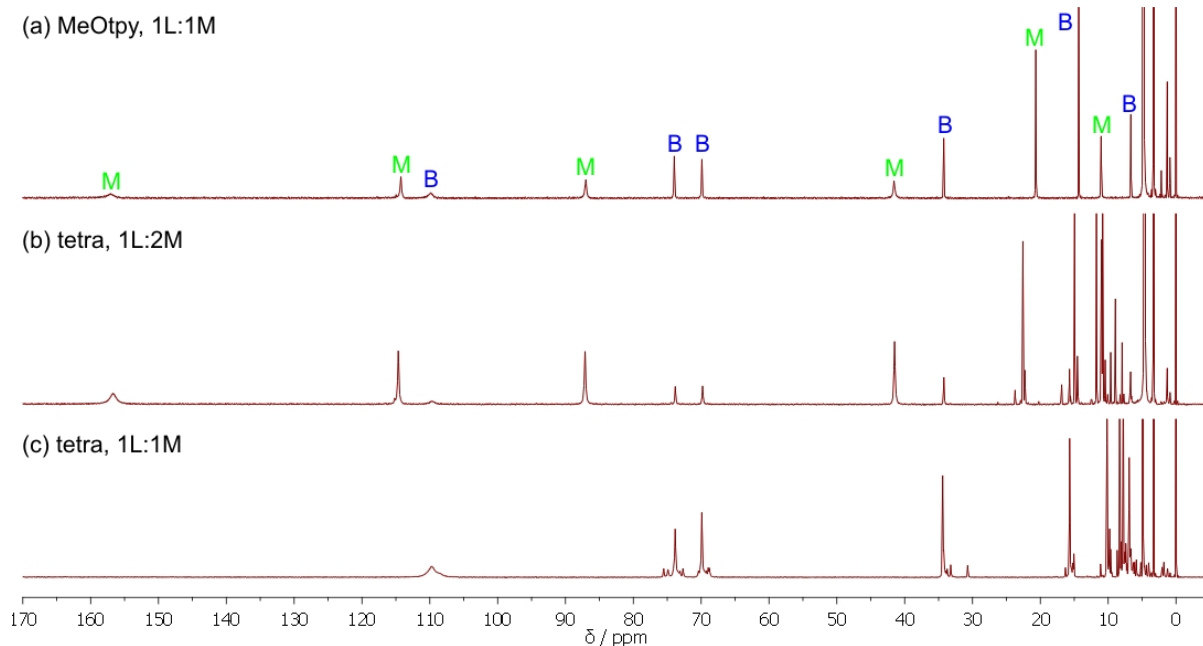


Figure 5.27 Full ^1H NMR spectra of mixtures of 4'-methoxy-2,2':6',2''-terpyridine (a) or bis(terpyridyl)tetra(ethylene glycol) (b and c) and cobalt(II) chloride hexahydrate (CD_3OD , 250 MHz). All samples have a concentration of cobalt(II) of 0.030 M. B = bis(4'-methoxy-2,2':6',2''-terpyridine)cobalt(II) complex, M = mono(4'-methoxy-2,2':6',2''-terpyridine)cobalt(II) complex.

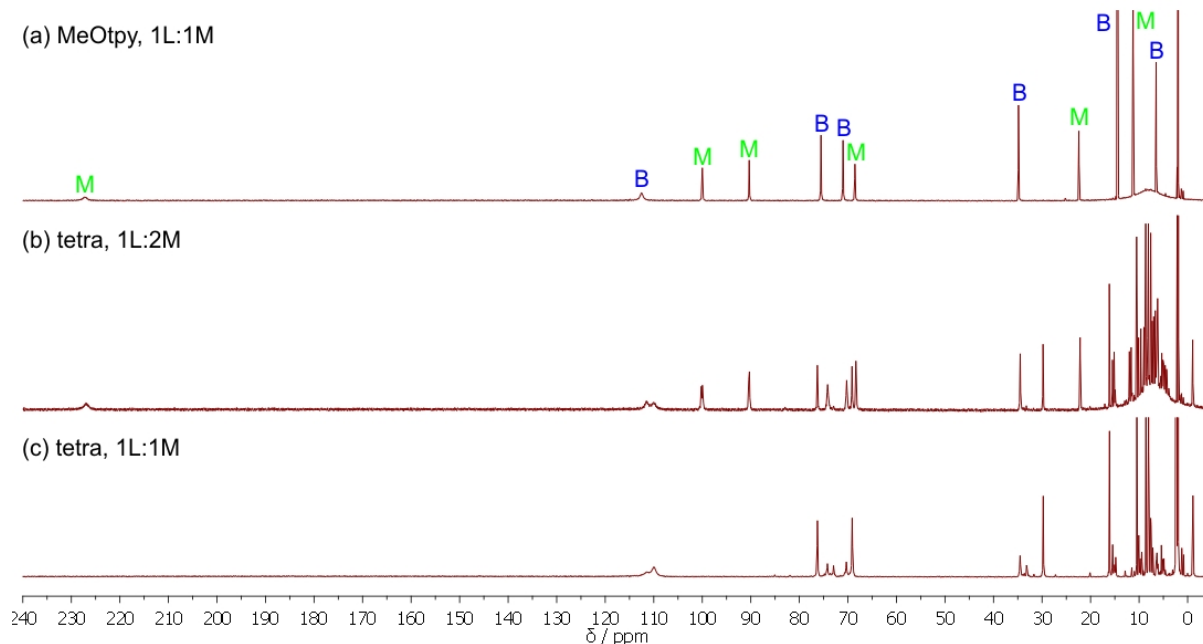


Figure 5.28 Full ^1H NMR spectra of mixtures of 4'-methoxy-2,2':6',2''-terpyridine (a) or bis(terpyridyl)tetra(ethylene glycol) (b and c) and cobalt(II) tetrafluoroborate hexahydrate (CD_3CN , 250 MHz). All samples have a concentration of cobalt(II) of 0.030 M. B = bis(4'-methoxy-2,2':6',2''-terpyridine)cobalt(II) complex, M = mono(4'-methoxy-2,2':6',2''-terpyridine)cobalt(II) complex.

The ^1H NMR spectra of the systems containing the ditopic ligand are in most cases extremely similar to those containing the monotopic 4'-methoxy-2,2':6',2''-terpyridine ligand, which suggests the presence of similar species in both systems. One exception to this is the mixture of one equivalent of bis(terpyridyl)tetra(ethylene glycol) with two equivalents of cobalt(II) acetate. The ^1H NMR spectrum shown in Figure 5.25(b) suggests the presence of two cobalt(II)-containing species in addition to the bis(2,2':6',2''-terpyridine)cobalt(II) moieties. This could indicate the formation of two different species with coordinated acetate anions, potentially monodentate and bidentate, or a complex with a solvent molecule in the sixth coordination site of the cobalt(II) centre. While it is possible to say that mono(2,2':6',2''-terpyridine)cobalt(II) units exist in the systems involving the ditopic ligands, it is not possible to determine whether these units form the ends of long polymers, short oligomers or dinuclear complexes involving only one ligand.

5.5 Conclusions

After observation of the formation of a second species in addition to the expected bis(2,2':6',2''-terpyridine)cobalt(II) complex on mixing monotopic and ditopic 2,2':6',2''-terpyridine ligands with cobalt(II) acetate tetrahydrate, a systematic study of the effect of the anion on these systems was undertaken. Using 4'-methoxy-2,2':6',2''-terpyridine as a model ligand, the speciation of mono- and bis(2,2':6',2''-terpyridine)cobalt(II) complexes in mixtures of the ligand and several cobalt(II) salts was analysed using ^1H NMR spectroscopy. The product mixtures were found to depend heavily on the anion, solvent and initial ratio of ligand to metal salt. While the ^1H NMR spectrum of the bis(4'-methoxy-2,2':6',2''-terpyridine)cobalt(II) complex was found to be essentially independent of the anion and solvent mixture, the signals corresponding to the mono(4'-methoxy-2,2':6',2''-terpyridine)cobalt(II) complex were significantly shifted by using different anions and solvent mixtures. Both solvent molecules and anions could coordinate to the metal centre in solution, and it is possible that the relative proportions of each could affect the spin state of the complex in solution. The use of a weakly coordinating anion still resulted in the formation of a mono(4'-methoxy-2,2':6',2''-terpyridine)cobalt(II) complex under appropriate conditions, and it was proposed that water molecules were coordinated to the metal ion as well as the 4'-methoxy-2,2':6',2''-terpyridine ligand. The X-ray crystal structures of four mono(4'-substituted-2,2':6',2''-terpyridine)cobalt(II) complexes with coordinated anions were

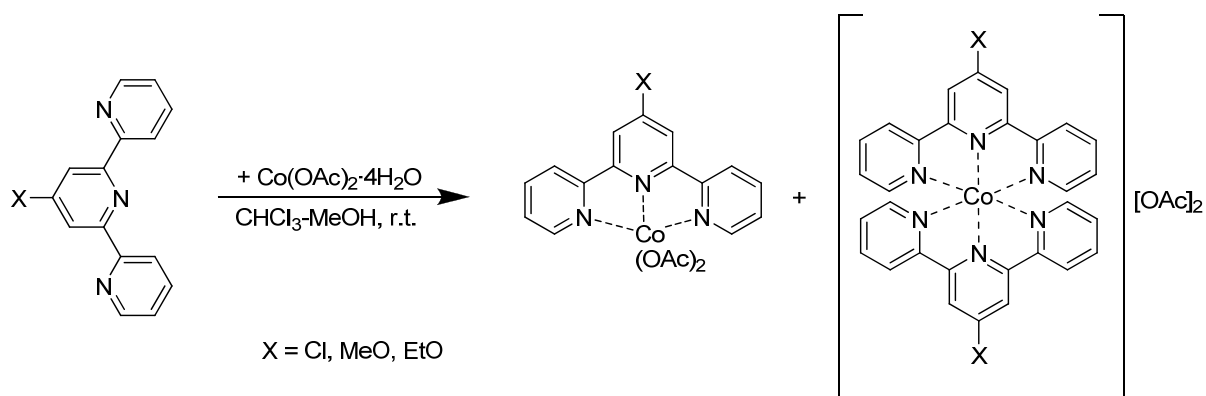
determined, as well as two mono(4'-chloro-2,2':6',2''-terpyridine) complexes of trivalent metal ions. The investigation was then extended to the ditopic ligand bis(terpyridyl)tetra(ethylene glycol), and similar behaviour was observed. The ratio of the mono- to bis(2,2':6',2''-terpyridine) units was not found to be dependent on the concentration of the solution, although polymer formation is usually expected to be favoured at higher concentrations. The formation of mono(2,2':6',2''-terpyridine)cobalt(II) moieties in systems based on bis(terpyridyl)oligo- or -poly(ethylene glycol) ligands gives rise to end-capping units and suggests that the extent of polymer or macrocycle formation in these systems will be enormously dependent on the reaction conditions used.

5.6 Experimental

5.6.1 Initial NMR spectroscopic experiments on the reaction of bis(terpyridyl)hexa(ethylene glycol) with cobalt(II) acetate tetrahydrate

Bis(terpyridyl)hexa(ethylene glycol) (0.005 g, 0.007 mmol) was dissolved in a CDCl₃-CD₃OD (9:1) solvent mixture (1.0 cm³). Cobalt(II) acetate tetrahydrate (0.002 g, 0.007 mmol) was added and ¹H NMR spectra (500 MHz, 295 K) were collected over 2 days. δ_H(500 MHz, CD₃CN)/ppm see discussion (section 5.2).

5.6.2 Reactions of monotopic 4'-substituted-2,2':6',2''-terpyridine ligands with cobalt(II) acetate tetrahydrate



5.6.2.1 Reactions with a ratio of 2L:1M (2tpy:1M)

The ligand (0.050 g, 2 eq) and cobalt(II) acetate tetrahydrate (1 eq) were dissolved in a chloroform-methanol solvent mixture (9:1, 10 cm³). The brown solution was stirred at room temperature, then the solvent was removed *in vacuo*. Yields were quantitative.

Reaction of 4'-chloro-2,2':6',2''-terpyridine (0.050 g, 0.19 mmol) and cobalt(II) acetate tetrahydrate (0.023 g, 0.093 mmol) for 45 minutes gave a dark pink solid. δ_H(250 MHz, CD₃CN)/ppm see discussion (section 5.3.1).

Reaction of 4'-methoxy-2,2':6',2''-terpyridine (0.050 g, 0.19 mmol) and cobalt(II) acetate tetrahydrate (0.024 g, 0.95 mmol) for 3 hours gave a pink-brown solid. δ_H(250 MHz, CD₃CN)/ppm see discussion (section 5.3.1).

Reaction of 4'-ethoxy-2,2':6',2''-terpyridine (0.050 g, 0.18 mmol) and cobalt(II) acetate tetrahydrate (0.023 g, 0.90 mmol) for 2 hours gave a lilac solid. δ_{H} (250 MHz, CD₃CN)/ppm see discussion (section 5.3.1).

5.6.2.2 Reactions with a ratio of 1L:1M (1tpy:1M)

The ligand (0.050 g, 1 eq) and cobalt(II) acetate tetrahydrate (1 eq) were dissolved in a chloroform-methanol solvent mixture (9:1, 10 cm³). The brown solution was stirred at room temperature, giving a red-pink solution, then the solvent was removed *in vacuo*. Yields were quantitative.

Reaction of 4'-chloro-2,2':6',2''-terpyridine (0.050 g, 0.19 mmol) and cobalt(II) acetate tetrahydrate (0.047 g, 0.19 mmol) for 6 days gave a dark pink solid. δ_{H} (250 MHz, CD₃CN)/ppm see discussion (section 5.3.1). Crystals of [Co(Cltpy)(OAc)₂] suitable for X-ray diffraction were obtained by slow evaporation of a solution of the complex in CDCl₃ containing a few drops of CD₃OD. Green crystals of [Co(Cltpy)Cl₃] \cdot CHCl₃ were obtained by slow diffusion over several weeks of diethyl ether into a chloroform-methanol solution of the acetate complex at room temperature.

Reaction of 4'-methoxy-2,2':6',2''-terpyridine (0.050 g, 0.19 mmol) and cobalt(II) acetate tetrahydrate (0.047 g, 0.19 mmol) for 3 hours gave a pink solid. δ_{H} (250 MHz, CD₃CN)/ppm see discussion (section 5.3.1).

Reaction of 4'-ethoxy-2,2':6',2''-terpyridine (0.050 g, 0.18 mmol) and cobalt(II) acetate tetrahydrate (0.045 g, 0.18 mmol) for 2 hours gave a lilac solid. δ_{H} (250 MHz, CD₃CN)/ppm see discussion (section 5.3.1).

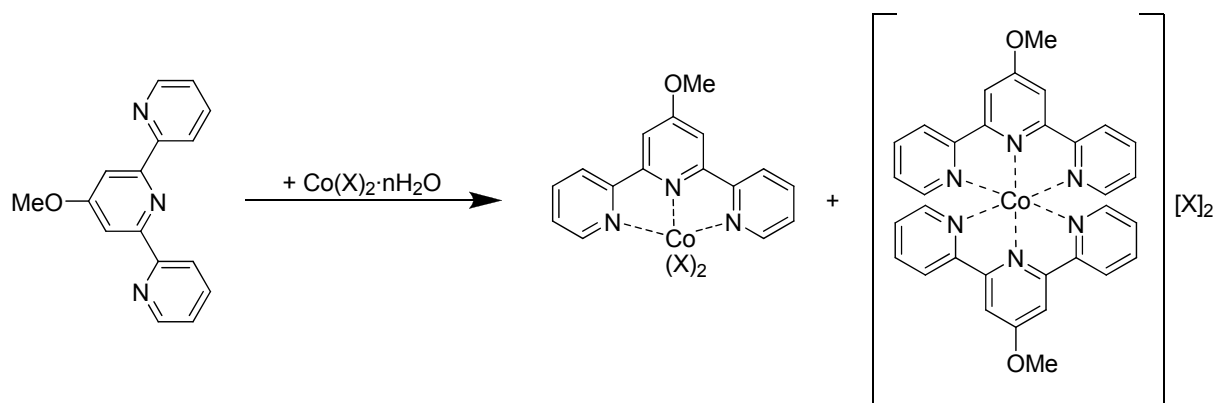
5.6.2.3 Reaction with a ratio of 1L:2M (1tpy:2M)

4'-chloro-2,2':6',2''-terpyridine (0.050 g, 0.19 mmol) and cobalt(II) acetate tetrahydrate (0.093 g, 0.37 mmol) were dissolved in a chloroform-methanol solvent mixture (9:1, 10 cm³). The red-brown solution was stirred at room temperature for 2 hours, then the solvent was removed *in vacuo* to give a dark lilac solid. The yield was quantitative. δ_{H} (250 MHz, CD₃CN)/ppm see discussion (section 5.3.1).

5.6.3 Reaction of 4'-chloro-2,2':6',2''-terpyridine with iron(II) chloride tetrahydrate (1L:1M, 1tpy:1M)

4'-chloro-2,2':6',2''-terpyridine (0.050 g, 0.19 mmol) and iron(II) chloride tetrahydrate (0.019 g, 0.19 mmol) were suspended in a chloroform-methanol solvent mixture (9:1, 10 cm³). The dark purple suspension was stirred at room temperature for 2 hours then the solvent was removed *in vacuo* to give a purple solid. Yellow crystals of [Fe(Cltpy)Cl₃]·CHCl₃ suitable for X-ray diffraction were grown by slow evaporation of a (purple) solution of the product mixture in CDCl₃ containing a few drops of CD₃OD. δ_{H} (250 MHz, CD₃CN)/ppm see discussion (section 5.3.1).

5.6.4 NMR spectroscopic studies on the reaction of 4'-methoxy-2,2':6',2''-terpyridine with cobalt(II) salts



5.6.4.1 Reactions in CDCl₃-CD₃OD with a ratio of 2L:1M (2tpy:1M)

4'-methoxy-2,2':6',2''-terpyridine (0.024 g, 0.091 mmol) was dissolved in a CDCl₃-CD₃OD solvent mixture (9:1, 1.5 cm³). The colourless solution was added to the solid cobalt(II) salt (0.0454 mmol) and the mixture was stirred at room temperature. The original solution (0.6 cm³) was diluted with the same solvent mixture (0.6 cm³), then the new solution (0.4 cm³) was diluted with the same solvent mixture (0.4 cm³), giving three samples with concentrations (of cobalt(II)) of 0.030 M, 0.015 M and 0.0076 M.

Reaction of 4'-methoxy-2,2':6',2''-terpyridine and cobalt(II) acetate tetrahydrate (0.0113 g, 0.0454 mmol) overnight gave a brown solution. δ_{H} (250 MHz, CD₃CN)/ppm see discussion (section 5.3.2). Crystals of [Co(MeOtpy)(OAc)₂] suitable for X-ray diffraction were obtained by slow diffusion of diethyl ether into the CDCl₃-CD₃OD solution at room temperature.

Reaction of 4'-methoxy-2,2':6',2''-terpyridine and cobalt(II) chloride hexahydrate (0.0108 g, 0.0454 mmol) overnight gave a brown solution. δ_{H} (250 MHz, CD₃CN)/ppm see discussion (section 5.3.2).

Reaction of 4'-methoxy-2,2':6',2''-terpyridine and cobalt(II) nitrate hexahydrate (0.0132 g, 0.0454 mmol) for 45 minutes gave a brown solution. δ_{H} (250 MHz, CD₃CN)/ppm see discussion (section 5.3.2).

5.6.4.2 Reactions in CD₃OD with a ratio of 2L:1M (2tpy:1M)

The cobalt(II) salt (0.0454 mmol) was dissolved in CD₃OD (1.5 cm³). The pink solution was added to solid 4'-methoxy-2,2':6',2''-terpyridine (0.024 g, 0.091 mmol) and the mixture was stirred at room temperature. The original solution (0.6 cm³) was diluted with the same solvent mixture (0.6 cm³), then the new solution (0.4 cm³) was diluted with the same solvent mixture (0.4 cm³), giving three samples with concentrations (of cobalt(II)) of 0.030 M, 0.015 M and 0.0076 M.

Reaction of 4'-methoxy-2,2':6',2''-terpyridine and cobalt(II) acetate tetrahydrate (0.0113 g, 0.0454 mmol) overnight gave a dark brown solution. δ_{H} (250 MHz, CD₃CN)/ppm see discussion (section 5.3.2). Crystals of [Co(MeOtpy)(OAc)₂] suitable for X-ray diffraction were obtained by slow diffusion of diethyl ether into the CD₃OD solution at room temperature.

Reaction of 4'-methoxy-2,2':6',2''-terpyridine and cobalt(II) chloride hexahydrate (0.0108 g, 0.0454 mmol) overnight gave a dark brown solution. δ_{H} (250 MHz, CD₃CN)/ppm see discussion (section 5.3.2).

Reaction of 4'-methoxy-2,2':6',2''-terpyridine and cobalt(II) nitrate hexahydrate (0.0132 g, 0.0454 mmol) for 2 hours gave a dark brown solution. δ_{H} (250 MHz, CD₃CN)/ppm see discussion (section 5.3.2).

5.6.4.3 Reactions in CD₃CN with a ratio of 2L:1M (2tpy:1M)

Cobalt(II) tetrafluoroborate hexahydrate (0.016 g, 0.046 mmol) was dissolved in CD₃CN (1.5 cm³). The red-pink solution was added to solid 4'-methoxy-2,2':6',2''-terpyridine (0.024 g, 0.091 mmol) and the mixture was stirred at room temperature for 45 minutes to give a brown solution. δ_{H} (250 MHz, CD₃CN)/ppm see discussion (section 5.3.2).

5.6.4.4 Reactions in CDCl₃-CD₃OD with a ratio of 1L:1M (1tpy:1M)

4'-methoxy-2,2':6',2''-terpyridine (0.0040 g, 0.015 mmol) was dissolved in a CDCl₃-CD₃OD solvent mixture (9:1, 0.5 cm³). The colourless solution was added to the solid cobalt(II) salt (0.015 mmol) and the mixture was stirred at room temperature.

Reaction of 4'-methoxy-2,2':6',2''-terpyridine and cobalt(II) acetate tetrahydrate (0.0038 g, 0.015 mmol) overnight gave a pink solution. δ_{H} (250 MHz, CD₃CN)/ppm see discussion (section 5.3.2).

Reaction of 4'-methoxy-2,2':6',2''-terpyridine and cobalt(II) chloride hexahydrate (0.0036 g, 0.015 mmol) overnight gave a mint green suspension. Crystals of [Co(MeOtpy)Cl₂] suitable for X-ray diffraction were grown by slow diffusion of a methanol solution of cobalt(II) chloride hexahydrate into a chloroform solution of 4'-methoxy-2,2':6',2''-terpyridine at room temperature.

Reaction of 4'-methoxy-2,2':6',2''-terpyridine and cobalt(II) nitrate hexahydrate (0.0044 g, 0.015 mmol) for 20 minutes gave a brown solution. δ_{H} (250 MHz, CD₃CN)/ppm see discussion (section 5.3.2). Crystals of [Co(MeOtpy)(NO₃)(H₂O)] suitable for X-ray diffraction formed overnight in the NMR tube.

5.6.4.5 Reactions in CD₃OD with a ratio of 1L:1M (1tpy:1M)

The cobalt(II) salt (0.015 mmol) was dissolved in CD₃OD (0.5 cm³). The pink solution was added to solid 4'-methoxy-2,2':6',2''-terpyridine (0.040 g, 0.015 mmol) and the mixture was stirred at room temperature.

Reaction of 4'-methoxy-2,2':6',2''-terpyridine and cobalt(II) acetate tetrahydrate (0.0038 g, 0.015 mmol) overnight gave a dark brown solution. δ_{H} (250 MHz, CD₃CN)/ppm see discussion (section 5.3.2).

Reaction of 4'-methoxy-2,2':6',2''-terpyridine and cobalt(II) chloride hexahydrate (0.0036 g, 0.015 mmol) overnight gave a dark brown suspension. δ_{H} (250 MHz, CD₃CN)/ppm see discussion (section 5.3.2).

Reaction of 4'-methoxy-2,2':6',2''-terpyridine and cobalt(II) nitrate hexahydrate (0.0044 g, 0.015 mmol) for 20 minutes gave a dark brown solution. δ_{H} (250 MHz, CD₃CN)/ppm see discussion (section 5.3.2).

5.6.4.6 Reactions in CD₃CN with a ratio of 1L:1M (1tpy:1M)

Cobalt(II) tetrafluoroborate hexahydrate (0.0052 g, 0.015 mmol) was dissolved in CD₃CN (0.5 cm³). The pink solution was added to solid 4'-methoxy-2,2':6',2''-terpyridine (0.0040 g, 0.015 mmol) and the mixture was stirred at room temperature for 45 minutes to give a dark brown solution. δ_{H} (250 MHz, CD₃CN)/ppm see discussion (section 5.3.2).

5.6.5 NMR spectroscopic studies on the reaction of bis(terpyridyl)tetra(ethylene glycol) with cobalt(II) salts

5.6.5.1 Reactions in CDCl₃-CD₃OD with a ratio of 1L:1M (2tpy:1M)

Bis(terpyridyl)tetra(ethylene glycol) (0.030 g, 0.046 mmol) was dissolved in a CDCl₃-CD₃OD solvent mixture (9:1, 1.5 cm³). The colourless solution was added to the solid cobalt(II) salt (0.0454 mmol) and the mixture was stirred at room temperature. The original solution (0.6 cm³) was diluted with the same solvent mixture (0.6 cm³), then the new solution (0.4 cm³) was diluted with the same solvent mixture (0.4 cm³), giving three samples with concentrations (of cobalt(II)) of 0.030 M, 0.015 M and 0.0076 M.

Reaction of bis(terpyridyl)tetra(ethylene glycol) and cobalt(II) acetate tetrahydrate (0.0113 g, 0.0454 mmol) overnight gave a brown solution. δ_{H} (250 MHz, CD₃CN)/ppm see discussion (section 5.4).

Reaction of bis(terpyridyl)tetra(ethylene glycol) and cobalt(II) chloride hexahydrate (0.0108 g, 0.0454 mmol) overnight gave a dark brown solution. δ_{H} (250 MHz, CD₃CN)/ppm see discussion (section 5.4).

5.6.5.2 Reactions in CD₃OD with a ratio of 1L:1M (2tpy:1M)

The cobalt(II) salt (0.0454 mmol) was dissolved in CD₃OD (1.5 cm³). The pink solution was added to solid bis(terpyridyl)tetra(ethylene glycol) (0.030 g, 0.046 mmol) and the mixture was stirred at room temperature. The original solution (0.6 cm³) was diluted with the same solvent mixture (0.6 cm³), then the new solution (0.4 cm³) was diluted with the same solvent mixture (0.4 cm³), giving three samples with concentrations (of cobalt(II)) of 0.030 M, 0.015 M and 0.0076 M.

Reaction of bis(terpyridyl)tetra(ethylene glycol) and cobalt(II) acetate tetrahydrate (0.0113 g, 0.0454 mmol) overnight gave a dark brown solution. δ_{H} (250 MHz, CD_3CN)/ppm see discussion (section 5.4).

Reaction of bis(terpyridyl)tetra(ethylene glycol) and cobalt(II) chloride hexahydrate (0.0108 g, 0.0454 mmol) overnight gave a dark brown solution. δ_{H} (250 MHz, CD_3CN)/ppm see discussion (section 5.4).

5.6.5.3 Reactions in CD_3CN with a ratio of 1L:1M (2tpy:1M)

Cobalt(II) tetrafluoroborate hexahydrate (0.0156 g, 0.0457 mmol) was dissolved in CD_3CN (1.5 cm^3). The red-pink solution was added to solid bis(terpyridyl)tetra(ethylene glycol) (0.030 g, 0.046 mmol) and the mixture was stirred at room temperature for 45 minutes to give a brown solution. δ_{H} (250 MHz, CD_3CN)/ppm see discussion (section 5.4).

5.6.5.4 Reactions in CDCl_3 - CD_3OD with a ratio of 1L:2M (1tpy:1M)

Bis(terpyridyl)tetra(ethylene glycol) (0.0050 g, 0.0076 mmol) was dissolved in a CDCl_3 - CD_3OD solvent mixture (9:1, 0.5 cm^3). The colourless solution was added to the solid cobalt(II) salt (0.015 mmol) and the mixture was stirred at room temperature.

Reaction of bis(terpyridyl)tetra(ethylene glycol) and cobalt(II) acetate tetrahydrate (0.0038 g, 0.015 mmol) overnight gave a lilac solution. δ_{H} (250 MHz, CD_3CN)/ppm see discussion (section 5.4).

Reaction of bis(terpyridyl)tetra(ethylene glycol) and cobalt(II) chloride hexahydrate (0.0036 g, 0.015 mmol) for 1 hour gave a green-blue solution. δ_{H} (250 MHz, CD_3CN)/ppm see discussion (section 5.4). Allowing the solution to stand overnight resulted in the precipitation of a green solid.

5.6.5.5 Reactions in CD_3OD with a ratio of 1L:2M (1tpy:1M)

The cobalt(II) salt (0.015 mmol) was dissolved in CD_3OD (0.5 cm^3). The pink solution was added to solid bis(terpyridyl)tetra(ethylene glycol) (0.0050 g, 0.0076 mmol) and the mixture was stirred at room temperature.

Reaction of bis(terpyridyl)tetra(ethylene glycol) and cobalt(II) acetate tetrahydrate (0.0038 g, 0.015 mmol) overnight gave a brown solution. δ_{H} (250 MHz, CD_3CN)/ppm see discussion (section 5.4).

Reaction of bis(terpyridyl)tetra(ethylene glycol) and cobalt(II) chloride hexahydrate (0.0036 g, 0.015 mmol) overnight gave a brown solution. δ_{H} (250 MHz, CD_3CN)/ppm see discussion (section 5.4).

5.6.5.6 Reactions in CD_3CN with a ratio of 1L:2M (1tpy:1M)

Cobalt(II) tetrafluoroborate hexahydrate (0.0052 g, 0.015 mmol) was dissolved in CD_3CN (0.5 cm^3). The pink solution was added to solid bis(terpyridyl)tetra(ethylene glycol) (0.0050 g, 0.0076 mmol) and the mixture was stirred at room temperature for 15 minutes to give a brown solution. δ_{H} (250 MHz, CD_3CN)/ppm see discussion (section 5.4).

6 Polymer or Macrocycle?

Cobalt Complexes of Ditopic Bis(terpyridyl)oligo(ethylene glycol)s

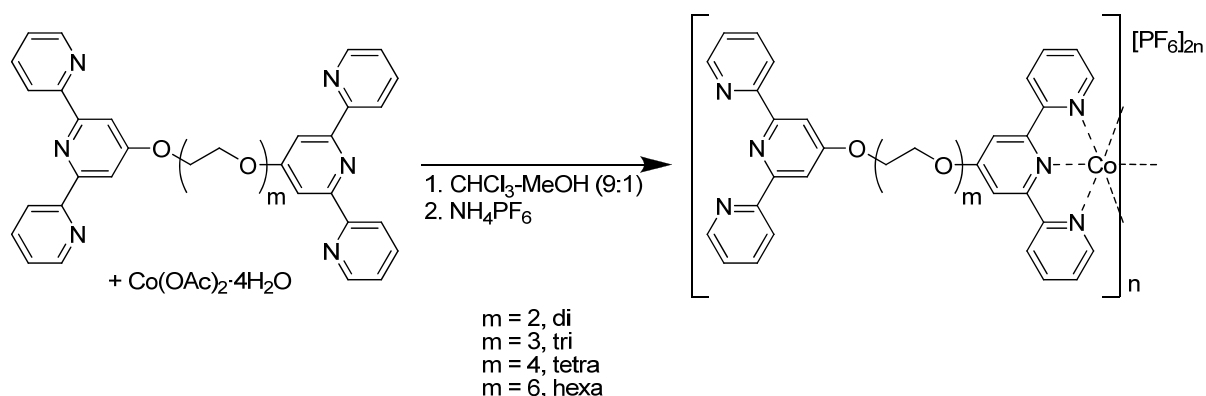
6.1 Introduction

As described in section 1.5, the overall aim of this project is to assess the extent of polymer or macrocycle formation from the reaction of flexible ditopic 2,2':6',2''-terpyridine ligands with cobalt(II) salts. Initial observations suggested that this is not a straightforward problem and the mixture of products obtained from the reaction of bis(terpyridyl)oligo(ethylene glycol) ligands with cobalt(II) salts is highly dependent on a large number of variables. Additionally (see Chapters 4 and 5), selection of an inappropriate cobalt(II) salt and solvent mixture can have even more dramatic consequences on the final product mixture. Depending on the metal salt and solvent used, the anion may coordinate to the metal centre, or even cause the decomposition of the ditopic ligand to give monotopic terpyridine units. In both cases, polymer end-units are created, which will have an effect on the position of the equilibrium between linear polymeric species and discrete molecular macrocycles. The equilibrium is also highly sensitive to many other more subtle changes in the reaction conditions and the effects of some these are considered in this chapter.

6.2 Cobalt(II) equilibria

6.2.1 Reactions with cobalt(II) acetate tetrahydrate

As described in Chapter 4, the complexation was initially carried out using 1:1 mixtures of the ditopic ligand and cobalt(II) acetate tetrahydrate in a chloroform-methanol solvent mixture (9:1) (Scheme 6.1). This solvent mixture was initially chosen for solubility reasons as the ligand is only sparingly soluble in pure methanol, and has been used by Schubert for the synthesis of metallopolymers based on similar bis(terpyridyl)poly(ethylene glycol) ligands.³⁹⁻
⁴¹ Use of this solvent mixture also reduces the amount of methanol available for the alkoxy exchange reaction which leads to the decomposition of the ditopic ligand when an acetate counterion is used.



Scheme 6.1 Reaction of bis(terpyridyl)oligo(ethylene glycol)s with cobalt(II) acetate tetrahydrate.

After a given amount of time at reflux or at room temperature, excess ammonium hexafluorophosphate in methanol was added to precipitate the product(s) and the ^1H NMR spectra were recorded in acetonitrile solution. The ^1H NMR spectra always showed a mixture of products, the composition of which changed with time. This has previously been observed for iron(II) complexes of a similar ligand.⁸⁴

6.2.1.1 Reactions with bis(terpyridyl)di(ethylene glycol)

A 1:1 mixture of bis(terpyridyl)di(ethylene glycol) and cobalt(II) acetate tetrahydrate was refluxed in a chloroform-methanol solvent mixture (9:1) for 1 hour, then excess ammonium hexafluorophosphate was added to the brown solution and the product was collected as the hexafluorophosphate salt. The ^1H NMR spectrum of this product immediately after precipitation is shown in Figure 6.1(a) and shows that one major species is present in solution with signals at δ 113, 76.2, 71.7, 35.3, 17.5, 13.0 and 6.91 ppm. Closer inspection of the peak corresponding to the H^5 proton of the terpyridine (inset in Figure 6.1(a)) shows that, in fact, several species are present in the mixture. As mentioned in Chapter 3, the ^1H NMR spectra of bis(2,2':6',2''-terpyridine)cobalt(II) complexes with an oxygen substituent in the 4'-position have been found to be very similar.⁹⁰ In this case also, the chemical shifts of the signals corresponding to the protons of the terpyridine unit are very similar to those in the spectrum of bis(4'-methoxy-2,2':6',2''-terpyridine)cobalt(II) hexafluorophosphate and assignments were made based on comparison with this complex. If this initial CD_3CN solution is left to stand for several days, the signals corresponding to the minor products increase in intensity as shown in Figure 6.1(b). The signals corresponding to the H^5 proton of the terpyridine are

particularly well separated and in this spectrum at least 7 species are clearly identifiable from this signal (inset in Figure 6.1(b)). All of the new signals associated with this proton are shifted to lower frequency in comparison with the signal corresponding to the major initial product. The exact composition of the equilibrium mixture is highly sensitive to the reaction conditions, including, amongst others, the temperature and concentration of the equilibration and the time and temperature of the initial reaction. While the same species were present in every attempt to study this equilibrium mixture, the relative proportions of each species were not reliably reproducible.

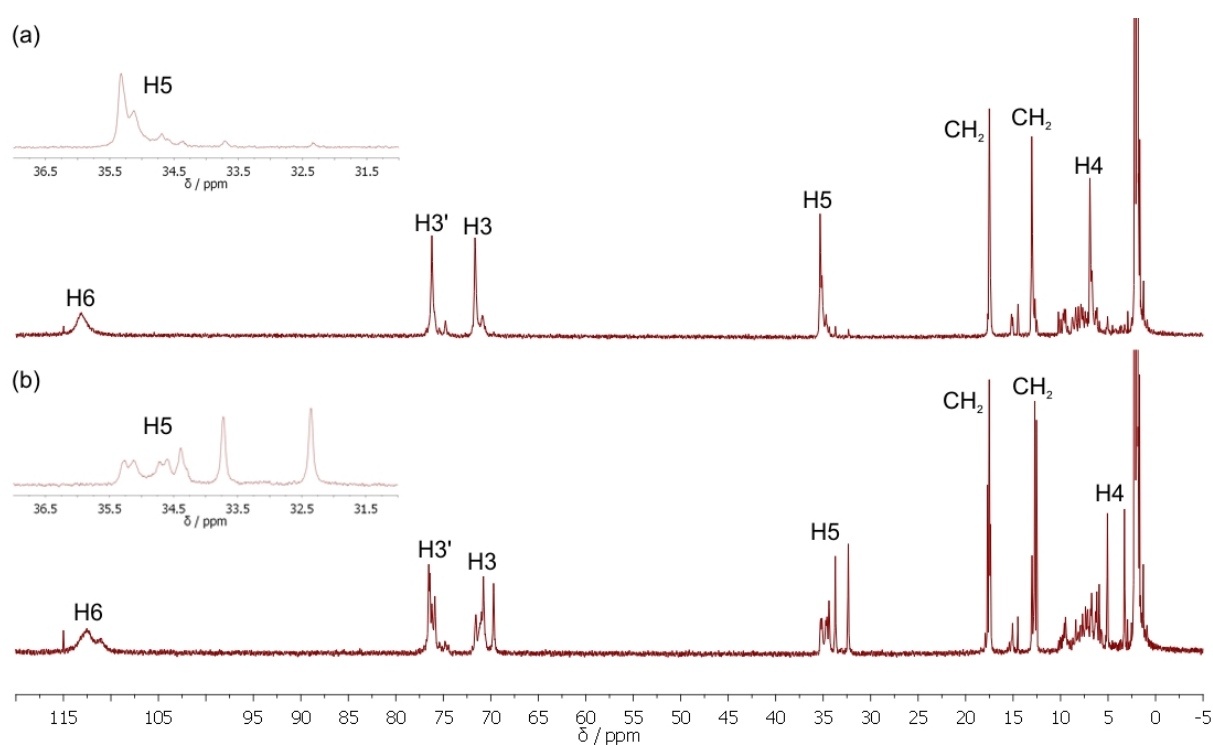


Figure 6.1 Full ^1H NMR spectra of the product mixture from the reaction of bis(terpyridyl)di(ethylene glycol) with cobalt(II) acetate tetrahydrate, (a) immediately after precipitation with excess ammonium hexafluorophosphate and (b) same sample after 2 days at room temperature and 5 days at 40 °C in CD_3CN solution (CD_3CN , 250 MHz). The inset shows the signal corresponding to the H^5 proton of the terpyridine.

The signals at approximately δ 15 ppm correspond to a coordinated 4'-methoxy- (see Chapter 3) or 4'-glycol-substituted-2,2':6',2''-terpyridine ligand,⁹⁰ and their presence shows that the decomposition of the ditopic ligand occurs to a limited extent under the reaction conditions

used (see Chapter 4). The intensity of these signals does not change over time in acetonitrile solution as can be seen in Figure 6.1.

A ^1H - ^1H COSY experiment was performed on another equilibrated sample of the same initial reaction mixture and a portion of the spectrum is shown in Figure 6.2. The assignment of signals in the ^1H - ^1H COSY experiment is explained in Chapters 2 and 3. In this case, the broad highest frequency set of signals (corresponding to H^6) again shows no cross peaks in the ^1H - ^1H COSY spectrum. Similarly, the set of signals at approximately δ 76 ppm does not couple with any other protons, confirming its assignment as H^3 . In this spectrum, cross peaks between four of the individual peaks within the groups of signals at approximately δ 70 (H^3), 34 (H^5) and 5 (H^4) ppm can also be observed, allowing signals belonging to the same species to be grouped together. Thus, the signals at δ 69.5, 32.3 and 3.26 ppm belong together, as do those at δ 70.6, 33.6 and 5.02 ppm, δ 70.8, 34.3 and 5.88 ppm and δ 71.4, 35.2 and 6.81 ppm. It is not possible, however, to gain any information about the size or nuclearity of the species in this mixture from these ^1H NMR spectroscopic studies, and it is possible that these sets of signals do not correspond to different discrete macrocyclic products, but instead to different environments within the same polymer or oligomer chain.

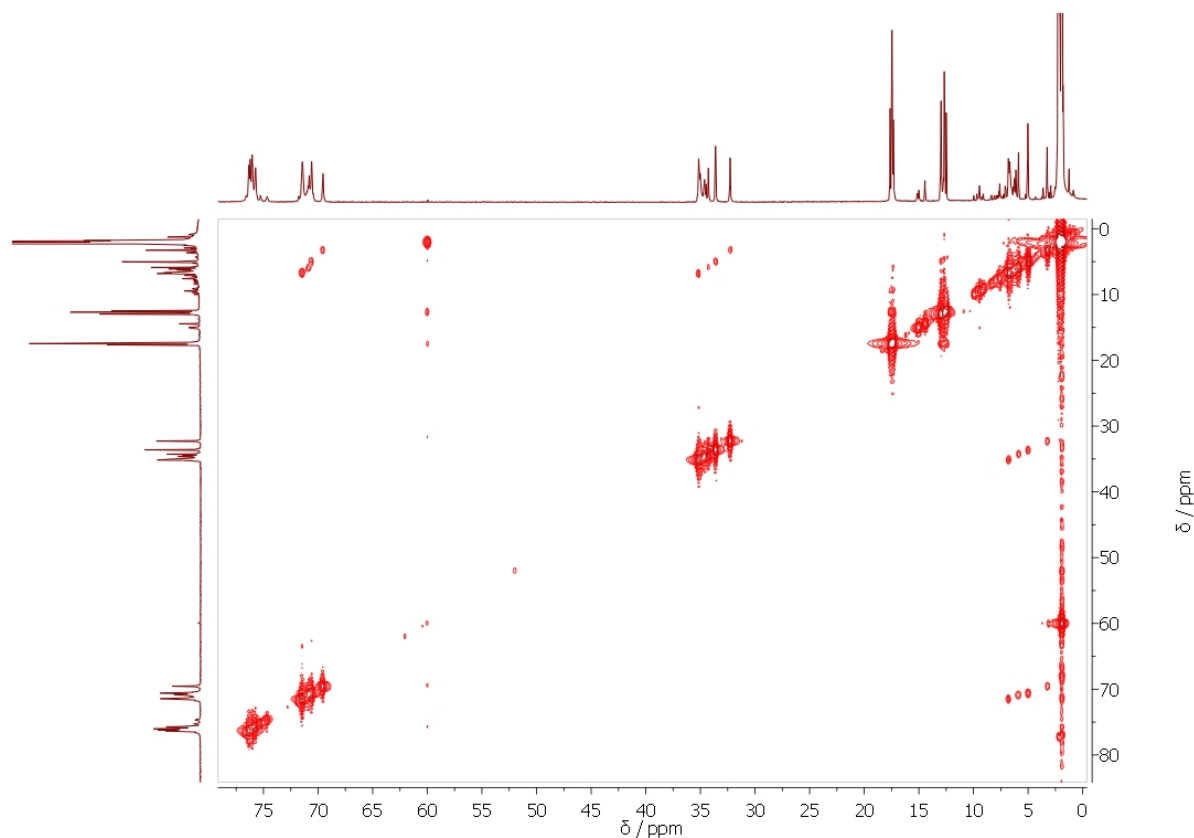


Figure 6.2 A portion of the ^1H - ^1H COSY spectrum (δ 0 – 80 ppm) of an equilibrated sample of the product from the reaction of bis(terpyridyl)di(ethylene glycol) with cobalt(II) acetate tetrahydrate after precipitation with excess ammonium hexafluorophosphate (CD_3CN , 500 MHz, 295 K).

The electrospray mass spectrum of the equilibrium mixture shows peaks at m/z 1231.2 and 1689.7, which correspond to $[\text{Co}_3(\text{di})_3(\text{PF}_6)_4]^{2+}$ and $[\text{Co}_4(\text{di})_4(\text{PF}_6)_6]^{2+}$ moieties, respectively. The presence of oligomeric or higher nuclearity species (whether polymeric or macrocyclic) is suggested by the presence of the signals at m/z 646.9 ($[\text{Co}(\text{di})\text{F}]^+$) and 1340.3 ($[\text{Co}(\text{di})_2\text{PF}_6]^+$). Decomposition products from the reaction of the ditopic ligand with the methanol in the solvent mixture can also be observed in the mass spectrum with peaks at m/z 1035.5 ($[(\text{MeOtpy})\text{Co}(\text{di})\text{PF}_6]^+$) and 1109.5 ($[(\text{HOCH}_2\text{CH}_2\text{OCH}_2\text{CH}_2\text{Otpy})\text{Co}(\text{di})\text{PF}_6]^+$).

6.2.1.2 Reactions with bis(terpyridyl)tri(ethylene glycol)

A similar reaction was performed with a 1:1 mixture of bis(terpyridyl)tri(ethylene glycol) and cobalt(II) acetate tetrahydrate at room temperature for 30 minutes. Excess ammonium hexafluorophosphate was added to the brown solution and the product was collected as the hexafluorophosphate salt. The ^1H NMR spectra of the product mixtures immediately after

precipitation from two different reactions under the same conditions are shown in Figure 6.3. As mentioned above, the exact composition of the mixture is not reproducible and the relative intensities of the signals shown in the two spectra are not the same. However, it is clear that the same species are present in the two mixtures and again one major initial product is formed with signals at δ 112, 74.9, 70.7, 34.7, 16.1, 11.0, 9.60 and 6.44 ppm.

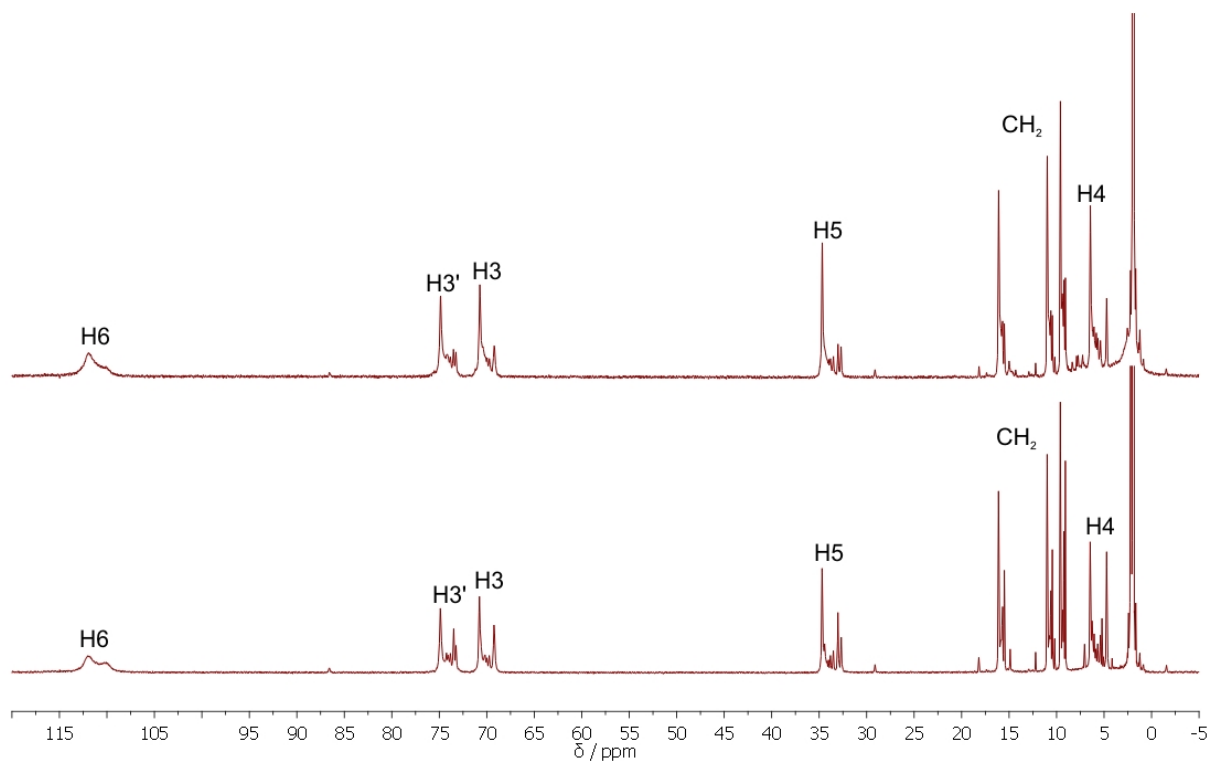


Figure 6.3 Full ^1H NMR spectra of the product mixtures from two different reactions of bis(terpyridyl)tri(ethylene glycol) with cobalt(II) acetate tetrahydrate in CHCl_3 -MeOH (9:1) at room temperature for 30 minutes, immediately after precipitation with ammonium hexafluorophosphate (CD_3CN , 250 MHz).

Leaving the NMR sample shown in Figure 6.3(b) to stand for several days led to an increase in the relative intensities of the second most intense set of signals in the initial mixture (δ 110, 73.4, 69.2, 33.0, 15.5, 10.5, 9.08 and 4.73 ppm). A bulk sample of the initial mixture was dissolved in acetonitrile and stirred at room temperature for two weeks. The solvent was removed *in vacuo* and the ^1H NMR spectrum of the product was measured in acetonitrile at several concentrations (Figure 6.4). Again, the signals in the group corresponding to the H^5

proton (δ 29 – 35 ppm) are particularly well separated and the presence of at least nine species can be observed (insets in Figure 6.4).

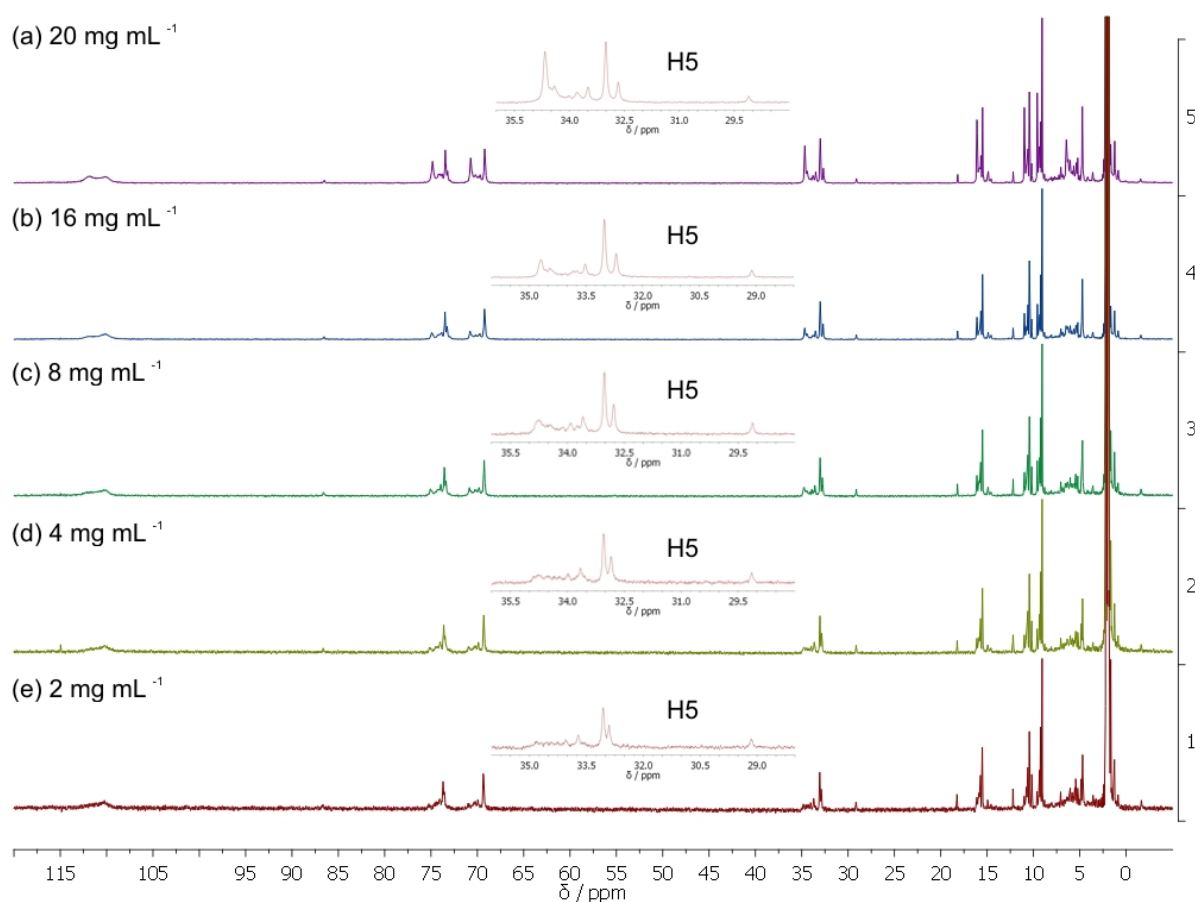


Figure 6.4 Full ^1H NMR spectra at several concentrations of the equilibrated product mixture from the reaction of bis(terpyridyl)tri(ethylene glycol) with cobalt(II) acetate tetrahydrate after precipitation with ammonium hexafluorophosphate and after two weeks in acetonitrile solution (CD_3CN , 250 MHz).

The speciation in the mixture is clearly concentration dependent, with higher proportions of the major product from the initial mixture present at higher concentrations and more of the new species with signals at lower frequency at lower concentrations. Assuming that the initial (kinetic) product of the reaction is polymeric, comparison of the ^1H NMR spectra of the initial and equilibrium mixtures shows that at equilibrium the formation of polymers is favoured at higher concentrations. Again, the relative concentrations of the different species are not readily reproducible between experiments, but the same species are always present in the mixture.

The electrospray mass spectrum of this solution (at low concentration) shows signals at m/z 335.8, 431.7 and 816.3. The isotope pattern in the signal at m/z 335.8 could not be resolved, and could belong to any $[\text{Co}_n(\text{tri})_n]^{2n+}$ species. The difference between the peaks in the signal at m/z 816.3 is 0.5 and can be assigned to the $[\text{Co}_2(\text{tri})_2(\text{PF}_6)_2]^{2+}$ moiety. The signal at m/z 431.7 is tentatively assigned to $[\text{Co}_3(\text{tri})_3(\text{PF}_6)_2]^{5+}$, although no isotope pattern could be resolved.

6.2.1.3 Reactions with bis(terpyridyl)tetra(ethylene glycol)

A 1:1 mixture of bis(terpyridyl)tetra(ethylene glycol) and cobalt(II) acetate tetrahydrate was stirred at room temperature for 30 minutes in a chloroform-methanol solvent mixture (9:1), then the product was precipitated by addition of excess ammonium hexafluorophosphate. The ^1H NMR spectra of the product immediately after precipitation and after eight days in CD_3CN solution are shown in Figure 6.5.

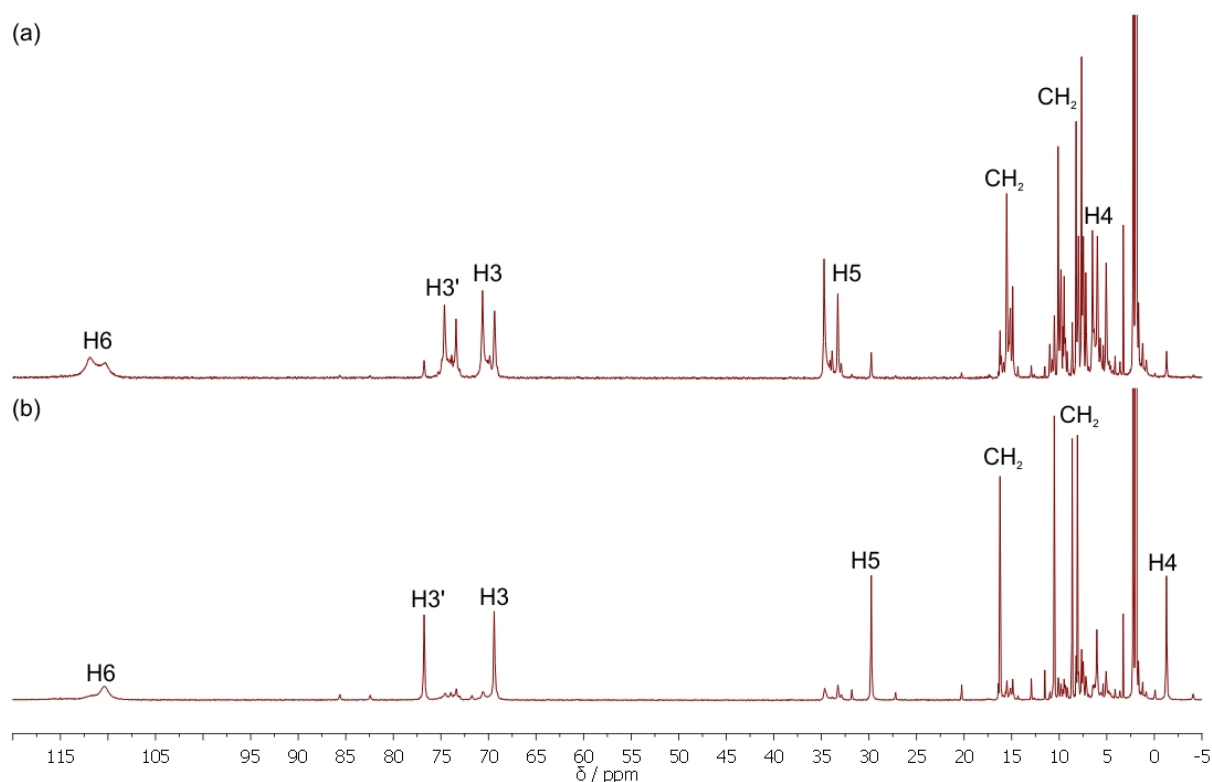


Figure 6.5 Full ^1H NMR spectra of the product mixture from the reaction of bis(terpyridyl)tetra(ethylene glycol) with cobalt(II) acetate tetrahydrate, (a) immediately after precipitation with excess ammonium hexafluorophosphate and (b) same sample after 8 days at room temperature in CD_3CN solution (CD_3CN , 250 MHz).

Similar behaviour to the complexes with the shorter chain ligands was observed. Immediately after precipitation with excess ammonium hexafluorophosphate, at least seven bis(2,2':6',2''-terpyridine)cobalt(II) species are present in the product mixture and the dominant species shows peaks at δ 112, 74.6, 70.6, 34.7, 15.5, 10.1, 8.24, 7.66 and 6.53 ppm in the ^1H NMR spectrum. In this case, equilibration in CD_3CN solution for several days leads to the formation of almost exclusively one product, exhibiting signals at δ 110, 76.8, 69.4, 29.8, 16.2, 10.5, 8.64, 8.08 and -1.28 ppm. Again, the relative proportions of all of the products in the mixtures could not be reproduced from one reaction to the next, but the same species were always present. Experiments with this ligand tended to equilibrate the most reliably towards a single equilibrium product.

The electrospray mass spectrum of the equilibrium mixture shows signals at m/z 1864.9, 860.2, 525.3 and 357.8, which correspond to $[\text{Co}_2(\text{tetra})_2(\text{PF}_6)_n]^{(4-n)+}$ species. The equilibrium product from this reaction was therefore proposed to be a [2+2] metallomacrocyclic species.

As described in section 6.2.1.2, the speciation in the equilibrium mixture of bis(terpyridyl)tri(ethylene glycol)cobalt(II) hexafluorophosphate is highly dependent on concentration. The effect of concentration on the equilibration process was considered for the system containing the bis(terpyridyl)tetra(ethylene glycol) ligand. The initial product obtained after precipitation with ammonium hexafluorophosphate from a reaction of bis(terpyridyl)tetra(ethylene glycol) with cobalt(II) acetate tetrahydrate for 24 hours at room temperature in a chloroform-methanol solvent mixture (9:1) was dissolved in CD_3CN at concentrations (of cobalt(II)) of 0.020, 0.010 and 0.005 M. ^1H NMR spectra of these solutions were measured at intervals over one month and the relative proportions of the proposed $[\text{Co}_2(\text{tetra})_2][\text{PF}_6]_4$ species were determined from the relative integrals of the signal at δ 29.8 ppm and the other signals assigned to the H^5 proton (δ 35 – 33 ppm). A graph of the relative proportions of the proposed $[\text{Co}_2(\text{tetra})_2][\text{PF}_6]_4$ species over time is shown in Figure 6.6.

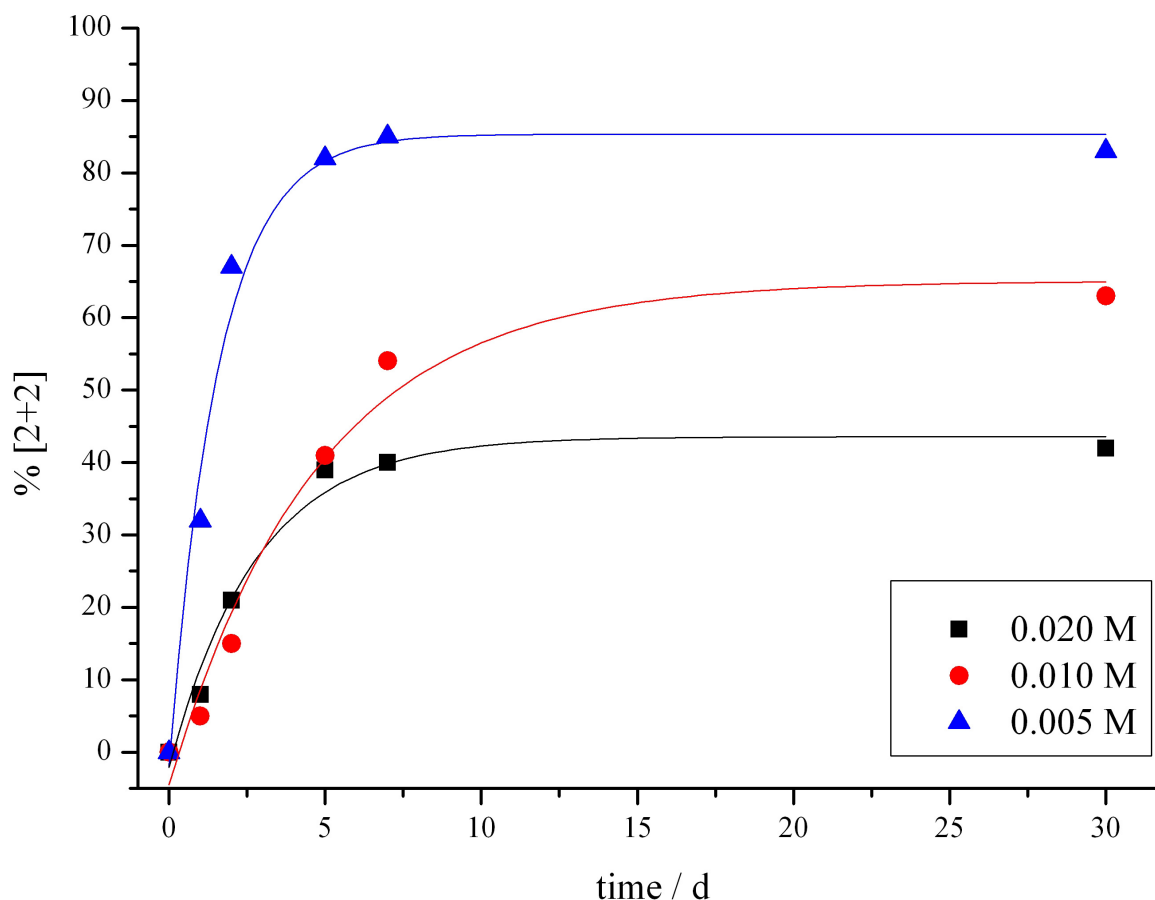


Figure 6.6 Graph showing the relative proportions (determined by ^1H NMR spectroscopy) of the proposed $[\text{Co}_2(\text{tetra})_2][\text{PF}_6]_4$ species present in mixtures of bis(terpyridyl)tetra(ethylene glycol)cobalt(II) hexafluorophosphate formed from the reaction of bis(terpyridyl)tetra(ethylene glycol) with cobalt(II) acetate tetrahydrate for 24 hours in chloroform-methanol (9:1) solution followed by precipitation with ammonium hexafluorophosphate (CD_3CN , 250 MHz).

The rate of the equilibration process is essentially independent of concentration and at all concentrations equilibrium was reached after approximately one week. However, the effect of the concentration on the equilibrium position is significant, with more of the proposed $[\text{Co}_2(\text{tetra})_2][\text{PF}_6]_4$ species being formed at lower concentrations, similar to the results described above for the system involving the bis(terpyridyl)tri(ethylene glycol) ligand.

The equilibration of a mixture of bis(terpyridyl)tetra(ethylene glycol)cobalt(II) hexafluorophosphate complexes formed from the reaction of the ligand with cobalt(II) chloride hexahydrate in methanol for 24 hours was also followed and the relative proportions of the proposed $[\text{Co}_2(\text{tetra})_2][\text{PF}_6]_4$ species in the CD_3CN solution over time are shown

graphically in Figure 6.7. In this experiment, higher proportions of the $[\text{Co}_2(\text{tetra})_2][\text{PF}_6]_4$ species were formed at the same concentrations with respect to the experiment with cobalt(II) acetate, however, the relative proportions of the species present in the mixture are not reliably reproducible. Use of a chloride counteranion eliminates the decomposition of the ditopic ligand to monotopic 2,2':6',2''-terpyridine units (see Chapter 4).

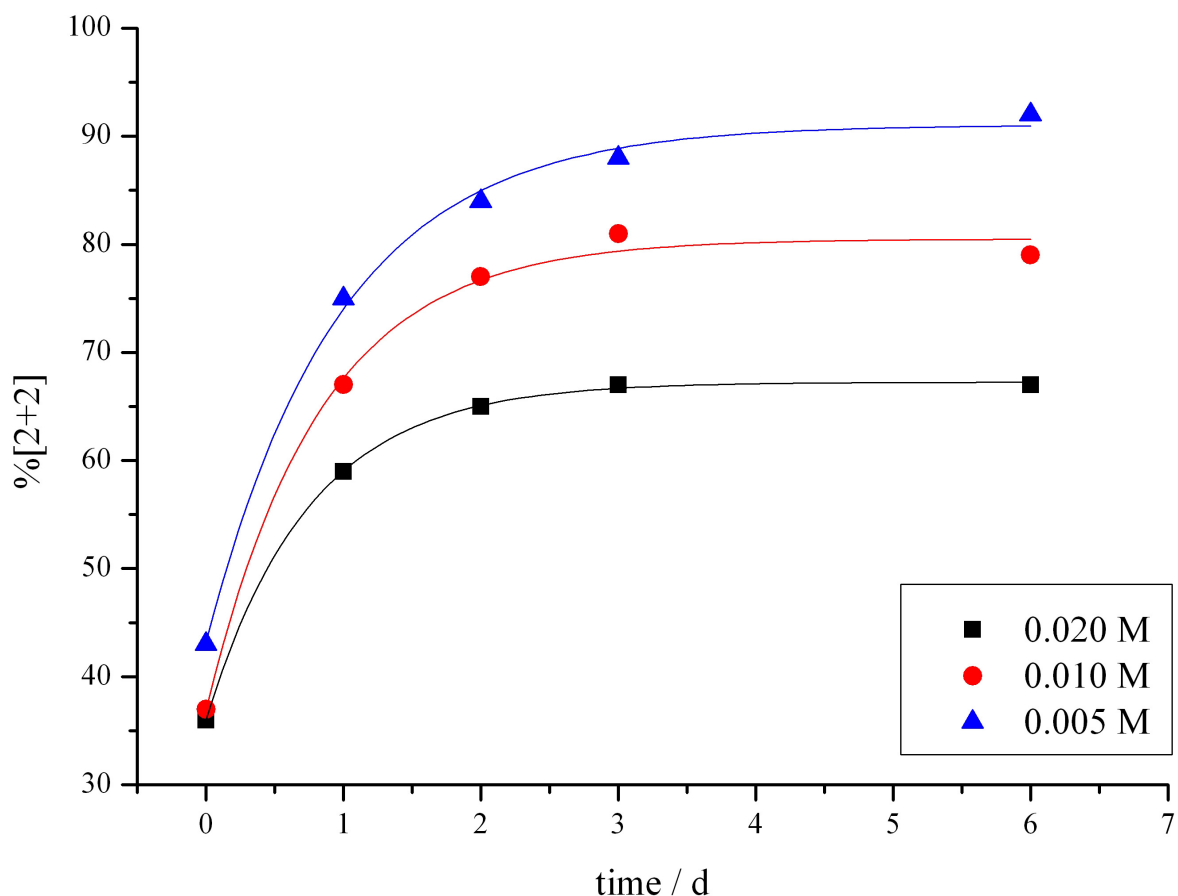


Figure 6.7 Graph showing the relative proportions (determined by ^1H NMR spectroscopy) of the proposed $[\text{Co}_2(\text{tetra})_2][\text{PF}_6]_4$ species present in mixtures of bis(terpyridyl)tetra(ethylene glycol)cobalt(II) hexafluorophosphate formed from the reaction of bis(terpyridyl)tetra(ethylene glycol) with cobalt(II) chloride hexahydrate for 24 hours in methanol solution followed by precipitation with ammonium hexafluorophosphate (CD_3CN , 250 MHz).

6.2.1.4 Reactions with bis(terpyridyl)hexa(ethylene glycol)

A 1:1 mixture of bis(terpyridyl)hexa(ethylene glycol) and cobalt(II) acetate tetrahydrate was refluxed in a chloroform-methanol solvent mixture (9:1) for 1 hour, then excess ammonium

hexafluorophosphate was added to the brown solution and the product was collected as the hexafluorophosphate salt. The ^1H NMR spectrum of the product immediately after precipitation is shown in Figure 6.8(a) and the spectrum of the product obtained after refluxing the bulk sample in acetonitrile for 17 hours is shown in Figure 6.8(b). Again, the relative proportions of all of the species in the mixtures could not be reproduced, but the same species were always present in the mixture. As observed for the other ligands, the product mixture immediately after precipitation contains several species, with the major product exhibiting signals at δ 115, 74.6, 70.6 and 34.8 ppm. The signals corresponding to H^4 and the glycol chains overlap considerably and are difficult to distinguish. After equilibration in acetonitrile solution, the mixture contains one major product, corresponding to one of the minor species in the initial mixture, with ^1H NMR signals at δ 110, 73.1, 69.0, 32.8, 14.3, 9.15, 7.16, 6.26, 5.57, 5.18 and 4.77 ppm. The signal at δ 4.77 ppm could be assigned to the H^4 proton using a ^1H - ^1H COSY experiment as it couples with the signals at δ 69.0 and 32.8 ppm. The two signals in the negative region of the spectrum couple only to each other and several broad signals between δ 11 and 3 ppm also appear to be independent of the other signals in the spectrum.

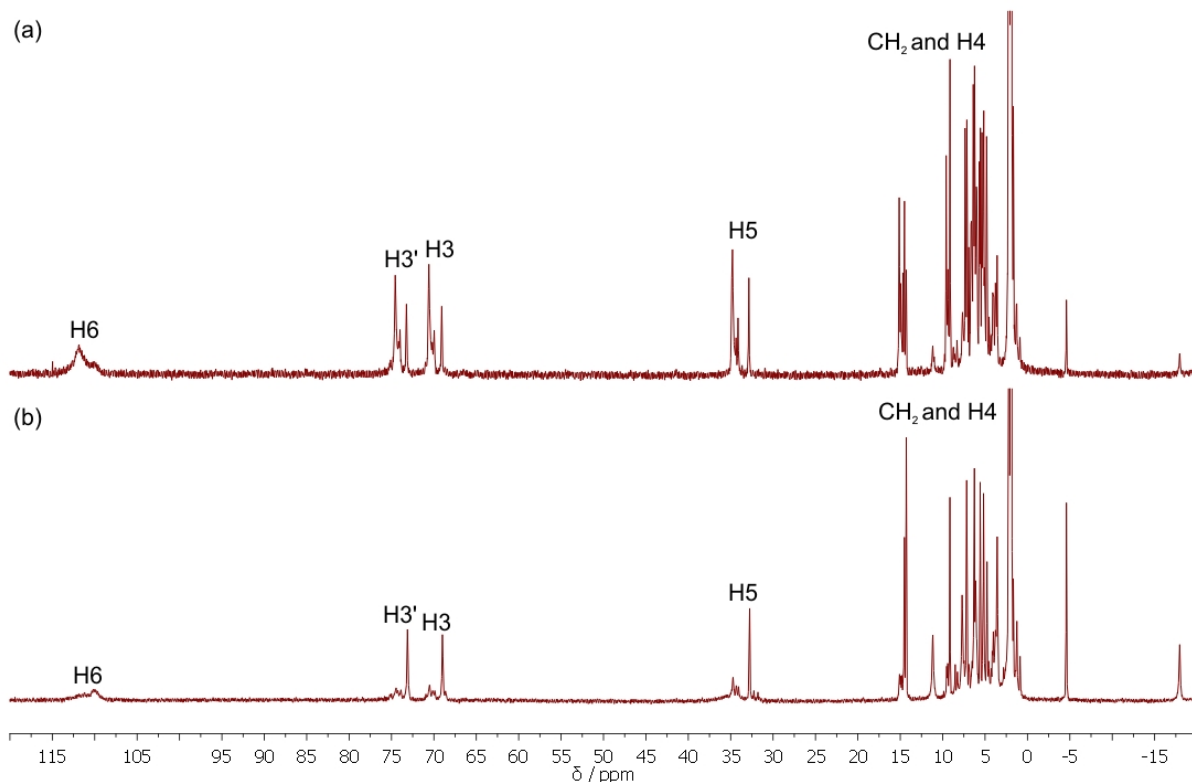


Figure 6.8 Full ^1H NMR spectra of the product mixture from the reaction of bis(terpyridyl)hexa(ethylene glycol) with cobalt(II) acetate tetrahydrate, (a) immediately after precipitation with excess ammonium hexafluorophosphate and (b) after the bulk sample was refluxed in acetonitrile solution for 17 hours (CD_3CN , 250 MHz).

The electrospray mass spectrum of the equilibrated sample showed peaks at m/z 948.1, 584.0 and 401.8 corresponding to the formation of a $[\text{Co}_2(\text{hexa})_2]^{4+}$ species. The equilibrium product from this reaction was therefore also proposed to be a [2+2] macrocyclic species.

6.2.1.5 Comparison of cobalt(II) complexes of bis(terpyridyl)oligo(ethylene glycol) ligands

A summary of the chemical shifts in the ^1H NMR spectra of the major species present in mixtures of bis(terpyridyl)oligo(ethylene glycol)cobalt(II) hexafluorophosphate complexes are shown in Table 6.1. The chemical shifts of the terpyridine protons (particularly $\text{H}^{3'}$) are largely dependent on the substituent in the 4'-position of the terpyridine. As these ligands have almost identical substituents, the ^1H NMR spectra are also expected to be very similar. In a small macrocycle, the environments of the terpyridine protons should also be affected by the surrounding glycol chain, so the chemical shifts of protons in smaller macrocycles would be expected to vary more significantly than in larger macrocycles or polymers.^{83, 84, 89} The

major species in the initial mixtures of cobalt(II) complexes of the three longest chain ligands have very similar ^1H NMR spectra in the terpyridine region, suggesting that the complexes themselves are also similar. Larger differences are observed in the ^1H NMR spectra of the equilibrium products. This observation therefore supports the hypothesis that polymers or large macrocycles are formed initially and then rearrange to smaller macrocyclic products.

	$\delta \text{H}^6 / \text{ppm}$	$\delta \text{H}^3 / \text{ppm}$	$\delta \text{H}^3 / \text{ppm}$	$\delta \text{H}^5 / \text{ppm}$	$\delta \text{H}^4 / \text{ppm}$
$[\text{Co}_n(\text{di})_n]^{2n+}$ (i)	113	76.2	71.7	35.3	6.91
$[\text{Co}_n(\text{tri})_n]^{2n+}$ (i)	112	74.9	70.7	34.7	6.44
$[\text{Co}_n(\text{tetra})_n]^{2n+}$ (i)	112	74.6	70.6	34.7	6.52
$[\text{Co}_n(\text{hexa})_n]^{2n+}$ (i)	115	74.6	70.6	34.8	-
$[\text{Co}_n(\text{di})_n]^{2n+}$ (eq)	-- ^a	-- ^a	70.6	33.6	5.02
	-- ^a	-- ^a	69.5	32.3	3.26
$[\text{Co}_n(\text{tri})_n]^{2n+}$ (eq)	110	73.4	69.2	33.0	4.73
$[\text{Co}_n(\text{tetra})_n]^{2n+}$ (eq)	110	76.8	69.4	29.8	-1.28
$[\text{Co}_n(\text{hexa})_n]^{2n+}$ (eq)	110	73.1	69.0	32.8	4.77

Table 6.1 Comparison of chemical shifts in the ^1H NMR spectra of the major species in initial (i) and equilibrium (eq) mixtures of bis(terpyridyl)oligo(ethylene glycol)cobalt(II) hexafluorophosphate complexes (CD_3CN , 250 MHz). (a = could not be distinguished due to overlapping signals).

6.2.2 NMR spectroscopic studies with other anions

Parallel to the studies of the effect of the anion on the equilibrium between mono- and bis(2,2':6',2''-terpyridine)cobalt(II) species in the reaction of bis(terpyridyl)tetra(ethylene glycol) with various cobalt(II) salts described in Chapter 5, the effect of changing the anion on the equilibrium between the different bis(2,2':6',2''-terpyridine)cobalt(II) species was also considered. The ditopic ligand bis(terpyridyl)tetra(ethylene glycol) was mixed with cobalt(II) acetate tetrahydrate, cobalt(II) chloride hexahydrate or cobalt(II) tetrafluoroborate hexahydrate at room temperature in a 1L:1M ratio in the solvents given in Table 6.2. This

ligand was chosen as a model system as the polymer-macrocycle equilibrium with the $[\text{PF}_6]^-$ anion tends to equilibrate towards a single product with well-separated signals in the ^1H NMR spectrum (see section 6.2.1.3). In all experiments the concentration of cobalt(II) was 0.030 M. The reaction mixtures were then diluted with the same solvent mixture to give three samples with concentrations of 0.030 M, 0.015 M and 0.0076 M, and all samples were characterised by ^1H NMR spectroscopy. Also shown in Table 6.2 are the relative proportions of the proposed $[\text{Co}_2(\text{tetra})_2]^{4+}$ species at equilibrium determined from the relative intensities of the signals corresponding to the H^5 proton of the terpyridine unit in the ^1H NMR spectra.

Anion	Solvent	% $[\text{Co}_2(\text{tetra})_2]^{4+}$		
		0.030 M	0.015 M	0.0076 M
OAc^-	$\text{CDCl}_3\text{-CD}_3\text{OD}$ (9:1)	0	0	0
OAc^-	CD_3OD	3	9	23
Cl^-	$\text{CDCl}_3\text{-CD}_3\text{OD}$ (9:1)	1	1	2
Cl^-	CD_3OD	6	15	30
$[\text{BF}_4]^-$	CD_3CN	55	80	95

Table 6.2 Relative proportions of the proposed $[\text{Co}_2(\text{tetra})_2]^{4+}$ species in equilibrium mixtures of bis(terpyridyl)tetra(ethylene glycol) and cobalt(II) salts. Percentages are based on integrals of the peaks corresponding to H^5 and do not include the signals corresponding to the mono(2,2':6',2''-terpyridine) units.

Figure 6.9 and Figure 6.10 show the ^1H NMR spectra in $\text{CDCl}_3\text{-CD}_3\text{OD}$ (9:1) solution of a 1:1 mixture of bis(terpyridyl)tetra(ethylene glycol) and cobalt(II) acetate tetrahydrate and cobalt(II) chloride hexahydrate, respectively. The presence of a small amount of a mono(2,2':6',2''-terpyridine)cobalt(II) acetate complex can clearly be seen in Figure 6.9 (signals at δ 85.6, 64.1 and 21.5 ppm), and a similar mono(2,2':6',2''-terpyridine)cobalt(II) chloride species is clearly absent from the spectra in Figure 6.10. In both cases, and at all concentrations, the amount of the proposed $[\text{Co}_2(\text{tetra})_2]^{4+}$ species, evidenced by the signal at δ 29.8 ppm for $[\text{Co}_2(\text{tetra})_2][\text{PF}_6]_4$ in CD_3CN and assumed to be in a similar position with other anions and in other solvents (see Chapter 5), is negligible. The major species is always similar to that seen in the reaction of the ligand with cobalt(II) acetate tetrahydrate immediately after precipitation with excess ammonium hexafluorophosphate. The concentration of the sample has little effect on the speciation of the mixture containing the

acetate counterion. When a chloride anion is used, lower concentrations disfavour this initial product and the minor signals at lower frequencies (although not those at the lowest frequency corresponding to the proposed $[\text{Co}_2(\text{tetra})_2]^{4+}$ species) start to become more significant.

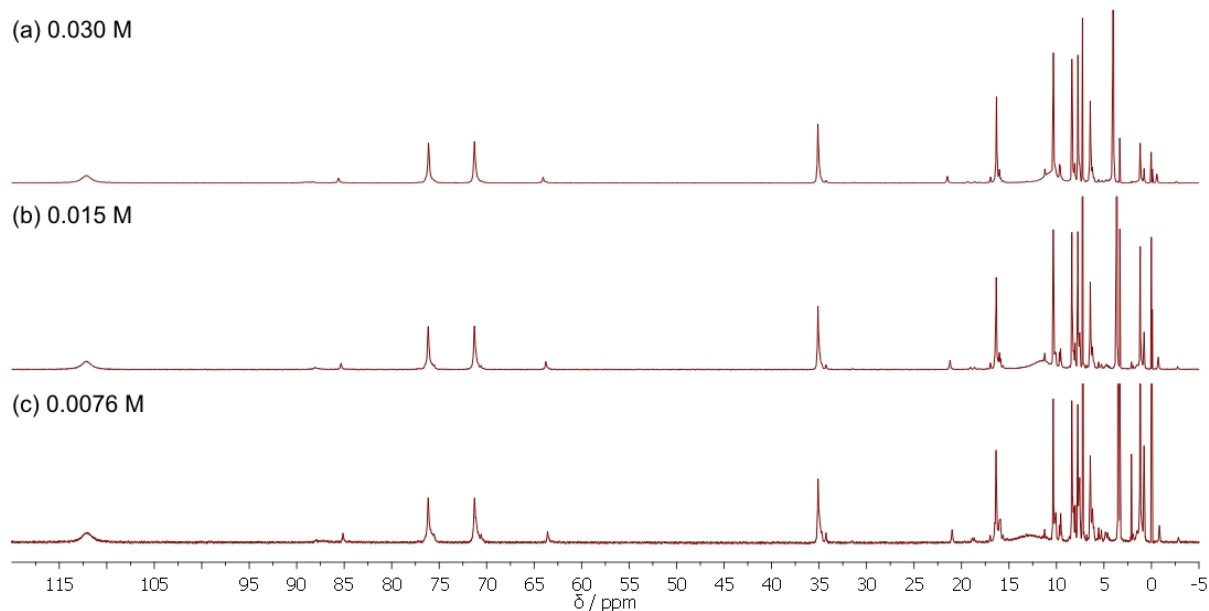


Figure 6.9 Full ^1H NMR spectra of a 1:1 mixture of bis(terpyridyl)tetra(ethylene glycol) and cobalt(II) acetate tetrahydrate at different concentrations ($\text{CDCl}_3\text{-CD}_3\text{OD}$ (9:1), 250 MHz).

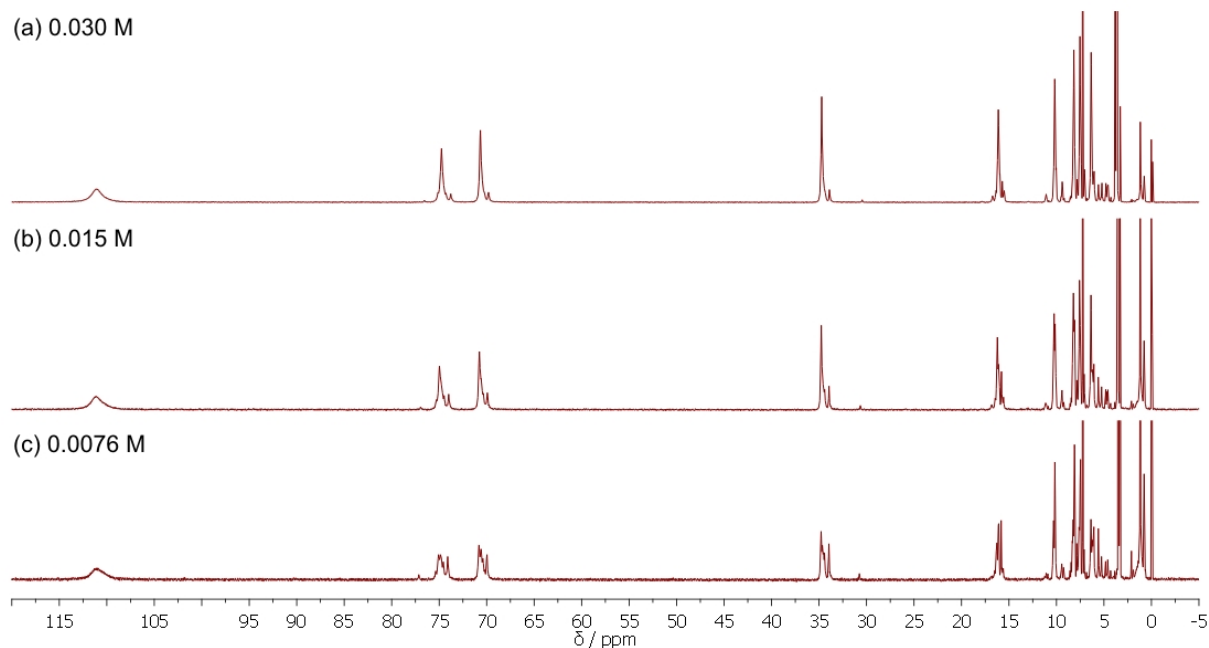


Figure 6.10 Full ^1H NMR spectra of a 1:1 mixture of bis(terpyridyl)tetra(ethylene glycol) and cobalt(II) chloride hexahydrate at different concentrations ($\text{CDCl}_3\text{-CD}_3\text{OD}$ (9:1), 250 MHz).

The ^1H NMR spectra in CD_3OD solution of similar mixtures of bis(terpyridyl)tetra(ethylene glycol) and cobalt(II) acetate tetrahydrate or cobalt(II) chloride hexahydrate are shown in Figure 6.11 and Figure 6.12, respectively. Again, the presence of mono(2,2':6',2''-terpyridine)cobalt(II) acetate units can be observed in the spectra shown in Figure 6.11, while signals corresponding to the equivalent chloride units are absent from the ^1H NMR spectra in Figure 6.12. Both systems follow approximately the same trend, and at higher concentrations the mixtures again contain almost exclusively one initial product. In this solvent, however, the effect of changing the concentration is more significant and the relative proportion of the proposed $[\text{Co}_2(\text{tetra})_2]^{4+}$ species (signal at δ 31.0 ppm for the acetate species and δ 30.8 ppm for the chloride species) increases considerably at lower concentrations (23 – 30%).

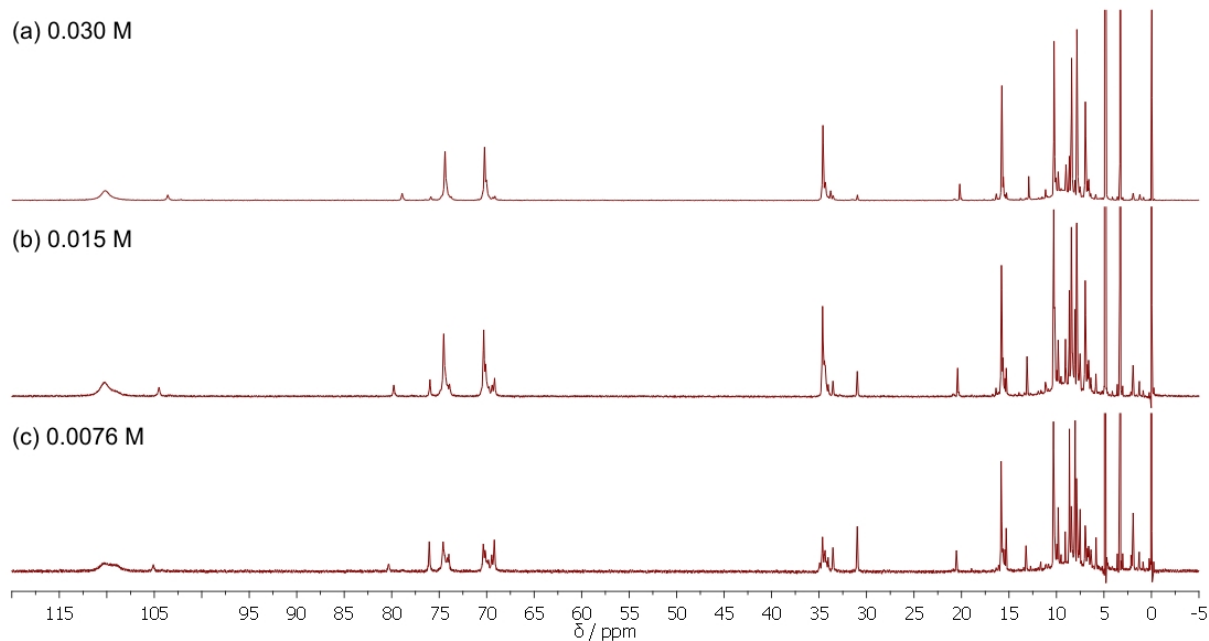


Figure 6.11 Portion of the ^1H NMR spectra (δ 120 – -5 ppm) of a 1:1 mixture of bis(terpyridyl)tetra(ethylene glycol) and cobalt(II) acetate tetrahydrate at different concentrations (CD_3OD , 250 MHz).

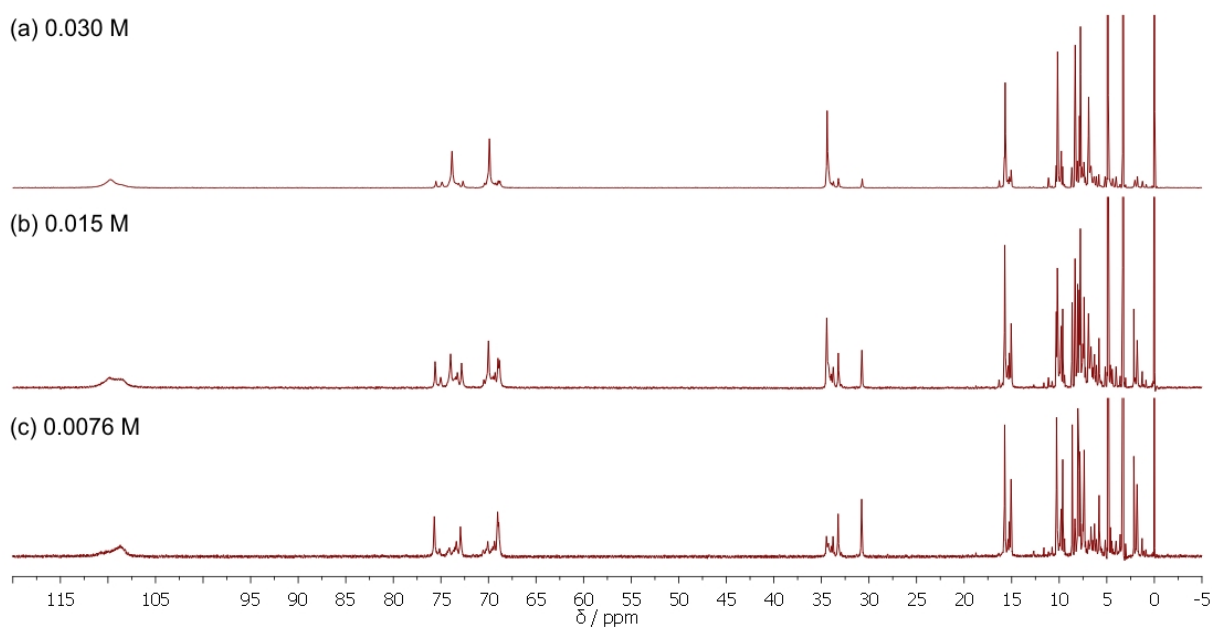


Figure 6.12 Full ^1H NMR spectra of a 1:1 mixture of bis(terpyridyl)tetra(ethylene glycol) and cobalt(II) chloride hexahydrate at different concentrations (CD_3OD , 250 MHz).

Using the weakly coordinating tetrafluoroborate anion gives somewhat different results and the ^1H NMR spectra of equilibrated mixtures of bis(terpyridyl)tetra(ethylene glycol) and cobalt(II) tetrafluoroborate hexahydrate at several concentrations are shown in Figure 6.13. At all concentrations, the proposed $[\text{Co}_2(\text{tetra})_2][\text{BF}_4]_4$ species is clearly the major product, with signals at δ 110, 76.3, 69.1, 29.8, 16.1, 10.5, 8.60, 8.04 and -1.09 ppm. At the lowest concentration, the mixture contains almost exclusively this species (95%).

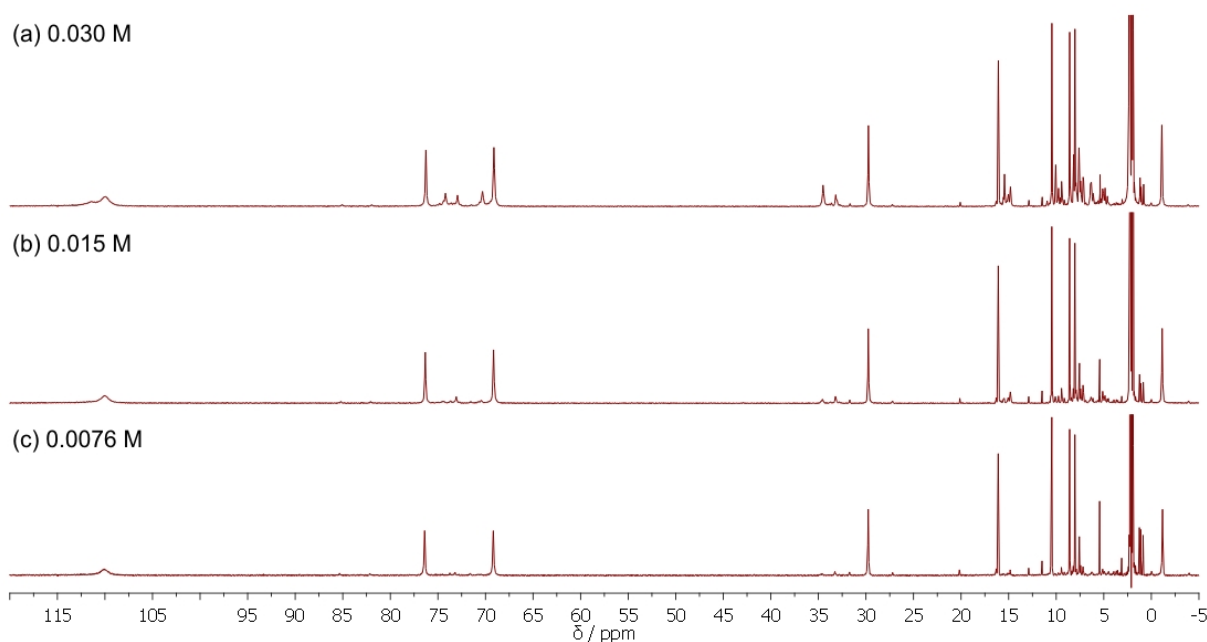


Figure 6.13 Full ^1H NMR spectra of a 1:1 mixture of bis(terpyridyl)tetra(ethylene glycol) and cobalt(II) tetrafluoroborate hexahydrate at different concentrations (CD_3CN , 250 MHz).

The bis(terpyridyl)tetra(ethylene glycol)cobalt(II) tetrafluoroborate system also reaches an equilibrium point significantly more slowly than the systems containing chloride or acetate anions. Using an acetate or chloride counteranion, equilibrium was reached immediately after diluting the sample to the new concentration (within the time taken to measure the ^1H NMR spectrum). When cobalt(II) tetrafluoroborate hexahydrate was used as the source of cobalt(II), equilibrium was only attained after six to nine days in acetonitrile solution. Determination of the relative integrals of the signals at δ 29.8 ppm and the other signals corresponding to the H^5 proton (δ 35 – 33 ppm) of the terpyridine unit allowed the relative proportion of the proposed

$[\text{Co}_2(\text{tetra})_2][\text{BF}_4]_4$ species to be followed over time. The study of the formation of this species is shown graphically in Figure 6.14.

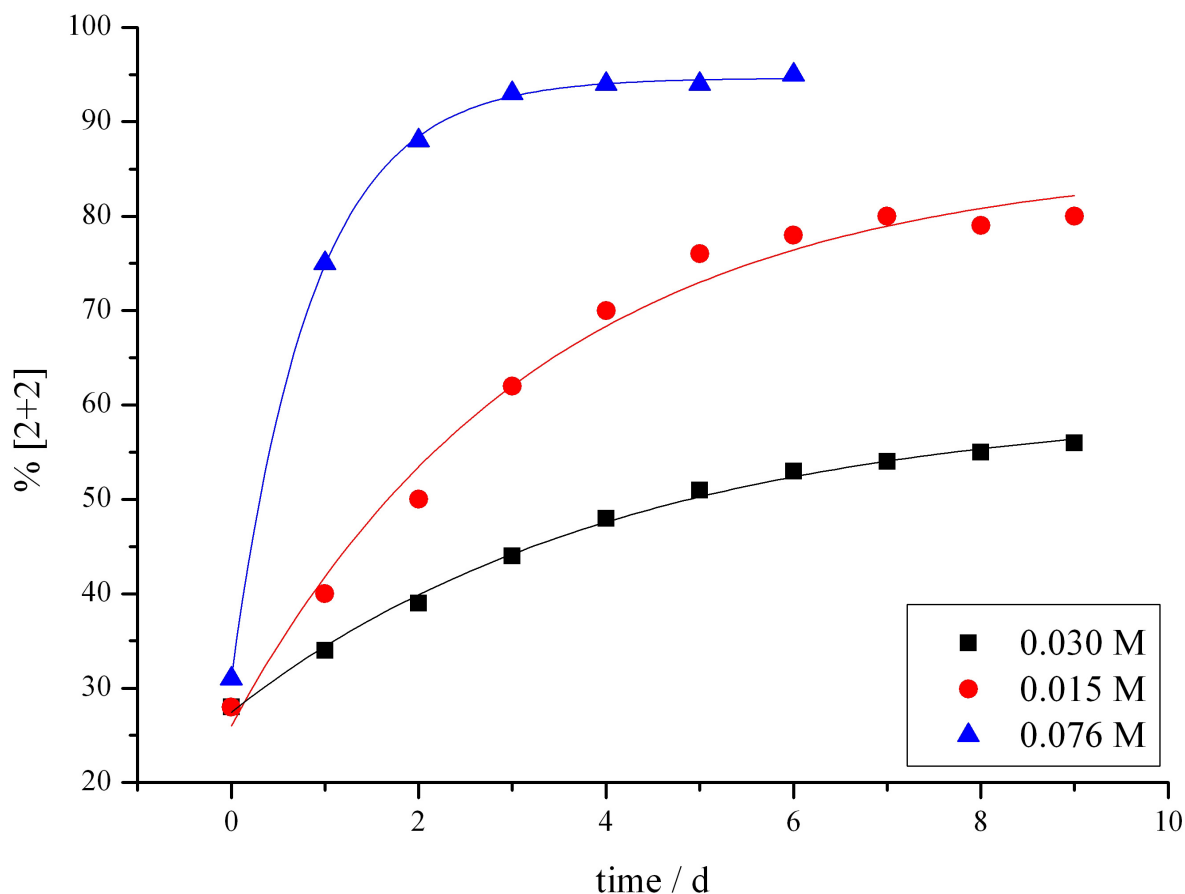


Figure 6.14 Graph showing the relative proportions (determined by ^1H NMR spectroscopy) of the proposed $[\text{Co}_2(\text{tetra})_2][\text{BF}_4]_4$ species present in solutions of a 1:1 mixture of bis(terpyridyl)tetra(ethylene glycol) and cobalt(II) tetrafluoroborate hexahydrate (CD_3CN , 250 MHz).

The systems under investigation are extremely complex. Equilibria exist between the uncoordinated ligand and cobalt(II) salt, macrocycles of different nuclearities and polymers, the end-units of which may be uncoordinated 2,2':6',2''-terpyridine units, metal centres with coordinated anions or solvent molecules, or even monotopic 2,2':6',2''-terpyridine ligands resulting from the decomposition of the ditopic ligand. Due to the reversibility of the formation of the metal–ligand coordination bond, the reaction is under thermodynamic control and entropy should favour the formation of the largest number of smallest nuclearity

macrocycle. The enthalpy difference between (unstrained) macrocycles of different sizes is expected to be insignificant as the coordination bonds present in, for example, three [2+2] cycles and two [3+3] cycles are identical. Thus, the energy differences between the species at equilibrium are expected to be very small. Small adjustments in minor reaction parameters which appear to play no important role in the final product, for example (uncoordinated) anions and solvent, can therefore have a large effect on the outcome of the reaction. The interactions between the mixture of complexes and the anions or solvent must be in the same order of magnitude as the energy differences between the complexes. Therefore, seemingly insignificant changes in these interactions can result in a slight increase in the stability of one of the complexes, enough to favour its formation over another.

The rate of ligand exchange is slower for the tetrafluoroborate species than for the acetate or chloride species, resulting in a longer equilibration time for the mixture of bis(terpyridyl)tetra(ethylene glycol) and cobalt(II) tetrafluoroborate hexahydrate. For ligand exchange to occur, one 2,2':6',2''-terpyridine unit must dissociate from the metal and another must coordinate. Dissociation of one of the pyridyl rings gives a free coordination site on the cobalt(II) centre, which must be filled with another pyridyl nitrogen atom, an anion or a solvent molecule. The dissociation of the three pyridyl rings of one 2,2':6',2''-terpyridine ligand is unfavourable due to the chelate effect, and coordination of three neutral solvent molecules offers no energetic advantage over three pyridine rings. However, coordination of an anion to the cobalt(II) centre is energetically favourable due to the charge difference and the intermediate is energetically stabilised. Coordination of an anion to the metal centre also increases the electron density at the metal, weakening the metal–nitrogen bonds to the remaining pyridine ligands and therefore increasing the rate at which the 2,2':6',2''-terpyridine ligand dissociates.^{190, 191} In the absence of a coordinating anion, this accelerating mechanism is not available.

6.2.3 Bulk synthesis

Taking into consideration the results described above and those described in Chapters 4 and 5, it was observed over many similar reactions that the highest proportion of (proposed) small macrocycles and fastest equilibration was obtained from the reaction of the bis(terpyridyl)oligo(ethylene glycol)s with cobalt(II) chloride hexahydrate in methanol, followed by the precipitation of the products as the hexafluorophosphate salts and

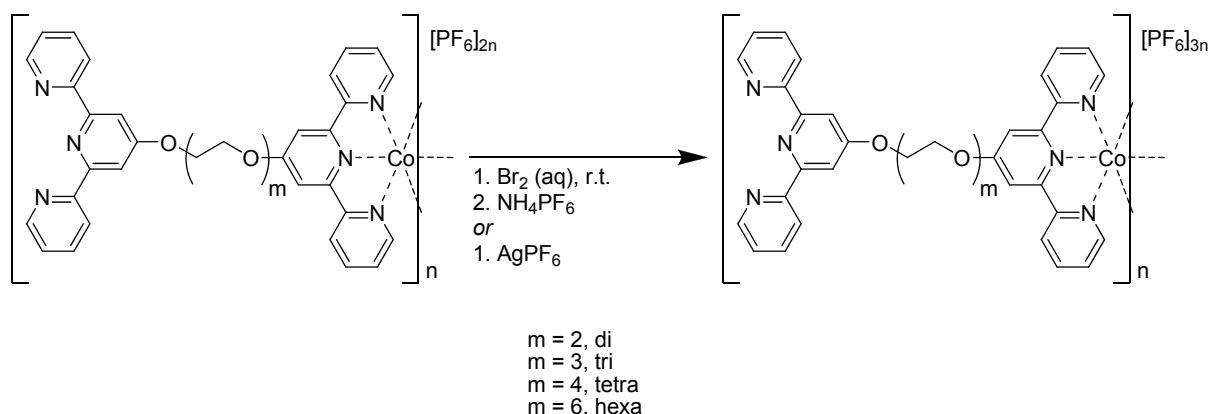
equilibration of this product mixture in acetonitrile solution. Only the bis(2,2':6',2''-terpyridine)cobalt(II) complex is present in solution during the reaction of bis(terpyridyl)tetra(ethylene glycol) with cobalt(II) chloride hexahydrate in a 1:1 ratio (i.e. there is no mono(2,2':6',2''-terpyridine)cobalt(II) complex) (see Chapter 5). In this way, the presence of polymer end-capping units with coordinated anions is minimised. Using cobalt(II) chloride hexahydrate in place of cobalt(II) acetate tetrahydrate also prevents the decomposition of the ditopic ligand as the less basic chloride anion cannot deprotonate the alcohol solvent as it attacks the ligand (see Chapter 4). This again minimises the presence of end-capping monotopic terpyridine units and allows reactions to be carried out in pure methanol instead of mixtures of alcohols with chloroform. Since the reaction appears to be highly sensitive to the reaction conditions, simplification of the system wherever possible is desirable. The results described in section 6.2.2 show that the proportion of the proposed $[\text{Co}_2(\text{tetra})_2]^{4+}$ species is greater in methanol than in the chloroform-methanol (9:1) solvent mixture and that the product mixtures of the chloride salts of the complex contain slightly more of this macrocycle than the acetate salts. Using cobalt(II) chloride hexahydrate as the cobalt(II) source and performing the reaction in methanol should therefore lead to the highest proportion of smaller macrocycles in the initial product mixture obtained immediately after precipitation of the product as the hexafluorophosphate salts. As the initial product mixture is therefore closer to the hexafluorophosphate equilibrium product in acetonitrile, the time required to reach the equilibrium position in acetonitrile solution should be reduced.

Cobalt(II) hexafluorophosphate complexes of all four bis(terpyridyl)oligo(ethylene glycol) ligands were synthesised on a larger scale (200 mg) from the reaction of the ligand with cobalt(II) chloride hexahydrate in methanol followed by precipitation of the products by addition of excess ammonium hexafluorophosphate. The initial products obtained immediately after precipitation were dissolved in acetonitrile at a concentration of approximately 10 mg of complex per mL acetonitrile and stirred at room temperature until equilibration was judged to be complete. This was estimated by following the equilibration of a sample of the mixture dissolved in CD_3CN at the same concentration. Mixtures of the same products described above (determined by ^1H NMR spectroscopy and electrospray mass spectrometry) were obtained in all cases; however the exact compositions of the mixtures were again not easily reproducible and must be influenced by small changes in reaction conditions that are almost impossible to control.

6.3 Oxidation

It is clear from the experiments described above that the speciation in mixtures of bis(terpyridyl)oligo(ethylene glycol)cobalt(II) complexes is very complex and highly dependent on many variables. In order to investigate further the product mixtures, the cobalt(II) complexes were oxidised to the corresponding kinetically inert cobalt(III) complexes in order to "freeze" the equilibrium at a specific point during the reaction. In addition, the oxidation step makes it possible to measure diffusion coefficients of the cobalt(III) complexes using PGSE NMR spectroscopy (see Chapters 2 and 3). From the measured diffusion coefficients, it should be possible to determine approximate sizes of the complexes at specific points in the reaction using the Stokes-Einstein equation (see Chapter 2).

The oxidation was initially carried out using aqueous bromine and the hexafluorophosphate salt of the cobalt(III) complex was precipitated by addition of excess ammonium hexafluorophosphate (Scheme 6.2). However, the presence of the bromide ions formed during the oxidation could influence the speciation of complexes in the mixtures, and oxidation of the cobalt(II) complexes using silver(I) hexafluorophosphate was also tested (Scheme 6.2), with good yields and a much simpler work-up. Comparison of the product mixtures between the two methods did not suggest that the bromide ions had a significant effect on the speciation but as the exact composition of the cobalt(II) mixtures were not reproducible (see section 6.2), the relative proportions of the species in the oxidised samples were also not consistent.



Scheme 6.2 Oxidation of bis(terpyridyl)oligo(ethylene glycol)cobalt(II) hexafluorophosphate complexes.

For each of the four ditopic ligands, a sample of the initial mixture of cobalt(II) complexes, obtained immediately after precipitation with ammonium hexafluorophosphate, and a second sample of the equilibrium mixture were oxidised. The ^1H NMR spectra of all the mixtures show signals within the normal diamagnetic range only, confirming the completion of the oxidation reaction (see section 3.2.3). Assignment of the signals (where possible) was by inspection of the coupling constants¹⁴² (^1H) and standard 2D methods. The advantage of using paramagnetic cobalt(II) salts for the investigation of the behaviour of these systems in solution is very obvious when comparing the ^1H NMR spectra of corresponding cobalt(II) and cobalt(III) systems. While it is relatively easy to obtain information on, for example, the number of species in solution and the relative proportions of these species from the ^1H NMR spectra of mixtures of bis(terpyridyl)oligo(ethylene glycol)cobalt(II) complexes, this is not the case with the spectra of the diamagnetic cobalt(III) complexes. Characterisation of the oxidised initial product mixtures using standard techniques was difficult as the ^1H NMR spectra showed broad, overlapping peaks from which little information could be obtained. Mass spectrometric studies were also not conclusive. The oxidised equilibrium mixtures showed sharper signals in the ^1H NMR spectra, however, the signals still overlapped considerably. In the case of the two longest chain ligands, bis(terpyridyl)tetra(ethylene glycol) and bis(terpyridyl)hexa(ethylene glycol), a single species could be isolated and was purified by preparative TLC. Separation of the complexes of the shorter chain ligands was not possible. The signal corresponding to the H^4 proton of the terpyridine unit was the most useful for distinguishing between different species in the mixture. This signal is well-separated from the other signals and its position appears to be highly sensitive to changes in the speciation of the mixture. In all cases, equilibration of the cobalt(II) sample and subsequent oxidation led to a shift of this signal to lower frequency with respect to its position in the oxidised initial mixture. A comparison of the initial and equilibrium mixtures of cobalt(III) complexes of the bis(terpyridyl)tetra(ethylene glycol) ligand is shown in Figure 6.15.

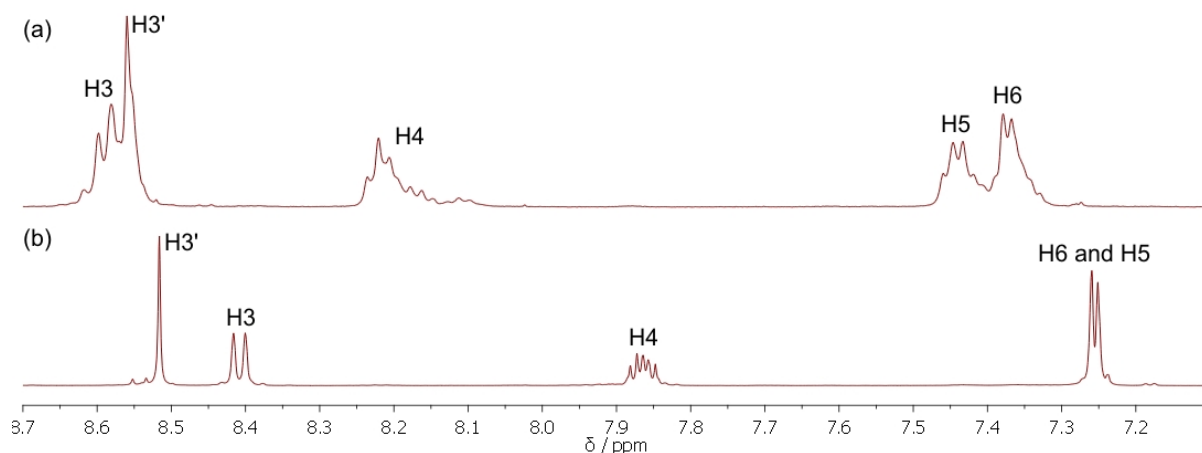


Figure 6.15 A portion of the ^1H NMR spectra (δ 8.7 – 7.1 ppm) of (a) the initial mixture of bis(terpyridyl)tetra(ethylene glycol)cobalt(III) hexafluorophosphate complexes and (b) the equilibrium mixture of bis(terpyridyl)tetra(ethylene glycol)cobalt(III) hexafluorophosphate complexes (after purification) (CD_3CN , 500 MHz, 295 K).

In all cases, electrospray mass spectrometric data supported that obtained for the corresponding cobalt(II) complexes and again intense peaks corresponding to the analogous cobalt(II) species were observed in addition to the expected signals. As described in Chapter 3, these cobalt(II) species are believed to form by reduction of the cobalt(III) complex in the mass spectrometer source.¹⁴³

6.4 X-ray structure determination of macrocycles

Although crystallisation of complexes of the bis(terpyridyl)oligo(ethylene glycol)s was anticipated to be difficult due to the size of the complexes and the flexibility of the ligands, it was possible to obtain single crystals of the dinuclear species, $[\text{Co}_2(\text{tetra})_2][\text{PF}_6]_4 \cdot 6\text{MeCN}$, $[\text{Co}_2(\text{tetra})_2][\text{PF}_6]_6 \cdot 10\text{MeCN}$, $[\text{Co}_2(\text{hexa})_2][\text{PF}_6]_5 \cdot 2\text{MeCN}$ and $[\text{Co}_2(\text{hexa})_2][\text{PF}_6]_6 \cdot 6\text{MeCN}$, and the trinuclear species, $[\text{Co}_3(\text{tri})_3][\text{PF}_6]_9 \cdot 2\text{MeCN} \cdot 0.5\text{MeOH} \cdot 2.75\text{H}_2\text{O}$. Cobalt–nitrogen bond lengths are given in Table 6.3 for comparison with the bond lengths in the mononuclear bis(2,2':6',2''-terpyridine)cobalt complexes described in Chapter 3.

Complex	Co–N1	Co–N2	Co–N3	Co–N4	Co–N5	Co–N6	av. Co–N _t	av. Co–N _c
[Co ₃ (tri) ₃][PF ₆] ₉ ·2MeCN· 0.5MeOH·2.75H ₂ O ^a	1.961(6)	1.879(6)	1.964(6)	1.957(6)	1.874(6)	1.955(6)	1.959	1.877
	1.950(7)	1.879(7)	1.951(6)	1.932(10)	1.887(10)	1.990(11)	1.956	1.883
	1.982(9)	1.883(8)	1.948(10)	1.945(7)	1.864(9)	1.953(8)	1.957	1.874
[Co ₂ (tetra) ₂][PF ₆] ₄ ·6MeCN	2.119(4)	1.991(4)	2.136(4)	2.126(4)	2.004(4)	2.137(4)	2.130	1.998
[Co ₂ (tetra) ₂][PF ₆] ₆ ·10MeCN	1.944(3)	1.849(3)	1.951(3)	1.957(3)	1.850(3)	1.946(3)	1.950	1.850
[Co ₂ (hexa) ₂][PF ₆] ₅ ·2MeCN	2.040(3)	1.890(3)	2.037(4)	1.982(3)	1.867(3)	1.982(3)	2.010	1.879
[Co ₂ (hexa) ₂][PF ₆] ₆ ·6MeCN	1.939(3)	1.857(3)	1.935(3)	1.941(3)	1.853(3)	1.944(3)	1.940	1.855

Table 6.3 Cobalt–nitrogen bond lengths (Å) in macrocyclic bis(terpyridyl)oligo(ethylene glycol)cobalt hexafluorophosphate complexes. The shading indicates the oxidation state of the complex; cobalt(II) (white), cobalt(III) (yellow) or mixed cobalt(II/III) (green). N1, N2 and N3 belong to one terpyridine ligand in the bis(2,2':6',2''-terpyridine)cobalt unit and N4, N5 and N6 belong to the other terpyridine ligand. N2 and N5 are the nitrogen atoms in the central pyridine rings. N_c = N_{central}, N_t = N_{terminal}. The numbering of the atoms in the table does not always correspond to the numbering of the atoms in the cif file. (a = The cobalt atoms are not equivalent and are numbered Co1, Co2 and Co3 in the cif file. The numbering of the nitrogen atoms coordinated to Co2 is N7–12 and those around Co3 are N13–18.)

Single crystals of $[\text{Co}_2(\text{tetra})_2][\text{PF}_6]_4 \cdot 6\text{MeCN}$ suitable for X-ray diffraction were obtained by slow diffusion of diethyl ether into an acetonitrile solution of the complex at room temperature, and the molecular structure of the cation is shown in Figure 6.16. The formation of a [2+2] metallomacrocylic species, predicted from the mass spectrometric data (see section 6.2.1.3) was confirmed and the structure is isostructural with the analogous ruthenium-containing metallomacrocycle, $[\text{Ru}_2(\text{tetra})_2][\text{PF}_6]_4 \cdot 6\text{MeCN}$.⁸³ The cobalt–nitrogen bond lengths are shown in Table 6.3 and are towards the higher end of the range seen for bis(2,2':6',2''-terpyridine)cobalt(II) complexes (see Chapter 3).

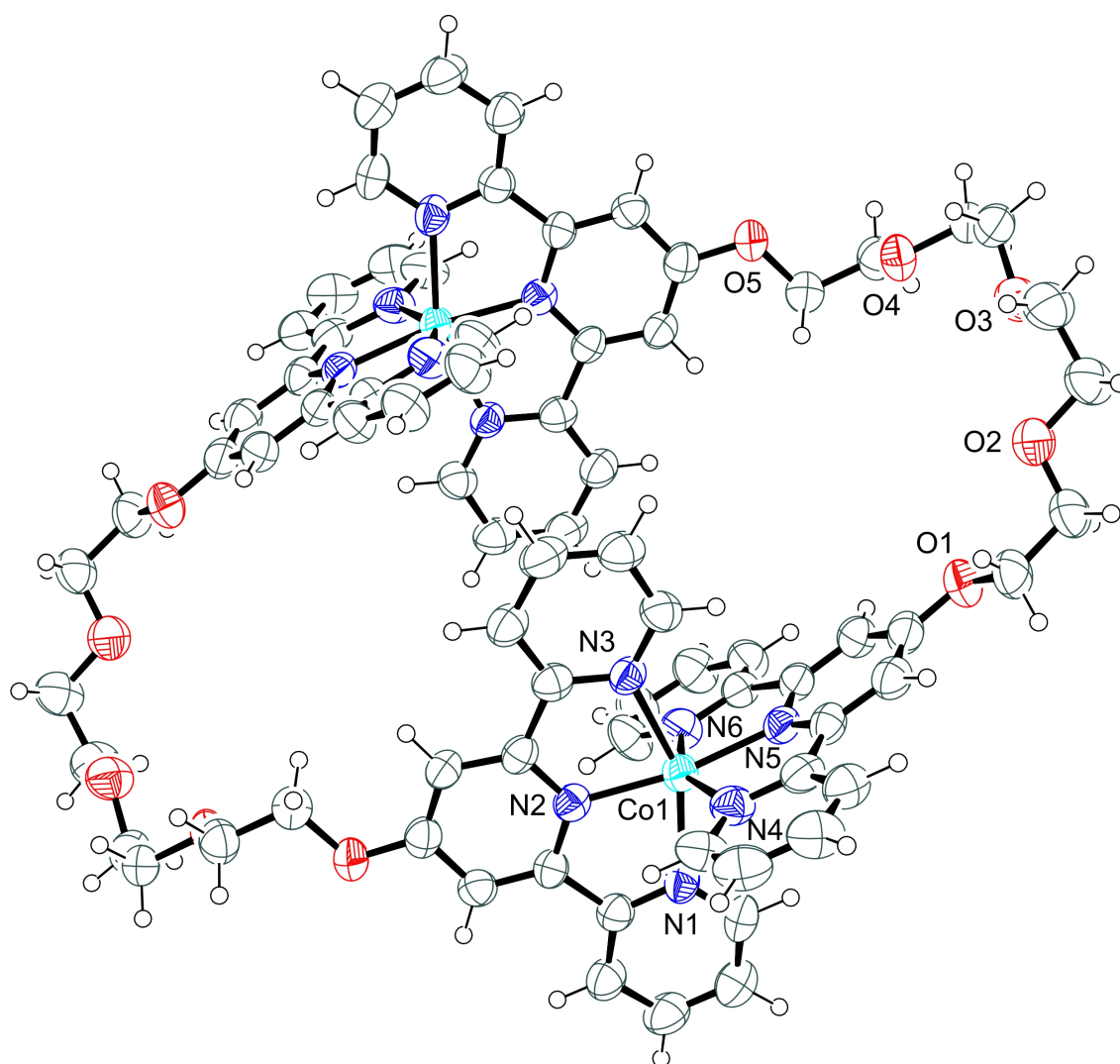


Figure 6.16 Molecular structure of the cation in $[\text{Co}_2(\text{tetra})_2][\text{PF}_6]_4 \cdot 6\text{MeCN}$ with anisotropic displacement ellipsoids drawn at the 50% probability level. Hydrogen atoms are shown as spheres of arbitrary radius.

The centre of the metallomacrocyclic lies on an inversion centre, relating the two halves of the cycle by symmetry. The distance between the two cobalt(II) centres across the macrocycle is 10.0879(10) Å, precluding any π - π interactions across the centre of the macrocycle between the pairs of symmetry-related pyridine rings. The cavity is dumbbell-shaped and large enough to accommodate one acetonitrile molecule in the enclosed space between the two bis(2,2':6,2''-terpyridine)cobalt(II) moieties (shown in Figure 6.17). This acetonitrile molecule sits on the inversion centre and is disordered over two positions. Two further acetonitrile molecules fill the open ends of the cavity, interacting with the glycol chains through weak C-H \cdots O hydrogen bonds (C42-H423 \cdots O2 = 2.55 Å, C42-H421 \cdots O4 = 2.92 Å). This interaction is also shown in Figure 6.17.

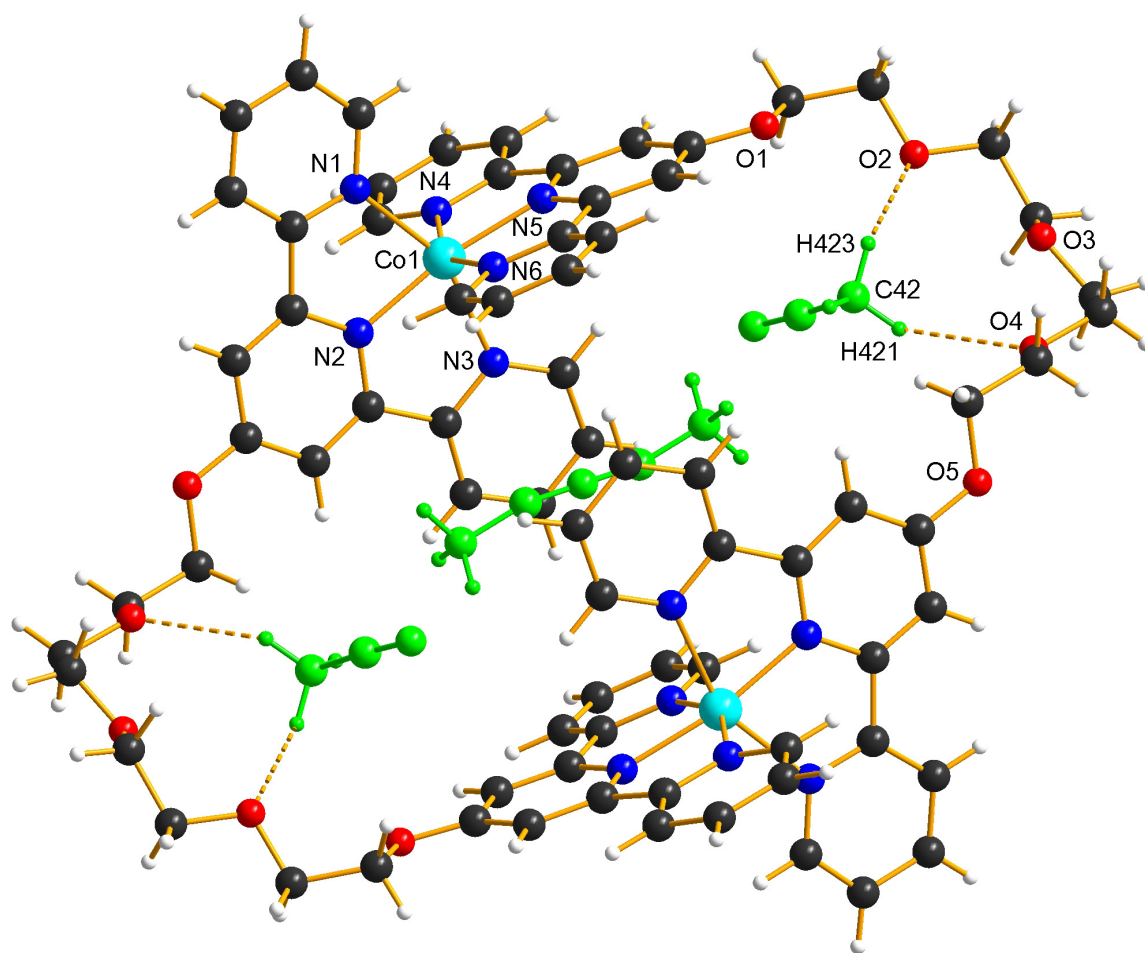


Figure 6.17 Molecular structure of the cation in $[\text{Co}_2(\text{tetra})_2][\text{PF}_6]_4 \cdot 6\text{MeCN}$, showing the acetonitrile molecules (green) in the macrocyclic cavity.

The macrocycles are arranged in one-dimensional chains in which the primary interaction is through C–H···F hydrogen bonds between the pyridyl rings and the anions, as shown in Figure 6.18. The chains then stack together in three dimensions, again mediated by C–H···F hydrogen bonds.

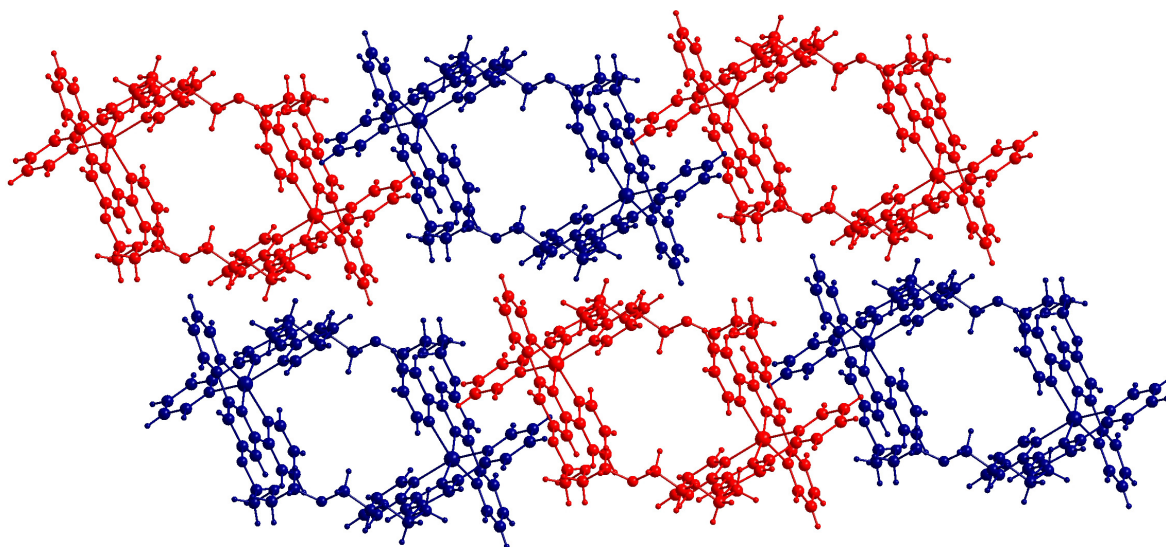


Figure 6.18 Packing of chains of $[\text{Co}_2(\text{tetra})_2]^{4+}$ cations (going into the page) in $[\text{Co}_2(\text{tetra})_2][\text{PF}_6]_4 \cdot 6\text{MeCN}$.

Single crystals of $[\text{Co}_2(\text{tetra})_2][\text{PF}_6]_6 \cdot 10\text{MeCN}$ suitable for X-ray diffraction were obtained by slow diffusion of diethyl ether into an acetonitrile solution of the complex at room temperature and the molecular structure of the cation is shown in Figure 6.19. The crystal structure determination confirms the formation of a [2+2] metallomacrocyclic species, and is consistent with the mass spectrometric data. The cobalt–nitrogen bond lengths are shown in Table 6.3 and are comparable with those in the mononuclear bis(2,2':6',2''-terpyridine)cobalt(III) complexes (see Chapter 3).

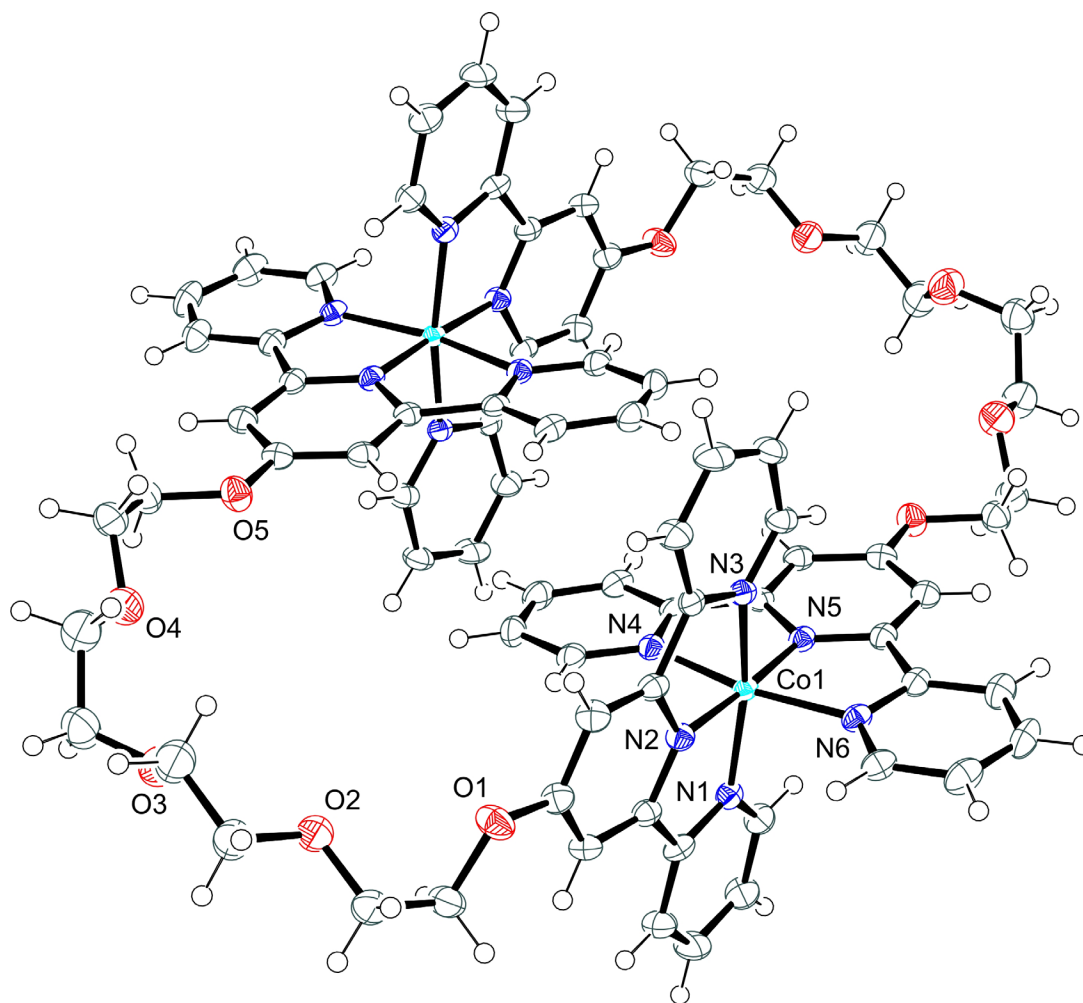


Figure 6.19 Molecular structure of the cation in $[\text{Co}_2(\text{tetra})_2][\text{PF}_6]_6 \cdot 10\text{MeCN}$ with anisotropic displacement ellipsoids drawn at the 50% probability level. Hydrogen atoms are shown as spheres of arbitrary radius.

The metallomacrocyclic is centrosymmetric and the distance between the two cobalt(III) centres is 8.9223(10) Å. Offset face-to-face π - π interactions between the pyridine rings facing each other across the centre of the macrocycle are observed (distance between the planes = 3.3 Å). The macrocycle can accommodate two acetonitrile molecules in each open end of the cavity, with one sitting slightly above and one slightly below the glycol chains. These interact with the glycol chains through weak C-H \cdots O and C-H \cdots N hydrogen bonds (C84ⁱ-H842ⁱ \cdots O3 = 2.50 Å, C82ⁱ-H823ⁱ \cdots O4 = 2.75 Å, C16-H161 \cdots N83ⁱ = 2.52 Å, C19ⁱⁱ-H191ⁱⁱ \cdots N81ⁱ = 2.64 Å; symmetry codes: *i* = 1 - *x*, 1 - *y*, 1 - *z*, *ii* = 2 - *x*, 1 - *y*, 1 - *z*). These interactions are shown in Figure 6.20.

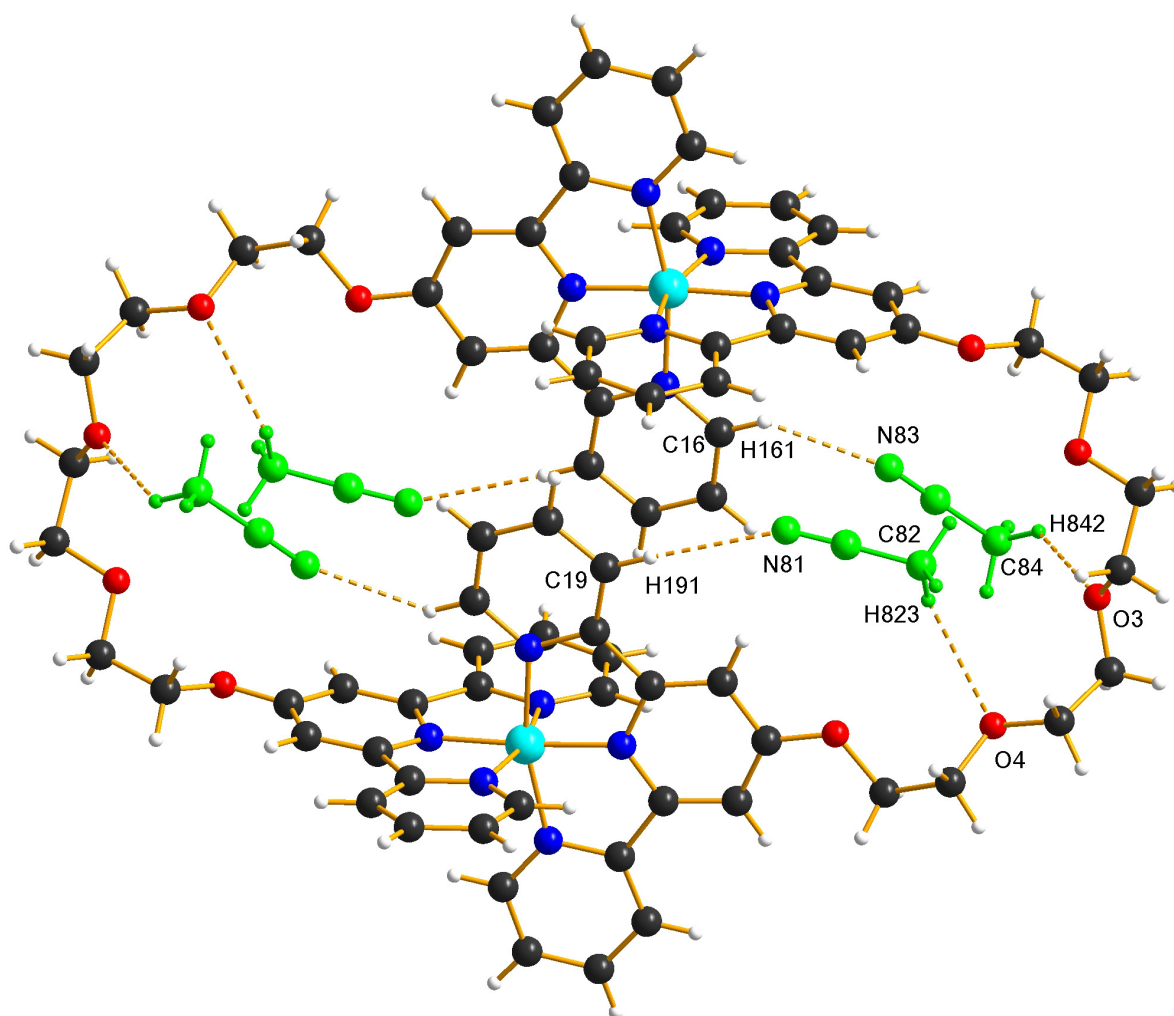


Figure 6.20 Molecular structure of the cation in $[\text{Co}_2(\text{tetra})_2][\text{PF}_6]_6 \cdot 10\text{MeCN}$, showing the acetonitrile molecules (green) in the macrocyclic cavity.

The packing of the macrocycles is again mediated by non-classical $\text{C}-\text{H}\cdots\text{F}$ hydrogen bonds between the cations and the hexafluorophosphate anions, and chains of macrocycles stack together to form the three-dimensional structure shown in Figure 6.21.

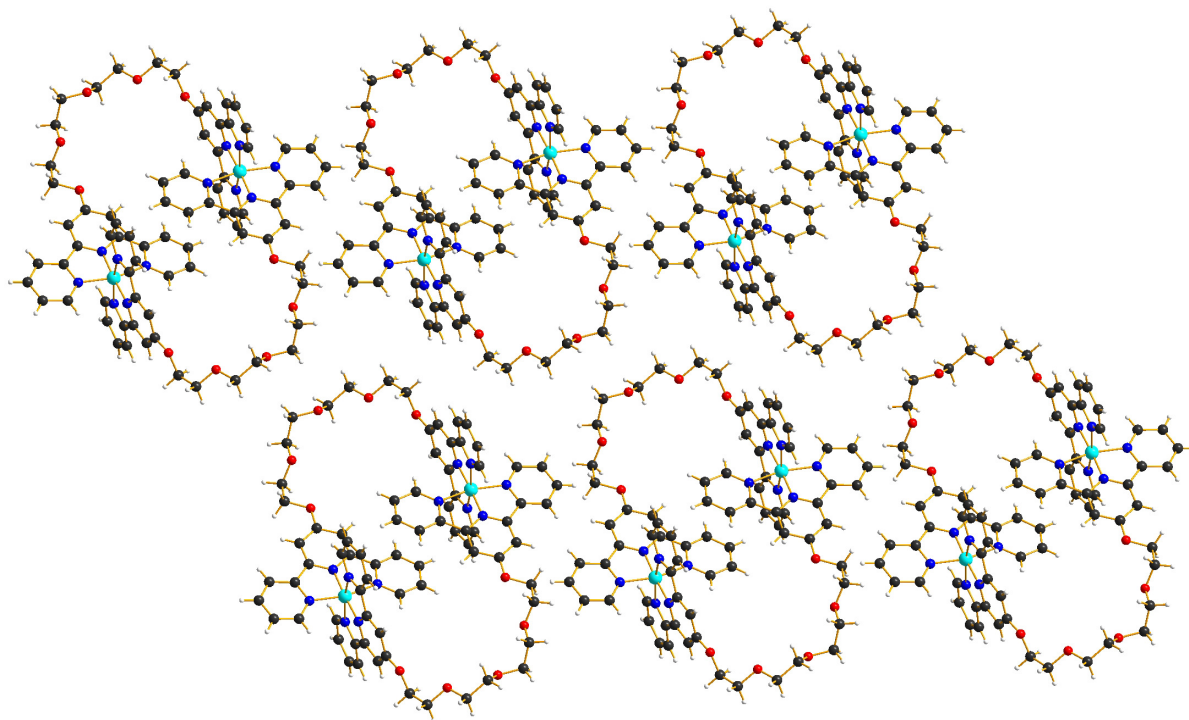


Figure 6.21 Packing of chains of $[\text{Co}_2(\text{tetra})_2]^{6+}$ cations (going into the page) in $[\text{Co}_2(\text{tetra})_2][\text{PF}_6]_6 \cdot 10\text{MeCN}$.

X-ray quality crystals of $[\text{Co}_2(\text{hexa})_2][\text{PF}_6]_5 \cdot 2\text{MeCN}$ were obtained by slow diffusion of diethyl ether into an acetonitrile solution of the bis(terpyridyl)hexa(ethylene glycol)cobalt(II) hexafluorophosphate complex at room temperature and the molecular structure of the cation is shown in Figure 6.22. The formation of a [2+2] metallomacrocyclic species is confirmed, supporting the mass spectrometric data.

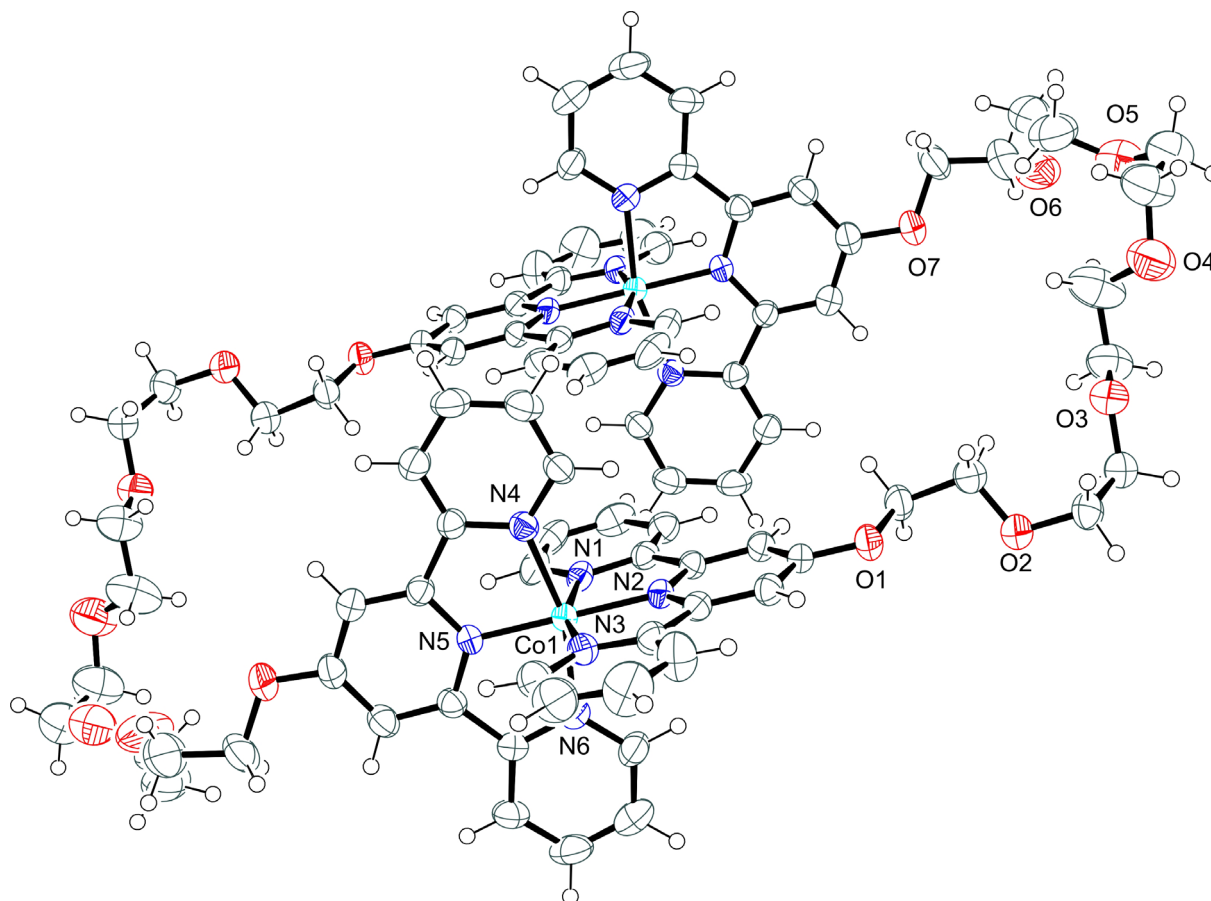


Figure 6.22 Molecular structure of the cation in $[\text{Co}_2(\text{hexa})_2][\text{PF}_6]_5 \cdot 2\text{MeCN}$ with anisotropic displacement ellipsoids drawn at the 50% probability level. The glycol chain is disordered and only one orientation is shown. Hydrogen atoms are shown as spheres of arbitrary radius.

The centre of the metallomacrocycle again lies on an inversion centre, but the unit cell contains one macrocyclic cation and five hexafluorophosphate anions, suggesting that the species has a mixed Co(II/III) oxidation state. Comparison of the cobalt–nitrogen bond lengths in this complex (shown in Table 6.3) with those for the mononuclear bis(2,2':6',2''-terpyridine)cobalt complexes described in Chapter 3 shows that the Co–N bond lengths are at the short end of the range expected for bis(2,2':6',2''-terpyridine)cobalt(II) complexes, but longer than those expected for bis(2,2':6',2''-terpyridine)cobalt(III) complexes. This lends support to the proposed mixed oxidation state complex, but the centre of symmetry means that the cobalt(II) and cobalt(III) centres must be disordered over the two positions in the macrocycle. However, it is also possible that one of the $[\text{PF}_6]^-$ anions is actually a $[\text{SiF}_6]^{2-}$ anion, giving the cation a 6+ charge. This anion could potentially arise from reaction of HF

(formed by decomposition of a hexafluorophosphate anion) with glass. Similarly to $[\text{Co}(\text{EtOtpy})_2][\text{PF}_6]_2 \cdot 2\text{MeCN}$ (see Chapter 3) and a small number of other previously reported cobalt(II) complexes,^{155, 160} one of the terpyridine units in this macrocyclic cation is bound more closely to the cobalt ion than the other ($\text{Co}-\text{N}_{\text{central}} = 1.890(3)$ and $1.867(3)$ Å). This has not previously been reported in bis(2,2':6',2''-terpyridine)cobalt(III) complexes.

The distance between the two cobalt centres is $9.8055(7)$ Å, and the tpy embrace motif^{d61} is observed in the centre of the macrocycle, as shown in Figure 6.23. Each terpyridine unit participates in one edge-to-face π - π interaction ($\text{C3}-\text{H31} \cdots \pi^i = 3.6$ Å; symmetry code: $i = 1 - x, 1 - y, 1 - z$) and the terpyridine units providing the edges for these interactions also participate in one offset face-to-face interaction (distance between the planes = 3.4 Å across the middle of the macrocyclic cavity).

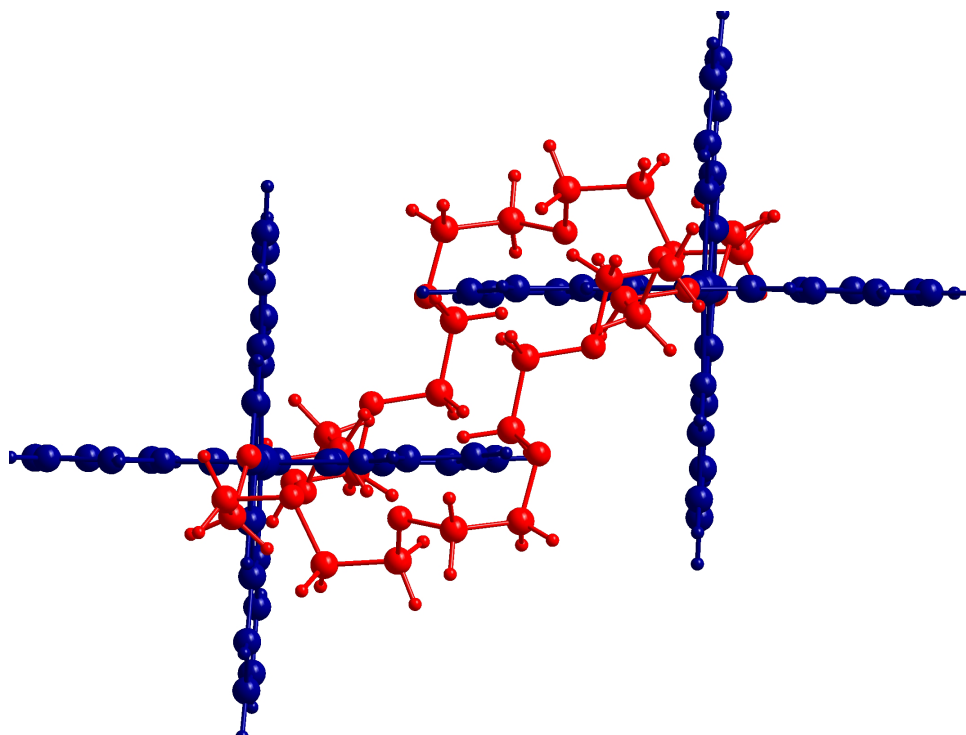


Figure 6.23 Terpy embrace in the middle of the macrocyclic cation in $[\text{Co}_2(\text{hexa})_2][\text{PF}_6]_5 \cdot 2\text{MeCN}$. Terpyridine units are shown in blue, glycol chains in red.

Due to the increased length of the glycol chain, the cavity in this macrocycle is larger than that in the two metallomacrocycles formed with the bis(terpyridyl)tetra(ethylene glycol) chain and can accommodate one hexafluorophosphate anion and one acetonitrile molecule in each open end of the cavity, slightly above or below the glycol chains. The hexafluorophosphate

anion is located towards the bis(2,2':6',2''-terpyridine)cobalt units and interacts with the macrocycle through non-classical C–H···F hydrogen bonds. One-dimensional chains of macrocycles held together by weak C–H···F hydrogen bonds pack together with the same type of interactions to form the three-dimensional structure as shown in Figure 6.24.

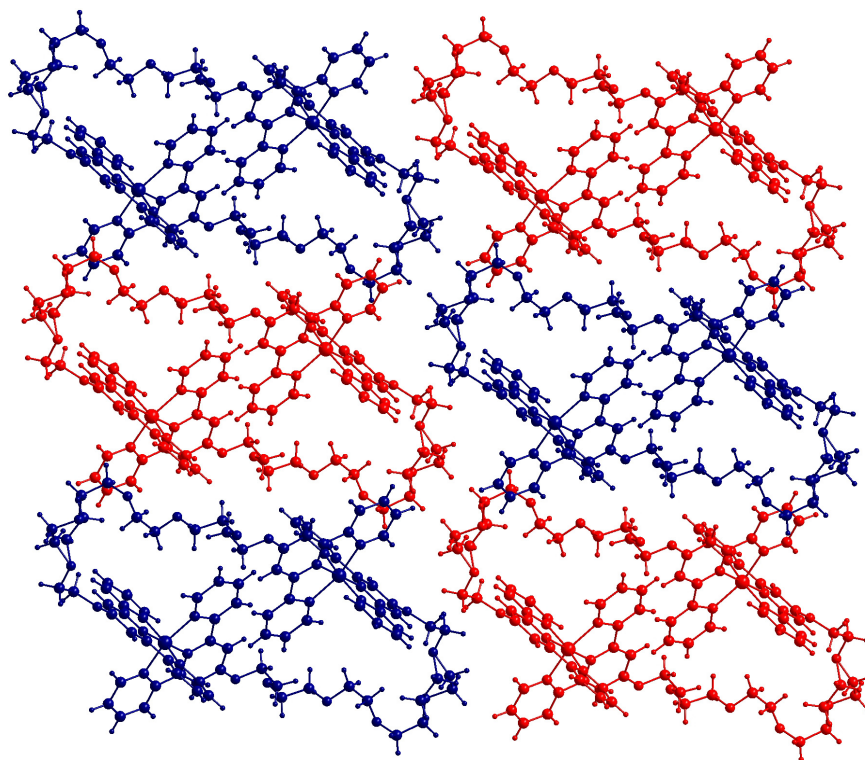


Figure 6.24 Packing of chains of $[\text{Co}_2(\text{hexa})_2]^{5+}$ cations (going into the page) in $[\text{Co}_2(\text{hexa})_2][\text{PF}_6]_5 \cdot 2\text{MeCN}$.

X-ray quality crystals of $[\text{Co}_2(\text{hexa})_2][\text{PF}_6]_6 \cdot 6\text{MeCN}$ were obtained by slow diffusion of *tert*-butyl methyl ether into an acetonitrile solution of the complex at room temperature and the molecular structure of the cation is shown in Figure 6.25. As predicted from the mass spectrometric data, determination of the structure confirms the formation of a [2+2] metallomacrocyclic species. The cobalt–nitrogen bond lengths are shown in Table 6.3 and are typical for bis(2,2':6',2''-terpyridine)cobalt(III) complexes (see Chapter 3).

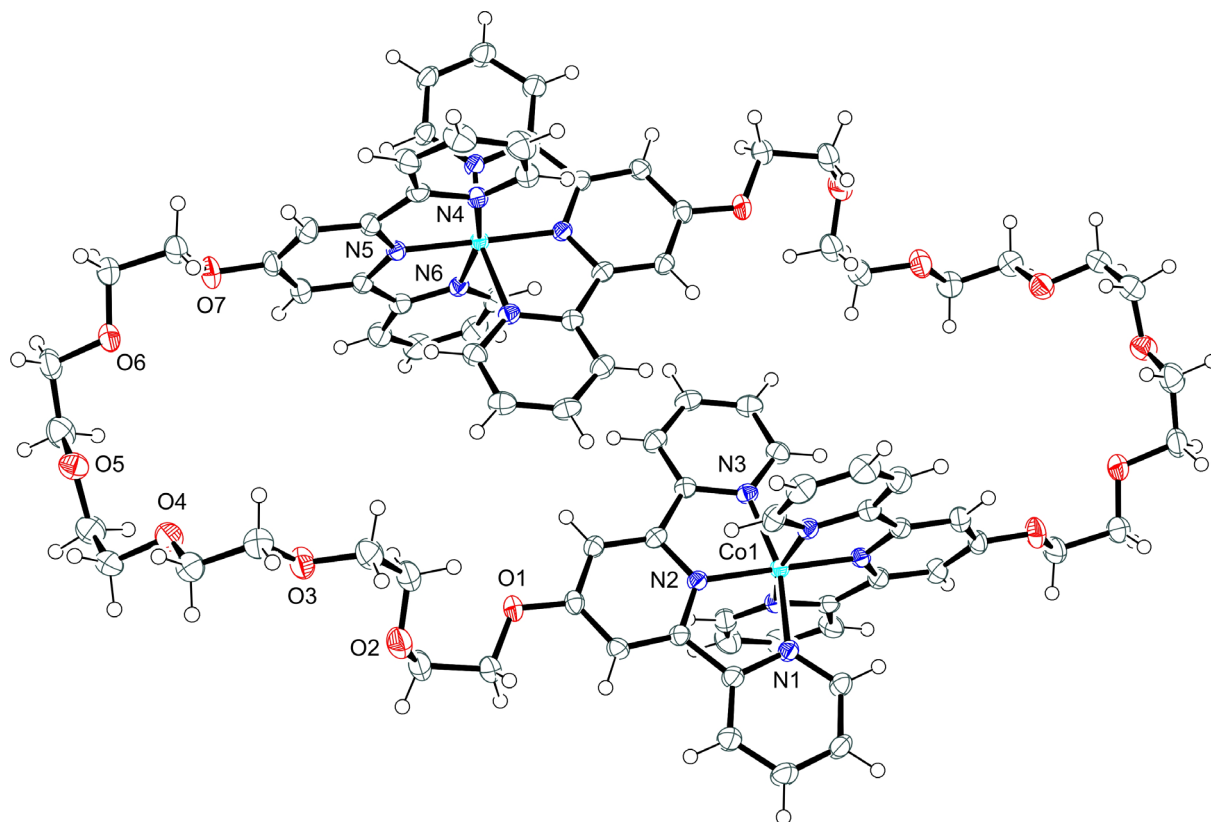


Figure 6.25 Molecular structure of the cation in $[\text{Co}_2(\text{hexa})_2][\text{PF}_6]_6 \cdot 6\text{MeCN}$ with anisotropic displacement ellipsoids drawn at the 50% probability level. Hydrogen atoms are shown as spheres of arbitrary radius.

The centre of the metallomacrocycle lies on an inversion centre as observed for the structures described above. However, this structure has a higher symmetry than the other macrocyclic structures and crystallises in the space group $P2_1/n$. The glycol chains are ordered and the macrocycle has a chair-like conformation. The distance between the two cobalt(III) centres is $9.6858(6)$ Å, but the bis(2,2':6',2'')-terpyridine)cobalt(III) units are offset such that no π - π interactions are observed across the centre of the macrocycle. One acetonitrile molecule is accommodated in each open end of the cavity and interaction with the macrocycle is through non-classical C-H \cdots O and C-H \cdots N hydrogen bonds (C46-H461 \cdots O4 = 2.33 Å, C46-H462 \cdots O6 = 2.84 Å, C15ⁱ-H151ⁱ \cdots N8 = 2.48 Å; symmetry code: $i = 1 - x, 1 - y, 1 - z$), as shown in Figure 6.26. One hexafluorophosphate anion sits above and below each acetonitrile molecule in the cavity, and these interact with the glycol chains and the acetonitrile molecule through weak C-H \cdots F hydrogen bonds.

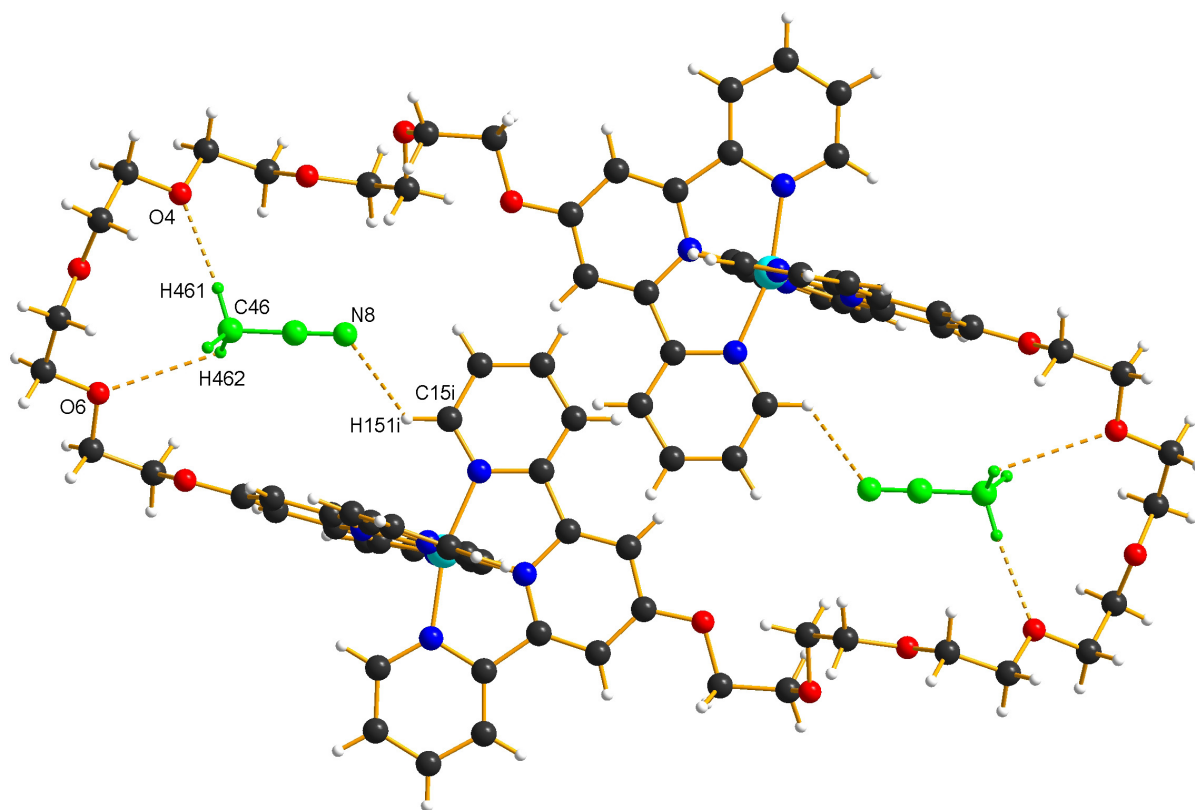


Figure 6.26 Molecular structure of the cation in $[\text{Co}_2(\text{hexa})_2][\text{PF}_6]_6 \cdot 6\text{MeCN}$, showing the acetonitrile molecules (green) in the macrocyclic cavity.

The packing in this structure is again dominated by weak $\text{C-H}\cdots\text{F}$ hydrogen bonds between the cations and the hexafluorophosphate anions. One dimensional chains of macrocyclic cations form two-dimensional layers (shown in different colours in Figure 6.27). Adjacent two-dimensional layers are offset by 90° due to the space group symmetry.

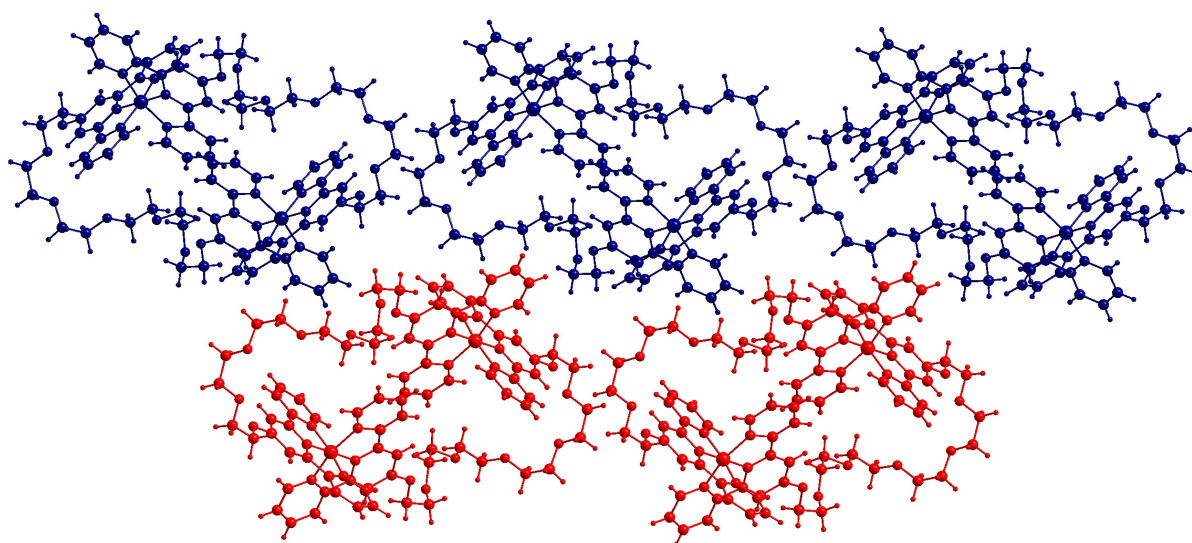


Figure 6.27 Packing of chains of $[\text{Co}_2(\text{hexa})_2]^{6+}$ cations (going into the page) in $[\text{Co}_2(\text{hexa})_2][\text{PF}_6]_6 \cdot 6\text{MeCN}$.

Single crystals of the trinuclear complex, $[\text{Co}_3(\text{tri})_3][\text{PF}_6]_9 \cdot 2\text{MeCN} \cdot 0.5\text{MeOH} \cdot 2.75\text{H}_2\text{O}$, were obtained by slow diffusion at room temperature of diethyl ether into an acetonitrile solution of an oxidised equilibrium mixture with a high proportion of one species, and the molecular structure of the cation is shown in Figure 6.28. The electrospray mass spectrum of a solution of the product used to obtain these crystals showed exclusively signals corresponding to a [3+3] species. Other samples, however, suggest the presence of both [2+2] and [3+3] metallomacrocycles, although the ^1H NMR spectra contain signals corresponding to a significantly higher number of compounds. The cobalt–nitrogen bond lengths are listed in Table 6.3 and are slightly higher than expected based on the bond lengths in mononuclear bis(2,2':6',2''-terpyridine)cobalt(III) complexes (see Chapter 3).

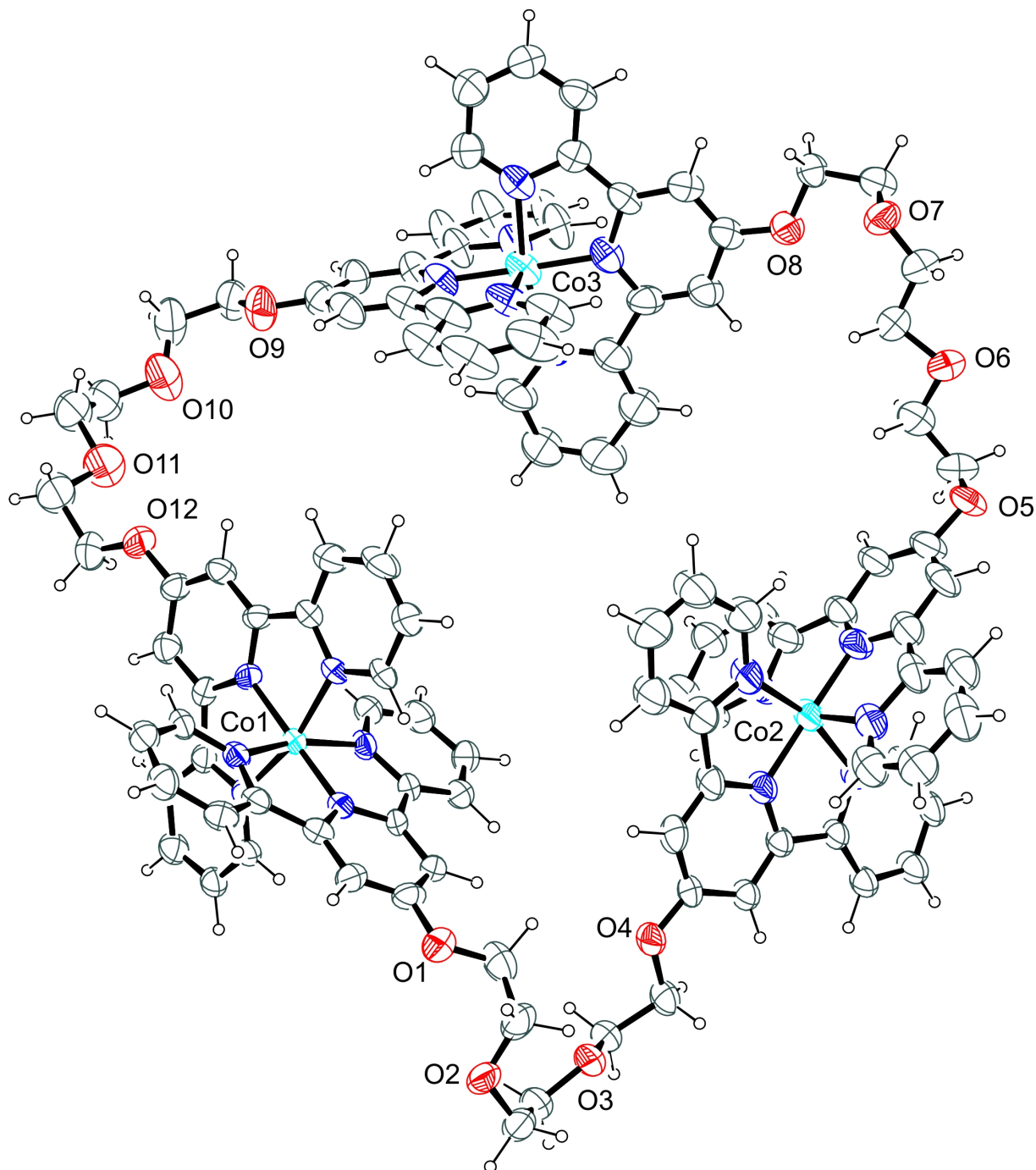


Figure 6.28 Molecular structure of the cation in $[\text{Co}_3(\text{tri})_3][\text{PF}_6]_9 \cdot 2\text{MeCN} \cdot 0.5\text{MeOH} \cdot 2.75\text{H}_2\text{O}$ with anisotropic displacement ellipsoids drawn at the 30% probability level. Two of the glycol chains are disordered and only one orientation is shown. Hydrogen atoms are shown as spheres of arbitrary radius.

The three cobalt atoms are approximately arranged in an isosceles triangle with cobalt–cobalt distances of 10.9768(19) Å (Co1–Co2), 12.1866(15) Å (Co1–Co3) and 12.145(3) Å (Co2–Co3). The arrangement of the glycol chains is such that the macrocyclic cation also

resembles a triangle. The cavity is filled with several hexafluorophosphate anions and solvent molecules, and the interactions between these and the macrocyclic cation are again via non-classical C–H···O, C–H···F and C–H···N hydrogen bonds.

The two cations in the unit cell are related by an inversion centre and pairs of macrocycles form one-dimensional chains held together by weak C–H···F hydrogen bonds. The chains also interact via weak C–H···F hydrogen bonds to form the three-dimensional structure (Figure 6.29).

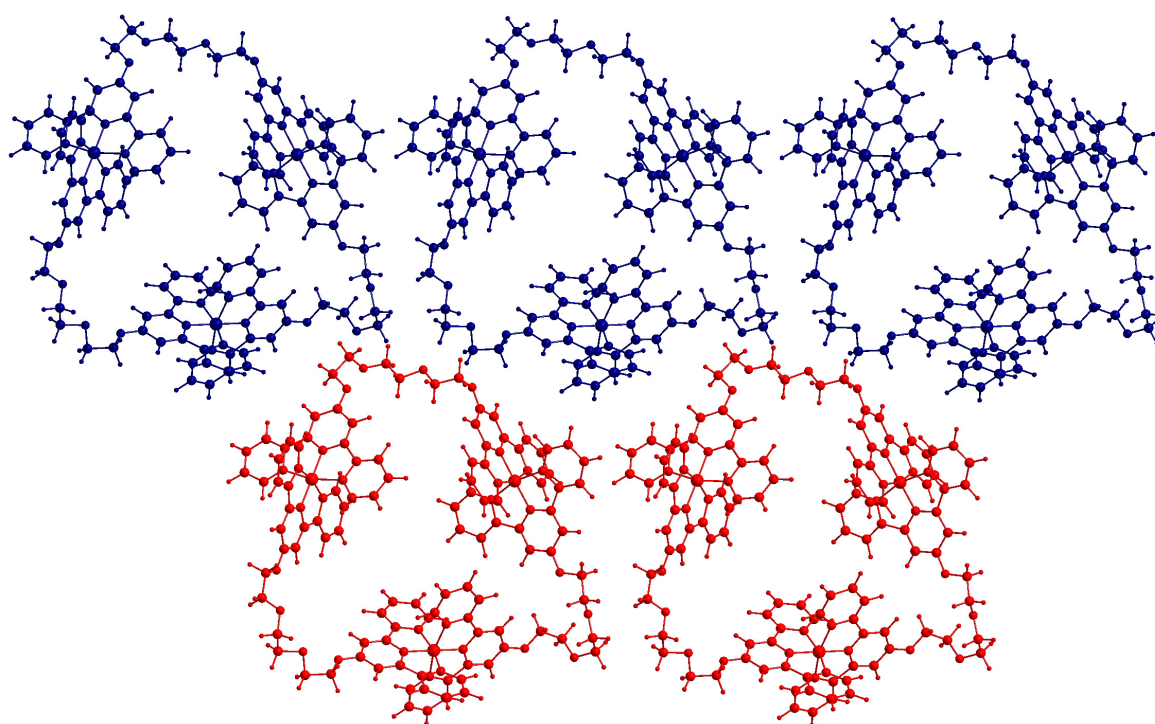


Figure 6.29 Packing of chains of $[\text{Co}_3(\text{tri})_3]^{9+}$ cations (going into the page) in $[\text{Co}_3(\text{tri})_3][\text{PF}_6]_9 \cdot 2\text{MeCN} \cdot 0.5\text{MeOH} \cdot 2.75\text{H}_2\text{O}$. Only one of the symmetry related macrocycles in the chains is shown.

6.5 Measurement of diffusion coefficients with PGSE NMR spectroscopy

6.5.1 Equilibrium mixtures

PGSE NMR spectroscopy has been shown to be useful in determining the sizes of mononuclear bis(2,2':6',2''-terpyridine)cobalt(III) complexes in solution (Chapter 3).

Comparison of experimental diffusion coefficients with diffusion coefficients determined using the modified Stokes-Einstein equation (see Chapter 2) from radii derived from several different models based on X-ray data showed that the best fit to the measured diffusion coefficients was provided by a spherical model with a radius of half the longest distance across the molecule.

PGSE NMR spectroscopy was consequently used to measure the diffusion coefficients of the species present in mixtures of bis(terpyridyl)oligo(ethylene glycol)cobalt(III) hexafluorophosphate complexes in DMSO-d₆ solution at concentrations of 8 mg mL⁻¹. Equilibrated samples of mixtures of cobalt(II) hexafluorophosphate complexes of the four bis(terpyridyl)oligo(ethylene glycol)s were oxidised with bromine and collected as the hexafluorophosphate salts. With the ligands bis(terpyridyl)tri(ethylene glycol), bis(terpyridyl)tetra(ethylene glycol) and bis(terpyridyl)hexa(ethylene glycol) the ¹H NMR spectra contain mostly one major species and several minor species with similar chemical shifts. However, the ¹H NMR spectrum of bis(terpyridyl)di(ethylene glycol)cobalt(III) hexafluorophosphate contains at least three species in significant amounts. No further purification of the mixtures was attempted before the diffusion NMR measurements were carried out. Diffusion coefficients were measured only for well-separated signals without systematic errors corresponding to the terpyridine protons of the major species and the average values over 3 experiments using different values for Δ and δ were taken. The viscosity of the solution was determined by the method described by Zuccaccia *et al.*¹¹⁹ The solvent viscosity (for DMSO-d₆ = 2.195 × 10⁻³ kg s⁻¹ m⁻¹)¹⁶⁶ was multiplied by a correction factor equal to the ratio of the diffusion coefficients of the residual solvent signal in the pure solvent and in the solution. The solution viscosity, averaged diffusion coefficients for the major species present in the mixtures and the signals in the ¹H NMR spectrum used for the analysis are shown in Table 6.4. DOSY-type plots for the four mixtures are shown in Figure 6.30.

Complex	$\eta_{solution}$ / $10^{-3} \text{ kg s}^{-1} \text{ m}^{-1}$	$D_{measured}$ / $10^{-10} \text{ m}^2 \text{ s}^{-1}$	Signals used / ppm
[Co _n (di) _n][PF ₆] _{3n} (eq)	2.27	0.40±0.01 ^a	8.38 (H ⁴), 7.53 (H ⁵)
		0.62±0.02	8.30 (H ⁴), 7.46 (H ⁵)
		0.75±0.02	8.17 (H ⁴), 7.41 (H ⁵)
[Co _n (tri) _n][PF ₆] _{3n} (eq)	2.26	0.69±0.02	8.92 (H ³), 8.90 (H ³), 8.26 (H ⁴), 7.42 (H ⁵)
[Co _n (tetra) _n][PF ₆] _{3n} (eq)	2.27	0.88±0.03	8.81 (H ³), 8.80 (H ³), 7.83 (H ⁴), 7.48 (H ⁶), 7.23 (H ⁵)
[Co _n (hexa) _n][PF ₆] _{3n} (eq)	2.25	0.88±0.03	9.11 (H ³), 8.94 (H ³), 8.26 (H ⁴), 7.54 (H ⁶), 7.39 (H ⁵)

Table 6.4 Measured solution viscosities and diffusion coefficients, and signals used for the analysis of the major species in equilibrium mixtures of cobalt(III) complexes of bis(terpyridyl)oligo(ethylene glycol)s. Experimental error is *ca.* ±3%. (a = this diffusion coefficient does not correspond to a single species, but was included as it is a significant component of the mixture).

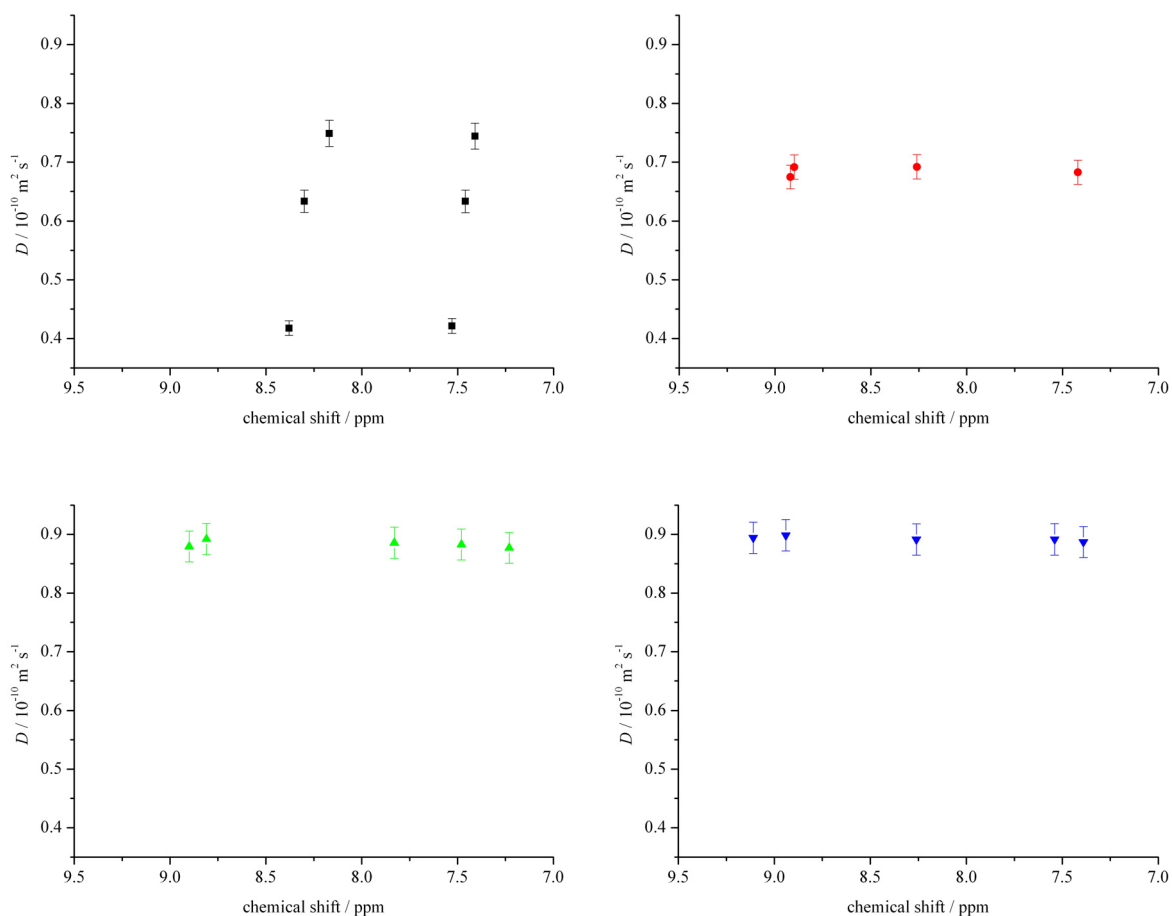


Figure 6.30 ^1H DOSY-type plots of oxidised equilibrium mixtures of $[\text{Co}_n(\text{di})_n][\text{PF}_6]_{3n}$ (black; $\Delta = 65.8$ ms, $\delta = 10.0$ ms), $[\text{Co}_n(\text{tri})_n][\text{PF}_6]_{3n}$ (red; $\Delta = 48.8$ ms, $\delta = 11.0$ ms), $[\text{Co}_n(\text{tetra})_n][\text{PF}_6]_{3n}$ (green; $\Delta = 48.8$ ms, $\delta = 9.0$ ms) and $[\text{Co}_n(\text{hexa})_n][\text{PF}_6]_{3n}$ (blue; $\Delta = 52.8$ ms, $\delta = 9.0$ ms) (500 MHz, DMSO-d_6 , 295 K).

6.5.1.1 Models of the macrocyclic complexes

The solid state structures of three of the bis(terpyridyl)oligo(ethylene glycol)cobalt(III) complexes, $[\text{Co}_3(\text{tri})_3][\text{PF}_6]_9 \cdot 2\text{MeCN} \cdot 0.5\text{MeOH} \cdot 2.75\text{H}_2\text{O}$, $[\text{Co}_2(\text{tetra})_2][\text{PF}_6]_6 \cdot 10\text{MeCN}$ and $[\text{Co}_2(\text{hexa})_2][\text{PF}_6]_6 \cdot 6\text{MeCN}$, have been determined by X-ray crystallography (see section 6.4), and were used as models to establish whether the PGSE NMR technique could be applied to determine the sizes of multinuclear macrocyclic complexes in solution. For each structure, two models were considered in order to calculate a diffusion coefficient for the macrocyclic cation. Firstly, the cations were assumed to be spherical with a radius of half the longest distance across the molecule as this was found to be the best model for the mononuclear

bis(2,2':6',2''-terpyridine)cobalt(III) complexes (see Chapter 3). From the results in Chapter 3, it was concluded that small, non-spherical molecules may be treated as spheres due to their rapid molecular motion in solution as suggested by Chen for disc-like crown ethers,¹⁰⁹ however, for larger molecules this assumption may not be correct. Secondly, the cations were considered to be ellipsoidal, with the $[\text{Co}_3(\text{tri})_3]^{9+}$ cation resembling an oblate (disc-like) ellipsoid (see Figure 2.3) and the $[\text{Co}_2(\text{tetra})_2]^{6+}$ and $[\text{Co}_2(\text{hexa})_2]^{6+}$ cations a prolate (rugby ball shaped) ellipsoid. In addition, a second spherical model was considered for the calculation of a diffusion coefficient for $[\text{Co}_2(\text{tetra})_2]^{6+}$ and $[\text{Co}_2(\text{hexa})_2]^{6+}$, in which the radius of the cation was determined from its Connolly solvent excluded volume (calculated from the crystal structure data using ChemBio3D Ultra (see equation 3.1)). As this model proved to be unsuitable (see below) and as the volume of the $[\text{Co}_3(\text{tri})_3]^{9+}$ cation could not be calculated easily using ChemBio3D Ultra, this model was not considered further.

The radii, r , of the spherical models and the calculated radii, r_e , of the ellipsoid models (see Table 2.3) are shown in Table 6.5. The length, 2α , of the major axis of the prolate ellipsoid is considered to be equal to the longest distance across the macrocycle in the crystal structure. The minor axis of length 2β is the longest distance perpendicular to the distance, 2α . For the oblate ellipsoid, the major axis has a length, 2α , again equal to the longest distance across the macrocycle. The minor axis, 2β , is the longest distance between the H^+ protons on two 2,2':6',2''-terpyridine units coordinated to the same cobalt ion, perpendicular to 2α .

Complex	$V / \text{\AA}^3$	$2\alpha / \text{\AA}$	$2\beta / \text{\AA}$	$r_{\text{volume}} / \text{\AA}$	$r_{\text{longest}} / \text{\AA}$	$r_e, \text{ellipsoid} / \text{\AA}$
$[\text{Co}_n(\text{tri})_n][\text{PF}_6]_{3n}$ (eq)	-- ^a	24.90	8.63	-- ^a	12.45	8.74 ^b
$[\text{Co}_n(\text{tetra})_n][\text{PF}_6]_{3n}$ (eq)	1087	21.77	19.10	6.38	10.91	9.97 ^c
$[\text{Co}_n(\text{hexa})_n][\text{PF}_6]_{3n}$ (eq)	1247	26.12	19.29	6.68	13.06	10.64 ^c

Table 6.5 Calculated volumes and radii for models of the macrocyclic complexes (a = volume not calculated, b = oblate ellipsoid model, c = prolate ellipsoid model).

Values for the two corrections to the Stokes-Einstein equation required when considering non-spherical particles of molecular size, f/f_0 , for the shape of the molecule (see Table 2.3),

and c , taking into account the size of the molecule (see Equation 2.10), are listed in Table 6.6. As described in Chapter 3, the radius of a DMSO molecule was calculated to be 2.50 Å.

Complex	f/f_0 , ellipsoid	C_{volume}	$C_{longest}$	$C_{ellipsoid}$
[Co _n (tri) _n][PF ₆] _{3n} (eq)	1.11 ^b	-- ^a	0.981	0.959 ^b
[Co _n (tetra) _n][PF ₆] _{3n} (eq)	1.00 ^c	0.921	0.975	0.969 ^c
[Co _n (hexa) _n][PF ₆] _{3n} (eq)	1.01 ^c	0.928	0.983	0.973 ^c

Table 6.6 Correction factors for models of the macrocyclic complexes (a = volume not calculated, b = oblate ellipsoid model, c = prolate ellipsoid model).

Finally, the calculated radii and correction factors for each model were substituted into the modified Stokes-Einstein equation (equation 2.11), to calculate a diffusion coefficient, D , for each model for comparison with the measured values. The measured and calculated diffusion coefficients are shown in Table 6.7. A comparison of the calculated and measured diffusion coefficients is given graphically in Figure 6.31.

Complex	$D_{measured}$ / $10^{-10} \text{ m}^2 \text{ s}^{-1}$	D_{volume} / $10^{-10} \text{ m}^2 \text{ s}^{-1}$	$D_{longest}$ / $10^{-10} \text{ m}^2 \text{ s}^{-1}$	$D_{ellipsoid}$ / $10^{-10} \text{ m}^2 \text{ s}^{-1}$
[Co _n (tri) _n][PF ₆] _{3n} (eq)	0.69±0.02	-- ^a	0.78	1.02 ^b
[Co _n (tetra) _n][PF ₆] _{3n} (eq)	0.88±0.03	1.62	0.89	0.98 ^c
[Co _n (hexa) _n][PF ₆] _{3n} (eq)	0.88±0.03	1.56	0.75	0.92 ^c

Table 6.7 Measured (500 MHz, DMSO-d₆, 295 K) and calculated diffusion coefficients for the macrocyclic complexes (a = volume not calculated, b = oblate ellipsoid model, c = prolate ellipsoid model).

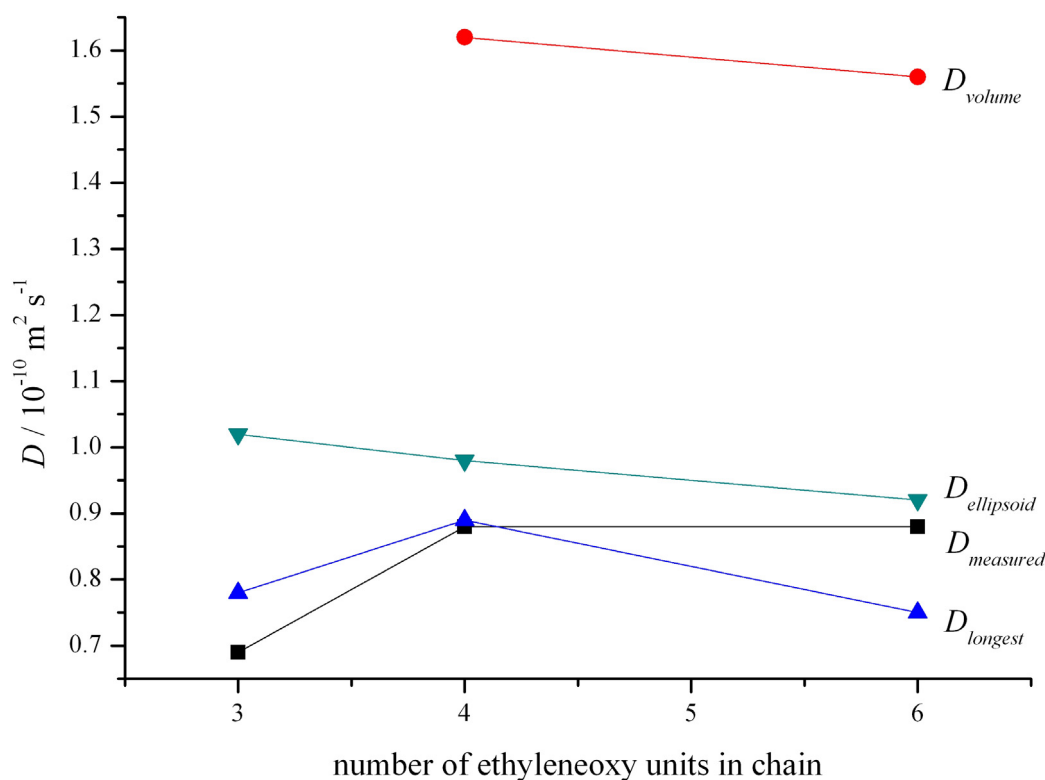


Figure 6.31 Graph of measured and calculated diffusion coefficients for models of the macrocyclic cations.

From the data in Table 6.7, represented graphically in Figure 6.31, it is clear that the calculated diffusion coefficient based on the volume of the cation is an inappropriate model for these systems. The ellipsoid model and the spherical model with the radius equal to half the longest distance across the molecule both give calculated diffusion coefficients with reasonably good agreement with the measured values. The measured diffusion coefficients for the bis(terpyridyl)tetra(ethylene glycol) and bis(terpyridyl)hexa(ethylene glycol) species are the same, although using both models, the bis(terpyridyl)hexa(ethylene glycol) species is expected to have a smaller diffusion coefficient due to its larger size in the solid state. The long flexible glycol chains in this cation can exist in many different conformations and in solution may be unlikely to adopt the extended conformation in the crystal structure, making the molecule appear smaller than expected. The shorter ethyleneoxy chains in the bis(terpyridyl)tetra(ethylene glycol) species are expected to be less flexible, and the solution structure should resemble more closely the structure found in the solid state. The spherical model based on the longest radius of the molecule was chosen the most appropriate model due to the excellent agreement between the calculated and measured diffusion coefficients

with the bis(terpyridyl)tetra(ethylene glycol) species. This model also gave the best agreement for the shorter chain (and therefore less flexible) bis(terpyridyl)tri(ethylene glycol) species. It can therefore be concluded that these molecules are not too large to be considered as spheres due to their rapid rotation in solution.

The spherical model based on the longest radius of the molecule was then used to determine the sizes, and to potentially identify the species present in the mixture of bis(terpyridyl)di(ethylene glycol)cobalt(III) hexafluorophosphate complexes, which showed two species with measured diffusion coefficients of $0.62 \pm 0.02 \times 10^{-10}$ and $0.75 \pm 0.02 \times 10^{-10} \text{ m}^2 \text{ s}^{-1}$. A diffusion coefficient of $0.40 \pm 0.01 \times 10^{-10} \text{ m}^2 \text{ s}^{-1}$ was determined for a third set of signals in the ^1H NMR spectrum, although the systematic errors in the data suggest that these signals do not belong to a single species, but are rather several overlapping signals. However, the smaller diffusion coefficient implies that these species are larger than the two species in the mixture with well separated signals in the ^1H NMR spectrum.

Rearrangement of the modified Stokes-Einstein equation (equation 2.11) gives equation 6.1:

$$rc = \frac{kT}{6\pi\eta D}$$

6.1

where r is the radius of the model sphere, c is the correction factor for the size of the diffusing particle (see equation 2.10), k is the Boltzmann constant, T is the absolute temperature, η is the viscosity of the solution and D is the diffusion coefficient. Consideration of a spherical model allows the correction for the shape of the particle (f/f_0) to be disregarded. The values of rc were calculated for each measured diffusion coefficient and are given in Table 6.8. For systems of this size, the value of the size correction factor, c , is between 0.98 and 1, and the radius is therefore very close to the value of rc .

$D_{measured} / 10^{-10} \text{ m}^2 \text{ s}^{-1}$	$rc / \text{Å}$	Assignment
0.40 ± 0.01^a	24 ± 1	mixed
0.62 ± 0.02	15.5 ± 0.5	$[\text{Co}_4(\text{di})_4]^{12+}$
0.75 ± 0.02	12.8 ± 0.4	$[\text{Co}_3(\text{di})_3]^{9+}$

Table 6.8 Measured diffusion coefficients (500 MHz, DMSO- d_6 , 295 K) and calculated radii based on a spherical model for the species present in a mixture of bis(terpyridyl)di(ethylene glycol)cobalt(III) hexafluorophosphate complexes. (a = this diffusion coefficient does not correspond to a single species, but was included as it is a significant component of the mixture).

As mentioned above, the systematic errors in the data corresponding to the smallest diffusion coefficient suggest that these signals belong to several species and the measured diffusion coefficient is a weighted average over all the species present. The fact that the measured diffusion coefficient of the mixed species is smaller than those of the two single species suggests that the unresolved signal corresponds to several larger species. Molecular modelling of several macrocycles of different nuclearities (MMFF-level SPARTAN¹⁶⁷ calculations) was carried out in an attempt to identify the two resolved species present in the mixture. The longest distances across $[\text{Co}_4(\text{di})_4]^{12+}$ and $[\text{Co}_3(\text{di})_3]^{9+}$ macrocycles were measured as 30 and 25 Å, respectively, corresponding to longest radii of 15 and 12.5 Å. The radii obtained are only approximate due to the low level of the calculations used. However, the agreement with the radii calculated from the measured diffusion coefficients is outstanding. The assignment of these signals to $[\text{Co}_4(\text{di})_4]^{12+}$ and $[\text{Co}_3(\text{di})_3]^{9+}$ macrocycles is also supported by the electrospray mass spectrometric data for the mixture of cobalt(II) complexes with this ligand.

6.5.2 Initial mixtures

After successfully applying the PGSE NMR technique to determine the sizes of macrocyclic species in equilibrium mixtures of bis(terpyridyl)oligo(ethylene glycol)cobalt(III) hexafluorophosphate complexes, the analysis of the initial mixtures of these complexes was also considered.

PGSE NMR spectroscopy was used to measure the diffusion coefficients of the species present in initial mixtures of bis(terpyridyl)oligo(ethylene glycol)cobalt(III)

hexafluorophosphate complexes in DMSO-d₆ solution at concentrations of 8 mg mL⁻¹. Samples of initial mixtures of cobalt(II) hexafluorophosphate complexes of the four bis(terpyridyl)oligo(ethylene glycol)s were oxidised with bromine and collected as the hexafluorophosphate salts. All of the ¹H NMR spectra showed broadened peaks suggesting the overlap of signals corresponding to several different species. No further purification of the mixtures was attempted before the diffusion NMR measurements were carried out. Diffusion coefficients were measured for each broad signal corresponding to the 2,2':6',2"-terpyridine unit and the average values over 3 experiments using different values for Δ and δ were taken. All signals displayed systematic errors, confirming that they do not correspond to a single species. The viscosity of the solution was determined by the method described by Zuccaccia *et al.*¹¹⁹ described above. The solution viscosity, averaged diffusion coefficients and signals used for the analysis are shown in Table 6.9. DOSY-type plots for the four complexes are shown in Figure 6.32.

Complex	$\eta_{solution}$ / 10 ⁻³ kg s ⁻¹ m ⁻¹	$D_{measured}$ / 10 ⁻¹⁰ m ² s ⁻¹	Signals used / ppm
[Co _n (di) _n][PF ₆] _{3n} (i)	2.27	0.32±0.01 ^a	9.25 (H ³), 9.14 (H ³), 8.38 (H ⁴), 7.66 (H ⁶), 7.53 (H ⁵)
[Co _n (tri) _n][PF ₆] _{3n} (i)	2.26	0.35±0.01 ^a	9.08 (H ³), 8.37 (H ⁴), 7.63 (H ⁶), 7.52 (H ⁵)
[Co _n (tetra) _n][PF ₆] _{3n} (i)	2.27	0.19±0.01 ^a	9.13 (H ³), 8.99 (H ³), 8.37 (H ⁴), 7.58 (H ⁶), 7.51 (H ⁵)
[Co _n (hexa) _n][PF ₆] _{3n} (i)	2.26	0.38±0.01 ^a	9.13 (H ³), 8.99 (H ³), 8.36 (H ⁴), 7.58 (H ⁶), 7.50 (H ⁵)

Table 6.9 Measured solution viscosity and diffusion coefficients (500 MHz, DMSO-d₆, 295 K), and signals used for the analysis of the major species in initial mixtures of cobalt(III) complexes of bis(terpyridyl)oligo(ethylene glycol)s. Experimental error is *ca.* ±3%. (a = this diffusion coefficient does not correspond to a single species).

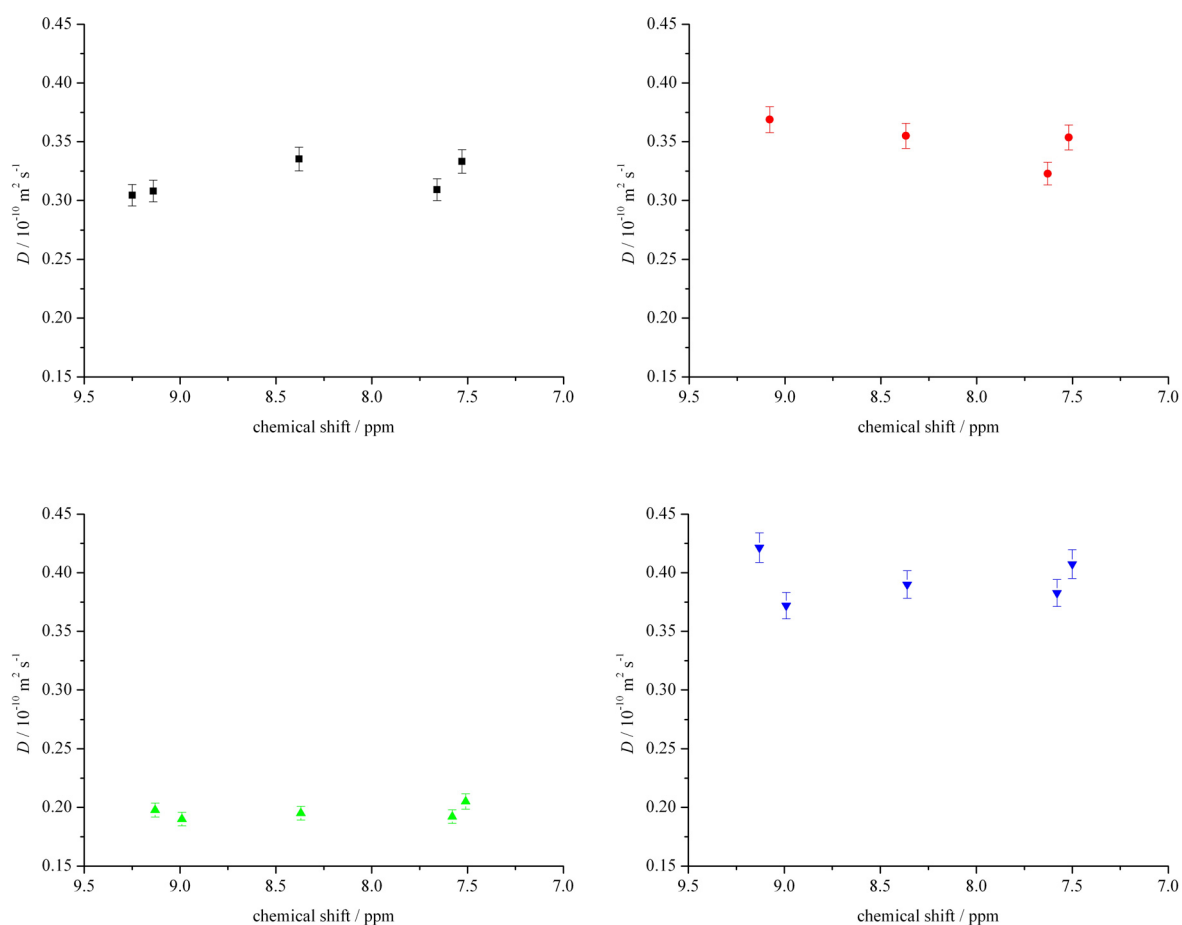


Figure 6.32 ^1H DOSY-type plots of oxidised initial mixtures of $[\text{Co}_n(\text{di})_n][\text{PF}_6]_{3n}$ (black; $\Delta = 80.8$ ms, $\delta = 12.0$ ms), $[\text{Co}_n(\text{tri})_n][\text{PF}_6]_{3n}$ (red; $\Delta = 67.8$ ms, $\delta = 12.0$ ms), $[\text{Co}_n(\text{tetra})_n][\text{PF}_6]_{3n}$ (green; $\Delta = 98.8$ ms, $\delta = 14.0$ ms) and $[\text{Co}_n(\text{hexa})_n][\text{PF}_6]_{3n}$ (blue; $\Delta = 79.8$ ms, $\delta = 11.0$ ms) (500 MHz, DMSO-d_6 , 295 K).

The measured diffusion coefficients can be converted to radii using equation 6.1 and the values of rc are given in Table 6.10. Again, the value of c , the correction factor for the size of the diffusing particle, is close to one, so the values of rc are very close to the calculated radii.

Complex	$D_{measured} / 10^{-10} \text{ m}^2 \text{ s}^{-1}$	$rc / \text{Å}$
$[\text{Co}_n(\text{di})_n][\text{PF}_6]_{3n} \text{ (i)}$	0.32 ± 0.01^a	30 ± 1
$[\text{Co}_n(\text{tri})_n][\text{PF}_6]_{3n} \text{ (i)}$	0.35 ± 0.01^a	28 ± 1
$[\text{Co}_n(\text{tetra})_n][\text{PF}_6]_{3n} \text{ (i)}$	0.19 ± 0.01^a	51 ± 3
$[\text{Co}_n(\text{hexa})_n][\text{PF}_6]_{3n} \text{ (i)}$	0.38 ± 0.01^a	25 ± 1

Table 6.10 Measured diffusion coefficients (500 MHz, DMSO- d_6 , 295 K) and calculated radii based on a spherical model for the species present in initial mixtures of cobalt(III) complexes of bis(terpyridyl)oligo(ethylene glycol)s. Experimental error is *ca.* $\pm 3\%$. (a = this diffusion coefficient does not correspond to a single species).

The systematic errors on the data used for the analysis of these oxidised initial product mixtures suggest that the spectra contain several overlapping sets of signals and the measured diffusion coefficients are therefore a weighted average over all the species present. As described in section 6.2, the exact compositions of the product mixtures from the reaction of bis(terpyridyl)oligo(ethylene glycol) ligands with cobalt(II) salts (and hence the oxidised product mixtures) are not reliably reproducible, with the mixtures containing the same species but with different relative proportions. As a result, the measured diffusion coefficients cannot be compared with each other. However, it is clear that the species present in the initial mixtures have significantly smaller diffusion coefficients than the single species present in the equilibrated mixtures, lending support to the hypothesis that large species (whether polymers or large macrocycles) form first and rearrange to smaller macrocycles over time.

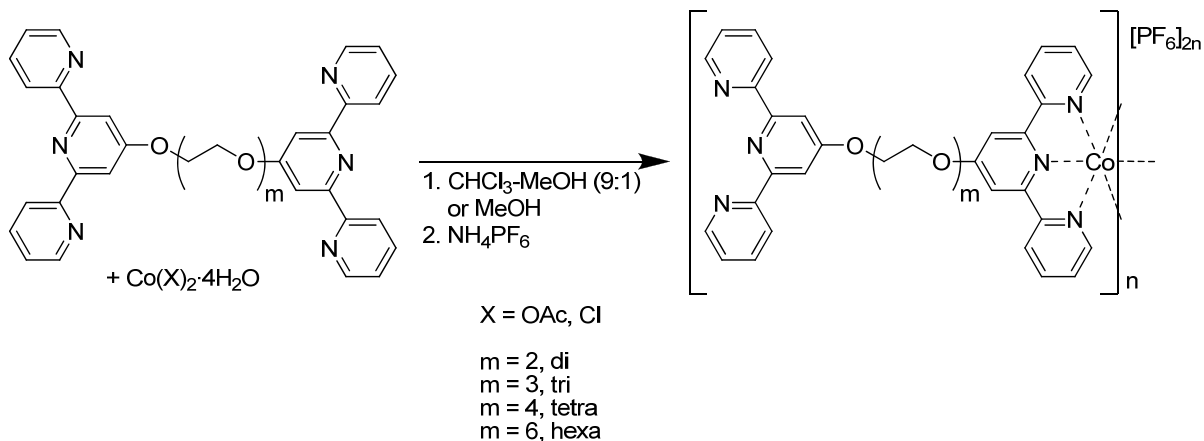
6.6 Conclusions

The reactions of four bis(terpyridyl)oligo(ethylene glycol) ligands with cobalt(II) salts were studied in detail. Preliminary studies on the reactions with cobalt(II) acetate tetrahydrate in a chloroform-methanol solvent mixture (9:1) showed that one major species was formed during the initial reaction, but on redissolving the hexafluorophosphate salt of the product in acetonitrile, re-equilibration of the mixture occurred and several new species were formed. These were proposed to be metallomacrocylic species based on ^1H NMR spectroscopic and mass spectrometric data. A systematic study of the effect of the anion, solvent mixture and concentration on the equilibrium between polymeric and macrocyclic species in the

bis(terpyridyl)tetra(ethylene glycol) system was performed. All three variables were found to have a significant influence on the composition of the equilibrium mixture. In addition, use of a weakly-coordinating tetrafluoroborate anion in place of chloride or acetate increased the time required to reach equilibrium. All initial and equilibrium mixtures could be oxidised to the corresponding cobalt(III) species in order to "freeze" the equilibrium at a specific point in the reaction. X-ray crystal structures could be determined for five metallomacrocyclic products, confirming the proposed structures based on mass spectrometric data. PGSE NMR spectroscopy was then used to determine the sizes of the species present in mixtures of bis(terpyridyl)oligo(ethylene glycol)cobalt(III) complexes in DMSO-d₆ solution. Several models were used to predict the diffusion coefficients of the metallomacrocycles for which it had been possible to determine X-ray crystal structures, and as for the simple model systems a spherical model was found to be most appropriate. This model was then used successfully to predict the sizes of the species present in mixtures of the di(ethylene glycol)-based system for which it had not been possible to obtain crystallographic data. Finally, the PGSE NMR technique was applied to solutions of the initial mixtures of bis(terpyridyl)oligo(ethylene glycol)cobalt(III) complexes in DMSO-d₆. These were found to be significantly larger than the major species present in the equilibrium mixtures.

6.7 Experimental

6.7.1 Reactions of bis(terpyridyl)oligo(ethylene glycol) ligands with cobalt(II) salts



6.7.1.1 Reaction with cobalt(II) acetate tetrahydrate

The bis(terpyridyl)oligo(ethylene glycol) (0.100 g) and cobalt(II) acetate tetrahydrate (1 eq) were dissolved in a chloroform-methanol solvent mixture (9:1, 20 cm³). The orange solution was stirred at room temperature or heated at reflux (time and temperature were varied depending on the experiment) to give a dark brown solution. The product was precipitated by addition of excess ammonium hexafluorophosphate in methanol, collected by filtration through Celite, washed well with methanol and diethyl ether and redissolved in acetonitrile. The solvent was removed *in vacuo* to give a brown solid in 70 – 90% yield.

6.7.1.2 Reaction with cobalt(II) chloride hexahydrate

The bis(terpyridyl)oligo(ethylene glycol) (0.200 g) was suspended in methanol (40 cm³) and cobalt(II) chloride hexahydrate (1 eq) was added. The orange solution was stirred at room temperature (1 – 3 h) to give a dark brown solution. The product was precipitated by addition of excess ammonium hexafluorophosphate in methanol, collected by filtration through Celite, washed well with methanol and diethyl ether and redissolved in acetonitrile. The solvent was removed *in vacuo* to give a brown solid in 80 – 100% yield.

6.7.1.3 Equilibration in acetonitrile

The hexafluorophosphate salt was dissolved in acetonitrile (concentration was varied depending on the experiment) and the dark brown solution was stirred at room temperature until equilibration was judged to be complete by ^1H NMR spectroscopy. The solvent was removed *in vacuo* to give a brown solid. Yields were quantitative.

6.7.1.4 Characterisation of the equilibrium mixtures

[Co_n(di)_n][PF₆]_{2n}: Found: C, 42.06; H, 3.20; N, 8.54%. C₃₄H₂₈N₆O₃CoP₂F₁₂·3H₂O (1L:1M) requires C, 42.03; H, 3.53; N, 8.65%; δ_{H} (250 or 500 MHz, CD₃CN)/ppm see discussion (section 6.2.1.1); *m/z* (ESI) 1689.7 ([Co₄L₄(PF₆)₆]²⁺, 10), 1340.3 ([CoL₂(PF₆)]⁺, 80), 1231.2 ([Co₃L₃(PF₆)₄]²⁺, 100), 1109.5 ([HOCH₂CH₂OCH₂CH₂Otpy)Co(L)(PF₆)]⁺, 70), 1035.5 [(MeOtpy)Co(L)(PF₆)]⁺, 55), 646.9 ([CoL(F)]⁺, 40),

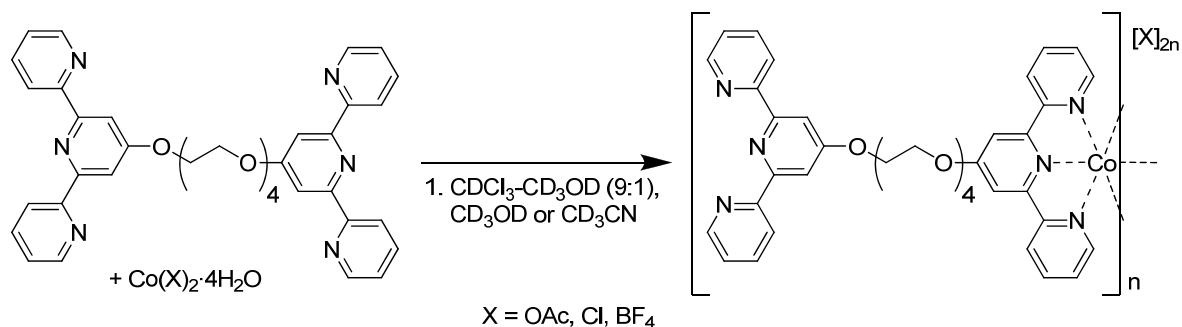
[Co_n(tri)_n][PF₆]_{2n}: δ_{H} (250 or 500 MHz, CD₃CN)/ppm see discussion (section 6.2.1.2); *m/z* (ESI) 1297.4 ([Co₃L₃(PF₆)₄]²⁺, 5), 816.3 ([Co₂L₂(PF₆)₂]²⁺ and [Co₃L₃(PF₆)₃]³⁺, 100), 576.3 ([Co₃L₃(PF₆)₂]⁴⁺, 50), 496.0 ([Co₂L₂(PF₆)₃]³⁺, 50), 432.0 ([Co₃L₃(PF₆)]⁵⁺, 50), 335.9 ([Co₂L₂]⁴⁺ and [Co₃L₃]⁶⁺, 90).

[Co_n(tetra)_n][PF₆]_{2n}: Found: C, 44.25; H, 3.77; N, 8.25%. C₃₈H₃₆N₆O₅CoP₂F₁₂·1.5H₂O (1L:1M) requires C, 44.20; H, 3.81; N, 8.14%; δ_{H} (250 or 500 MHz, CD₃CN)/ppm see discussion (section 6.2.1.3) Major component (500 MHz): 110 (s, br, 8 H, H⁶), 76.8 (s, 8 H, H^{3'}), 69.4 (s, 8 H, H³), 29.7 (s, 8 H, H⁵), 16.2 (s, 8 H, tpyOCH₂CH₂), 10.5 (s, 8 H, tpyOCH₂CH₂), 8.62 (s, 8 H, tpyOCH₂CH₂OCH₂CH₂), 8.07 (s, 8 H, tpyOCH₂CH₂OCH₂CH₂), -1.32 (s, 8 H, H⁴); *m/z* (ESI) 1864.9 ([Co₂L₂(PF₆)₃]⁺, 20), 860.2 ([Co₂L₂(PF₆)₂]²⁺, 70), 525.3 ([Co₂L₂(PF₆)₃]³⁺, 15), 357.8 ([Co₂L₂]⁴⁺, 100). Crystals of [Co₂(tetra)₂][PF₆]₄·6MeCN suitable for X-ray diffraction were obtained by slow diffusion of diethyl ether into an acetonitrile solution of the complex at room temperature.

[Co_n(hexa)_n][PF₆]_{2n}: δ_{H} (250 or 500 MHz, CD₃CN)/ppm see discussion (section 6.2.1.4) Major component (500 MHz): 110 (s, br, 8 H, H⁶), 73.1 (s, 8 H, H^{3'}), 69.0 (s, 8 H, H³), 32.8 (s, 8 H, H⁵), 14.3 (s, 8 H, tpyOCH₂CH₂), 9.15 (s, 8 H, tpyOCH₂CH₂), 7.16 (s, 8 H, tpyOCH₂CH₂OCH₂CH₂), 6.26 (s, 8 H, tpyOCH₂CH₂OCH₂CH₂), 5.57 (s, 8 H, tpyOCH₂CH₂OCH₂CH₂OCH₂CH₂), 5.18 (s, 8 H, tpyOCH₂CH₂OCH₂CH₂OCH₂CH₂), 4.77 (s, 8 H, H⁴); *m/z* (ESI) 948.1 ([Co₂L₂(PF₆)₂]²⁺, 45), 584.0 ([Co₂L₂(PF₆)]³⁺, 40), 401.8 ([Co₂L₂]⁴⁺, 100). Crystals of [Co₂(hexa)₂][PF₆]₅·2MeCN suitable for X-ray diffraction were obtained by

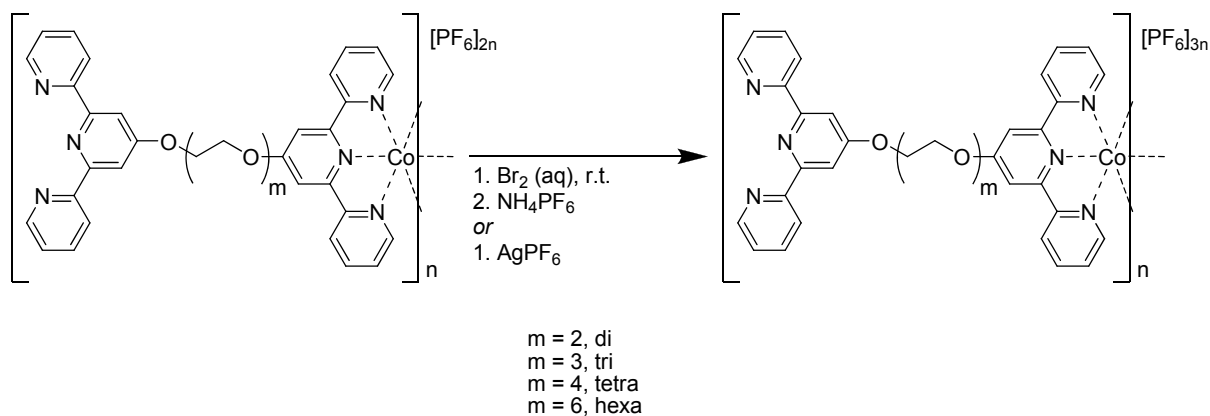
slow diffusion of diethyl ether into an acetonitrile solution of the complex at room temperature.

6.7.2 NMR studies on the reaction of bis(terpyridyl)tetra(ethylene glycol) with cobalt(II) salts



Reactions with bis(terpyridyl)tetra(ethylene glycol) and cobalt(II) acetate tetrahydrate, cobalt(II) chloride hexahydrate and cobalt(II) tetrafluoroborate hexahydrate (1L:1M) are described in section 5.6.5. ¹H NMR spectra were run at regular intervals until equilibrium was attained.

6.7.3 Oxidation



6.7.3.1 Oxidation with bromine

The bis(terpyridyl)oligo(ethylene glycol)cobalt(II) hexafluorophosphate complex (0.050 g) was suspended in water (5 cm³). A saturated solution of bromine in water (*ca.* 5 drops in 5 cm³) was added to give a yellow suspension. This was stirred at room temperature for 20 hours, then excess ammonium hexafluorophosphate in water was added to give a yellow precipitate. This was collected by filtration through Celite, washed well with water, ethanol

and diethyl ether, then redissolved in acetonitrile. The solvent was removed *in vacuo* to give a yellow-orange solid in 50 – 80% yield.

Alternatively, after stirring at room temperature for 20 hours, acetonitrile was added and the mixture was stirred until all the solid dissolved to give an orange-yellow solution. Excess solid ammonium hexafluorophosphate was added and the solution was transferred to a separating funnel. A few drops of dichloromethane was added and two layers formed. The yellow-orange layer was collected and the solvent was removed *in vacuo*. The resulting yellow-orange solid was dissolved in a minimum amount of acetonitrile and water was added to give a yellow-orange precipitate. This was collected by filtration through Celite, washed well with water, ethanol and diethyl ether and redissolved in acetonitrile. The solvent was removed *in vacuo* to give a yellow-orange solid in 70 – 90% yield.

6.7.3.2 Oxidation with silver(I) hexafluorophosphate

Silver hexafluorophosphate (1 eq) was suspended in acetonitrile (*ca.* 1 cm³) and added to a (dark brown) solution of the equilibrated bis(terpyridyl)oligo(ethylene glycol)cobalt(II) hexafluorophosphate complex (*ca.* 0.200 g, 1 eq) in acetonitrile (*ca.* 20 cm³). The colour of the solution immediately lightened and the mixture was stirred at room temperature for 20 hours. The orange yellow solution was concentrated to approximately half volume *in vacuo* and filtered through Celite to remove elemental silver. The solvent was removed *in vacuo* to give an orange solid in quantitative yield.

6.7.3.3 Separation of the species and characterisation of the oxidised equilibrium mixtures

[Co_n(di)_n][PF₆]_{3n}: δ_{H} (500 MHz, CD₃CN)/ppm see discussion (section 6.3); *m/z* (ESI) 917.5 ([Co₃L₃(PF₆)₆]³⁺, 705.0 ([Co₄L₄(PF₆)₇]⁵⁺, 675.9 ([Co₄L₄(PF₆)₆]⁵⁺, 563.3 ([Co₄L₄(PF₆)₆]⁶⁺.

[Co_n(tri)_n][PF₆]_{3n}: δ_{H} (500 MHz, CD₃CN)/ppm see discussion (section 6.3); *m/z* (ESI) 518.6 ([Co₃L₃(PF₆)₄]⁵⁺, 60), 408.0 ([Co₃L₃(PF₆)₃]⁶⁺, 100), 329.1 ([Co₃L₃(PF₆)₂]⁷⁺, 10). Crystals of [Co₃(tri)₃][PF₆]₉·2MeCN·0.5MeOH·2.75H₂O suitable for X-ray diffraction were obtained by slow diffusion of diethyl ether into an acetonitrile solution of the complex at room temperature.

[Co_n(tetra)_n][PF₆]_{3n}: The product was purified by preparative TLC chromatography on Al₂O₃ using acetonitrile-water-saturated aqueous KNO₃ solution (7:2:2) as eluent. The fractions were concentrated *in vacuo* and excess aqueous ammonium hexafluorophosphate was added

to the yellow solution to give a yellow precipitate. This was collected by filtration through Celite, washed well with water, ethanol and diethyl ether and redissolved in acetonitrile. The solvent was removed *in vacuo* to give a yellow solid. Found: C, 38.02; H, 2.91; N, 7.27%. $C_{76}H_{72}N_{12}O_{10}Co_2P_6F_{36}\cdot 4H_2O$ requires C, 38.46; H, 3.40; N, 7.08%; $\tilde{\nu}_{max}(solid)/cm^{-1}$ 3630w, 3620w, 3092w, 3043w, 2874w, 1684w, 1653w, 1614m, 1562m, 1555w, 1481m, 1433m, 1379w, 1352m, 1254w, 1215m, 1163w, 1099m, 1063m, 1041m, 1032m, 968w, 877w, 820s, 781s, 750s, 741s, 719m, 698m, 663m, 640w, 619m; $\delta_H(500\text{ MHz, }CD_3CN)/ppm$ 8.52 (s, 4 H, H^3), 8.41 (d, J 7.9 Hz, 4 H, H^3), 7.90 – 7.84 (m, 4 H, H^4), 7.26 (d, J 4.1 Hz, 8 H, H^5 and H^6), 4.87 – 4.80 (m, 4 H, tpyOCH₂CH₂), 4.12 – 4.05 (m, 4 H, tpyOCH₂CH₂), 3.83 – 3.76 (m, 4 H, tpyOCH₂CH₂OCH₂CH₂), 3.70 – 3.63 (m, 4 H, tpyOCH₂CH₂OCH₂CH₂); $\delta_C(126\text{ MHz, }CD_3CN)/ppm$ 173.8 (C^4), 157.7 (C^2), 157.1 (C^2), 153.2 (C^6), 143.8 (C^4), 131.8 (C^5), 127.8 (C^3), 116.1 (C^3), 72.4 (tpyOCH₂CH₂), 71.5 (tpyOCH₂CH₂OCH₂CH₂), 71.1 (tpyOCH₂CH₂OCH₂CH₂), 69.9 (tpyOCH₂CH₂); m/z (ESI) 1864.8 ($[Co_2L_2][PF_6]_3^+$, 2), 1005.3 ($[Co_2L_2][PF_6]_4^{2+}$, 20), 932.8 ($[Co_2L_2][PF_6]_3^{2+}$, 60), 860.3 ($[Co_2L_2][PF_6]_2^{2+}$, 65), 622.0 ($[Co_2L_2][PF_6]_3^{3+}$, 10), 573.8 ($[Co_2L_2][PF_6]_2^{3+}$, 15), 525.4 ($[Co_2L_2][PF_6]^{3+}$, 20), 430.5 ($[Co_2L_2][PF_6]_2^{4+}$, 2), 394.0 ($[Co_2L_2][PF_6]^{4+}$, 55), 358.0 ($[Co_2L_2]^{4+}$, 100). Crystals of $[Co_2(tetra)_2][PF_6]_6\cdot 10MeCN$ suitable for X-ray diffraction were obtained by slow diffusion of diethyl ether into an acetonitrile solution of the complex at room temperature.

$[Co_n(hexa)_n][PF_6]_{3n}$: The product was purified by preparative TLC chromatography on Al_2O_3 using acetonitrile-water-saturated aqueous KNO_3 solution (7:2:2) as eluent. The fractions were concentrated *in vacuo* and excess aqueous ammonium hexafluorophosphate was added to the yellow solution to give a yellow precipitate. This was collected by filtration through Celite, washed well with water, ethanol and diethyl ether and redissolved in acetonitrile. The solvent was removed *in vacuo* to give a yellow solid. Found: C, 39.53; H, 3.80; N, 6.86%. $C_{42}H_{44}N_6O_7CoP_3F_{18}\cdot 2H_2O$ requires C, 39.57; H, 3.80; N, 6.59%; $\tilde{\nu}_{max}(solid)/cm^{-1}$ 3096w, 2868w, 1618m, 1566m, 1485m, 1435m, 1352m, 1256w, 1220m, 1170w, 1099m, 1067m, 1043m, 1032m, 822s, 781s, 750s, 741s, 719m, 698m, 663m, 623m; $\delta_H(500\text{ MHz, }CD_3CN)/ppm$ 8.51 (s, 4 H, H^3), 8.50 (d, J 8.8 Hz, 4 H, H^3), 8.12 (t, J 7.7 Hz, 4 H, H^4), 7.37 (t, J 6.7 Hz, 4 H, H^5), 7.32 (d, J 5.6 Hz, 4 H, H^6), 4.83 – 4.76 (m, 4 H, tpyOCH₂CH₂), 4.10 – 4.04 (m, 4 H, tpyOCH₂CH₂), 3.80 – 3.73 (m, 4 H, tpyOCH₂CH₂OCH₂CH₂), 3.67 – 3.62 (m, 4 H, tpyOCH₂CH₂OCH₂CH₂), 3.60 – 3.54 (m, 8 H, tpyOCH₂CH₂OCH₂CH₂OCH₂CH₂); $\delta_C(126\text{ MHz, }CD_3CN)/ppm$ 173.7 (C^4), 157.8 (C^2), 157.2 (C^2), 153.3 (C^6), 144.0 (C^4), 131.8 (C^5),

127.8 (C³), 115.9 (C³), 72.5 (tpyOCH₂CH₂), 71.6 (tpyOCH₂CH₂OCH₂CH₂), 71.12 (tpyOCH₂CH₂OCH₂CH₂), 71.11 (tpyOCH₂CH₂OCH₂CH₂OCH₂CH₂), 71.09 (tpyOCH₂CH₂OCH₂CH₂OCH₂CH₂), 69.73 (tpyOCH₂CH₂); *m/z* (ESI) 1093.2 ([Co₂L₂][PF₆]₄²⁺, 25), 1020.8 ([Co₂L₂][PF₆]₃²⁺, 50), 947.9 ([Co₂L₂][PF₆]₂²⁺, 55), 680.6 ([Co₂L₂][PF₆]₃³⁺, 40), 632.3 ([Co₂L₂][PF₆]₂³⁺, 65), 584.1 ([Co₂L₂][PF₆]₃³⁺, 55), 474.2 ([Co₂L₂][PF₆]₂⁴⁺, 75), 438.1 ([Co₂L₂][PF₆]₄⁴⁺, 65), 401.8 ([Co₂L₂]⁴⁺, 65), 350.3 ([Co₂L₂][PF₆]₅⁵⁺, 20), 321.5 ([Co₂L₂]⁵⁺, 35), 267.8 ([Co₂L₂]⁶⁺, 100). Crystals of [Co₂(hexa)₂][PF₆]₆·6MeCN suitable for X-ray diffraction were obtained by slow diffusion of *tert*-butyl methyl ether into an acetonitrile solution of the complex at room temperature.

7 General Conclusions

The overall aim of this thesis was to assess the extent of polymer or macrocycle formation from the reaction of cobalt(II) salts with ditopic bis(2,2':6',2''-terpyridine) ligands linked by flexible oligo(ethylene glycol) spacers. The speciation of product mixtures obtained from the reaction of bis(terpyridyl)oligo(ethylene glycol) ligands was found to be extremely complex and highly dependent on the ligand, anion, solvent, concentration and many other seemingly minor reaction parameters. Use of alcohol-containing solvents and an acetate counterion brings about the decomposition of the ditopic ligand to form mononuclear bis(4'-alkoxy-2,2':6',2''-terpyridine)cobalt(II) complexes, providing potential polymer end units. Similarly, polymer end units (in this case, mono(2,2':6',2''-terpyridine)cobalt(II) complexes) are formed when cobalt(II) salts of coordinating anions are used for the coordination. The formation of polymer end units disfavors the assembly of the components into discrete metallomacrocyclic species. The counteranion was also found to influence the relative proportions of several bis(2,2':6',2''-terpyridine)cobalt(II) complexes present in solutions of the ditopic ligands and various cobalt(II) salts. Analysis of initial product mixtures obtained immediately after reaction of the ditopic ligands with cobalt(II) acetate and precipitation with ammonium hexafluorophosphate suggested that the kinetic products of the reaction are large multinuclear species. However, whether these species are polymeric or macrocyclic has yet to be determined. Equilibration of the hexafluorophosphate salts of these initial product mixtures in acetonitrile solution resulted in a change in the composition of the mixture and the formation of several new cobalt(II)-containing complexes. Several components of the equilibrium mixtures could be identified using X-ray crystallography and PGSE NMR spectroscopy and were found to be metallomacrocyclic species. These components were present in significant amounts (up to 95%) at equilibrium in cobalt(II) hexafluorophosphate complexes of the ditopic ligands.

The answer to the question raised in the title of this thesis: "Polymer or Macrocycle?" is therefore dependent on a huge number of variables, some of which are almost impossible to control.

8 Appendix

8.1 General experimental

All chemicals and solvents were obtained from Acros Organics, Alfa Aesar, Fluka, Sigma Aldrich or VWR and, unless otherwise stated, were used without further purification. Chloroform and dichloromethane were distilled before use. Microwave reactions were carried out in sealed tubes in a Biotage Initiator 8 reactor.

8.1.1 Analytical instrumentation

Melting points were determined on a Stuart Scientific Melting Point Apparatus SMP3. Elemental analyses were performed by W. Kirsch with a Leco CHN-900 microanalyser. UV-Vis absorption spectra were recorded on a Varian-Cary 5000 spectrophotometer. Infrared spectra were measured on a Shimadzu FTIR-8400S spectrophotometer with neat samples using a Golden Gate diamond ATR attachment. ^1H and ^{13}C NMR spectra were recorded on Bruker AM250 (250 MHz) or Bruker Avance DRX500 (500 MHz) NMR spectrometers. Chemical shifts are referenced to residual solvent peaks (TMS δ 0 ppm). MALDI-TOF mass spectra were recorded with a PerSeptive Biosystems Voyager mass spectrometer, using a supporting matrix (sinapinic acid or α -cyano-4-hydroxycinnamic acid). Electrospray mass spectra were measured on Finnigan MAT LCQ or Bruker esquire 3000^{plus} mass spectrometers.

8.1.2 PGSE NMR spectroscopy

All PGSE NMR measurements were performed on a Bruker Avance DRX500 NMR spectrometer equipped with a 5 mm BBO or BBI probe and a z-gradient coil with a maximum strength of $55 \times 10^{-4} \text{ T cm}^{-1}$ at 295 K. The 90° pulse lengths were determined for each sample. A standard BPPLIED sequence¹⁹² was used with sinusoidal pulse field gradients and two spoiler gradients. A recovery delay of 1 ms and an LED delay of 5 ms were employed to reduce eddy current effects. The gradient strength was calibrated by using the self-diffusion coefficient of residual HOD in D_2O ($1.9 \times 10^{-9} \text{ m}^2 \text{ s}^{-1}$).¹⁹³ For each experiment, the gradient strength was increased from 5 – 95% in sixteen equally spaced steps with eight scans per increment. Values of δ (gradient pulse length) and Δ (diffusion time) were selected to give an intensity of between 5 and 10% of the initial intensity at 95% gradient strength. For each sample, several experiments with different values of δ and Δ were measured to verify the

integrity of the data. The diffusion coefficients for each sample were calculated as previously described.¹⁹⁴ The data were plotted as $\ln(I/I_0)$ vs. $\gamma^2 \delta^2 G^2 (\Delta - \delta/3)$ and the gradient of the straight line ($-D$) was fitted using a least-squared regression fit on 14 – 16 points with an r^2 value greater than 0.99. The signal intensity at a gradient strength of 5% was taken as an approximation for the value for the signal intensity without gradients. The value of I_0 has no effect on the gradient of the straight line.

8.2 X-Ray crystallography

X-ray crystallographic data were collected on Bruker-Nonius Kappa CCD or Stoe IPDS diffractometers. The data reduction, solution and refinement were carried out using the programs COLLECT,¹⁹⁵ SIR92,¹⁹⁶ DENZO/SCALEPACK,¹⁹⁷ and CRYSTALS,¹⁹⁸ or Stoe IPDS software,¹⁹⁹ and SHELXL97.²⁰⁰

Compound	MeOtpy	tri	[Co(tpy) ₂][PF ₆] ₂ ·2MeCN
Empirical Formula	C ₁₆ H ₁₃ N ₃ O	C ₃₆ H ₃₂ N ₆ O ₄	C ₃₄ H ₂₈ N ₈ P ₂ F ₁₂ Co
Formula Weight	263.30	612.69	897.51
Temperature / K	123	173	123
Crystal System	Monoclinic	Monoclinic	Tetragonal
Space Group	<i>P</i> 2 ₁ / <i>c</i>	<i>P</i> 2 ₁ / <i>n</i>	<i>P</i> 4 ₃
Unit cell dimensions:			
a / Å	16.4972(4)	5.8461(2)	12.3479(5)
b / Å	5.04890(10)	22.5122(10)	12.3479(5)
c / Å	16.9712(4)	11.6542(5)	49.146(2)
α / °	90	90	90
β / °	114.7110(10)	94.589(3)	90
γ / °	90	90	90
Volume / Å³	1284.13(5)	1528.88(11)	7493.3(5)
Z	4	2	8
Crystal Description	colourless needle	colourless block	blue block
Crystal Size / mm³	0.07 × 0.09 × 0.28	0.04 × 0.17 × 0.23	0.11 × 0.14 × 0.26
Density / Mg m⁻³	1.362	1.331	1.591
Absorption Coefficient / mm⁻¹	0.088	0.089	0.642
Theta range for data collection / °	2.414 to 33.267	1.809 to 27.817	1.649 to 29.369
Reflections collected	37220	12355	63132
Independent reflections	4912	3623	20080
R(int)	0.023	0.094	0.038
Completeness to theta / ° (%)	32.601 (99.5)	27.261 (99.7)	29.369 (99.8)
Parameters	181	208	1156
Goodness of fit	1.0511	1.0209	1.0941
wR₂	0.0482	0.0687	0.0504
Final R₁ [I > 2σ(I)]	0.0410	0.0906	0.0484

Table 8.1 Crystal data and structure refinement for 4'-methoxy-2,2':6',2''-terpyridine, bis(terpyridyl)tri(ethylene glycol) and [Co(tpy)₂][PF₆]₂·2MeCN.

Compound	$2\{[\text{Co}(\text{tpy})_2][\text{PF}_6]_3\} \cdot 5\text{MeCN}$	$[\text{Co}(\text{Cltpy})_2][\text{PF}_6]_2$	$[\text{Co}(\text{Cltpy})_2][\text{PF}_6]_3 \cdot \text{MeCN}$
Empirical Formula	$\text{C}_{70}\text{H}_{59}\text{N}_{17}\text{P}_6\text{F}_{36}\text{Co}_2$	$\text{C}_{30}\text{H}_{20}\text{Cl}_2\text{N}_6\text{P}_2\text{F}_{12}\text{Co}$	$\text{C}_{32}\text{H}_{23}\text{Cl}_2\text{N}_7\text{P}_3\text{F}_{18}\text{Co}$
Formula Weight	2125.99	884.29	1070.31
Temperature / K	123	173	173
Crystal System	Triclinic	Tetragonal	Orthorhombic
Space Group	$P\bar{1}$	$P\bar{4}2_1c$	$Pna2_1$
Unit cell dimensions:			
a / Å	11.3947(8)	8.9400(13)	16.3767(6)
b / Å	17.8294(13)	8.9400(13)	12.2742(4)
c / Å	20.2985(15)	20.236(4)	19.5992(7)
α / °	89.555(4)	90	90
β / °	87.865(4)	90	90
γ / °	83.293(4)	90	90
Volume / Å³	4092.8(5)	1617.3(5)	3939.7(2)
Z	2	2	4
Crystal Description	yellow plate	red plate	orange plate
Crystal Size / mm³	$0.06 \times 0.15 \times 0.32$	$0.02 \times 0.25 \times 0.28$	$0.04 \times 0.17 \times 0.37$
Density / Mg m⁻³	1.725	1.816	1.804
Absorption Coefficient / mm⁻¹	0.660	0.900	0.817
Theta range for data collection / °	1.801 to 26.452	3.78 to 27.49	1.958 to 30.087
Reflections collected	79437	13275	134907
Independent reflections	16786	1822	11536
R(int)	0.032	0.0723	0.052
Completeness to theta / ° (%)	25.923 (99.8)	27.49 (97.6)	30.087 (99.8)
Parameters	1180	127	569
Goodness of fit	1.0986	1.160	1.0876
wR₂	0.0322	0.0806	0.0364
Final R₁ [I > 2sigma(I)]	0.0316	0.0319	0.0309

Table 8.2 Crystal data and structure refinement for $2\{[\text{Co}(\text{tpy})_2][\text{PF}_6]_3\} \cdot 5\text{MeCN}$, $[\text{Co}(\text{Cltpy})_2][\text{PF}_6]_2$ and $[\text{Co}(\text{Cltpy})_2][\text{PF}_6]_3 \cdot \text{MeCN}$.

Compound	[Co(MeOtpy) ₂][PF ₆] ₂	[Co(MeOtpy) ₂][PF ₆] ₂ ·MeCN	[Co(MeOtpy) ₂][PF ₆] ₃ ·MeCN
Empirical Formula	C ₃₂ H ₂₆ O ₂ N ₆ P ₂ F ₁₂ Co	C ₃₄ H ₂₉ O ₂ N ₇ P ₂ F ₁₂ Co	C ₃₄ H ₂₉ O ₂ N ₇ P ₃ F ₁₈ Co
Formula Weight	875.45	916.51	1061.47
Temperature / K	173	173	173
Crystal System	Monoclinic	Orthorhombic	Orthorhombic
Space Group	<i>P</i> 2 ₁ / <i>c</i>	<i>Pccn</i>	<i>Pna</i> 2 ₁
Unit cell dimensions:			
a / Å	18.9611(17)	30.2955(4)	16.7813(7)
b / Å	9.3533(9)	12.46980(10)	12.3488(5)
c / Å	19.6865(18)	19.6441(2)	19.8304(8)
α / °	90	90	90
β / °	102.360(4)	90	90
γ / °	90	90	90
Volume / Å³	3410.5(5)	7421.12(14)	4109.4(3)
Z	4	8	4
Crystal Description	red plate	green plate	orange plate
Crystal Size / mm³	0.06 × 0.34 × 0.40	0.05 × 0.23 × 0.32	0.08 × 0.20 × 0.30
Density / Mg m⁻³	1.705	1.641	1.716
Absorption Coefficient / mm⁻¹	0.705	0.653	0.660
Theta range for data collection / °	2.118 to 27.618	1.344 to 27.881	2.048 to 32.515
Reflections collected	15519	34884	53310
Independent reflections	6626	8864	13777
R(int)	0.084	0.046	0.055
Completeness to theta / ° (%)	25.132 (87.3)	27.881 (100)	30.889 (99.8)
Parameters	496	524	596
Goodness of fit	0.9258	1.0935	1.1536
wR₂	0.1845	0.0432	0.0480
Final R₁ [I>2sigma(I)]	0.0738	0.0373	0.0442

Table 8.3 Crystal data and structure refinement for [Co(MeOtpy)₂][PF₆]₂, [Co(MeOtpy)₂][PF₆]₂·MeCN and [Co(MeOtpy)₂][PF₆]₃·MeCN.

Compound	[Co(EtOtpy) ₂][PF ₆] ₂ ·2MeCN	[Co(EtOtpy) ₂][PF ₆] ₃ ·MeCN	[Co(EtOtpy) ₂][Br] ₃ ·MeCN·H ₂ O
Empirical Formula	C ₃₈ H ₃₆ O ₂ N ₈ P ₂ F ₁₂ Co	C ₃₆ H ₃₃ O ₂ N ₇ P ₃ F ₁₈ Co	C ₃₆ H ₃₅ O ₃ N ₇ Br ₃ Co
Formula Weight	985.61	1089.52	912.36
Temperature / K	173	123	173
Crystal System	Monoclinic	Orthorhombic	Monoclinic
Space Group	<i>P2</i> ₁ / <i>c</i>	<i>Pbca</i>	<i>P2</i> ₁ / <i>n</i>
Unit cell dimensions:			
a / Å	9.82930(10)	13.4160(13)	14.7647(4)
b / Å	21.7694(3)	20.1202(18)	13.8679(3)
c / Å	19.6786(2)	30.775(3)	19.3849(5)
α / °	90	90	90
β / °	103.1996(7)	90	110.8046(11)
γ / °	90	90	90
Volume / Å³	4099.54(8)	8307.1(14)	3710.36(16)
Z	4	8	4
Crystal Description	dark red plate	orange plate	orange plate
Crystal Size / mm³	0.11 × 0.13 × 0.32	0.08 × 0.19 × 0.42	0.02 × 0.21 × 0.21
Density / Mg m⁻³	1.597	1.742	1.633
Absorption Coefficient / mm⁻¹	0.598	0.655	3.739
Theta range for data collection / °	3.002 to 27.869	1.941 to 30.508	1.849 to 27.533
Reflections collected	37341	102047	22616
Independent reflections	9749	12571	8451
R(int)	0.075	0.031	0.059
Completeness to theta / ° (%)	27.869 (99.8)	29.288 (99.5)	26.707 (99.5)
Parameters	568	604	452
Goodness of fit	0.9868	1.1507	1.0274
wR₂	0.0917	0.0593	0.0567
Final R₁ [I>2sigma(I)]	0.0445	0.0381	0.0511

Table 8.4 Crystal data and structure refinement for [Co(EtOtpy)₂][PF₆]₂·2MeCN, [Co(EtOtpy)₂][PF₆]₃·MeCN and [Co(EtOtpy)₂][Br]₃·MeCN·H₂O.

Compound	[Co(PrOtpy) ₂][PF ₆] ₂ ·MeCN	[Co(PrOtpy) ₂][PF ₆] ₂ ·MeCN·Et ₂ O	2{[Co(PrOtpy) ₂][PF ₆] ₃ }·5MeCN
Empirical Formula	C ₃₈ H ₃₇ O ₂ N ₇ P ₂ F ₁₂ Co	C ₄₂ H ₄₇ O ₃ N ₇ P ₂ F ₁₂ Co	C ₈₂ H ₈₃ O ₄ N ₁₇ P ₆ F ₃₆ Co ₂
Formula Weight	972.61	1046.74	1179.15
Temperature / K	173	173	173
Crystal System	Triclinic	Monoclinic	Triclinic
Space Group	<i>P</i> -1	<i>P</i> 2 ₁ / <i>n</i>	<i>P</i> -1
Unit cell dimensions:			
a / Å	15.7438(4)	15.7364(3)	10.5795(4)
b / Å	16.2492(4)	15.6546(3)	13.4992(4)
c / Å	16.5825(4)	19.2908(4)	20.4174(8)
α / °	79.1230(10)	90	72.619(2)
β / °	79.0640(10)	107.7770(10)	89.8082(17)
γ / °	79.6200(10)	90	78.331(2)
Volume / Å³	4044.22(17)	4525.32(16)	2720.17(17)
Z	4	4	2
Crystal Description	orange block	orange block	orange plate
Crystal Size / mm³	0.12 × 0.21 × 0.36	0.12 × 0.29 × 0.38	0.02 × 0.22 × 0.23
Density / Mg m⁻³	1.597	1.536	1.440
Absorption Coefficient / mm⁻¹	0.604	0.548	0.507
Theta range for data collection / °	1.861 to 35.700	1.881 to 36.038	1.047 to 27.843
Reflections collected	223440	134082	23232
Independent reflections	36189	20138	12782
R(int)	0.045	0.042	0.044
Completeness to theta / ° (%)	27.489 (99.5)	33.155 (99.6)	25.894 (99.5)
Parameters	1252	640	739
Goodness of fit	1.1267	1.0788	1.1113
wR₂	0.0511	0.0424	0.0645
Final R₁ [I>2sigma(I)]	0.0422	0.0387	0.0598

Table 8.5 Crystal data and structure refinement for [Co(PrOtpy)₂][PF₆]₂·MeCN, [Co(PrOtpy)₂][PF₆]₂·MeCN·Et₂O and 2{[Co(PrOtpy)₂][PF₆]₃}·5MeCN.

Compound	[Co(MeOtpy)(OAc) ₂]	[Co(MeOtpy)Cl ₂]	[Co(MeOtpy)(NO ₃) ₂ (OH ₂)]
Empirical Formula	C ₂₀ H ₁₉ O ₅ N ₃ Co	C ₁₆ H ₁₃ OC ₁₂ N ₃ Co	C ₁₆ H ₁₅ O ₈ N ₅ Co
Formula Weight	440.31	393.14	464.26
Temperature / K	173	123	123
Crystal System	Triclinic	Monoclinic	Monoclinic
Space Group	<i>P</i> -1	<i>P</i> 2 ₁ / <i>c</i>	<i>P</i> 2 ₁ / <i>n</i>
Unit cell dimensions:			
a / Å	8.1976(16)	19.5517(6)	8.8923(2)
b / Å	10.949(2)	8.9285(3)	20.3307(4)
c / Å	11.250(2)	17.7411(5)	10.2934(2)
α / °	93.90(3)	90	90
β / °	107.00(3)	92.4040(10)	105.8910(10)
γ / °	94.79(3)	90	90
Volume / Å³	957.7(3)	3094.29(17)	1789.79(6)
Z	2	8	4
Crystal Description	red block	red block	yellow prism
Crystal Size / mm³	0.09 × 0.09 × 0.23	0.21 × 0.22 × 0.48	0.04 × 0.11 × 0.23
Density / Mg m⁻³	1.527	1.688	1.723
Absorption Coefficient / mm⁻¹	0.934	1.461	1.019
Theta range for data collection / °	2.61 to 31.50	2.085 to 36.366	2.003 to 33.728
Reflections collected	35684	108956	34162
Independent reflections	6260	15003	7115
R(int)	0.0772	0.030	0.044
Completeness to theta / ° (%)	31.50 (98.4)	36.366 (99.8)	33.728 (99.7)
Parameters	265	415	271
Goodness of fit	1.106	1.0497	1.1071
wR₂	0.0899	0.0232	0.0322
Final R₁ [I>2sigma(I)]	0.0344	0.0228	0.0328

Table 8.6 Crystal data and structure refinement for [Co(MeOtpy)(OAc)₂], [Co(MeOtpy)Cl₂] and [Co(MeOtpy)(NO₃)₂(OH₂)].

Compound	[Co(Cltpy)(OAc) ₂]	[Co(Cltpy)Cl ₃] ₂ ·CHCl ₃	[Fe(Cltpy)Cl ₃] ₂ ·CHCl ₃
Empirical Formula	C ₁₉ H ₁₆ O ₄ N ₃ ClCo	C ₁₆ H ₁₁ Cl ₇ N ₃ Co	C ₁₆ H ₁₁ Cl ₇ N ₃ Fe
Formula Weight	444.74	552.39	549.28
Temperature / K	173	173	173
Crystal System	Triclinic	Triclinic	Monoclinic
Space Group	<i>P</i> -1	<i>P</i> -1	<i>P</i> 2 ₁ / <i>c</i>
Unit cell dimensions:			
a / Å	8.5363(1)	8.4093(2)	11.035(2)
b / Å	10.9131(2)	10.7388(2)	12.192(2)
c / Å	11.4735(2)	11.6666(2)	16.177(3)
α / °	104.3090(8)	93.6671(11)	90
β / °	97.0490(8)	109.6238(11)	100.48(3)
γ / °	110.5235(8)	90.8995(9)	90
Volume / Å³	943.78(3)	989.56(4)	2140.1(7)
Z	2	2	4
Crystal Description	yellow plate	green plate	orange needle
Crystal Size / mm³	0.04 × 0.07 × 0.20	0.02 × 0.05 × 0.51	0.03 × 0.03 × 0.26
Density / Mg m⁻³	1.565	1.854	1.705
Absorption Coefficient / mm⁻¹	1.082	1.820	1.586
Theta range for data collection / °	1.883 to 27.876	1.858 to 27.895	2.66 to 25.05
Reflections collected	8942	9304	14422
Independent reflections	4499	4714	3715
R(int)	0.019	0.019	0.1289
Completeness to theta / ° (%)	27.876 (99.9)	27.895 (99.9)	25.05 (98.0)
Parameters	253	244	244
Goodness of fit	1.0738	1.0685	1.115
wR₂	0.0328	0.0335	0.1090
Final R₁ [I>2σ(I)]	0.0298	0.0321	0.0396

Table 8.7 Crystal data and structure refinement for [Co(Cltpy)(OAc)₂], [Co(Cltpy)Cl₃]₂·CHCl₃ and [Fe(Cltpy)Cl₃]₂·CHCl₃.

Compound	[Co ₂ (tetra) ₂][PF ₆] ₄ ·6MeCN	[Co ₂ (tetra) ₂][PF ₆] ₆ ·10MeCN	[Co ₂ (hexa) ₂][PF ₆] ₅ ·2MeCN
Empirical Formula	C ₈₈ H ₉₀ O ₁₀ N ₁₈ P ₄ F ₂₄ Co ₂	C ₉₆ H ₁₀₂ O ₁₀ N ₂₂ P ₆ F ₃₆ Co ₂	C ₈₈ H ₉₄ O ₁₄ N ₁₄ P ₅ F ₃₀ Co ₂
Formula Weight	2257.51	2711.64	2414.48
Temperature / K	173	173	173
Crystal System	Triclinic	Triclinic	Triclinic
Space Group	<i>P</i> -1	<i>P</i> -1	<i>P</i> -1
Unit cell dimensions:			
a / Å	13.6827(7)	9.6391(6)	10.9291(2)
b / Å	14.7422(6)	17.2240(10)	12.1180(2)
c / Å	15.2050(7)	18.7747(10)	20.5108(4)
α / °	101.324(3)	71.629(2)	85.1137(12)
β / °	111.052(2)	80.633(2)	87.2782(11)
γ / °	110.394(3)	74.851(2)	72.6510(10)
Volume / Å³	2495.1(2)	2844.4(3)	2582.73(8)
Z	1	1	1
Crystal Description	red block	orange needle	purple plate
Crystal Size / mm³	0.06 × 0.08 × 0.31	0.01 × 0.04 × 0.33	0.08 × 0.15 × 0.50
Density / Mg m⁻³	1.502	1.583	1.552
Absorption Coefficient / mm⁻¹	0.507	0.501	0.519
Theta range for data collection / °	2.175 to 26.084	2.197 to 26.090	1.765 to 27.537
Reflections collected	18344	48447	23192
Independent reflections	9806	11040	11879
R(int)	0.055	0.045	0.034
Completeness to theta / ° (%)	25.562 (99.6)	25.047 (98.4)	27.537 (99.6)
Parameters	667	811	709
Goodness of fit	1.0280	1.1505	1.0897
wR₂	0.0897	0.0758	0.0836
Final R₁ [I>2sigma(I)]	0.0957	0.0663	0.0717

Table 8.8 Crystal data and structure refinement for [Co₂(tetra)₂][PF₆]₄·6MeCN, [Co₂(tetra)₂][PF₆]₆·10MeCN and [Co₂(hexa)₂][PF₆]₅·2MeCN.

Compound	[Co ₂ (hexa) ₂][PF ₆] ₆ ·6MeCN	[Co ₃ (tri) ₃][PF ₆] ₉ ·2MeCN·0.5MeOH·2.75H ₂ O
Empirical Formula	C ₉₆ H ₁₀₆ O ₁₄ N ₁₈ P ₆ F ₃₆ Co ₂	C _{112.5} H _{109.5} O _{15.25} N ₂₀ P ₉ F ₅₄ Co ₃
Formula Weight	2723.65	3467.19
Temperature / K	123	173
Crystal System	Monoclinic	Triclinic
Space Group	<i>P</i> 2 ₁ / <i>n</i>	<i>P</i> -1
Unit cell dimensions:		
a / Å	11.8008(4)	19.4562(5)
b / Å	20.2110(7)	21.1099(6)
c / Å	24.1339(8)	23.1829(5)
α / °	90	114.3039(15)
β / °	96.660(2)	107.0917(15)
γ / °	90	94.3568(13)
Volume / Å³	5717.2(3)	8079.8(4)
Z	2	2
Crystal Description	orange needle	orange block
Crystal Size / mm³	0.04 × 0.06 × 0.34	0.20 × 0.26 × 0.28
Density / Mg m⁻³	1.582	1.423
Absorption Coefficient / mm⁻¹	0.501	0.514
Theta range for data collection / °	1.699 to 30.034	1.032 to 25.094
Reflections collected	86390	53869
Independent reflections	16708	28513
R(int)	0.068	0.052
Completeness to theta / ° (%)	30.034 (99.9)	25.094 (99.1)
Parameters	803	2137
Goodness of fit	1.1142	1.0954
wR₂	0.0626	0.1277
Final R₁ [I>2sigma(I)]	0.0612	0.1353

Table 8.9 Crystal data and structure refinement for [Co₂(hexa)₂][PF₆]₆·6MeCN and [Co₃(tri)₃][PF₆]₉·2MeCN·0.5MeOH·2.75H₂O.

References

1. J. W. Steed and J. L. Atwood, *Supramolecular Chemistry*, 2nd edn., Wiley, Chichester, 2009.
2. I. Dance, *New J. Chem.*, 2003, **27**, 1-2.
3. A. J. Goshe, J. D. Crowley and B. Bosnich, *Helv. Chim. Acta*, 2001, **84**, 2971-2985.
4. E. C. Constable, *Pure Appl. Chem.*, 1996, **68**, 253-260.
5. M. Fujita, M. Tominaga, A. Hori and B. Therrien, *Acc. Chem. Res.*, 2005, **38**, 371-380.
6. C.-L. Chen, Z.-Q. Yu, Q. Zhang, M. Pan, J.-Y. Zhang, C.-Y. Zhao and C.-Y. Su, *Cryst. Growth Des.*, 2008, **8**, 897-905.
7. T. Weilandt, R. W. Troff, H. Saxell, K. Rissanen and C. A. Schalley, *Inorg. Chem.*, 2008, **47**, 7588-7598.
8. U. S. Schubert and C. Eschbaumer, *Angew. Chem., Int. Ed.*, 2002, **41**, 2893-2926.
9. P. R. Andres and U. S. Schubert, *Adv. Mater.*, 2004, **16**, 1043-1068.
10. E. C. Constable, *Chem. Soc. Rev.*, 2007, **36**, 246-253.
11. E. C. Constable and A. Thompson, *J. Chem. Soc., Dalton Trans.*, 1992, 3467-3475.
12. J.-P. Collin, P. Laine, J.-P. Launay, J.-P. Sauvage and A. Sour, *J. Chem. Soc., Chem. Commun.*, 1993, 434-435.
13. F. Barigelletti, L. Flamigni, V. Balzani, J.-P. Collin, J.-P. Sauvage, A. Sour, E. C. Constable and A. M. W. Cargill Thompson, *J. Am. Chem. Soc.*, 1994, **116**, 7692-7699.
14. E. C. Constable and A. M. W. Cargill Thompson, *J. Chem. Soc., Dalton Trans.*, 1995, 1615-1627.
15. F. Barigelletti, L. Flamigni, G. Calogero, L. Hammarstrom, J.-P. Sauvage and J.-P. Collin, *Chem. Commun.*, 1998, 2333-2334.
16. J.-P. Collin, P. Gavina, V. Heitz and J.-P. Sauvage, *Eur. J. Inorg. Chem.*, 1998, 1-14.
17. Z. Ji, S. Li, Y. Li and W. Sun, *Inorg. Chem.*, 2010, **49**, 1337-1346.
18. A. C. Benniston, V. Grosshenny, A. Harriman and R. Ziessel, *Angew. Chem., Int. Ed.*, 1994, **33**, 1884-1885.
19. V. Grosshenny, A. Harriman and R. Ziessel, *Angew. Chem., Int. Ed. Engl.*, 1995, **34**, 1100-1102.
20. V. Grosshenny, A. Harriman and R. Ziessel, *Angew. Chem., Int. Ed.*, 1995, **34**, 2705-2708.
21. M. Hissler, A. El-ghayoury, A. Harriman and R. Ziessel, *Angew. Chem., Int. Ed.*, 1998, **37**, 1717-1720.
22. M. Schütte, D. G. Kurth, M. R. Linford, H. Cölfen and H. Möhwald, *Angew. Chem., Int. Ed.*, 1998, **37**, 2891-2893.
23. T. E. Janini, J. L. Fattore and D. L. Mohler, *J. Organomet. Chem.*, 1999, **578**, 260-263.
24. D. G. Kurth and R. Osterhout, *Langmuir*, 1999, **15**, 4842-4846.

25. S. Kelch and M. Rehahn, *Chem. Commun.*, 1999, 1123-1124.
26. S. Kelch and M. Rehahn, *Macromolecules*, 1999, **32**, 5818-5828.
27. D. G. Kurth, P. Lehmann and M. Schütte, *Proc. Natl. Acad. Sci. USA*, 2000, **97**, 5704-5707.
28. J. A. Barron, S. Glazier, S. Bernhard, K. Takada, P. L. Houston and H. D. Abruña, *Inorg. Chem.*, 2003, **42**, 1448-1455.
29. D. Hinderberger, O. Schmelz, M. Rehahn and G. Jeschke, *Angew. Chem., Int. Ed.*, 2004, **43**, 4616-4621.
30. A. Lindner, M. Menzel, F. Renz, D. G. Kurth and A. F. Thünemann, *Hyperfine Interact.*, 2005, **166**, 465-468.
31. F. S. Han, M. Higuchi and D. G. Kurth, *Adv. Mater.*, 2007, **19**, 3928-3931.
32. F. S. Han, M. Higuchi, Y. Akasaka, Y. Otsuka and D. G. Kurth, *Thin Solid Films*, 2008, **516**, 2469-2473.
33. F. S. Han, M. Higuchi and D. G. Kurth, *J. Am. Chem. Soc.*, 2008, **130**, 2073-2081.
34. W. Y. Ng, X. Gong and W. K. Chan, *Chem. Mater.*, 1999, **11**, 1165-1170.
35. V. Stepanenko, M. Stocker, P. Müller, M. Büchner and F. Würthner, *J. Mater. Chem.*, 2009, **19**, 6816-6826.
36. A. Winter, C. Friebe, M. Chiper, M. D. Hager and U. S. Schubert, *J. Polym. Sci., Part A: Polym. Chem.*, 2009, **47**, 4083-4098.
37. U. S. Schubert, O. Hien and C. Eschbaumer, *Macromol. Rapid Commun.*, 2000, **21**, 1156-1161.
38. S. Schmatloch, M. Fernández González and U. S. Schubert, *Macromol. Rapid Commun.*, 2002, **23**, 957-961.
39. S. Schmatloch and U. S. Schubert, *Macromol. Symp.*, 2003, **199**, 483-497.
40. H. Hofmeier, S. Schmatloch, D. Wouters and U. S. Schubert, *Macromol. Chem. Phys.*, 2003, **204**, 2197-2203.
41. S. Schmatloch, A. M. J. van den Berg, A. S. Alexeev, H. Hofmeier and U. S. Schubert, *Macromolecules*, 2003, **36**, 9943-9949.
42. S. Schmatloch, A. M. J. van den Berg, M. W. M. Fijten and U. S. Schubert, *Macromol. Rapid Commun.*, 2004, **25**, 321-325.
43. S. Schmatloch, A. M. J. Van den Berg, H. Hofmeier and U. S. Schubert, *Des. Monomers Polym.*, 2004, **7**, 191-201.
44. M. A. R. Meier, H. Hofmeier, C. H. Abeln, C. Tziatzios, M. Rasa, D. Schubert and U. S. Schubert, *e-Polymers*, 2006, No. 016.
45. M. Chiper, R. Hoogenboom and U. S. Schubert, *e-Polymers*, 2008, No. 157.
46. H. Hofmeier, M. Wouters, D. Wouters and U. S. Schubert, *ACS Symp. Ser.*, 2006, **928**, 113-125.
47. R. H. Holyer, C. D. Hubbard, S. F. A. Kettle and R. G. Wilkins, *Inorg. Chem.*, 1966, **5**, 622-625.

-
48. R. Hogg and R. G. Wilkins, *J. Chem. Soc.*, 1962, 341-350.
 49. M. Raşa, B. G. G. Lohmeijer, H. Hofmeier, H. M. L. Thijs, D. Schubert, U. S. Schubert and C. Tziatzios, *Macromol. Chem. Phys.*, 2006, **207**, 2029-2041.
 50. U. S. Schubert, S. Schmatloch and A. A. Precup, *Des. Monomers Polym.*, 2002, **5**, 211-221.
 51. M. Chipper, M. A. R. Meier, D. Wouters, S. Hoepfener, C.-A. Fustin, J.-F. Gohy and U. S. Schubert, *Macromolecules*, 2008, **41**, 2771-2777.
 52. M. A. R. Meier, D. Wouters, C. Ott, P. Guillet, C.-A. Fustin, J.-F. Gohy and U. S. Schubert, *Macromolecules*, 2006, **39**, 1569-1576.
 53. C. Ott, J. M. Kranenburg, C. Guerrero-Sanchez, S. Hoepfener, D. Wouters and U. S. Schubert, *Macromolecules*, 2009, **42**, 2177-2183.
 54. J.-F. Gohy, B. G. G. Lohmeijer and U. S. Schubert, *Macromolecules*, 2002, **35**, 4560-4563.
 55. B. G. G. Lohmeijer and U. S. Schubert, *Angew. Chem., Int. Ed.*, 2002, **41**, 3825-3829.
 56. J.-F. Gohy, B. G. G. Lohmeijer and U. S. Schubert, *Macromol. Rapid Commun.*, 2002, **23**, 555-560.
 57. P. Guillet, C.-A. Fustin, B. G. G. Lohmeijer, U. S. Schubert and J.-F. Gohy, *Macromolecules*, 2006, **39**, 5484-5488.
 58. C. Mugemana, P. Guillet, S. Hoepfener, U. S. Schubert, C.-A. Fustin and J.-F. Gohy, *Chem. Commun.*, 2010, **46**, 1296-1298.
 59. E. C. Constable, A. M. W. Cargill Thompson, D. A. Tocher and M. A. M. Daniels, *New J. Chem.*, 1992, **16**, 855-867.
 60. J. B. Beck and S. J. Rowan, *J. Am. Chem. Soc.*, 2003, **125**, 13922-13923.
 61. Y. Q. Zhao, J. B. Beck, S. J. Rowan and A. M. Jamieson, *Macromolecules*, 2004, **37**, 3529-3531.
 62. S. J. Rowan and J. B. Beck, *Faraday Discuss.*, 2005, **128**, 43-53.
 63. J. B. Beck, J. M. Ineman and S. J. Rowan, *Macromolecules*, 2005, **38**, 5060-5068.
 64. W. Weng, J. B. Beck, A. M. Jamieson and S. J. Rowan, *J. Am. Chem. Soc.*, 2006, **128**, 11663-11672.
 65. W. G. Weng, A. M. Jamieson and S. J. Rowan, *Tetrahedron*, 2007, **63**, 7419-7431.
 66. W. Weng, Z. Li, A. M. Jamieson and S. J. Rowan, *Macromolecules*, 2009, **42**, 236-246.
 67. F. M. Romero, R. Ziessel, A. Dupont-Gervais and A. Van Dorselaer, *Chem. Commun.*, 1996, 551-553.
 68. S.-H. Hwang, C. N. Moorefield, F. R. Fronczek, O. Lukoyanova, L. Echegoyen and G. R. Newkome, *Chem. Commun.*, 2005, 713-715.
 69. S.-H. Hwang, P. S. Wang, C. N. Moorefield, L. A. Godínez, J. Manríquez, E. Bustos and G. R. Newkome, *Chem. Commun.*, 2005, 4672-4674.

-
70. G. R. Newkome, T. J. Cho, C. N. Moorefield, G. R. Baker, R. Cush and P. S. Russo, *Angew. Chem., Int. Ed.*, 1999, **38**, 3717-3721.
 71. G. R. Newkome, T. J. Cho, C. N. Moorefield, R. Cush, P. S. Russo, L. A. Godínez, M. J. Saunders and P. Mohapatra, *Chem. Eur. J.*, 2002, **8**, 2946-2954.
 72. G. R. Newkome, T. J. Cho, C. N. Moorefield, P. P. Mohapatra and L. A. Godínez, *Chem. Eur. J.*, 2004, **10**, 1493-1500.
 73. P. Wang, C. N. Moorefield and G. R. Newkome, *Org. Lett.*, 2004, **6**, 1197-1200.
 74. S.-H. Hwang, P. Wang, C. N. Moorefield, J.-C. Jung, J.-Y. Kim, S.-W. Lee and G. R. Newkome, *Macromol. Rapid Commun.*, 2006, **27**, 1809-1813.
 75. T. J. Cho, C. N. Moorefield, S.-H. Hwang, P. S. Wang, L. A. Godínez, E. Bustos and G. R. Newkome, *Eur. J. Org. Chem.*, 2006, 4193-4200.
 76. S.-H. Hwang, C. N. Moorefield, P. Wang, J.-Y. Kim, S.-W. Lee and G. R. Newkome, *Inorg. Chim. Acta*, 2007, **360**, 1780-1784.
 77. Y.-T. Chan, X. Li, M. Soler, J.-L. Wang, C. Wesdemiotis and G. R. Newkome, *J. Am. Chem. Soc.*, 2009, **131**, 16395-16397.
 78. S.-H. Hwang, C. N. Moorefield, P. Wang, F. R. Fronczek, B. H. Courtney and G. R. Newkome, *Dalton Trans.*, 2006, 3518-3522.
 79. S.-H. Hwang, C. N. Moorefield, H.-C. Cha, P. Wang and G. R. Newkome, *Des. Monomers Polym.*, 2006, **9**, 413-424.
 80. I. Eryazici and G. R. Newkome, *New J. Chem.*, 2009, **33**, 345-357.
 81. P. Wang, C. N. Moorefield and G. R. Newkome, *Angew. Chem., Int. Ed.*, 2005, **44**, 1679-1683.
 82. E. C. Constable, C. E. Housecroft and C. B. Smith, *Inorg. Chem. Commun.*, 2003, **6**, 1011-1013.
 83. E. C. Constable, C. E. Housecroft, M. Neuburger, S. Schaffner and C. B. Smith, *Dalton Trans.*, 2005, 2259-2267.
 84. P. R. Andres and U. S. Schubert, *Synthesis*, 2004, 1229-1238.
 85. P. R. Andres and U. S. Schubert, *Macromol. Rapid Commun.*, 2004, **25**, 1371-1375.
 86. C. B. Smith, E. C. Constable, C. E. Housecroft and B. M. Kariuki, *Chem. Commun.*, 2002, 2068-2069.
 87. H. S. Chow, E. C. Constable, C. E. Housecroft and M. Neuburger, *Dalton Trans.*, 2003, 4568-4569.
 88. H. S. Chow, E. C. Constable, R. Frantz, C. E. Housecroft, J. Lacour, M. Neuburger, D. Rappoport and S. Schaffner, *New J. Chem.*, 2009, **33**, 376-385.
 89. H. S. Chow, E. C. Constable, C. E. Housecroft, M. Neuburger and S. Schaffner, *Polyhedron*, 2006, **25**, 1831-1843.
 90. H. S. Chow, Ph.D. Thesis, University of Basel, 2005.
 91. G. U. Priimov, P. Moore, P. K. Maritim, P. K. Butalanyi and N. W. Alcock, *J. Chem. Soc., Dalton Trans.*, 2000, 445-449.

-
92. E. C. Constable, in *Education in Advanced Chemistry - Perspectives in Coordination Chemistry*, eds. A. M. Trzeciak, P. Sobota and J. J. Ziółkowski, Wydawnictwo Poznańskie, Poznań-Wrocław, 2000, vol. 7, pp. 159-183.
 93. I. Bertini, C. Luchinat and S. Aime, *Coord. Chem. Rev.*, 1996, **150**, 1-292.
 94. E. C. Constable, T. Kulke, M. Neuburger and M. Zehnder, *New J. Chem.*, 1997, **21**, 1091-1102.
 95. H. S. Chow, E. C. Constable, C. E. Housecroft, K. J. Kulicke and Y. Tao, *Dalton Trans.*, 2005, 236-237.
 96. Y. Tao, Ph.D. Thesis, University of Birmingham, 2004.
 97. J. K. Beattie and H. Elsbernd, *Inorg. Chim. Acta*, 1995, **240**, 641-644.
 98. E. C. Constable, C. P. Hart and C. E. Housecroft, *Appl. Organometal. Chem.*, 2003, **17**, 383-387.
 99. E. C. Constable, C. E. Housecroft and Y. Tao, *Synthesis*, 2004, 869-874.
 100. E. C. Constable, C. E. Housecroft, T. Kulke, C. Lazzarini, E. R. Schofield and Y. Zimmermann, *J. Chem. Soc., Dalton Trans.*, 2001, 2864-2871.
 101. P. W. Atkins, *Physical Chemistry*, 6th edn., Oxford University Press, Oxford, 2001.
 102. A. Einstein, *Ann. Phys.*, 1906, **19**, 371-381.
 103. A. Einstein, *Ann. Phys.*, 1906, **19**, 289-306.
 104. M. v. Smoluchowski, *Ann. Phys.*, 1906, **326**, 756-780.
 105. J. T. Edward, *J. Chem. Educ.*, 1970, **47**, 261-270.
 106. A. Macchioni, G. Ciancaleoni, C. Zuccaccia and D. Zuccaccia, *Chem. Soc. Rev.*, 2008, **37**, 479-489.
 107. K. E. v. Holde, W. C. Johnson and P. S. Ho, *Principles of Physical Biochemistry*, 2nd edn., Pearson Prentice Hall, Upper Saddle River, 2006.
 108. A. F. Olea and J. K. Thomas, *J. Am. Chem. Soc.*, 1988, **110**, 4494-4502.
 109. E. Yumet, H. C. Chen and S. H. Chen, *AIChE J.*, 1985, **31**, 76-81.
 110. M. Ihnat and D. A. I. Goring, *Can. J. Chem.*, 1967, **45**, 2353-2361.
 111. H. H. Schuh and H. Fischer, *Helv. Chim. Acta*, 1978, **61**, 2130-2164.
 112. E. R. Nightingale, *J. Phys. Chem.*, 1959, **63**, 1381-1387.
 113. R. A. Robinson and R. H. Stokes, *Electrolyte Solutions*, 2nd revised edn., Butterworths, London, 1965.
 114. A. Spornol and K. Wirtz, *Z. Naturforsch., A: Astrophys. Phys. Phys. Chem.*, 1953, **8**, 522-532.
 115. A. Spornol, *J. Phys. Chem.*, 1956, **60**, 703-704.
 116. S. G. Schultz and A. K. Solomon, *J. Gen. Physiol.*, 1961, **44**, 1189-1199.
 117. A. Gierer and K. Wirtz, *Z. Naturforsch., A: Astrophys. Phys. Phys. Chem.*, 1953, **8**, 532-538.

-
118. H. C. Chen and S. H. Chen, *J. Phys. Chem.*, 1984, **88**, 5118-5121.
119. D. Zuccaccia and A. Macchioni, *Organometallics*, 2005, **24**, 3476-3486.
120. P. S. Pregosin, P. G. A. Kumar and I. Fernandez, *Chem. Rev.*, 2005, **105**, 2977-2998.
121. M. Valentini, H. Ruegger and P. S. Pregosin, *Helv. Chim. Acta*, 2001, **84**, 2833-2853.
122. P. S. Pregosin, *Prog. Nucl. Magn. Reson. Spectrosc.*, 2006, **49**, 261-288.
123. Y. Cohen, L. Avram and L. Frish, *Angew. Chem., Int. Ed.*, 2005, **44**, 520-554.
124. W. S. Price, *Concepts Magn. Reson.*, 1997, **9**, 299-336.
125. E. O. Stejskal and J. E. Tanner, *J. Chem. Phys.*, 1965, **42**, 288-292.
126. T. Brand, E. J. Cabrita and S. Berger, *Prog. Nucl. Magn. Reson. Spectrosc.*, 2005, **46**, 159-196.
127. W. S. Price, *Concepts Magn. Reson.*, 1998, **10**, 197-237.
128. C. S. Johnson, *Prog. Nucl. Magn. Reson. Spectrosc.*, 1999, **34**, 203-256.
129. T. Brand, E. J. Cabrita and S. Berger, in *Modern Magnetic Resonance*, ed. G. A. Webb, Springer, Dordrecht, 2006, pp. 135-143.
130. P. S. Pregosin, E. Martinez-Viviente and P. G. A. Kumar, *Dalton Trans.*, 2003, 4007-4014.
131. P. S. Pregosin, *Pure Appl. Chem.*, 2009, **81**, 615-633.
132. A. Pastor and E. Martinez-Viviente, *Coord. Chem. Rev.*, 2008, **252**, 2314-2345.
133. T. Megyes, H. Jude, T. Grósz, I. Bakó, T. Radnai, G. Tárkányi, G. Pálinkás and P. J. Stang, *J. Am. Chem. Soc.*, 2005, **127**, 10731-10738.
134. W. H. Otto, M. H. Keefe, K. E. Splan, J. T. Hupp and C. K. Larive, *Inorg. Chem.*, 2002, **41**, 6172-6174.
135. J. E. Beves, B. E. Chapman, P. W. Kuchel, L. F. Lindoy, J. McMurtrie, M. McPartlin, P. Thordarson and G. Wei, *Dalton Trans.*, 2006, 744-750.
136. J. E. Beves, E. C. Constable, C. E. Housecroft, M. Neuburger, S. Schaffner and E. J. Shardlow, *Dalton Trans.*, 2007, 1593-1602.
137. M. Ikeda, Y. Tanaka, T. Hasegawa, Y. Furusho and E. Yashima, *J. Am. Chem. Soc.*, 2006, **128**, 6806-6807.
138. J. Chambers, B. Eaves, D. Parker, R. Claxton, P. S. Ray and S. J. Slattery, *Inorg. Chim. Acta*, 2006, **359**, 2400-2406.
139. G. Lowe, A. S. Droz, T. Vilaivan, G. W. Weaver, L. Tweedale, J. M. Pratt, P. Rock, V. Yardley and S. L. Croft, *J. Med. Chem.*, 1999, **42**, 999-1006.
140. M. G. B. Drew, M. J. Hudson, P. B. Iveson, M. L. Russell, J. O. Liljenzin, M. Skalberg, L. Spjuth and C. Madic, *J. Chem. Soc., Dalton Trans.*, 1998, 2973-2980.
141. M. Chipper, M. A. R. Meier, J. M. Kranenburg and U. S. Schubert, *Macromol. Chem. Phys.*, 2007, **208**, 679-689.
142. H. Elsbernd and J. K. Beattie, *J. Inorg. Nucl. Chem.*, 1972, **34**, 771-774.

143. V. Goral, M. I. Nelen, A. V. Eliseev and J.-M. Lehn, *Proc. Natl. Acad. Sci. USA*, 2001, **98**, 1347-1352.
144. H. A. Goodwin, *Top. Curr. Chem.*, 2004, **234**, 23-47.
145. B. N. Figgis, E. S. Kucharski and A. H. White, *Aust. J. Chem.*, 1983, **36**, 1563-1571.
146. R. Indumathy, M. Kanthimathi, T. Weyhermuller and B. U. Nair, *Polyhedron*, 2008, **27**, 3443-3450.
147. Z. Yu, A. Nabei, T. Izumi, T. Okubo and T. Kuroda-Sowa, *Acta Crystallogr., Sect. C: Cryst. Struct. Commun.*, 2008, **64**, M209-M212.
148. E. N. Maslen, C. L. Raston and A. H. White, *J. Chem. Soc., Dalton Trans.*, 1974, 1803-1807.
149. C. L. Raston and A. H. White, *J. Chem. Soc., Dalton Trans.*, 1976, 7-12.
150. W. Henke and S. Kremer, *Inorg. Chim. Acta*, 1982, **65**, L115-L117.
151. B. N. Figgis, E. S. Kucharski and A. H. White, *Aust. J. Chem.*, 1983, **36**, 1537-1561.
152. B. N. Figgis, E. S. Kucharski and A. H. White, *Aust. J. Chem.*, 1983, **36**, 1527-1535.
153. F. Takusagawa, P. G. Yohannes and K. B. Mertes, *Inorg. Chim. Acta*, 1986, **114**, 165-169.
154. A. B. Gaspar, M. C. Muñoz, V. Niel and J. A. Real, *Inorg. Chem.*, 2001, **40**, 9-10.
155. A. Galet, A. B. Gaspar, M. C. Muñoz and J. A. Real, *Inorg. Chem.*, 2006, **45**, 4413-4422.
156. G. Agustí, C. Bartual, V. Martinez, F. J. Muñoz-Lara, A. B. Gaspar, M. C. Muñoz and J. A. Real, *New J. Chem.*, 2009, **33**, 1262-1267.
157. S. Hayami, Y. Shigeyoshi, M. Akita, K. Inoue, K. Kato, K. Osaka, M. Takata, R. Kawajiri, T. Mitani and Y. Maeda, *Angew. Chem., Int. Ed.*, 2005, **44**, 4899-4903.
158. S. Hayami, R. Moriyama, Y. Shigeyoshi, R. Kawajiri, T. Mitani, M. Akita, K. Inoue and Y. Maeda, *Inorg. Chem.*, 2005, **44**, 7295-7297.
159. S. Hayami, K. Murata, D. Urakami, Y. Kojima, M. Akita and K. Inoue, *Chem. Commun.*, 2008, 6510-6512.
160. P. Nielsen, H. Toftlund, A. D. Bond, J. F. Boas, J. R. Pilbrow, G. R. Hanson, C. Noble, M. J. Riley, S. M. Neville, B. Moubaraki and K. S. Murray, *Inorg. Chem.*, 2009, **48**, 7033-7047.
161. M. L. Scudder, H. A. Goodwin and I. G. Dance, *New J. Chem.*, 1999, **23**, 695-705.
162. E. R. Schofield, Ph.D. Thesis, University of Basel, 1999.
163. G. D. Storrier, K. Takada and H. D. Abruña, *Inorg. Chem.*, 1999, **38**, 559-565.
164. T. Yutaka, I. Mori, M. Kurihara, N. Tamai and H. Nishihara, *Inorg. Chem.*, 2003, **42**, 6306-6313.
165. K. T. Potts, D. A. Usifer, A. Guadalupe and H. D. Abruna, *J. Am. Chem. Soc.*, 1987, **109**, 3961-3967.
166. A. Sacco and E. Matteoli, *J. Solution Chem.*, 1997, **26**, 527-535.

-
167. SPARTAN '04, 1991-2004, Wavefunction Inc.
168. D. L. Jameson and L. E. Guise, *Tetrahedron Lett.*, 1991, **32**, 1999-2002.
169. E. C. Constable and M. D. Ward, *J. Chem. Soc., Dalton Trans.*, 1990, 1405-1409.
170. C. Arana, S. Yan, M. Keshavarz-K, K. T. Potts and H. D. Abruña, *Inorg. Chem.*, 1992, **31**, 3680-3682.
171. C. Arana, M. Keshavarz, K. T. Potts and H. D. Abruña, *Inorg. Chim. Acta*, 1994, **225**, 285-295.
172. D. J. Hathcock, K. Stone, J. Madden and S. J. Slattery, *Inorg. Chim. Acta*, 1998, **282**, 131-135.
173. D. N. Hague and A. R. White, *J. Chem. Soc., Dalton Trans.*, 1995, 449-453.
174. G. U. Priimov, P. Moore, L. Helm and A. E. Merbach, *Inorg. React. Mech.*, 2001, **3**, 1-23.
175. E. C. Constable, *Inorg. Chim. Acta*, 1984, **82**, 53-57.
176. E. C. Constable and T. A. Leese, *Inorg. Chim. Acta*, 1988, **146**, 55-58.
177. J. Clayden, N. Greeves, S. Warren and P. Wothers, *Organic Chemistry*, 1st edn., Oxford University Press, Oxford, 2001.
178. M. Jones, *Organic Chemistry*, 2nd edn., W. W. Norton & Company, New York, 2000.
179. H. Lettau, *Chemie der Heterocyclen*, 1st edn., VEB Deutscher Verlag für Grundstoffindustrie, Leipzig, 1980.
180. A. F. Holleman, E. Wiberg and N. Wiberg, *Lehrbuch der Anorganischen Chemie*, 33rd edn., Walter de Gruyter, Berlin, 1985.
181. J. E. Beves, E. C. Constable, C. E. Housecroft, M. Neuburger, S. Schaffner and J. A. Zampese, *Inorg. Chem. Commun.*, 2008, **11**, 1006-1008.
182. J. S. Judge and W. A. Baker, *Inorg. Chim. Acta*, 1967, **1**, 239-244.
183. J. S. Judge and W. A. Baker, *Inorg. Chim. Acta*, 1967, **1**, 245-248.
184. J. S. Judge, W. M. Reiff, G. M. Intille, P. Ballway and W. A. Baker, *J. Inorg. Nucl. Chem.*, 1967, **29**, 1711-1716.
185. C. M. Harris, T. N. Lockyer, R. L. Martin, H. R. H. Patil, E. Sinn and I. M. Stewart, *Aust. J. Chem.*, 1969, **22**, 2105-2116.
186. E. Goldschmied and N. C. Stephenson, *Acta Crystallogr., Sect. B: Struct. Sci*, 1970, **B26**, 1867-1875.
187. E. C. Constable, C. E. Housecroft, V. Jullien, M. Neuburger and S. Schaffner, *Inorg. Chem. Commun.*, 2006, **9**, 504-506.
188. A. G. Vinogradov and A. N. Glebov, *Russ. J. Coord. Chem.*, 2001, **27**, 803-807.
189. S. A. Cotton, V. Franckevicius and J. Fawcett, *Polyhedron*, 2002, **21**, 2055-2061.
190. R. A. Henderson, *The Mechanisms of Reactions at Transition Metal Sites*, Oxford University Press, Oxford, 1993.
191. P. K. Chattopadhyay and J. F. Coetzee, *Inorg. Chem.*, 1976, **15**, 400-405.

References

192. D. H. Wu, A. D. Chen and C. S. Johnson, *J. Magn. Reson., Ser. A*, 1995, **115**, 260-264.
193. R. Mills, *J. Phys. Chem.*, 1973, **77**, 685-688.
194. E. Martínez-Viviente and P. S. Pregosin, *Helv. Chim. Acta*, 2003, **86**, 2364-2378.
195. COLLECT Software, 1997-2001, Nonius BV.
196. A. Altomare, G. Cascarano, C. Giacovazzo, A. Guagliardi, M. C. Burla, G. Polidori and M. Camalli, *J. Appl. Cryst.*, 1994, **27**, 435.
197. Z. Otwinowski and W. Minor, in *Methods in Enzymology*, eds. C. W. Carter Jr. and R. M. Sweet, Academic Press, New York, 1997, vol. 276, p. 307.
198. P. W. Betteridge, J. R. Carruthers, R. I. Cooper, K. Prout and D. J. Watkin, *J. Appl. Cryst.*, 2003, **36**, 1487-1487.
199. Stoe & Cie, IPDS software v 1.26, 1996, Stoe & Cie, Darmstadt, Germany.
200. G. M. Sheldrick, *Acta Crystallogr., Sect. A: Fundam. Crystallogr.*, 2008, **64**, 112-122.

References

CV

Emily Kate Harris

Address: Oberwilerstr. 112
4054 Basel
Switzerland

Date of Birth: 2nd November 1982
Telephone: +41 61 321 3791
E-mail: kate.harris@unibas.ch

Education

01/2006 – 03/2010 University of Basel
PhD in Inorganic Chemistry *Summa cum Laude*
Thesis Title: Polymer or Macrocycle? Cobalt Complexes of Ditopic 2,2':6',2''-Terpyridine Ligands with Flexible Spacers
Research under the supervision of Prof. Edwin C. Constable and Prof. Catherine E. Housecroft in the area of supramolecular chemistry involving the synthesis of ditopic terpyridine ligands and investigation of their co-ordination behaviour.

10/2001 – 06/2005 University of Edinburgh
MChem Chemistry with a Year in Europe *First Class Honours*
Final year project with Prof. Peter Tasker requiring the synthesis of four new phenolic oxime ligands and investigation of their co-ordination compounds with a view to their use in "clean" metal extraction procedures.

10/2003 – 08/2004 Ludwig-Maximilians University, Munich
ERASMUS Exchange
Extended research projects with Prof. Dr. Thomas Klapötke involving a mainly theoretical investigation of the decomposition of explosive nitramines in the presence of an energetic binder and attempts to synthesise a previously unknown ligand-stabilised gold(I) fluoride.

09/1994 – 06/2001 Alcester Grammar School
4 A-levels in Chemistry (A), German (A), French (A), Mathematics (A)
11 GCSEs at grades A* and A

Awards
Lang Scholarship for the best degree with a Year in Europe/Industry (2005)
Second and third year Chemistry Class Medals (2002, 2003)
Second and third year Physical Laboratory prize (2002, 2003)
School Modern Languages prize (2001)

Practical Skills

Instrumentation Extensive experience in measurement (Bruker) and analysis of NMR data including:
Standard 1-D (multinuclear) and 2-D methods
PGSE NMR methods
NMR spectra of paramagnetic complexes
Measurement and analysis of mass spectra, IR spectra, UV-vis spectra

Language Skills Native speaker of English
Fluent spoken and written German
Good understanding of French
Working knowledge of Japanese (JLPT Level 3 – December 2009)

IT Skills Confident with Microsoft Office, MestreNova, ChemDraw, SciFinder, Beilstein, Origin, Mercury, Diamond

Teaching Experience

- 06/2008** **Supervisor of high school work experience student (University of Basel)**
- 04/2006 –**
(5 semesters) **Laboratory course in inorganic chemistry for 4th semester chemistry students (University of Basel)**
Assisting students with basic and advanced laboratory technique including inert atmosphere techniques. Assessment of reports and oral examinations.
- 10/2006 – 01/2010** **Exercises accompanying introductory chemistry lecture course for 1st semester students (University of Basel)**
(4 semesters) Solution of general chemistry problems on the blackboard in German for 350 students, answering individual students' questions and invigilating and marking exam papers.

Work History

- 04/2006 –** **Elsevier, Editorial Assistant to Catherine E. Housecroft for Polyhedron**
Selection of appropriate reviewers and liaison with authors and referees.
- 10/2005 – 12/2005** **Electrophotography Business, Avecia Ltd., Chemist**
Lab-scale formulation, screen testing, physical characterisation and quality control of current and new coloured toner for laser printers using blending equipment, microscopy, particle size analysis and print testing techniques.

Personal Interests and Activities

Japanese Language and Culture

Scottish Country Dancing and other Folk Dance

- 2002 – 2003 Committee Member (Publicity) for Edinburgh University New Scotland Country Dance Society
- 2009 – Committee Member for Scottish Country Dance Group Basel

Student Membership of the RSC and the Swiss Chemical Society

References

Professor Edwin C. Constable

Department of Chemistry, University of Basel, Spitalstr. 51, 4056 Basel, Switzerland.
Tel.: + 41 61 267 1001 Email: edwin.constable@unibas.ch

Professor Catherine E. Housecroft

Department of Chemistry, University of Basel, Spitalstr. 51, 4056 Basel, Switzerland.
Tel.: + 41 61 267 1008 Email: catherine.housecroft@unibas.ch

Professor Peter A. Tasker

School of Chemistry, University of Edinburgh, West Mains Road, Edinburgh, EH9 3JJ, U.K.
Tel.: + 44 131 650 4706 Email: peter.tasker@ed.ac.uk

Professor Thomas M. Klapötke

Department of Chemistry and Biochemistry, LMU Munich, Butenandtstr. 5-13 (D), 81377 Munich, Germany.
Tel.: + 49 89 2180 77491 Email: thomas.m.klapoetke@cup.uni-muenchen.de

List of Publications

Journal Articles

4. **Turning $\{M(\text{tpy})_2\}^{n+}$ Embraces and $\text{CH}\cdots\pi$ Interactions On and Off in Homoleptic Cobalt(II) and Cobalt(III) Bis(2,2':6',2''-terpyridine) Complexes.** Edwin C. Constable, Kate Harris, Catherine E. Housecroft, Markus Neuburger and Jennifer A. Zampese, *CrystEngComm*, **2010**, DOI: 10.1039/c002834g.
3. **A Metallopolymer Case-History: Polymer, Ring or Ligand Reaction?** Edwin C. Constable, Kate Harris, Catherine E. Housecroft, Markus Neuburger and Silvia Schaffner, *Chem. Commun.*, **2008**, 5360-5362.
2. **Further Decomposition Pathways of Mixtures of the Nitramines HMX, RDX and CL-20 with the Energetic Binder Glycidyl Azide Polymer (GAP) – A Computational Study II.** Manfred A. Bohn, Anton Hammerl, Kate Harris and Thomas M. Klapötke, *Central European Journal of Energetic Materials*, **2005**, 2(3), 3-19.
1. **The Elimination of NO_2 from Mixtures of the Nitramines HMX, RDX and CL-20 with the Energetic Binder Glycidyl Azide Polymer (GAP) – A Computational Study I.** Manfred A. Bohn, Anton Hammerl, Kate Harris and Thomas M. Klapötke, *Central European Journal of Energetic Materials*, **2005**, 2(2), 29-44.

Conference Proceedings

1. **Interactions between the Nitramines RDX, HMX and CL-20 with the Energetic Binder GAP.** Manfred A. Bohn, Anton Hammerl, Kate Harris and Thomas M. Klapötke, *New Trends in Research of Energetic Materials, Proceedings of the 7th Seminar, Pardubice, Czech Republic, 19.04 – 21.04.2005*, **2005**, 2, 490-497.

Oral Presentations

1. **Synthesis of Cobalt(II)- and Cobalt(III)-Containing Metallomacrocycles from Ditopic 2,2':6',2''-Terpyridine Ligands with Flexible Spacers.** Edwin C. Constable, Kate Harris, Catherine E. Housecroft, Markus Neuburger and Silvia Schaffner, *235th ACS National Meeting*, New Orleans, LA, USA, 06.04.2008 – 10.04.2008.

Poster Presentations

12. **Anion and Solvent Effects on the Synthesis of Cobalt Complexes of Ditopic 2,2':6',2''-Terpyridine Ligands with Flexible Spacers.** Edwin C. Constable, Kate Harris, Catherine E. Housecroft, Markus Neuburger and Silvia Schaffner, *SCS Fall Meeting 2009*, Lausanne, Switzerland, 04.09.2009.

11. **Anion and Solvent Effects on the Synthesis of Cobalt Complexes of Ditopic 2,2':6',2"-Terpyridine Ligands with Flexible Spacers.** Edwin C. Constable, Kate Harris, Catherine E. Housecroft, Markus Neuburger and Silvia Schaffner, *IV International Symposium on Macrocyclic and Supramolecular Chemistry*, Maastricht, Netherlands, 21.06 – 25.06.2009.
10. **Cobalt(II) Catalysed Alkoxy Group Exchange in 4'-Alkoxy-2,2':6',2"-Terpyridines.** Edwin C. Constable, Kate Harris, Catherine E. Housecroft, Markus Neuburger and Silvia Schaffner, *2nd European Chemistry Congress*, Torino, Italy, 16.09 – 20.08.2008.
9. **Cobalt Complexes of Ditopic 2,2':6',2"-Terpyridine Ligands with Flexible Spacers – Polymers or Metallomacrocycles?** Edwin C. Constable, Kate Harris, Catherine E. Housecroft, Markus Neuburger and Silvia Schaffner, *SCS Fall Meeting 2008*, Zürich, Switzerland, 11.09.2008.
8. **Assembly of Metallomacrocycles from Ditopic 2,2':6',2"-Terpyridine Ligands with Flexible Spacers.** Edwin C. Constable, Kate Harris, Catherine E. Housecroft, Markus Neuburger and Silvia Schaffner, *SCS Fall Meeting 2007*, Lausanne, Switzerland, 12.09.2007.
7. **Assembly of Metallomacrocycles from Ditopic 2,2':6',2"-Terpyridine Ligands with Flexible Spacers.** Edwin C. Constable, Kate Harris, Catherine E. Housecroft, Markus Neuburger and Silvia Schaffner, *II International Symposium on Macrocyclic and Supramolecular Chemistry*, Salice Terme, Italy, 24.06 – 28.06.2007.
6. **Metallopolymer or Metallomacrocycle?** Hoi-Shan Chow, Edwin C. Constable, Kate Harris, Catherine E. Housecroft, Markus Neuburger and Silvia Schaffner, *SCS Fall Meeting 2006*, Zürich, Switzerland, 13.10.2006.
5. **Metallopolymer or Metallomacrocycle?** Hoi-Shan Chow, Edwin C. Constable, Kate Harris, Catherine E. Housecroft, Markus Neuburger and Silvia Schaffner, *1st European Chemistry Congress*, Budapest, Hungary, 27.08 – 31.08.2006.
4. **Interactions between the Nitramines RDX, HMX and CL20 with the Energetic Binder GAP.** Manfred A. Bohn, Anton Hammerl, Kate Harris and Thomas M. Klapötke, *New Trends in Research of Energetic Materials, 7th Seminar*, Pardubice, Czech Republic, 19.04 – 21.04.2005.
3. **Interaction between Energetic Nitramines and the Energetic Binder GAP.** Manfred A. Bohn, Anton Hammerl, Kate Harris and Thomas M. Klapötke, *Münchner Industrietag 2004*, LMU München, 14.10.2004.
2. **Reactions of Silver Phosphanes with Fluoride Ions.** Anton Hammerl, Kate Harris and Thomas M. Klapötke, *11^a Reunión Científica Plenaria de Química Inorgánica, 5^a Reunión Científica Plenaria de Química del Estado Sólido*, Santiago de Compostela, Spain, 12.09 – 16.09.2004.
1. **Decomposition of Nitramines with GAP.** Manfred A. Bohn, Anton Hammerl, Kate Harris and Thomas M. Klapötke, *11^a Reunión Científica Plenaria de Química Inorgánica, 5^a Reunión Científica Plenaria de Química del Estado Sólido*, Santiago de Compostela, Spain, 12.09 – 16.09.2004.